MARIANA SPONCHIADO

Deciphering the embryo-maternal interactome: Embryo-dependent programming of endometrial function during early pregnancy in cattle

São Paulo
2019

MARIANA SPONCHIADO

Deciphering the embryo-maternal interactome: Embryo-dependent programming of endometrial function during early pregnancy in cattle

Thesis submitted to the Postgraduate Program in Animal Reproduction of the School of Veterinary Medicine and Animal Science of the University of São Paulo – Brazil and Faculty of Pharmaceutical, Biomedical, and Veterinary Sciences of the University of Antwerp – Belgium to obtain the Doctor's double-degree in Sciences and Veterinary Sciences.

Department:

Animal Reproduction

Area:

Animal Reproduction

Advisors:

Prof. Mario Binelli, Ph.D.

Prof. Jo Leroy, Ph.D.

São Paulo

2019

DADOS INTERNACIONAIS DE CATALOGAÇÃO NA PUBLICAÇÃO

(Biblioteca Virginie Buff D'Ápice da Faculdade de Medicina Veterinária e Zootecnia da Universidade de São Paulo)

T. 3794
FMVZ

Sponchiado, Mariana
Deciphering the embryo-maternal interactome: embryo-dependent programming of endometrial function during early pregnancy in cattle / Mariana Sponchiado. – 2019.
224 f. : il.

Título traduzido: Decifrando o interactoma materno-embrionário: programação do funcionamento do endométrio dependente do embrião durante a gestação inicial em bovinos.

Tese (Doutorado) – Universidade de São Paulo. Faculdade de Medicina Veterinária e Zootecnia. Departamento de Reprodução Animal, São Paulo, 2019.

Programa de Pós-Graduação: Reprodução Animal.
Área de concentração: Reprodução Animal.
Orientador: Prof. Dr. Mario Binelli.
Coorientador: Prof. Dr. Jo L. M. Leroy.

1. Útero. 2. Sinalização materno-embrionária. 3. Mórula. 4. Blastocisto. I. Título.

Ficha catalográfica elaborada pela bibliotecária Maria Aparecida Laet, CRB 5673-8, da FMVZ/USP.

CERTIFICADO

Certificamos que a proposta intitulada "Composição regional do histotrofo uterino e efeito local do embrião no endométrio bovino", protocolada sob o CEUA nº 3167260815 (ID 002263), sob a responsabilidade de **Mário Binelli** - que envolve a produção, manutenção e/ou utilização de animais pertencentes ao filo Chordata, subfilo Vertebrata (exceto o homem), para fins de pesquisa científica ou ensino - está de acordo com os preceitos da Lei 11.794 de 8 de outubro de 2008, com o Decreto 6.899 de 15 de julho de 2009, bem como com as normas editadas pelo Conselho Nacional de Controle da Experimentação Animal (CONCEA), e foi **aprovada** pela Comissão de Ética no Uso de Animais da Faculdade de Medicina Veterinária e Zootecnia da Universidade de São Paulo (CEUA/FMVZ) na reunião de 13/04/2016.

We certify that the proposal "Regional composition of the uterine histotroph and local effect of the embryo in the bovine endometrium", utilizing 50 Bovines (50 females), protocol number CEUA 3167260815 (ID 002263), under the responsibility of **Mário Binelli** - which involves the production, maintenance and/or use of animals belonging to the phylum Chordata, subphylum Vertebrata (except human beings), for scientific research purposes or teaching - is in accordance with Law 11.794 of October 8, 2008, Decree 6899 of July 15, 2009, as well as with the rules issued by the National Council for Control of Animal Experimentation (CONCEA), and was **approved** by the Ethic Committee on Animal Use of the School of Veterinary Medicine and Animal Science (University of São Paulo) (CEUA/FMVZ) in the meeting of 04/13/2016.

Finalidade da Proposta: Pesquisa

Vigência da Proposta: de 01/2016 a 06/2016 Área: Reprodução Animal

Origem:	Prefeitura do Campus da USP de Pirassununga						
Espécie:	Bovinos	sexo:	Fêmeas	idade:	2 a 8 anos	N:	50
Linhagem:	Nelore (Bos indicus)			Peso:	450 a 640 kg		

Local do experimento: Os animais ficarão alojados e serão manejados no Centro de Biotecnologia de Reprodução Animal (CBRA) - VRA/FMVZ/USP - Campus Fernando Costa, Pirassununga-SP. As amostras serão coletadas no Laboratório de Fisiologia e Endocrinologia Molecular localizado neste mesmo centro.

São Paulo, 23 de abril de 2019

Profa. Dra. Anneliese de Souza Traldi
Presidente da Comissão de Ética no Uso de Animais
Faculdade de Medicina Veterinária e Zootecnia da Universidade de São Paulo

Roseli da Costa Gomes
Secretária
Faculdade de Medicina Veterinária e Zootecnia da Universidade de São Paulo

CERTIFICADO

Certificamos que a proposta intitulada "Células epiteliais endometriais bovinas como um modelo para estudar interação materno-embrionária", protocolada sob o CEUA nº 1655180718 (ID 006407), sob a responsabilidade de **Mario Binelli** *e equipe; Mariana Sponchiado* - que envolve a produção, manutenção e/ou utilização de animais pertencentes ao filo Chordata, subfilo Vertebrata (exceto o homem), para fins de pesquisa científica ou ensino - está de acordo com os preceitos da Lei 11.794 de 8 de outubro de 2008, com o Decreto 6.899 de 15 de julho de 2009, bem como com as normas editadas pelo Conselho Nacional de Controle da Experimentação Animal (CONCEA), e foi **aprovada** pela Comissão de Ética no Uso de Animais da Faculdade de Medicina Veterinária e Zootecnia da Universidade de São Paulo (CEUA/FMVZ) na reunião de 17/04/2019.

We certify that the proposal "Bovine endometrial epithelial cells as a model to address early embryo-maternal cross-talk", utilizing 1000 Bovines (1000 females), protocol number CEUA 1655180718 (ID 006407), under the responsibility of **Mario Binelli** *and team; Mariana Sponchiado* - which involves the production, maintenance and/or use of animals belonging to the phylum Chordata, subphylum Vertebrata (except human beings), for scientific research purposes or teaching - is in accordance with Law 11.794 of October 8, 2008, Decree 6899 of July 15, 2009, as well as with the rules issued by the National Council for Control of Animal Experimentation (CONCEA), and was **approved** by the Ethic Committee on Animal Use of the School of Veterinary Medicine and Animal Science (University of São Paulo) (CEUA/FMVZ) in the meeting of 04/17/2019.

Finalidade da Proposta: Pesquisa

Vigência da Proposta: de 04/2019 a 06/2019 Área: Reprodução Animal

Origem:	Animais de proprietários						
Espécie:	Bovinos	sexo:	Fêmeas	idade:	1 a 10 anos	N:	1000
Linhagem:	Bos taurus			Peso:	250 a 700 kg		

Local do experimento: O isolamento e cultivo de células, bem como a produção in vitro de embriões bovinos, será realizado no Gamete Research Centre (supervisionado pelo Prof. Dr. Jo Leroy, Department of Veterinary Sciences, University of Antwerp).

São Paulo, 23 de abril de 2019

Profa. Dra. Anneliese de Souza Traldi
Presidente da Comissão de Ética no Uso de Animais
Faculdade de Medicina Veterinária e Zootecnia da Universidade de São Paulo

Roseli da Costa Gomes
Secretária
Faculdade de Medicina Veterinária e Zootecnia da Universidade de São Paulo

EVALUATION FORM

Author: SPONCHIADO, Mariana

Title: **Deciphering the embryo-maternal interactome:** Embryo-dependent programming of endometrial function during early pregnancy in cattle

Thesis submitted to the Postgraduate Program in Animal Reproduction of the School of Veterinary Medicine and Animal Science of the University of São Paulo – Brazil, and Faculty of Pharmaceutical, Biomedical and Veterinary Sciences of the University of Antwerp – Belgium to obtain the Doctor's double-degree in Sciences and Veterinary Sciences.

Date: _____/_____/_____

Committee Members

Prof. _____

Institution:_____ Decision: _____

Prof. _____

Institution:_____ Decision: _____

Prof. _____

Institution:_____ Decision: _____

Prof. _____

Institution:_____ Decision: _____

Prof. _____

Institution:_____ Decision: _____

I dedicate this thesis to my parents, whose example is my treasure, and whose love, my inspiration.

ACKNOWLEDGEMENTS

I would like to express my deepest gratitude to all the people who have made this PhD possible. I would particularly like to thank my advisors Dr. Mario Binelli and Dr. Jo Leroy. I was fortunate to train under two great scientists and I will be forever indebted to both of you for the critical sense, personal and professional skills I have developed under your supervision.

To my mentor, Dr. Mario Binelli, who gave the knowledge and tools to pursuit the highest academic degree, thank you for your continued support and guidance. It has been an honor learning from your scientific philosophy. Thank you for the opportunity to work with a great and respected team. Dear Mario, thank you for teaching me that we should not be afraid of embracing new challenges. Your integrity and resilience deeply inspire me.

To my step mentor, Dr. Jo Leroy, thank you for receiving me in your wonderful research group, and for all the time, knowledge and belief that you invested me. Thank you for having taught many aspects about mentorship under your navigation. Dear Jo, thank you for all the self-reflections. Your efficiency managing your time and the way you care about your PhD-students beyond their academic lives are remarkable and inspiring.

.

I am grateful to the graduate programs of the University of São Paulo and University of Antwerp for providing me all the conditions to conduct my research. It has been an honor to be part of two Universities of excellence. I would also like to extend my gratitude to the Department of Animal Sciences, University of Florida, for receiving me in the last months of my PhD. Being among a diverse scientific community represents a unique and enriching opportunity in my short scientific career and I will always be grateful for that.

I would like to thank all the people from the international offices, represented by Isabela Furegatti at the University of São Paulo, and Simone Kramer at the University of Antwerp, that made the double-PhD possible and for their endless support with the bureaucratic parts of the process.

I would also like to thank all the professors, staff and colleagues from the Department of Animal Reproduction, University of São Paulo, and from the Department of Veterinary Sciences, University of Antwerp.

I was very fortunate to have had the opportunity to work with two great research teams along this journey. I want to thanks all my LFEM-mattes: Estela, Milena, Mae, Saara, Moana, Everton, Roney, Rafaela, Bia, Angela, Cecilia, Veerle, Guilherme and Emiliana. Each and every one of you has a space in my memories and in my heart. Thank you for all the good moments and for your friendship.

To my GRC-mattes, Waleed, Jessie, Anouk, Lies, Karolien, Anniek, Chiara and Lotte, thank you all for welcoming me and for making my stay in Belgium lighter and funnier. To Dr. Peter Bols, thank you for your hospitality during my stay at the Gamete Research Centre. It was a pleasure to meet you and to listen to your many stories about Brazil. Els and Silke, thank you very much for your

outstanding technical assistance in performing the *in vitro* experiments. You are the best! Britt, thank you for all your help with the paperwork to keep me legal in Belgium. You all together made my research stay incredibly memorable.

To my LFEM/Florida-mattes, Gabriela and Felipe, thank you for bringing lightness to our routine.

I would also like to acknowledge all the LMMD colleagues for always being supportive and for sharing their facilities and equipment with us.

A special thank you to my guinea pigs Nathália and Jens. I hope you both learned as much as I did during our time working together in the lab.

.

This study was financed in part by the Coordenação de Aperfeiçoamento de Pessoal de Nível Superior - Brasil (CAPES) - Finance Code 001 (PDSE program; 88881.132730/2016-01). I am grateful to CNPq and the Special Research Fund of the University of Antwerp for the scholarships granted during my PhD.

.

To the jury members, Drs. Felipe Perecin, Marcella Pecora Milazzotto, and Mayra Elena Ortiz D' Avila Assumpção, thank you for your time, critical reading, advice and suggestions to improve the quality of this thesis.

.

To my family, who supported me through the process. Specially, to my wonderful parents, Benhur and Rosi, who have all my admiration. Thank you for having taught me that I have to do my best always. Thank you for allowing me to fly and pursuit my dreams, even though for many times I was absent. Thank you for the example, support and encouragement.

To my sister, Julhana, and my brother, Mateus, thank you for filling my life with love and joy. I am very proud of what you both became. I consider myself the luckiest one in the world for having both of you by my side. Thank you for being there when I was missing.

To my brother-in-law Nelson, and my sister-in-law July, for completing our family.

To my family-in-law, specially D. Norma, who has taught me many lessons about life. You are an inspiring human being. Thank you for taking care of Nina better than I would do.

.

To my friends, both near and far, for the good moments, for keeping me sane and grounded.

To my beloved Belgian family, Julie, Shanty and Billy. You were there!

.

Finally, I thank my husband Thiago for his ever-sustaining support, encouragement and love. You are my balance and my ground. You are an example of human being in any aspect and it has been a privilege to share my life with you.

.

I extend my sincere gratitude to all the animals that were part of the experiments during these years.

“pensava que quando se sonha tão grande a realidade aprende”

–Valter Hugo Mãe, O Filho de Mil Homens

RESUMO

SPONCHIADO, M. **Decifrando o interactoma materno-embrionário:** Programação do funcionamento do endométrio dependente do embrião durante a gestação inicial em bovinos. 224 p. Tese (Doutorado em Ciências e Ciências Veterinárias) – Faculdade de Medicina Veterinária e Zootecnia, Universidade de São Paulo, São Paulo, e Faculdade de Ciências Farmacêuticas, Biomédicas e Veterinárias, Universidade da Antuérpia, Antuérpia, 2019.

O sucesso gestacional depende do programa embrionário intrínseco, operando em conjunto com fatores extrínsecos que emanam do trato reprodutivo materno, bem como de uma coordenada interação entre as unidades materna e embrionária. Atualmente, o conhecimento sobre a programação do funcionamento do endométrio dependente do embrião pré-elongado é limitado. A hipótese central desta tese é que embriões bovinos são capazes de modular a função endometrial no dia 7 após o estro. No primeiro estudo, regiões espacialmente definidas do transcriptoma endometrial foram interrogadas quanto a respostas a um embrião no dia 7 *in vivo*. Amostras de endométrio foram coletadas da junção útero-tubárica, região anterior, medial e posterior do corno uterino ipsilateral ao corpo lúteo 7 dias após o estro de vacas Nelore artificialmente inseminadas e confirmadas gestantes, ou de vacas em que a inseminação foi mimetizada. A abundância de 12 dos 87 transcritos analisados foi modulada no endométrio de animais gestantes, incluindo genes estimulados por interferon (ISGs) e genes associados à biossíntese de eicosanoides. As alterações foram predominantemente nas porções mais craniais do corno uterino, onde o embrião estava localizado. Além disso, a abundância de 71 transcritos variou de acordo com a região do trato reprodutivo, independentemente da presença do embrião. Quantificação baseada em espectrometria de massa de 205 metabólitos no fluido luminal uterino (ULF) recuperado da porção mais cranial do corno uterino ipsilateral mostrou que a exposição ao embrião altera a composição do ULF no dia 7 *in vivo*. Modulações induzidas pelo embrião incluem aumento nas concentrações de metabólitos derivados da via das lipoxigenases e diminuição nas concentrações de aminoácidos, aminas biogênicas, acilcarnitinas e fosfolipídios. Alterações na composição do ULF podem ser devido à secreção ou depleção de moléculas específicas, executadas pelo embrião ou pelo endométrio, mas iniciadas por sinais provenientes do embrião. No segundo estudo, um modelo *in vitro* foi usado para estudar as alterações induzidas por embriões no transcriptoma de células epiteliais endometriais bovinas (BEEC) e investigar modos de comunicação molecular entre tecidos. Mórulas produzidas *in vitro* foram co-cultivadas em justaposição ou sem contato direto com BEECs. Grupos de BEECs ou embriões sozinhos

foram cultivados como controles. Independentemente da justaposição à monocamada, o co-cultivo com BEECs melhorou as taxas de blastocistos no dia 7,5. A proximidade física entre embriões e a monocamada de células, no entanto, alterou a natureza e a intensidade das alterações induzidas pelos embriões no transcriptoma das células endometriais. Embriões justapostos modularam a transcrição de 1.797 versus 230 genes em BEECs não contactando diretamente os embriões, quando comparadas às células cultivadas na ausência de embriões. Vias moduladas pela presença de embriões incluíram resposta imune mediada por interferon, regulação do ciclo celular e apoptose, sinalização via prolactina e biossíntese de prostanoides. Coletivamente, a partir dos resultados obtidos nesta tese, concluímos que embriões bovinos pré-elongamento são capazes de modular a função endometrial. A presente tese fornece vias candidatas que parecem ser importantes para o condicionamento do ambiente uterino para o desenvolvimento do concepto. A sinalização embrionária precoce pode ser necessária para garantir o desenvolvimento ideal e o estabelecimento da gestação em bovinos.

Palavras-chave: Útero. Sinalização materno-embrionária. Mórulas. Blastocisto.

OVERZICHT

SPONCHIADO, M. **Ontcijferen van de embryo-maternale interactoom:** Embryo-afhankelijke programmering van endometriale werking gedurende de vroege dracht bij runderen. 224 p. Tese (Doutorado em Ciências) – Faculdade de Medicina Veterinária e Zootecnia, Universidade de São Paulo, São Paulo, e Faculdade de Ciências Farmacêuticas, Biomédicas e Veterinárias, Universidade da Antuérpia, Antuérpia, 2019.

Een succesvolle dracht is afhankelijk van de intrinsieke embryonale programmering en collaboreert met de extrinsieke signalen die het maternale voortplantingsstelsel afgeeft, alsook door een gecoördineerde interactie tussen de embryonale en de moedereenheden. Actuele kennis is beperkt van de pre verlengende embryonaal afhankelijke programmering van de endomitriale werking in runderen. De algemene hypothese is dat embryo's van runderen vanaf ten vroegste dag 7 na de bronst de endomitriale werking kunnen regelen. In de eerste studie werden ruimtelijk gedefinieerde regio's van het endometrium transcriptoom geobserveerd voor responsen op een dag 7 embryo *in vivo*. Endomitriale stalen werden verzameld van de uterotubale aansluiting, de anterieure, mediale en posterieure regio's van de baarmoederlijke hoorn, ipsilateraal tegenover de corpus luteum 7 dagen na de brons van schijn geïnsemineerde of kunstmatige geïnsemineerde, bevestigd zwangere Nelore koeien. Een aanzienlijke 12 van de 87 geanalyseerde transcripten waren gemoduleerd in het bevruchte endometrium, inclusief klassieke interferon-opgewekte genen en transcripten die geassocieerd worden met eicosanoide biosynthese. De voornaamste veranderingen vonden plaats in de craniale portie van de baarmoederlijke hoorn, waar de embryo's gelegen zijn. Bovendien varieerde het merendeel van de 71 transcripten in overeenstemming met de regio van het voortplantingsgestel, onafhankelijk van de drachtstatus. Gerichte massa spectrometrie-gebaseerde kwantificatie van 205 metabolieten in het baarmoederlijk luminaal vocht, gerecupereerd van het meest craniale deel van de ipsilaterale baarmoederlijke hoorn, toonde aan dat blootstelling aan een dag-7 embryo de baarmoederlijk luminaal vocht (ULF) composiet *in vivo* verandert. Embryonaal opgewekte modulatie zorgde voor een stijging van de concentraties van lipoxygenase-afgeleide metabolieten en een daling van de concentratie van aminozuren, biogenische amines, acylcarnitienen en phospholipieden. De veranderde samenstelling van de ULF kan afhankelijk zijn van afscheiding of afname van specifieke moleculen, veroorzaakt door ofwel de embryo of het endometrium, maar geïnitieerd door de signalen die het embryo uitstuurt. Voor de tweede studie werd een *in vitro* model gebruikt om

de embryonaal opgewekte veranderingen in runder-endomitriale epitheliale cellen (BEECs) transcriptoom door te lichten en te onderzoeken op welke manieren de tussenweefsel moleculaire communicatie gebeurt. *In vitro*-geproduceerde morulae werden samen gekweekt in juxtapositie of zonder direct contact met een BEEC-monolaag. Extra groepen BEECs of enkelvoudige embryo's warden gekweekt als controle. Onafhankelijk van de juxtapositie tegenover de cellulaire monolaag, verbeterde co-cultuur met BEECs blastocysten ratio's op dag 7.5. Echter, de fysieke nabijheid tussen de embryo's en de BEEC-monolaag wijzigde de natuur en de intensiteit van de embryonaal opgewekte veranderingen op het BEEC transcriptoom. Embryo's juxtapositioneerden gemoduleerde transcriptie van 1,797 versus 230 genen in BEECs zonder direct contact, in relatie tot cellen die zonder nabijheid van embryo's geweekt werden. Trajecten die gemoduleerd waren door de nabijheid van embryo's bevatten interferon-gemedieerde immuunreacties, celcyclus regulatie en apoptose, prolactine signalisatie en prostanoide biosynthese. Uiteindelijk, op basis van de behaalde resultaten gedurende deze thesis, concluderen wij dat peri-ontwikkelde runderembryo's de endomitriale functie moduleren. Op basis hiervan voorzien wij kandidaat systemen die belangrijk kunnen zijn om de baarmoederlijke omgeving te conditioneren voor conceptus ontwikkeling. Vroege embryonale signalisatie kan nodig zijn om optimale ontwikkeling en de succesvolle aantoning van dracht in runderen te garanderen.

Zoekwoorden: Baarmoeder. Embryo-maternale signalisatie. Morula. Blastocyste.

ABSTRACT

SPONCHIADO, M. **Deciphering the embryo-maternal interactome:** Embryo-dependent programming of endometrial function during early pregnancy in cattle. 224 p. Tese (Doutorado em Ciências e Ciências Veterinárias) – Faculdade de Medicina Veterinária e Zootecnia, Universidade de São Paulo, São Paulo, e Faculdade de Ciências Farmacêuticas, Biomédicas e Veterinárias, Universidade da Antuérpia, Antuérpia, 2019.

A successful pregnancy is dependent on the intrinsic embryonic program, operating in conjunction with extrinsic signals emanating from the maternal reproductive tract, as well as on a coordinated interaction between the embryonic and the maternal units. Current knowledge about the pre-elongation embryo-dependent programming of endometrial function in cattle is limited. Central hypothesis is that bovine embryos are able to modulate the endometrial function as early as day 7 after estrus. In the first study, spatially defined regions of the endometrium transcriptome were interrogated for responses to a day 7 embryo *in vivo*. Endometrial samples were collected from the uterotubal junction, anterior, medial and posterior regions of the uterine horn ipsilateral to the corpus luteum 7 days after estrus from sham-inseminated or artificially inseminated, confirmed pregnant Nellore cows. Abundance of 12 out of 87 transcripts analyzed was modulated in the pregnant endometrium, including classic interferon-induced genes and transcripts associated to eicosanoid biosynthesis. Changes were predominantly in the most cranial portion of the uterine horn, where the embryos were located. In addition, abundance of 71 transcripts varied according to region of the reproductive tract, irrespective to the pregnancy status. Targeted mass spectrometry-based quantification of 205 metabolites in the uterine luminal fluid (ULF) recovered from the most cranial portion of the ipsilateral uterine horn showed that exposure to a day-7 embryo changes ULF composition *in vivo*. Embryo-induced modulation included an increase in concentrations of lipoxygenase-derived metabolites and a decrease in concentrations of amino acids, biogenic amines, acylcarnitines and phospholipids. The changed composition of the ULF could be due to secretion or depletion of specific molecules, executed by either the embryo or the endometrium, but initiated by signals coming from the embryo. In the second study, an *in vitro* model was used to probe embryo-induced changes on bovine endometrial epithelial cells (BEECs) transcriptome and investigate modes of inter-tissues molecular communication. *In vitro*-produced morulae were co-cultured in juxtaposition or without a direct contact with a BEEC monolayer. Extra groups of BEECs or embryos alone were cultured as controls.

Irrespective of juxtaposition to the cell monolayer, co-culture with BEECs improved blastocyst rates on day 7.5. Physical proximity between embryos and the BEEC monolayer, nevertheless, did alter nature and intensity of embryo-induced changes on BEEC transcriptome. Embryos juxtapositioned modulated transcription of 1,797 versus 230 genes in BEECs not contacting embryos directly, in relation to cells cultured in the absence of embryos. Pathways modulated by presence of embryos included interferon-mediated immune responses, cell cycle regulation and apoptosis, prolactin signaling, and prostanoid biosynthesis. Overall, from the results obtained in the course of this thesis, we conclude that peri-hatching bovine embryos modulate the endometrial function. Herein, we provide candidate systems that might be important for conditioning the uterine environment for conceptus development. Early embryonic signaling might be necessary to guarantee optimal development and successful establishment of pregnancy in cattle.

Keywords: Uterus. Embryo-maternal signaling. Morula. Blastocyst.

TABLE OF CONTENTS

CHAPTER 1

GENERAL INTRODUCTION

1 GENERAL INTRODUCTION

Reproductive efficiency is a major factor impacting the profitability of livestock systems. Subfertility often manifests as early embryonic death. This is especially true in cattle. Indeed, up to 40% of all pregnancies are terminated before maternal recognition of pregnancy, which occurs around day 16 post-estrus (Diskin *et al*., 2011), indicating that early embryonic mortality is a major cause of reproductive inefficiency in the bovine species. One major reason for this is the disturbance of the embryo-maternal dialogue. Fundamentally, a successful pregnancy requires a balance between a properly programmed embryo and a receptive endometrium. Although both mother and embryo contribute to the establishment of pregnancy, in the present thesis the role of the maternal unit will be the main subject, with emphasis on the endometrium.

The overall hypothesis of this Thesis is that bovine embryos are able to modulate the endometrial function as early as day 7 after conception. The existence of a complex embryo-maternal interactome between a pre-elongation embryo and the endometrium provides the theoretical basis for the present thesis. The concept of embryo-maternal interactome comprises molecular processes by which the embryo may affect the mother and vice versa. **The central objective of this Thesis was to characterize/gain insights into the embryo-induced changes on the endometrial function during early gestation in cattle**. In this Introduction, aspects of early gestation in cattle will be discussed, with a focus on individual and mutual contributions of the embryonic and the maternal units to the establishment of a successful pregnancy. Further, evidences from other studies in literature of an early cross-talk between the embryo and the maternal reproductive tract that supported our central hypothesis will be provided. Last, we will discuss the microenvironment that surrounds the embryo *in vivo* and the possible modes of inter-tissues molecular communication. The studies that were conducted to test the central and specific hypotheses of this Thesis are presented in three Chapters, each organized as a scientific manuscript. The final pages of this PhD Thesis have been reserved for a General Discussion, which summarizes the main findings presented in the previous chapters, and provides directions for future research.

1.1 THE ENDOMETRIUM, THE EMBRYO, AND THEIR INTERACTOME: A SYSTEM OF ADDITIVE COMPLEXITY

The embryo starts to interact directly with the endometrium around days 4-5 after insemination/breeding, when the zona-enclosed morula enters the lumen of the uterine horn ipsilateral to the ovary containing the corpus luteum (CL; Bazer *et al.*, 1991). From then onwards, the embryo *in utero* undergoes rapid and dynamic morphological changes including blastulation, hatching from the zona pellucida, elongation, apposition and attachment to the uterine epithelium, around day 20 after insemination/breeding, leading to initial formation of the placenta. An overview of the main events taking place in the uterus during the pre-implantation period in the cow is provided in Figure 1. From its arrival in the uterus, the embryo grows from approximately 200 µm in diameter to several centimeters in length by day 16 of pregnancy. At that time, the elongated conceptus (embryo and associated membranes) becomes able to abrogate the endometrium-driven, pre-programed release of pulses of PGF_{2a} that cause luteolysis. Once maternal recognition of pregnancy has occurred, the uterus stays under the long-term influence of luteal progesterone and pregnancy is maintained.

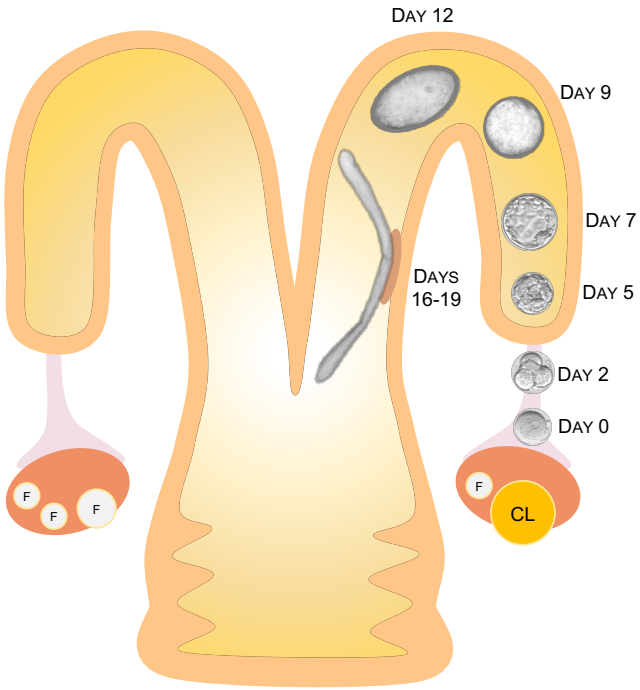

Figure 1. Overview of embryo/conceptus development in relation to position in the female reproductive tract during early pregnancy in cattle. Following ovulation, fertilization of the bovine oocyte takes place in the oviduct. The resulting zygote moves towards the utero-tubal junction as it undergoes the first cellular divisions. The zona pellucida-enclosed morula enters the uterus on days 4-5 after estrus and is only about 120-200 µm in diameter. The blastocyst is formed by day 7, and consists of an inner cell mass which forms the embryo/fetus, and a blastocoele surrounded by a monolayer of trophectoderm, which gives rise to the extraembryonic membranes. The hatched-blastocyst (day 9) grows and changes in morphology from a spherical to an ovoid shape (day 12). By day 14, the 6 mm conceptus (embryo and extraembryonic membranes) elongates to a filamentous form, and reaches a length of several cm by day 19. The elongation process marks the beginning of an anatomical union between the embryonic and maternal units, which involves apposition (day 16), transient attachment (day 17-18) and adhesion (day 19-21) of the trophectoderm cells to the lining endometrium (Guillomot, 1995). F Follicles, CL Corpus luteum.

The bovine embryo that develops successfully utilizes a set of mechanisms that depend on its intrinsic capacity to develop, as well as on external cues originating from the surrounding tissues.

On the **embryonic side**, it is well conceived that a successful embryo maintains basic tools for its own development. Decades of *in vitro* embryo production have taught us that embryos of a variety of species can thrive successfully beyond the blastocyst stage in culture, independently of exposure to the maternal reproductive tract. Moreover, the fact that a relatively simple culture medium composition allows embryo survival leads to the idea that the uterus might provide not more than a permissive milieu for the early developing embryo. However, it is clear that the maternal reproductive tract, including the uterus, exerts considerable control over the ability of a conceptus to develop. For example, several studies have demonstrated that *in vivo* cultured embryos are of superior quality compared to their *in vitro*-produced counterparts in many aspects, including quality and developmental competence (Rizos *et al*., 2002a), morphology (Van Soom & De Kruif, 1992), incidence of chromosome abnormalities (Viuff *et al*., 1999), relative transcript abundance (Rizos *et al*., 2002b; Lonergan *et al*., 2003), and cryotolerance (Fair *et al*., 2001). Additionally, exposure to uterus-derived factors seems to be a prerequisite for conceptus elongation post-hatching in domestic ruminants. This is based on the fact that elongation does not occur in the absence of uterine glands (Gray *et al*., 2000) and that attempts to artificially induce elongation of bovine conceptuses *in vitro* have been unsuccessful (Brandao *et al*., 2004).

The uterine lumen contains a unique milieu that has embryotrophic properties. Endocrine factors that regulate the maternal reproductive tract function have been investigated extensively. In this respect, it is known that the **ovarian sex-steroids** (i.e. estradiol and progesterone) exert temporal and spatial control over many uterine functions that support embryonic development. For example, progesterone produced by the CL, acts on its cognate receptors in the endometrial tissue in a classical endocrine fashion, regulating endometrial secretions essential for stimulating and mediating changes in conceptus growth and differentiation throughout early pregnancy (Carter *et al*., 2008; Clemente *et al*., 2009; Forde *et al*., 2009; Forde *et al*., 2010; Forde *et al*., 2011a; Mesquita *et al*., 2015). Aspects of the spatial-programming of endometrial function exerted by ovarian steroids and systemic factors are discussed in **Chapter 2 of the present thesis**, entitled “Pre-hatching embryo-dependent and -independent programming of endometrial function in cattle".

In addition to the endocrine, sex-steroidal control of endometrial function, we hypothesize that the developing embryo/conceptus *in uterus* provides local signals that

program the endometrium towards a more receptive status. Although specific factors orchestrating the embryo-maternal interactome are currently unknown, it is reasonable to conceive that the embryonic contribution to the embryo-maternal interactome would primarily depend upon the intrinsic competence of the embryo to develop, and on its capacity of synthesis and secretion of signaling molecules. In this scenario, the endometrial contribution would rely on an appropriate exposure of the maternal genital tract to sex steroids to ensure endometrial receptivity to the developing embryo and responsiveness to the embryo-derived signals.

1.2 EMBRYO-MATERNAL COMMUNICATION IN CATTLE PRIOR TO ELONGATION: IS THE ENDOMETRIUM THE SOLE SPEAKER?

While the influence of the uterine milieu on proper embryo development and pregnancy establishment is well accepted, the embryonic contribution in modulating the endometrium has not been investigated to the same extent. Holistic analysis comparing the bovine endometrium transcriptome of pregnant versus cyclic animals was first reported by Klein *et al*. (2006). In this study, endometrial tissues collected on day 18 of pregnancy from monozygotic twin heifers that were sham-transferred or had a confirmed pregnancy were compared by using a combination of subtraction cDNA libraries and cDNA array hybridization. A number of 87 genes were identified as upregulated in pregnant animals. Authors stated that almost one half of the genes that were upregulated in pregnant animals are known to be stimulated by type I interferons. Subsequently, a number of studies reported that embryos of different developmental fates elicited different responses from the endometrial transcriptome on day 18 of pregnancy (Bauersachs *et al*., 2009; Mansouri-Attia *et al*., 2009). Forde *et al.* (2011b) conducted a critical study comparing the endometrial transcriptome between cyclic and inseminated (pregnant) heifers on days 5, 7, 13 or 16 of pregnancy/estrous cycle. A clear separation between cyclic and pregnant endometrial transcriptome profiles was only detectable on day 16, coinciding with the window of maternal pregnancy recognition. In agreement with previous reports later in pregnancy, Forde and coauthors (2011) found that the abundance of transcripts increased to the greatest extent in pregnant endometria were associated with type I interferon-signaling. Taken together, these studies supported the idea that embryo-mediated modulation of endometrial function would occur after conceptus elongation in cattle. Earlier communication between embryo and endometrium seems not to be present.

In vitro studies, however, indicate that the pre-elongation bovine embryo is active in releasing a range of signaling factors into the culture medium (reviewed by Wydooghe *et al*., 2011). These molecules, referred as to embryotropins, are secreted in several ways including passive outflow, regulated or constitutive active secretion, bound to a carrier molecule or transport within extracellular vesicles (Wydooghe *et al*., 2017). Embryotropins have the potential to act upon the embryo itself in an autocrine way, or on maternal tissues, in juxtacrine, paracrine or endocrine fashion. It is reasonable, nonetheless, to assume that the capacity of synthesis and secretion of signals by the pre-elongation embryo is limited to its size or cellular machinery of roughly 200 cells. In this regard, the lack of differences on the endometrial transcriptome triggered by the pre-elongation embryo might be attributed to its disproportional small size and limited capacity of secretion of factors in the context of the uterine horn, that is several centimeters in length. Thus, the pre-elongation embryo is hypothesized to evoke local effects, confined to the surrounding tissues.

In the past few years a number of studies have shown that pre-hatching bovine embryos are able to induce transcriptional changes in the oviduct *in vivo* (Almiñana *et al*., 2014; Maillo *et al*., 2015) and *in vitro* (García *et al*., 2017). In the study of Maillo *et al*. (2015), the authors failed to detect an effect of a single 8-cell embryo on the transcriptome of the oviduct; conversely, when 50 embryos were laparoscopically transferred per heifer, in an attempt to amplify and detect putative local oviductal responses to embryos, significant transcriptome changes were detected. Therefore, the authors attributed the failure to detect changes in the oviductal transcriptome in the presence of a single embryo to the fact that any effects of the embryo on the oviduct would be spatially restricted and would not be detected due to the miniscule "embryo to oviduct tissue ratio". Furthermore, the migratory feature of the embryo inside the oviduct could lead to a transitory change on the local oviductal transcriptome. The emerging indication of a local effect elicited by the embryo from its vicinities drove the first hypothesis of the present thesis. **We hypothesized that exposure to an embryo changes the abundance of specific transcripts in the endometrial regions in closest proximity to the embryo in the pregnant uterine horn.** Therefore, in our first study, we interrogated spatially defined regions of the ipsilateral uterine horn for responses to a day 7 embryo *in vivo*. We demonstrated for the first time that a day 7 embryo modulates interferon signaling and eicosanoid biosynthesis pathways in the endometrium, at the transcriptional level, and that most changes were found in the most cranial portions (i.e. uterotubal-junction and anterior third) of the ipsilateral uterine horn, where the embryos were

located (Sponchiado *et al*., 2017). This *in vivo* study was conducted at the University of São Paulo, Pirassununga, São Paulo – Brazil, and composes the **Chapter 2 of this Thesis**.

A remaining open question was whether the embryo-induced changes in the endometrial transcriptome *in vivo* lead to changes in the uterine luminal fluid (ULF) composition. The ULF is the ultimate link between the pre-implantation embryo and the uterus. Thus, the second study was centered in the **hypothesis that the embryo modulates the biochemical composition of the ULF in the most cranial portion of the uterine horn ipsilateral to the CL.** Using a mass spectrometry-based quantification of over 200 compounds, we demonstrated that the pre-hatching embryo changes uterine luminal metabolite composition *in vivo*. These results are compiled and discussed in **Chapter 3 of this Thesis**, entitled "The pre-hatching bovine embryo transforms the uterine luminal metabolite composition *in vivo*", that has been submitted for publication in Nature Scientific Reports journal.

How does the embryo communicate with the surrounding tissues; what are the molecules involved in this process; and whether the embryo would benefit from the local cross-talk with the endometrium during its journey throughout the uterine lumen are examples of the many unanswered questions that remain in this topic. To understand how the embryo interacts with the underlying endometrium, we first needed to probe the microenvironment that surrounds it in the uterine lumen *in vivo*.

1.3 THE EMBRYO-MATERNAL INTERACTOME IN A UNIQUE INTERFACE

When one thinks about the context of the preimplantation embryo *in uterus,* the image that comes will likely show the pre-hatching embryo bathing in maternal secretions. However, this does not represent the *in vivo* situation. Ultrasound images in the horse, for example, show that a day-12 blastocyst is tightly surrounded by the maternal endometrium (Herrler *et al*., 2003). The fact is that the embryo-maternal interface during early pregnancy is poorly known for most mammalian species, including cattle.

The embryo-endometrial interactome comprises dynamic molecular processes elicited by the embryo on the endometrium and vice-versa. Signaling molecules are understood to play an important role in the cross-talk between the maternal and the embryonic units. The concept of communication implies in a **cellular origin of the signaling agent**, a **cellular target that is able to decode the message,** and ultimately a **response triggered by the primary signal or associated messengers**.

Regarding signaling agents, they are molecules that play a functional role in the early embryo-maternal communication in cattle, given that there is no anatomical adhesion between the non-invasive embryo and the underlying endometrium until day 20 of pregnancy. Signaling factors involved in the embryo-maternal dialogue are secreted by the embryo to act on the maternal tissue, and vice-versa, in four putative mechanisms. Fundamentally, a signaling factor can activate receptors on the cell of its origin in a so-called **autocrine** stimulation, or it can be released into the extra-cellular milieu, spreading through the surrounding tissue in a **paracrine** fashion, or it can be secreted in the blood stream and reach the target cell or tissue in an **endocrine** mode. Additionally, effector cells may communicate with adjacent recipient cells in a **juxtacrine** fashion. Figure 2 illustrates the mechanism by which embryo-derived molecules could participate in the embryo-maternal dialogue. One classical example of paracrine and endocrine signaling triggered by the bovine embryo towards the mother is Interferon-tau (IFNτ). The conceptus-derived IFNτ is released into the uterine lumen and exerts paracrine antiluteolytic effects on the endometrium inhibiting the upregulation of oxytocin receptors in the endometrial epithelia, thereby preventing the production of luteolytic prostaglandin F2 alpha ($PGF_{2\alpha}$) pulses. Also, IFNτ upregulates a large number of classical interferon-stimulated genes (ISGs) and regulates expression of many other genes in a cell-specific manner in the endometrium that are likely important for conceptus elongation, implantation and establishment of pregnancy. Further, IFNT has endocrine effects on extrauterine cells and tissues, such as the CL, and blood cells (reviewed by Hansen *et al*. 2017).

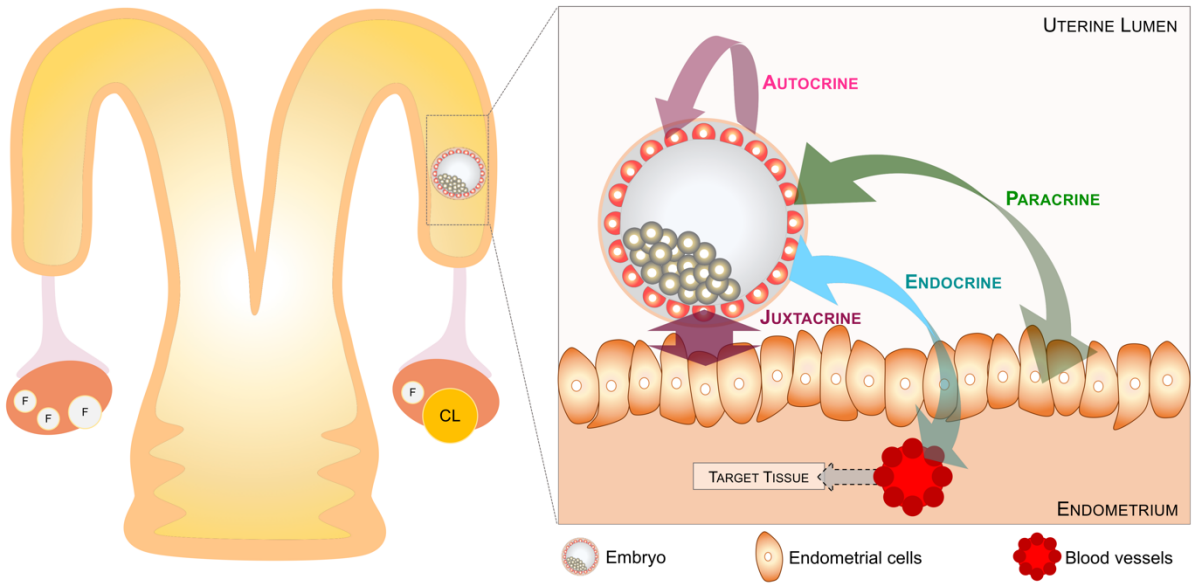

Figure 2. Schematic illustration of putative mechanisms by which embryo-derived signaling molecules would act in the maternal reproductive tract.

Effects of the embryo on the directly adjacent endometrial cells are poorly defined. In the **third study of this Thesis** we addressed the question of whether the endometrial responses differ between the juxtacrine and the non-juxtacrine fashion. **We hypothesized that embryo-induced changes on endometrial transcriptome depend on physical proximity between the embryos and the endometrium.** Therefore, we used an *in vitro* co-culture system of bovine endometrial epithelial cells (BEEC) and morula-to-blastocyst embryos to interrogate the embryo-maternal interface for embryo-induced changes on the endometrial epithelial cells transcriptome. This study was carried out at the Gamete Research Centre, University of Antwerp – Belgium, and composes the **Chapter 4** of this thesis, entitled "The bovine embryo-endometrium interactome deciphered *in vitro*".

1.4 REFERENCES

Almiñana, C. *et al*. The battle of the sexes starts in the oviduct: modulation of oviductal transcriptome by X and Y-bearing spermatozoa. **BMC genomics,** v. 15, n. 1, p. 293, 2014.

Bauersachs, S. *et al*. The endometrium responds differently to cloned versus fertilized embryos. **Proceedings of the National Academy of Sciences,** v. 106, n. 14, p. 5681-5686, 2009.

Bazer, F. W. *et al*. Physiological mechanisms of pregnancy recognition in ruminants. **Journal of reproduction and fertility.** Supplement, v. 43, p. 39-47, 1991.

Brandao, D. O. *et al*. Post hatching development: a novel system for extended *in vitro* culture of bovine embryos. **Biology of Reproduction,** v. 71, n. 6, p. 2048-2055, 2004.

Carter, F. *et al*. Effect of increasing progesterone concentration from Day 3 of pregnancy on subsequent embryo survival and development in beef heifers. **Reproduction, Fertility and Development,** v. 20, n. 3, p. 368-375, 2008.

Clemente, M. *et al*. Progesterone and conceptus elongation in cattle: a direct effect on the embryo or an indirect effect via the endometrium? **Reproduction,** v. 138, n. 3, p. 507-517, 2009.

Diskin, M. G.; Parr, M. H.; Morris, D. G. Embryo death in cattle: an update. **Reproduction, Fertility and Development,** v. 24, n. 1, p. 244-251, 2011.

Fair, T. *et al*. Ultrastructure of bovine blastocysts following cryopreservation: effect of method of blastocyst production. **Molecular reproduction and development,** v. 58, n. 2, p. 186-195, 2001.

Forde, N. *et al*. Progesterone-regulated changes in endometrial gene expression contribute to advanced conceptus development in cattle. **Biology of Reproduction,** v. 81, n. 4, p. 784-794, 2009.

Forde, N. *et al*. Effect of pregnancy and progesterone concentration on expression of genes encoding for transporters or secreted proteins in the bovine endometrium. **Physiological genomics,** v. 41, n. 1, p. 53-62, 2010.

Forde, N. *et al*. Changes in the endometrial transcriptome during the bovine estrous cycle: effect of low circulating progesterone and consequences for conceptus elongation. **Biology of reproduction,** v. 84, n. 2, p. 266-278, 2011a.

Forde, N. *et al*. Conceptus-induced changes in the endometrial transcriptome: how soon does the cow know she is pregnant? **Biology of Reproduction,** v. 85, n. 1, p. 144-156, 2011b.

Forde, N. *et al*. Effect of lactation on conceptus-maternal interactions at the initiation of implantation in cattle: I. Effects on the conceptus transcriptome and amino acid composition of the uterine luminal fluid. **Biology of Reproduction,** v. 97, n. 6, p. 798-809, 2017.

García, E. V. *et al*. Bovine embryo-oviduct interaction *in vitro* reveals an early cross talk mediated by BMP signaling. **Reproduction,** v. 153, n. 5, p. 631-643, 2017.

Gray, C. A. *et al*. Ovine uterine gland knock-out model: effects of gland ablation on the estrous cycle. **Biology of reproduction,** v. 62, n. 2, p. 448-456, 2000.

Guillomot, M. Cellular interactions during implantation in domestic ruminants. **Journal of reproduction and fertility.** Supplement, v. 49, p. 39-51, 1995.

Hansen, T. R.; Sinedino, L. D. P.; Spencer, T. E. Paracrine and endocrine actions of interferon tau (IFNT). **Reproduction,** v. 154, n. 5, p. F45-F59, 2017.

Herrler, A.; Von Rango, U.; Beier, H. M. Embryo-maternal signalling: how the embryo starts talking to its mother to accomplish implantation. **Reproductive biomedicine online,** v. 6, n. 2, p. 244-256, 2003.

Klein, C. *et al*. Monozygotic twin model reveals novel embryo-induced transcriptome changes of bovine endometrium in the preattachment period. **Biology of Reproduction,** v. 74, n. 2, p. 253-264, 2006.

Lonergan, P. *et al*. Temporal divergence in the pattern of messenger RNA expression in bovine embryos cultured from the zygote to blastocyst stage *in vitro* or *in vivo*. **Biology of Reproduction,** v. 69, n. 4, p. 1424-1431, 2003.

Maillo, V. *et al*. Oviduct-Embryo Interactions in Cattle: Two-Way Traffic or a One-Way Street?. **Biology of Reproduction,** v. 92, n. 6, p. 144-152, 2015.

Mansouri-Attia, N. *et al*. Endometrium as an early sensor of *in vitro* embryo manipulation technologies. **Proceedings of the National Academy of Sciences,** v. 106, n. 14, p. 5687-5692, 2009.

Mesquita, F. S. *et al*. The receptive endometrial transcriptomic signature indicates an earlier shift from proliferation to metabolism at early diestrus in the cow. **Biology of reproduction**, v. 93, n. 2, p. 52-64, 2015.

Rizos, D. *et al*. Consequences of bovine oocyte maturation, fertilization or early embryo development *in vitro* versus *in vivo*: implications for blastocyst yield and blastocyst quality. **Molecular reproduction and development,** v. 61, n. 2, p. 234-248, 2002a.

Rizos, D. *et al*. Analysis of differential messenger RNA expression between bovine blastocysts produced in different culture systems: implications for blastocyst quality. **Biology of reproduction,** v. 66, n. 3, p. 589-595, 2002b.

Sponchiado, M. *et al*. Pre-hatching embryo-dependent and-independent programming of endometrial function in cattle. **PloS one,** v. 12, n. 4, p. e0175954, 2017.

Van Soom, A.; De Kruif, A. A comparative study of *in vivo* and *in vitro* derived bovine embryos. In: Proceedings of the International Congress on Animal Reproduction and Artificial Insemination, v. 3, p. 1365-1367, 1992.

Viuff, D. *et al*. A high proportion of bovine blastocysts produced *in vitro* are mixoploid. **Biology of reproduction,** v. 60, n. 6, p. 1273-1278, 1999.

Wydooghe, E. *et al*. Differential apoptotic staining of mammalian blastocysts based on double immunofluorescent CDX2 and active caspase-3 staining. **Analytical biochemistry,** v. 416, n. 2, p. 228-230, 2011.

Wydooghe, E. *et al*. Autocrine embryotropins revisited: how do embryos communicate with each other *in vitro* when cultured in groups? **Biological Reviews,** v. 92, n. 1, p. 505-520, 2017.

CHAPTER 2

PRE-HATCHING EMBRYO-DEPENDENT AND -INDEPENDENT PROGRAMMING OF ENDOMETRIAL FUNCTION IN CATTLE

M. Sponchiado[1], N. S. Gomes[1], P. K. Fontes[2], T. Martins[1], M. del Collado[3], A. de A. Pastore[4], G. Pugliesi[5], M. F. G. Nogueira[6], M. Binelli[1]

1 School of Veterinary Medicine and Animal Science, University of São Paulo, Pirassununga, São Paulo, Brazil

2 Department of Pharmacology, São Paulo State University, Botucatu, São Paulo, Brazil

3 Department of Veterinary Medicine, Faculty of Animal Science and Food Engineering, University of São Paulo, Pirassununga, São Paulo, Brazil

4 Androvet, Sertãozinho, São Paulo, Brazil

5 Department of Clinic and Surgery of Veterinary, School of Veterinary, Minas Gerais Federal University, Belo Horizonte, Minas Gerais, Brazil

6 Department of Biological Science, São Paulo State University, Assis, São Paulo, Brazil

PUBLISHED IN PLOS ONE, APRIL 2017; https://doi.org/10.1371/journal.pone.0175954

Appendix A

2 PRE-HATCHING EMBRYO-DEPENDENT AND -INDEPENDENT PROGRAMMING OF ENDOMETRIAL FUNCTION IN CATTLE

2.1 ABSTRACT

The bovine pre-implantation embryo secretes bioactive molecules from early development stages, but effects on endometrial function are reported to start only after elongation. Here, we interrogated spatially defined regions of the endometrium transcriptome for responses to a day 7 embryo *in vivo*. We hypothesize that exposure to an embryo changes the abundance of specific transcripts in the cranial region of the pregnant uterine horn. Endometrium was collected from the uterotubal junction (UTJ), anterior (IA), medial (IM) and posterior (IP) regions of the uterine horn ipsilateral to the CL 7 days after estrus from sham-inseminated (Con) or artificially inseminated, confirmed pregnant (Preg) cows. Abundance of 86 transcripts was evaluated by PCR using a microfluidic platform. Abundance of 12 transcripts was modulated in the Preg endometrium, including classical interferon-stimulated genes (*ISG15*, *MX1*, *MX2* and *OAS1Y*), prostaglandin biosynthesis genes (*PTGES*, *HPGD* and *AKR1C4*), water channel (*AQP4*) and a solute transporter (*SLC1A4*) and this was in the UTJ and IA mainly. Additionally, for 71 transcripts, abundance varied according to region of the reproductive tract. Regulation included downregulation of genes associated with proliferation (*IGF1*, *IGF2*, *IGF1R* and *IGF2R*) and extracellular matrix remodeling (*MMP14*, *MMP19* and *MMP2*) and upregulation of anti-adhesive genes (*MUC1*) in the cranial regions of uterine horn. Physical proximity to the embryo provides paracrine regulation of endometrial function. Embryo-independent regulation of the endometrial transcriptome may support subsequent stages of embryo development, such as elongation and implantation. We speculate that successful early embryo-dependent and -independent programming fine-tune endometrial functions that are important for maintenance of pregnancy in cattle.

2.2 INTRODUCTION

In cattle, pre-implantation embryo development starts after successful fertilization and continues until initial migration of giant trophoblast cells from the conceptus trophectoderm to the maternal luminal epithelium and lasts approximately 20 days (Spencer *et al*., 2007). The morula-stage embryo reaches the uterus 4 to 5 days post-estrus, develops to the blastocyst stage by day 7, hatches from the zona pellucida on days 9-10 and develops into a tubular conceptus that begins to elongate on day 15 to a filamentous form that occupies the entire length of the ipsilateral uterine horn by day 19 (Guillomot, 1994). Around day 16 the apposition and transient attachment of the trophoblastic cells to the uterine epithelium begins. After day 19, the elongating conceptus is adhered to the luminal epithelium and placentation starts (Guillomot *et al*., 1981).

An important feature of the pre-implantation embryo development in cattle is that the embryo/conceptus relies solely on uterine secretions (i.e., the histotroph) to supply required nutrients and growth factors. The histotroph is composed of molecules synthesized and secreted by the endometrial glandular and luminal epithelia as well as selectively transported from blood (Bazer *et al*., 2011). Endometrial secretion and transport of molecules to the uterine lumen are spatially and temporally programmed processes. Programming can be put forth by embryo-independent and -dependent factors and their interaction.

Fluctuations of sex steroid concentrations during the periovulatory period and throughout pre-implantation development exert classical endocrine, embryo-independent programming, while secretions from the developing embryo/conceptus act on a paracrine fashion inside the uterine lumen to modulate endometrial function. Dysregulation of this complex interplay leads to early embryonic mortality, which ranges from 25 to 30% in beef cattle (Diskin & Sreenan, 1980).

Regarding embryo/conceptus-mediated programming of endometrial function, a critical unanswered question is when in pre-implantation development does it start (Thatcher *et al*., 2001). It is well established that after starting elongation, there is an increasing capacity of the conceptus to secrete interferon-tau (IFNτ; Kubisch *et al*., 1998), which modulates prostaglandin synthesis in the endometrium to block luteolytic pulses of prostaglandin F2α ($PGF_{2\alpha}$) and to favor prostaglandin E2 (PGE_2) secretion (Arosh *et al*., 2016; Spencer *et al*., 2013). However, to the best of our knowledge, there is no evidence that the embryo affects endometrial function before elongation, which begins 13 days after AI (Forde *et al*., 2011). However, *in vitro* culture studies demonstrated that preimplantation embryos secrete a range

of biochemical messengers that act in concert to promote embryonic development, referred to as embryotropins (reviewed by Wydooghe *et al*., 2015). Interestingly, many of these factors have cognate receptors expressed in the uterus. Activation of such receptors could lead to cellular and tissue responses such as transcription and *de novo* synthesis of proteins and metabolites, as well as post-transcriptional and post-translational modifications of molecules pre-existing in the endometrium (Salamonsen *et al*., 2013). It is reasonable to expect that pre-elongation embryo-derived factors regulate endometrial transcription in regions that are in close physical association to the embryo. In the present study we interrogated spatially defined regions of the endometrium transcriptome for responses to a day 7 embryo *in vivo*. We hypothesize that exposure to an embryo changes the abundance of specific transcripts in the cranial region of the pregnant uterine horn.

Regarding sex-steroid programming of endometrial function, (1) manipulation of pre-ovulatory follicle growth and associated changes in proestrus estradiol (E2) and diestrus progesterone (P4) concentrations (Mesquita *et al*., 2015; Ramos *et al*., 2015; Scolari *et al*., 2016) and (2) exogenous supplementation of P4 during early diestrus regulates the endometrial transcriptome and function (Forde *et al*., 2009, 2010), and fertility (Pugliesi *et al*., 2016). More importantly, the effects of sex steroid hormones depend on their bioavailability to the endometrium and the nature and abundance of specific receptors in the endometrium. Regarding bioavailability, anatomical evidence indicates a distinct sex-steroids input according to the region of the reproductive tract. Specifically, the vascular arrangement of vessels that irrigate the uterus allows a greater input of ovarian steroids to the cranial portion of the uterine horn ipsilateral to the ovary containing the CL compared to the cranial portion of the contralateral horn and compared to the mid-caudal region of either horn (Pope *et al*., 1982). Araújo *et al*. (2015) proposed that such spatial changes in ovarian steroid input regulate local endometrium gene expression and function. Furthermore, they showed decreasing endometrial abundance of *PGR* and *ESR2* transcripts from the cranial to the caudal region of the uterine horn. This suggests that responsiveness to steroids may also be regionally controlled. Despite the clear implications of such regional specificities on the regulation of uterine function to support conceptus development, there is a lack of information on target pathways that could be modulated along the uterine horn.

Objective was to measure pre-hatching embryo-dependent and -independent effects on the abundance of select transcripts associated with uterine function to support gestation along the uterine horn in beef cows.

2.3 MATERIALS AND METHODS

Experiments were carried out at the University of São Paulo in Pirassununga, São Paulo, Brazil. All experimental procedures involving animals were approved by the Ethics and Animal Handling Committee of the School of Veterinary Medicine and Animal Science of the University of São Paulo (CEUA-FMVZ/USP, n3167260815). Protocol was in accordance with the ethical principles in animal research.

2.3.1 Reproductive management and treatments

All animals were maintained in a single *Brachiaria brizantha* pasture, supplemented with chopped sugarcane, concentrate and minerals to fulfill their maintenance requirements and received water *ad libitum*.

The estrous cycles of reproductively normal multiparous Nelore (*Bos taurus indicus*, n = 36; average body weight 531 ± 12 kg) cows were synchronized by insertion of an intravaginal P4-releasing device (1 g; Sincrogest®, Ourofino Saúde Animal, Cravinhos, São Paulo, Brazil) and i.m. administrations of $PGF_{2\alpha}$ analogue (500 μg of sodium cloprostenol; Sincrocio®, Ourofino Saúde Animal) and estradiol benzoate (2 mg; Sincrodiol®, Ourofino Saúde Animal) on day –10 (D–10; Fig. 1). At the time of P4-device removal (D–3), animals received an i.m. administration of $PGF_{2\alpha}$ and an Estrotect™ heat detector patch (Rockway, Inc. Spring Valley, WI, USA). Cows were visually observed for signs of estrus activity twice a day between 48 and 84 h after P4-releasing device withdrawal. Cows observed in standing heat or presenting an activated heat detector patch were considered in estrus (n = 30; D0 of the study). Animals were allocated randomly to one of two experimental groups 12 h after standing estrus. In the control group (Con; n = 8), cows were sham-inseminated with deposition of semen extender in the uterine body; in the Pregnant group (Preg; n = 16), cows were artificially inseminated with frozen-thawed semen from the same batch of a bull of proven fertility. All procedures were performed by a single technician. Ovulation was checked 12 hours later by B-mode transrectal ultrasonography, and only cows with a confirmed, single ovulation were maintained in the experiment (n = 24).

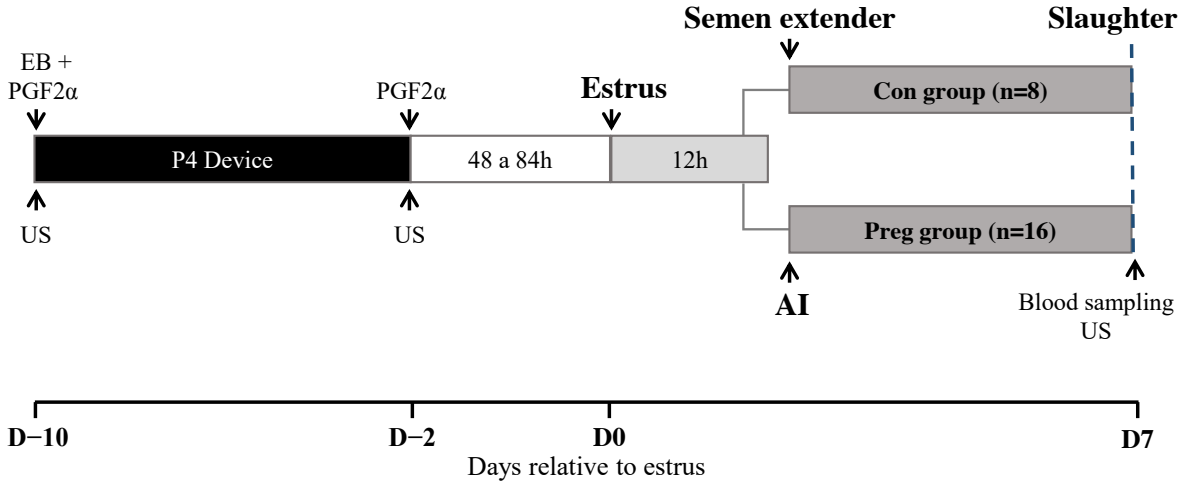

Figure 1. Experimental design. The estrous cycles of Nelore cows (n = 36) were synchronized using an 8-day progesterone-releasing intravaginal device. On day –10 (D–10), cows received a progesterone-releasing device (1 g; Sincrogest; Ourofino) and an injection of 2 mg estradiol benzoate (EB; Sincrodiol, Ourofino) and an injection of prostaglandin F2α (PGF2α; 500 µg of sodium cloprostenol; Sincrocio, Ourofino). On D–3, when the progesterone-releasing device was removed, all cows received an extra injection of PGF2α. At estrus (D0), cows were allocated to one of two experimental groups: Control (Con), cows were sham-inseminated and received semen extender; Pregnant (Preg), cows were inseminated with semen from the same batch of semen from a bull of proven fertility, 12 h post-estrus. All cows were slaughtered on D7.

Transrectal ultrasonography (7.5-MHz transducer, DP-50 vet; Mindray, Shenzhen, Guangdong, China) was also performed to measure CLs and follicles on D–10 and D–3, side and size of the preovulatory follicle and ovulation on D0 and D1, and to confirm the CL development on D7.

2.3.2 Endometrial sample collection

Animals were slaughtered on D7 after estrus. Between 4 and 8 animals, from both experimental groups, were slaughtered in each of four independent sessions. Reproductive tracts were isolated and transported on ice to the laboratory within 10 min to uterus processing. Uterus were trimmed free of surrounding tissues. The ipsi and contralateral horns relative to ovary containing the CL were isolated. Average uterine horns length was 27.12 ± 0.70 cm [mean ± SEM]. For each uterine horn, always starting from the horn ipsilateral to the CL, forceps were placed every 8 cm starting from the utero-tubal junction (UTJ) to delimit the anterior, medial and posterior uterine thirds (Fig. 2). The anterior, medial and posterior thirds were individually washed with 3, 5 and 6 mL of PBS, respectively, and the flushing was recovered in a petri dish. The presence and location of an embryo in the flushings was verified under a stereomicroscope in the Preg group animals. All embryos found (n = 10/16) were at

the expected stage of development (compact morula or early, not-hatched blastocyst) and were in the flushing obtained from the anterior third. Inseminated cows from which no embryo was recovered (n = 6) were excluded from the experiment.

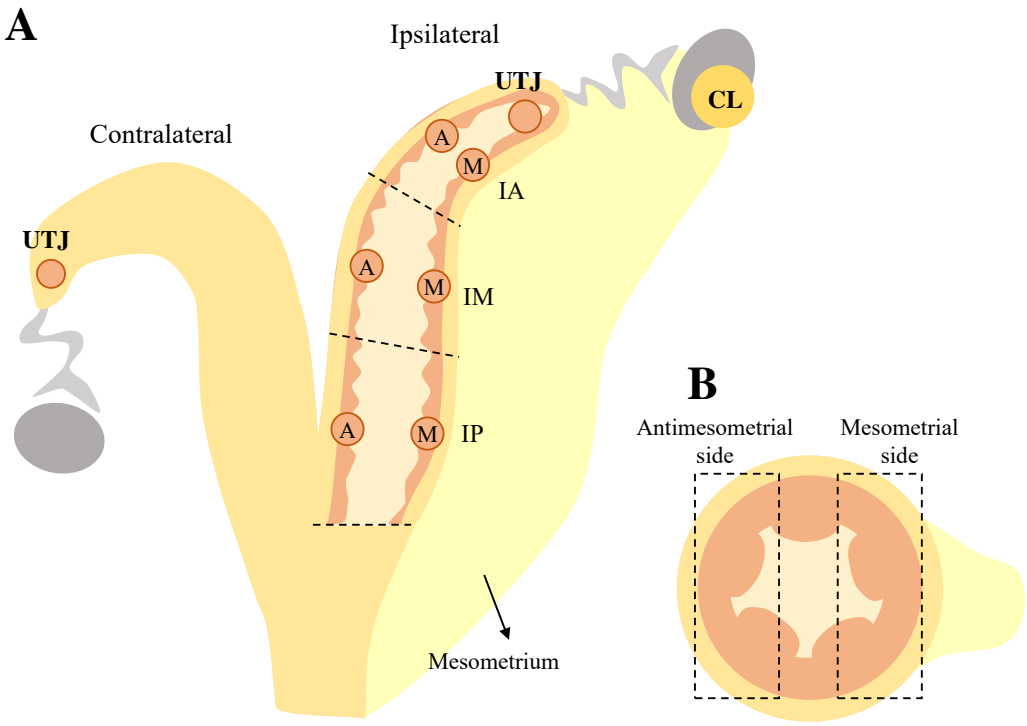

Figure 2. Schematic representation of sites selected for collection of endometrial samples. Panel A: Endometrial tissue samples were collected from 8 regions of the uterus: uterotubal junction (UTJ) ipsi and contralateral to the ovary containing the CL and the intermediate portion of the anterior, medial and posterior thirds of the ipsilateral uterine horn, that were further divided in mesometrial (M) and antimesometrial (A) sides. Panel B: Representative cross-section of the uterine horn indicating the sites for endometrium collection according to the mesometrium insertion.

After flushing, the ipsilateral uterine thirds were incised longitudinally at the mesometrial insertion. From each third, a 1 cm-wide strip of intercaruncular endometrium was dissected transversally from the lengthwise intermediate portion of the third. Then, each strip was subdivided in mesometrial and antimesometrial sides. Endometrial component of the ipsi and contralateral UTJ was collected, but not further subdivided. Once collected, the endometrial samples were immediately transferred to cryotubes and snap frozen in liquid nitrogen. Samples were stored at –80ºC until further processing. Only intercaruncular endometrium was collected because there are no caruncles in the UTJ region. In addition, only intercaruncular endometrium contains endometrial glands, which are functional units that play a major role on histotroph secretion.

2.3.3 Blood sampling and progesterone concentration measurements

Prior to slaughter, blood samples were collected via jugular venipuncture for subsequent measurement of P4. Blood samples were collected into 10 mL heparinized evacuated tubes (BD, São Paulo, SP, Brazil) and were maintained in ice for 1 hour until plasma separation. Samples were centrifuged at 4 °C, 1,500 x g for 15 min and plasma was extracted and stored in sterile 2 mL vials at –20 °C until assayed.

Plasma P4 concentrations were measured by solid-phase radioimmunoassay (Immuchem Double Antibody Progesterone Kit, MP Biomedicals, Germany GmbH, Eschwege) according to manufacturer's instructions. The intra-assay coefficients of variation were 0.17% (low concentration reference) and 7.39% (high concentration reference). The detection limit (sensibility) of the assay was 0.1 ng/mL.

2.3.4 RNA extraction and quality analysis

Endometrial fragments (~40mg) were mechanically macerated in liquid nitrogen using a stainless-steel apparatus. Subsequently, the macerate was homogenized in lysis buffer from PureLink® RNA mini kit (Ambion™, Life Technologies, Carlsbad, California, USA) and further RNA extraction performed as per manufacturer's instructions. To maximize lysis, tissue suspension was passed at least ten times through a 21-ga needle, and centrifuged at 12,000 g for 1 min at 4 ºC for removal of cellular debris. Supernatant was loaded and processing in RNeasy columns. Total RNA was eluted with 30 µL of RNase free water. Concentration and purity of total RNA in extracts were evaluated using spectrophotometry (NanoVue™ Plus Spectrophotometer, GE Healthcare, UK) by the absorbance at 260 nm and the 260/280 nm ratios, respectively.

RNA integrity was assessed using automated capillary gel electrophoresis on a Bioanalyzer 2100 with RNA 6000 Nano Lab-chips (Agilent Technologies Ireland, Dublin, Ireland) according to manufacturer's instructions. Absorbance ratios (28S/18S) and RNA integrity values recorded for all RNA samples extracted ranged between 1.8 and 2.0, and 6.9 and 9.8, respectively.

Samples of RNA (200 ng) were treated for contaminating genomic DNA using DNase I Amplification Grade (Invitrogen™, Life Technologies) in accordance with manufacturer's guidelines supplied. First strand cDNA was synthesized using the High Capacity cDNA Reverse Transcription kit (Applied Biosystems™, Life Technologies) with RNaseOUT

Recombinant Ribonuclease Inhibitor (Invitrogen™, Life Technologies) according to manufacturer's instructions. Total RNA was reverse transcribed using random hexamers and incubated at 25 ºC for 10 min, followed by incubation at 37 ºC for 2 h and reverse-transcriptase inactivation at 85 ºC for 5 min. The cDNA was stored at −20 °C for subsequent analyses.

2.3.5 Primers pairs selection and validation

Transcript abundance was determined by microfluidic dynamic array using BioMark HD (Fluidigm, South San Francisco, CA, USA) platform in a 96.96 Dynamic Array™ Integrated Fluidic Circuits (Fluidigm), which enables reaction of 96 cDNA samples with 96 genes assays in a single run. Representative genes were selected from 11 key pathways known to influence endometrial function, in addition to endogenous controls (Table 1). Primer details are provided on Supplemental S1 Table.

Table 1. Representative genes selected from key pathways known to influence endometrial function and endogenous controls.

Cell-cell adhesion	Eicosanoid metabolic process	Growth factor signaling	Secretory activity	Solute and water transport	Sex steroid signaling
FN1	*AKR1B1*	*EDN3*	*GRP*	*AQP1*	*ESR1*
ICAM1	*AKR1C4*	*EGFR*	*LTF*	*AQP4*	*ESR2*
ICAM3	*HPGD*	*FGF2*	*MCOLN3*	*CLDN10*	*GPER*
ITFG3	*PTGES*	*FGFR2*	*PIP*	*SLC13A5*	*OXTR*
ITGAV	*PTGES2*	*FLT1*	*RBP4*	*SLC1A4*	*PAQR8*
ITGB1	*PTGES3*	*GRB7*	*SCAMP1*	*SLC2A1*	*PGR1*
LGALS1	*PTGIS*	*IGF1*	*SCAMP2*	*SLC5A6*	*PGRMC1*
LGALS7B	*PTGS1*	*IGF1R*	*SCAMP3*	*SLC7A8*	*PGRMC2*
LGALS9	*PTGS2*	*IGF2*	*SERPINA14*		
MUC1	*SLCO2A1*	*IGF2R*	*SPP1*		
VIL1		*IGFBP7*			
		KDR			

Interferon Signaling	Extracellular matrix assembly	Extracellular matrix remodeling	Oxidative Stress	Polyamine Regulation and proteolysis	Endogenous control
IFI6	*HAS3*	*MMP14*	*CAT*	*AMD1*	*ACTB*
IFNAR2	*HMMR*	*MMP19*	*GPX4*	*ODC1*	*GAPDH*
IRF6	*HYAL1*	*MMP2*	*SOD1*	*ANPEP*	*PPIA*
ISG15	*HYAL2*	*TIMP2*	*SOD2*	*EED*	
MX1		*TIMP3*			
MX2					
OAS1Y					

Optimized primer pairs were designed using the Primer Express 3.0 based on GenBank Ref-Seq mRNA sequences of target genes. Oligos were aligned by Primer-BLAST (http://www.ncbi.nlm.nih. gov/tools/primer-blast/), to verify their identity and homology to the bovine genome. Oligonucleotides were commercially synthesized as purified salt-free products by Invitrogen (Life Technologies, São Paulo, SP, Brazil). All primer pairs were tested for their sensitivity and specificity first in conventional Real Time qPCR analysis to verify amplification conditions. Briefly, reactions were carried out in 96-well plates sealed with MicroAmp optical adhesive cover (Life Technologies) using the Step One Plus apparatus (Applied Biosystems Real-Time PCR System; Life Technologies). Reactions were conducted in a final volume of 20 µL using 10 µL of Power SYBR Green PCR Master Mix (Life Technologies). The PCR program consisted of an initial denaturation step at 95 ºC for 10 min, followed by 40 cycles of 15 seconds at 95 ºC and annealing at 60 ºC for 1 min. Melting curves were obtained by stepwise increases in the temperature from 60 to 95 ºC. Primer validation consisted of meeting the following criteria: i) a melt curve containing a sharp peak and devoid of additional peak(s), ii) efficiency of the standard curve ranging between 85% and 115% (based on the slope calculated for 3-fold serial dilution of a pooled cDNA sample), and iii) no amplification of the negative control (diethyl pyrocarbonate treated water replacing template cDNA on the qPCR reaction). The qPCR products identities were confirmed by sequencing and agarose gel electrophoresis for all target genes.

2.3.6 Transcript abundance analysis

Transcript abundance analysis in endometrial samples was performed using pre-selected bovine-specific primers. The mRNA abundance of 86 genes was analyzed, as indicated in Table 1, according to functional categories. Prior to qPCR thermal cycling, each sample was submitted to sequence-specific pre-amplification process as follows: 0.5 µL assay (bovine-specific primer forward and reverse, final concentration of 500nM), 2.5 µL 2X TaqMan® PreAmp Master Mix (Applied Biosystems, Foster City, CA, USA), 0.75 µL DNase-free water and 1.25 µL cDNA. The reactions were activated at 95 ºC for 10 min followed by denaturing at 95 ºC for 15 s, and annealing and amplification at 60 ºC for 4 min for 10 cycles. After thermal-cycling, the pre-amplification reactions products were submitted to the process of clean up with Exonuclease I (New England BioLabs, Ipswich, MA, New England): 1.4 µL DNase-free water, 0.2 µL Exonuclease I Reaction Buffer and 0.4 µL Exonuclease I, 20 U/µL, the digest phase was performed by 30 minutes at 37ºC, followed by inactivate phase at 80 ºC

for 15 minutes. The final product was diluted 7-fold prior to qPCR analysis. For gene expression analysis, the sample solution prepared consisted of 2.25 µL cDNA (pre-amplified products), 2.5 µL of SsoFast EvaGreen Supermix with low ROX (Bio-Rad, Hercules, CA, EUA) and 0.25 µL of 20X DNA Binding Dye (Fluidigm); and the assay solution: 0.25 µL of 100 µM combined forward and reverse primers, 2.25 µL of 1X DNA Suspension Buffer and 2.5 µL of 2X Assay Loading Reagent (Fluidigm). The 96.96 Dynamic Array™ Integrated Fluidic Circuits (Fluidigm) chip was used to data collection. After priming, the chip was loaded with 5 µL of each assay solution and 5 µL of each sample solution. The qPCR thermal cycling was performed in the Biomark HD System (Fluidigm) running 25 cycles using the protocol GE Fast 96x96 PCR+Melt. A negative control (diethyl pyrocarbonate treated water) was included and a primer pair (*GAPDH*) was essayed in duplicate. Quantitative analysis was carried out by using the crossing point (Cq) values during the log-linear phase of the reaction at which fluorescence increased above background for each primer assay.

Analysis of putative reference genes for qPCR studies was carried out using GeNorm version 3.5 Microsoft Excel Add in (Microsoft, Redmond, WA; Vandesompele *et al*., 2002). The stability of the transcript abundance of reference genes including peptidylprolyl isomerase A (*PPIA*), actin beta (*ACTB*) and glyceraldehyde-3-phosphate dehydrogenase (*GAPDH*) was investigated across all samples in this study. Relative abundance was obtained after normalization of the target genes Cq values by the geometric mean of *PPIA*, *GAPDH* and *ACTB* transcript abundance values.

2.3.7 Statistical analysis

Data were analyzed using the Statistical Analysis Systems software package (SAS Inst. Inc., Cary, NC, USA) version 9.3. Continuous data were tested with Shapiro-Wilk and Levene's test to check the normality of residues and homogeneity of variances, respectively. Group effect (Con *vs.* Preg) was determined by one-way ANOVA using Type III sums of squares.

Transcript abundance data were analyzed by repeated measures in space using the MIXED procedure in two distinct models. The first model estimated the effects of group and uterine regions by Split-plot ANOVA. Fixed effects included the main plot: experimental groups (Con *vs.* Preg); sub-plot: regions (UTJ *vs.* IA *vs.* IM *vs.* IP) and the group by region interaction. The experimental unit was a plot with its unique combination of experimental group and region. Animal within treatment was used as the error term. The type of variance-

covariance structure was chosen according to the magnitude of the Akaike information criterion corrected (AICc). The matrix with the least AICc value to each variable was deem best. When the effect of a categorical variable was significant, the Pdiff *post-hoc* test was used to determine differences between means. In the case of a significant interaction, the slice command was incorporated to the procedure to measure group effects within each region. In these analyzes, the mean relative abundance of a transcript on the antimesometrial and mesometrial sides within each uterine region was calculated to represent the region on comparisons.

The second repeated-measures analyzes aimed to compare transcript abundance between groups, uterine regions and sides, by Split-split-plot ANOVA. Fixed effects included the main plot: experimental groups (Con *vs.* Preg); sub-plot: regions (IA *vs.* IM *vs.* IP); sub-sub-plot: sides (Antimesometrial *vs.* Mesometrial) and the resulting double and triple interactions. The experimental unit was a plot with its unique combination of experimental group, region and side. Animal within treatment was used as the error term. The criteria to select the variance-covariance structure and means test were the same as described above.

Pearson's coefficient of correlation was calculated by CORR procedure. All data are expressed as means ± standard error of the mean (±SEM). Treatment differences with $P \leq 0.05$ were considered significant and probability of $0.05 < P \leq 0.10$ were considered to approach significance.

2.3.8 Cluster analysis by region

Transformed group means were used for K-means clustering by Euclidian distances using the multivariate tool in Minitab statistical software (Minitab Inc., State College, PA, USA) version 17.1.0. Dendrogram was used for preliminary assessments of the number of gene clusters. Genes with significant group by region interaction were excluded from this analysis.

2.4 RESULTS

2.4.1 Animal model, ovarian and endocrine variables

Hormonal synchronization successfully generated groups of animals presenting similar ovarian morphologies and sex steroid endocrine profiles (Table 2), as expected. Specifically,

POF diameter and CL area, plasma P4 concentration and diameter of the largest follicle on D7 were similar between groups (P > 0.1). In the present study, plasma E2 concentrations were not quantified, but the similar largest follicle diameter measured both prior to ovulation and on D7 indicated that groups experienced similar exposure to E2 both during pre-ovulatory period and early diestrus.

Table 2. Size of ovarian structures and P4 concentrations in pregnant (Preg) and sham inseminated (Con) cows. Values are expressed as means ± SEM.

Variables	Group		*P*-value
	Con (n = 8)	Preg (n = 10)	
Pre-ovulatory follicle diameter (mm)	13.57 ± 0.71	13.87 ± 0.41	0.70
CL area on D7 (cm^2)	2.84 ± 0.24	2.69 ± 0.17	0.62
Plasma P4 concentrations on D7 (ng/mL)	3.67 ± 0.52	3.43 ± 0.45	0.72
Largest follicle diameter on D7 (mm)	11.90 ± 0.45	11.56 ± 0.51	0.68

2.4.2 Confirmation of transcript abundance data generated by the microfluidic dynamic array method

To measure the repeatability of measurements taken by the Biomark HD system, the same primer pair for a reference gene (*GAPDH*) was ran twice in the same assay for all samples. The correlation coefficient (r) of this test was r = 0.99. To validate transcript abundance results measured by the Biomark microfluidic dynamic array system, abundance of *PPIA*, *IRF6*, *MX2* and *ISG15* transcripts from the same samples were measured by conventional Real time PCR. For each primer pair the correlation between Cqs obtained from Step One Plus and BioMark HD PCR analysis was 0.89, 0.94, 0.93 and 0.89 for *PPIA*, *IRF6*, *MX2* and *ISG15*, respectively.

2.4.3 Pre-hatching embryo modulation of endometrial transcript abundance

There was no main effect of group (Con vs. Preg) for the abundance of any of the transcripts measured; but there was a significant group by region (UTJ, IA, IM or IP) interaction for 12 of the 83 transcripts (Table 3). Interpretation of these interactions revealed that the group effect manifested predominantly in the regions in which the embryos were found (i.e. UTJ and anterior third). Remarkably, four differentially expressed genes were

classical interferon stimulated genes. The abundances of *ISG15*, *MX1*, *MX2* and *OAS1Y* mRNAs were respectively 1.98, 1.77, 2.00 and 1.50-fold greater in the UTJ of Preg vs. Con cows, but abundances were similar between groups in the remaining regions (Fig. 3). These results suggest that early embryo-derived IFNT locally induced the expression of ISGs in the endometrium. Furthermore, three differentially expressed genes were related to eicosanoid biosynthesis. The abundance of *PTGES* (a PGE2 synthase) in the UTJ from Preg cows was upregulated (1.35-fold). Further, in the IA region from Preg group the abundance of *AKR1C4* (a PGF2α synthase) and *HPGD* (an enzyme involved in prostaglandin catabolism) transcripts was reduced 0.67 and 0.76-fold, respectively (Fig. 4). Such expression patterns are consistent with the early embryo-mediated induction of PGE_2 and inhibition of $PGF_{2\alpha}$ synthesis in the endometrium. The proportion of transcript abundance between Preg and Con groups for the remaining genes differentially expressed ($P \leq 0.1$) in the UTJ were *AQP4* (1.58-fold), *ITGAV* (1.30-fold) and *SLC1A4* (0.52-fold). Transcripts abundance for *AMD1* (0.72-fold), *APQ4* (1.64-fold) and *ITGB1* (0.83-fold) differed ($P < 0.05$) between groups in the IA region. Only *AMD1* mRNA differed (0.77-fold; $P < 0.05$) in the IM region. A summary of embryo-dependent regional modulation of endometrial transcript abundance is presented in Figure 5.

To confirm that the up regulation of ISGs abundance in Preg UTJ was not caused by the presence or passage of sperm, we compared the abundances of *ISG15*, *MX1* and *MX2* transcripts in the UTJ from the uterine horn contralateral to the CL between Preg (contacted sperm but not the embryo) and Con (did not contact sperm or embryo) groups. Abundance of ISGs was similar between groups for all genes tested *(P* > 0.1; data in Figure S1) in the contralateral horns. Therefore, group effect noted in the ipsilateral horn was due the passage or presence of the embryo, which was unique to the ipsilateral horn and not sperm, which contacted both uterine horns.

Table 3. Effects of Group (Preg vs. Con), Region (UTJ, IA, IM vs. IP) and Group by Region in the abundance of transcripts showing significant Group by Region (G*R) interaction.

Gene symbol	Overall effects *P*-value			Ratio of mean transcript abundance (Preg:Con)[a,b]			
	Group	Region	G*R	UTJ	IA	IM	IP
Interferon Signaling							
ISG15	ns[c]	0.04	0.02	1.98*	1.00	1.12	1.18
MX1	ns	0.02	0.06	1.77*	0.89	0.89	0.94
MX2	ns	0.05	0.03	2.00*	1.15	1.26	1.07
OAS1Y	ns	0.01	0.08	1.50 ×	0.77	0.76	0.80
Eicosanoid metabolic process							
AKR1C4	ns	0.02	0.07	0.52	0.67×	0.81	0.99
HPGD	ns	0.00	0.08	0.64	0.76*	0.80	1.24
PTGES	ns	ns	0.04	1.35*	0.94	1.10	1.14
Cell-cell adhesion							
ITGAV	ns	ns	0.07	1.30×	0.87	1.05	1.17
ITGB1	ns	0.00	0.04	1.03	0.83*	0.91	1.04
Polyamine Regulation							
AMD1	ns	0.00	0.04	0.98	0.72**	0.77*	0.99
Solute and water transport							
AQP4	ns	0.01	0.07	1.58*	1.64*	1.06	0.98
SLC1A4	ns	ns	0.09	0.52*	1.11	0.72	0.93

Within each region, the abundance of each transcript was compared between Pregnant (Preg) and Control (Con) groups.
[a]Magnitude of effect of group (Preg *vs.* Con) within each region is indicated by: $^{**}P \leq 0.01$; $^{*}P \leq 0.05$; $^{\times}P \leq 0.1$.
[b]Data are presented as the ratio of mean transcript abundance between Preg and Con groups
[c]Not significant ($P > 0.1$).

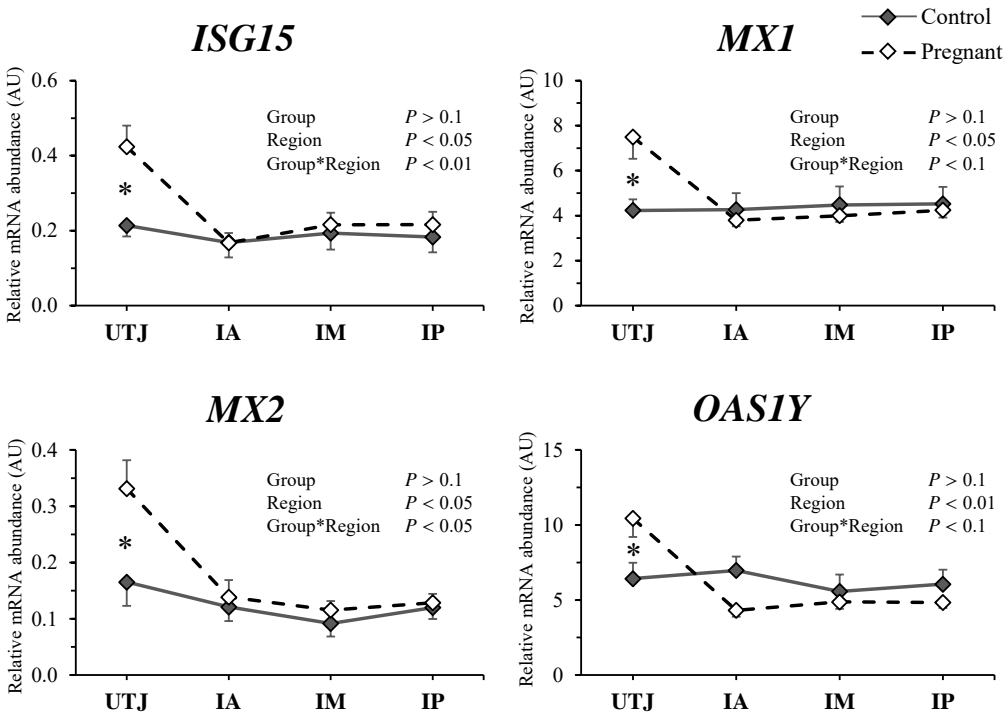

Figure 3. Relative mRNA abundance of interferon-stimulated genes (arbitrary units; AU; mean ± SEM) for control (solid lines) and pregnant (dashed lines) cows in the uterotubal junction (UTJ), anterior (IA), medial (IM) and posterior (IP) regions of the uterine horn ipsilateral to the CL. *$P < 0.05$ and ×$P < 0.1$ denotes that significant differences were reached or approached, respectively, between groups at each specific region.

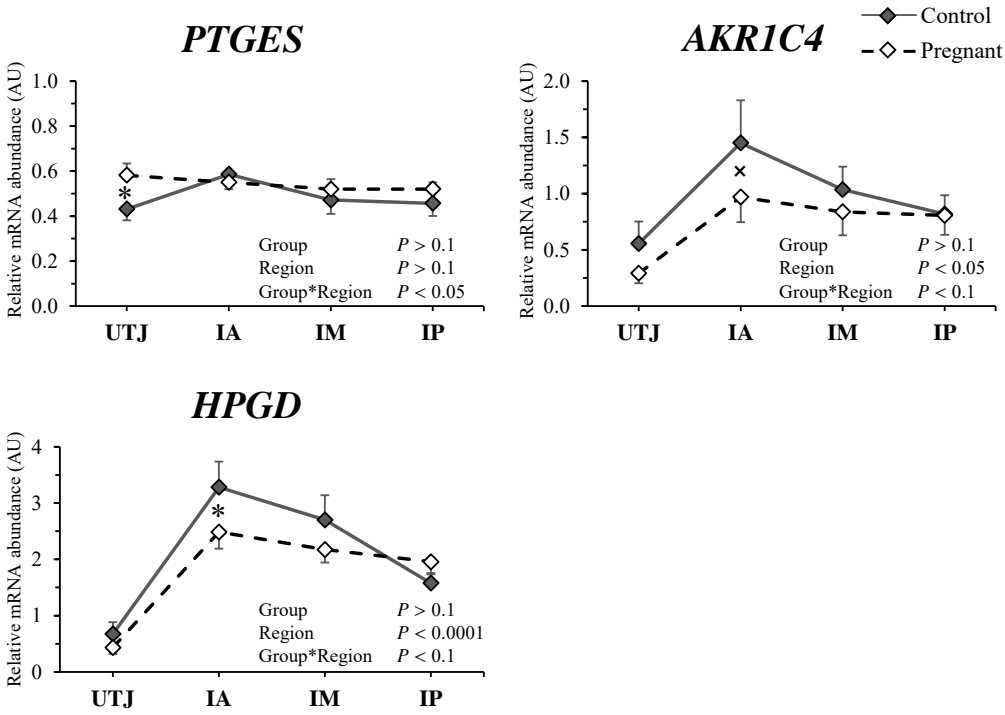

Figure 4. Relative mRNA abundance of eicosanoid biosynthesis related genes (arbitrary units; AU; mean ± SEM) for control (solid lines) and pregnant (dashed lines) cows in the uterotubal junction (UTJ), anterior (IA), medial (IM) and posterior (IP) regions of the uterine horn ipsilateral to the CL. *$P < 0.05$ and ×$P < 0.1$ denotes that significant differences were reached or approached, respectively, between groups at each specific region.

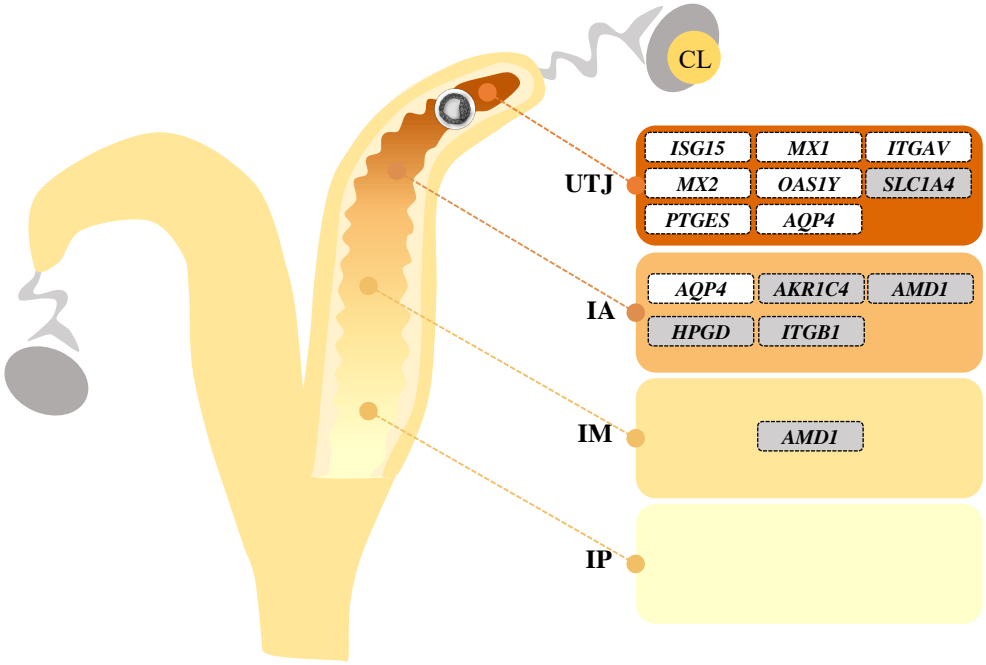

Figure 5. Summary of embryo-dependent effects. Schematic representation of distribution of transcripts affected by Group by Region (UTJ, uterotubal junction; IA, anterior; IM, medial; IP, posterior) interaction in the uterine horn ipsilateral to the CL. The position of each differentially expressed gene in the figure indicate an upregulation (placed inside a white box) or downregulation (placed inside a gray box) in the Pregnant compared to Control cows within each region.

2.4.4 Pre-hatching embryo-independent regional regulation of endometrial transcript abundance

We evaluated transcript abundance of 83 key genes associated with endometrial receptivity to the embryo in 4 regions along the ipsilateral uterine horn and established a spatial signature of endometrial transcript abundance. There was an effect of region in the expression pattern of most genes (85.5% [71/83]; Supplemental S2 Table). Genes with similar abundance patterns along the ipsilateral uterine horn were grouped by K-means analysis in four clusters. Regional patterns of expression are represented in Figure 6; a list of gene symbols assigned to each cluster is in Table 4. In general, we observed a contrasting pattern of transcript abundance in the UTJ compared to the other regions. It is remarkable that in the UTJ region there were many genes that were downregulated compared to the remaining regions, in which the expression patterns were more balanced (Clusters 2 and 3). Specifically, Cluster 1 presents a strikingly different pattern of expression in comparison to Clusters 2 and 3; there are 11 genes upregulated in the UTJ region, which are associated with developing embryo support, (*FGF2*, *PTGIS* and *SLCO2A1*), interferon signaling (*IFNAR2* and *IFI6*) and adhesive glycoproteins (*FN1* and *MUC1*). Cluster 2 was composed of 25 genes that were

downregulated in the UTJ and whose expression increased gradually in the IA, IM and IP thirds. Interestingly, some of these genes are associated with a non-receptive endometrium. For example, *IGF1*, *IGF1R*, *IGF2*, *IGF2R*, and *KDR* are associated with proliferation, and *MMP14*, *MMP19*, *MMP2* and *TIMP3* are linked to extracellular matrix remodeling. The Cluster 3 included 11 genes whose expression was drastically downregulated in the UTJ and similar among others regions, including *AKR1B1*, *ANPEP*, *SLC13A5* and *SLC5A6*. Finally, the genes in cluster 4 (24 genes) presented similar expression pattern across the four uterine regions.

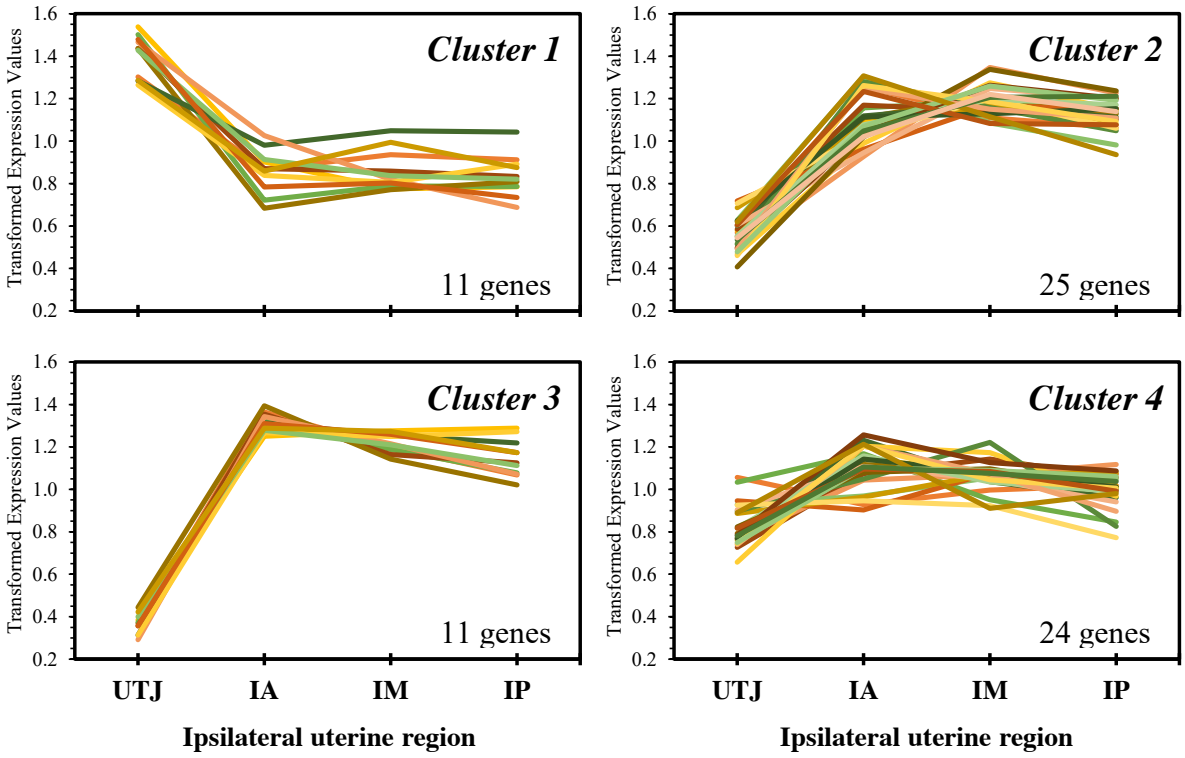

Figure 6. Cluster analysis showing uterine spatial signatures of transcript abundance in the uterotubal junction (UTJ), anterior (IA), medial (IM) and posterior (IP) regions of the ipsilateral uterine horn. Relative expression was mean-centered and clustered by K-means. Genes present in each cluster are in Table 4.

Table 4. Genes representing clusters shown in Figure 6.

Cluster	Gene Symbols
1	*FGF2, FGFR2, FN1, GRP, IFI6, IFNAR2, MUC1, OXTR, PTGIS, PTGS1, SLCO2A1*
2	*EED, FLT1, GPX4, HMMR, HYAL1, HYAL2, ICAM1, IGF1, IGF1R, IGF2, IGF2R, ITFG3, KDR, LGALS7B, MMP14, MMP19, MMP2, PGR1, PGRMC1, PTGES2, RBP4, SCAMP3, SLC7A8, TIMP3, VIL1*
3	*AKR1B1, ANPEP, EDN3, ESR2, GRB7, IRF6, MCOLN3, ODC1, PAQR8, SLC13A5, SLC5A6*
4	*AQP1, CAT, CLDN10, EGFR, ESR1, GPER, HAS3, ICAM3, IGFBP7, LGALS1, LGALS9, LTF, PGRMC2, PIP, PTGES3, PTGS2, SCAMP1, SCAMP2, SERPINA14, SLC2A1, SOD1, SOD2, SPP1, TIMP2*

2.4.5 Pre-hatching embryo-independent side regulation of endometrial transcript abundance

Transcript abundance in the mesometrial and antimesometrial sides of the uterine horn was evaluated on IA, IM and IP uterine thirds. In general, the effect of side was slight. From the 83 genes evaluated, the abundance of only eight genes [~10% (8/83)] was affected by side (Fig. 7A) and the abundance of nine genes [~11% (9/83)] was affected by a region by side interaction (Fig. 7B). These analyzes revealed that the main effect of side was predominant in the IM and IP uterine thirds. In general, transcript abundance was less in the mesometrial side, indicating the presence of inhibitory effects in proximity to larger vessel blood supply. A summary of side-dependent modulation of endometrial transcript abundance is presented in Figure 8.

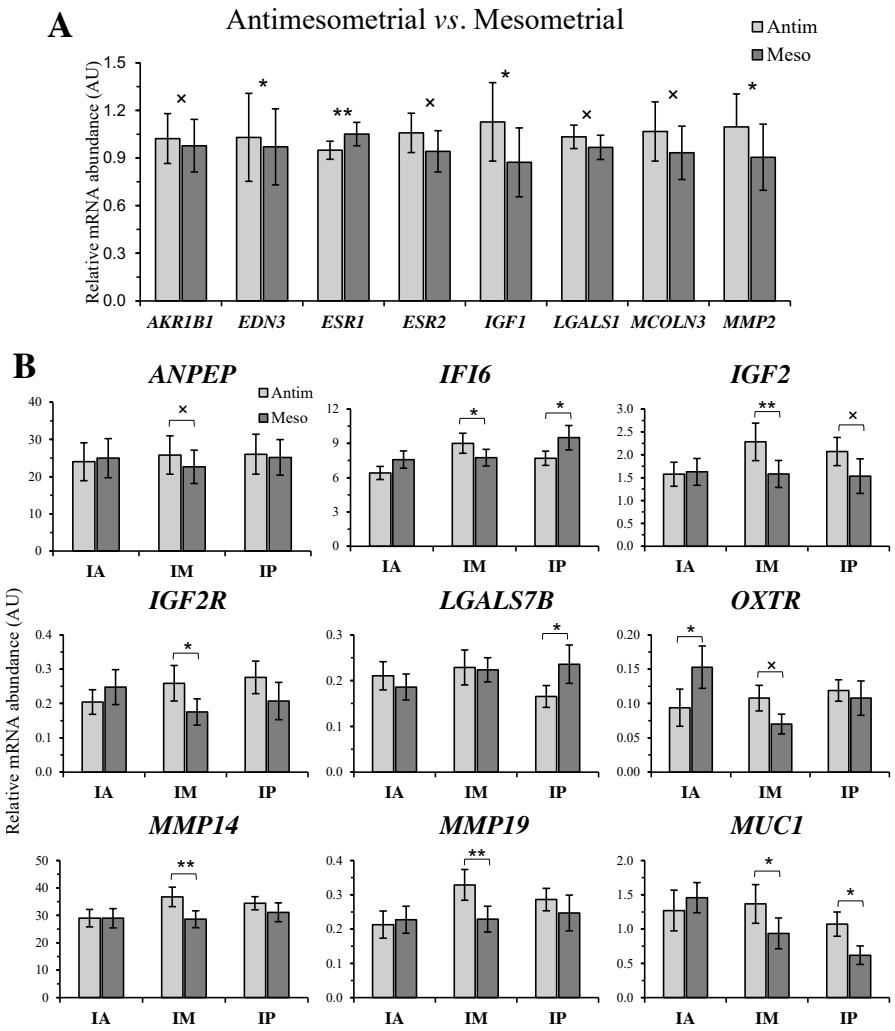

Figure 7. Relative mRNA abundance of genes affected by Side (antimesometrial *vs*. mesometrial; Panel A; arbitrary units: AU; mean ± SEM) and by the Side by Region (IA, IM *vs*. IP; Panel B; arbitrary units: AU; mean ± SEM) interaction in the uterine horn ipsilateral to the CL. *$P < 0.05$ and ×$P < 0.1$ denotes that significant differences were reached or approached, respectively, between sides at each specific region.

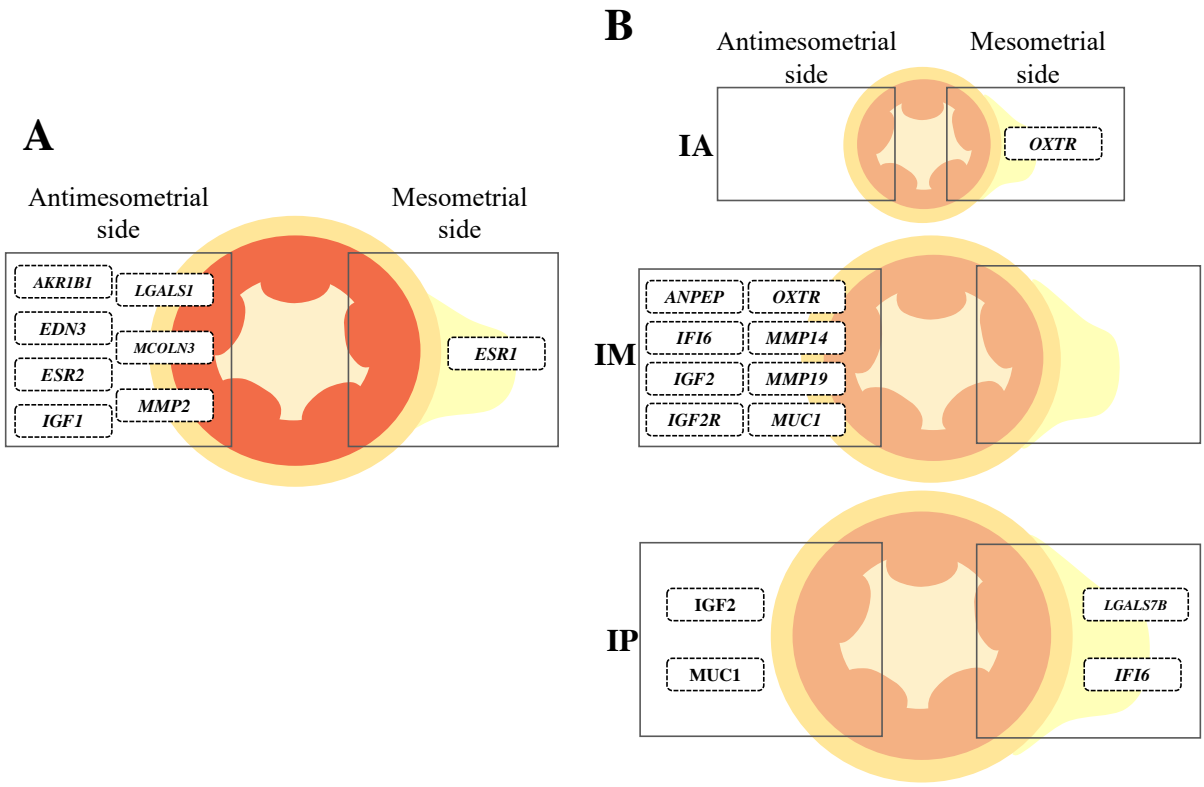

Figure 8. Summary of side-dependent differences in gene expression. Schematic representation of distribution of genes affected by Side (antimesometrial *vs*. mesometrial; Panel A) and by the Side by Region (IA, anterior; IM, medial; IP, posterior; Panel B) interaction in the uterine horn ipsilateral to the CL. The position of each differentially expressed gene in the figure indicate an upregulation in the side.

2.5 DISCUSSION

A critical unanswered question surrounding early pregnancy in cattle is how early is the embryo able to regulate endometrial function to favor its development. Studies over the past 20 years have indicated the existence of complex paracrine and endocrine *in vivo* communication between early embryo and the maternal tract in mammalians (Kane *et al*., 1997; Hardy & Spanos, 2002). *In vitro* culture studies demonstrated that preimplantation embryos secrete a range of biochemical messengers that act in concert to promote embryonic development, referred to as embryotropins (reviewed by Wydooghe *et al*. 2015). The aim of the present study was to compare the abundance of specific transcripts between cycling and pregnant bovine endometria to elucidate whether presence of a pre-hatching embryo might influence the endometrial function at a time-point coinciding with apical uterine position of the embryo. We demonstrated for the first time that a day 7 embryo was able to locally regulate interferon signaling and eicosanoid biosynthesis pathways in the endometrium.

Furthermore, embryo-independent, uterine region and side regulation of transcript abundance was discovered.

The pre-hatching, day 7 embryo is located in the cranial portion of the uterine horn ipsilateral to the CL, that comprehended the UTJ and cranial-most 8 cm of the horn. In agreement, Dinskin & Sreenan (Diskin & Sreenan, 1980) reported that embryos recovered 8 days post-estrus were located at the tip of the uterine horn, close to the UTJ, in inseminated beef cows. The dynamic of migration of the early bovine embryo along the uterine horn remains poorly known. According to Wolf *et al*. (2003) the embryo does not float in a recognizable volume of maternal secretions, but is surrounded tightly by the endometrium through a thin fluid layer stabilized by glycoproteins.

Exposure to a day 7 embryo stimulates local expression of classic interferon-induced genes. The fact that the abundance of transcripts for ISGs (*ISG15*, *MX1*, *MX2* and *OAS1Y*) was increased in the UTJ region of Preg cows is suggestive of signaling by embryo secreted interferon-tau. Furthermore, there was a greater abundance of transcripts for *IFNAR2*, a classical interferon type I receptor, in the UTJ than other uterine regions. This could be associated with a more pronounced interferon-mediated response in this region. The expression of *IFNT* mRNA and protein is first evident as the trophoblast cell lineage develops at the late morula and early blastocyst stage in cattle (D6–7 of pregnancy; Farin *et al*., 1989; Lonergan *et al*, 2003). *In vivo* or *in vitro* derived day 7 bovine blastocysts produce very low amounts of IFNT (~ 100 to 1000 pM/day) as measured by antiviral cell protection assay (Kubisch *et al*., 1998). Indeed, *in vitro* stimulation of endometrial cells with 25 nmol of IFNT was needed to increased *ISG15* mRNA and ISG15 protein abundance (Austin *et al*., 1996). Thus, it is remarkable that such early embryos were capable to change endometrial transcript abundance as reported here. Probably, such limited capacity of synthesis and secretion of signals by the early embryo (Robinson *et al*., 2006) is the reason of the locally restricted effects verified. Substantial endometrial expression of ISGs was reported previously (Dorniak *et al*., 2011) in embryo recipients on D13 after estrus.

To rule out the possibility of non-specific ISGs stimulation by exposure to sperm in Preg cows, we compared ISGs expression between Con and Preg cows in the contralateral UTJ. The similar ISGs transcript abundances between the groups further indicated that the significant differences found in the ipsilateral UTJ were induced by the embryo. Thus, although IFNT signaling is likely to have occurred in the present study, functional relevance of such early communication is currently unknown.

Exposure to a day 7 embryo changes the abundance of eicosanoid metabolism transcripts to favor a greater PGE_2/PGF_{2a} ratio. Prostaglandins evidently regulate endometrial functions and conceptus elongation during early pregnancy (Robinson *et al*., 2006). Dorniak *et al*. (2011) showed that intrauterine infusion of meloxican, a selective PTGS2 inhibitor, prevented conceptus elongation in early pregnant sheep. In the present report, the expression of *PTGES* (prostaglandin E synthase) was upregulated, while that of *AKR1C4* (aldo-keto reductase family 1, member C4) and *HPGD* [hydroxyprostaglandin dehydrogenase 15-(NAD)] was downregulated in pregnant endometria. The PTGES enzyme converts PGH_2 to PGE_2 and is mainly responsible for the production of the PGE_2 in the bovine endometrium (Arosh *et al*., 2004). The AKR1C4 enzyme converts PGH_2 to $PGF_{2\alpha}$, while HPGD is responsible for prostaglandins catabolism (Parent *et al*., 2006). Interpretation of these data suggests an increase in PGE_2 synthesis and secretion and decrease in $PGF_{2\alpha}$ synthesis, which is a pro-gestation phenotype. Indeed, PGE_2 has been associated to multiple roles as an embryo and luteotrophic signal and as an important mediator in endometrial receptivity, myometrial quiescence, and immune function at the fetal-maternal interface during the establishment of pregnancy (Arosh *et al*., 2006; Magness *et al*., 1981; Emond *et al*., 1998). Conversely, uterine production of $PGF_{2\alpha}$ has a direct negative effect on continued embryonic development (Senna *et al*., 2004). Seals *et al*. (1998) verified that most susceptible period of embryonic growth to the negative effects of $PGF_{2\alpha}$ was during the development from morula to blastocyst, which happens at the apical uterine portion. Consistent with our findings, Beltman *et al*. (2010) analyzed the tip of the uterus and verified that the expression of *PTGES* was upregulated in the endometria of heifers with a viable embryo compared to that of a retarded embryo, while the expression of *HGPD* was significantly decreased in this group.

Remaining transcripts regulated by the embryo locally were *ITGB1* (in the IA region) and *AMD1* (in the IA and IM regions), both downregulated in the Preg group, and *AQP4* (in the UTJ and IA regions), upregulated by the embryo. The integrin subunit beta 1 (ITGB1) is a glycoprotein involved in the cell-cell adhesion, cell-extracellular matrix adhesion and signal transduction, and is expressed along the basolateral membranes of the luminal and glandular epithelial cells as well as around the blood capillaries throughout the endometrium (Pfarrer *et al*., 2003). Guillomot (1999) provided evidence that major components of the ECM and the ITGB1 are lost in a progressive local pattern during the trophoblastic adhesion process in the caprine endometrium. The adenosylmethionine decarboxylase 1 is an enzyme coded by *AMD1* gene and is implicated in polyamine biosynthesis. The biological relevance of this finding during early pregnancy has not been established. However, Heald (1979) observed

that local embryonic signals seems to regulate polyamine synthesis in the pregnant uterus of rats. The embryo-induced regulation of *AQP4* transcripts indicates an increased water transport to the portion of the horn containing the embryo. The aqueous transport through the aquaporin channel is driven by osmotic gradients. Secretion, absorption and homeostasis of uterine fluid are crucial for embryo development (Zho *et al*., 2014).

Regional differences in transcript abundance along the uterine horn ipsilateral to the CL define a functional spatial signature associated with receptivity to the embryo. Cluster analysis grouped four patterns of transcript abundance along the ipsilateral uterine horn. Cluster 1 represents 11 genes that showed overexpression in the UTJ region and that support the developing embryo, such as *FGF2, FGFR2, PTGIS* and *SLCO2A1,* are associated with interferon response (*IFNAR2* and *IFI6*) and provide embryo adhesiveness (*FN1* and *MUC1*). FGF2 has been described as a strong mediator of IFNT production in bovine trophectoderm cells and blastocyst-stage bovine embryos (Michael *et al*., 2006) and greater amounts of *FGF2* mRNA in the ipsilateral apical uterine horn can be a reasonable explanation to support the early embryo development. Excess mucin, coded by the *MUC1* gene, prevents embryo attachment to the endometrial luminal epithelium (Bowen *et al*., 1997; Surveyor *et al*., 1995). Thus, upregulation of this gene in the Preg UTJ probably stimulates embryo transit to the subsequent regions of the uterine horn.

Cluster 2 was composed of 25 transcripts whose abundance was lowest in the UTJ and continuously increased in the IA, IM and IP regions. Interestingly, some of these transcripts are associated with a non-receptive endometrium, that expresses proliferation- (*IGF1, IGF1R, IGF2, IGF2R,* and *KDR*) rather than secretion-associated genes (Mesquita *et al*., 2015) and extracellular matrix remodeling genes (*MMP14*, *MMP19*, *MMP2* and *TIMP3;* Scolari *et al*., 2016). The gradual uterine cranial-wise downregulation of these genes may be related to local requirements of the embryo, that are specific to each stage of development. The UTJ-IA location of embryos in the present report are consistent with the concept that an endometrium that is less engaged in proliferation and remodeling is receptive compatible with early embryo requirements. Findings were similar to those described by Bauersachs *et al*. (2005), which identified differential mRNA expression between different regions (anterior, middle and posterior) of the ipsi and contralateral uterine horns. Specifically, that study showed an increase in *UTMP* (also known as *SERPINA14*) transcripts abundance at the cranial ipsilateral uterine horn, similarly to our study. Regulation of region-specific transcript profiles may be exerted through differential vascularization along the uterine horn. Specifically, there is a preferential input of blood draining the ovaries to the cranial region of the uterus compared to

the mid and posterior regions (Pope *et al*., 1982). Thus, sex steroid regulation of endometrial transcription may explain regional differences in transcript abundance (Araújo *et al*., 2015).

A collective finding that was consistent to clusters 1 to 3 relates to the uniqueness of the transcription profile in the UTJ compared to the remaining regions of the uterus. To the best of our knowledge, there are no studies comparing the gene expression of UTJ with the remaining uterine horn. The bovine UTJ is composed of three parts: terminal isthmic segment, transition region proper and uterine apex (Wrobel *et al*., 1983). The uterine apex extends to the point of the first caruncles, approximately 1-1.5 cm caudally to the oviductal transition into the uterine horn. Only the endometrial component of the UTJ was collected and analyzed in this study. The luminal epithelium of the bovine UTJ consists of a simple columnar epithelium containing ciliated and non-ciliated cells, and its surface is covered by varying amounts of a mucous secretion that tends to agglomerate the cilia and microvilli (Wrobel *et al*., 1983). The existence of glands in the bovine UTJ remains controversial (Hook & Hafez, 1968), although we clearly detected glands in histologic sections of the uterus (data not shown). Discrepant differences verified at transcriptional level may be due to differences in cellular compartments between regions.

Side differences in transcript abundance along the uterine horn ipsilateral to the CL define a second layer of functional spatial signature associated with receptivity to the embryo. Because the main blood vessels supplying the bovine uterus are inserted through the mesometrium, we hypothesized that there would be a greater input of systemic factors and ovarian steroids in the endometrium close to the mesometrium insertion (Dyce *et al*., 2004). Perhaps this could evoke side-specific regulation of gene expression. Furthermore, to the best of our knowledge, there are no reports showing evidence of differential gene expression between mesometrial and antimesometrial sides in the bovine endometrium during pre-hatching embryo development. In the present study, abundance of eight transcripts was affected by side, seven of which were upregulated in the antimesometrial side. One such gene is endothelin 3 (*EDN3*), which is a potent vasoconstrictor. The EDN3 is synthetized by endometrial stromal and glandular epithelial cells and acts in a paracrine manner in the uterine vasculature (Cameron *et al*., 1993, 1995). A decrease in *EDN3* mRNA abundance in the mesometrial side of endometrium may point to a local vasodilatation and, thus, increased blood supply in this region. Study of region by side interactions revealed additional 9 genes (Fig. 7B) whose transcript abundance was regulated between sides in least one uterine region (IA, IM or IP). Interpretation of interactions showed that the majority of side effects are concentrated in the IM and IP regions in comparison to the IA. It is possible that because the

caudal-wise increase in the uterine horn diameter, the distance between the mesometrial and antimesometrial sides are greater and regulation is more prone to occur. In many rodents, including mice and rats, attachment always occurs at the antimesometrial side of the uterine lumen, opposite the entry site of blood vessels into the uterus, whereas implantation is mesometrial in bats, mare and pigs (Spencer & Hansen *et al*., 2015). However, relevance of side-specific transcript abundance in cattle is unknown and remains to be discovered. Although not examined in the present study, there are probably embryo-dependent and -independent effects on caruncular endometrium function. Such effects were reported earlier before (Correia-Alvarez *et al*., 2015) and at implantation (Mansouri-Attia *et al*., 2009).

The functional relevance of uterine programming during pre-hatching early embryo development can be questioned due to the fact that *in vitro* produced bovine embryos can be caudally transferred to the uterus and are able to establish gestations successfully. However, it has been demonstrated clearly in embryo transfer programs that there is a greater pregnancy success when an embryo was transferred deep in ipsilateral uterine horn compared to a shallow transfer (65.9% *vs*. 29.6%; Beal *et al*., 1988). Furthermore, Newcomb *et al*. (1980) transferred single embryos surgically, bilaterally on day 7 to a combination of sites (tip or base) of uterine horns in cows. They concluded that the tip of the ipsilateral uterine horn is the optimal site for fetal survival and that to ensure a high twin fetal survival one embryo must had been placed in this site. Collectively, these findings and ours provide evidence that although the sequential exposure of the embryo to a regionally programmed uterus is not absolutely required to establishment of pregnancy, absence of exposure may be implied as a contributing factor to reduced establishment of pregnancy, such as when embryo is transferred caudally in cattle. Thus, exposure to the pre-hatching embryo may fine-tune endometrial function to support subsequent pregnancy events.

In conclusion, the present study showed that the expression pattern of specific genes in the endometrium respond to pre-hatching embryo-dependent and -independent programming (Fig. 9). Embryo-dependent programming requires physical proximity to the embryo probably because of the limited capacity of synthesis and secretion of signals by the early embryo. Clear regional and side changes in transcript abundance were observed in this study and their critical role for further embryo development and survival and, ultimately, pregnancy success, deserves further research. Mechanisms that regulate regional expression of transcripts have not been elucidated, but may include vascular specializations to deliver different sex-steroid concentrations to particular regions of the reproductive tract and specific intrinsic regional programming of expression across the uterine horn. We propose that successful pre-hatching

embryo-dependent and -independent programming of endometrial function fine-tune endometrial functions that are important for a successful pregnancy in cattle.

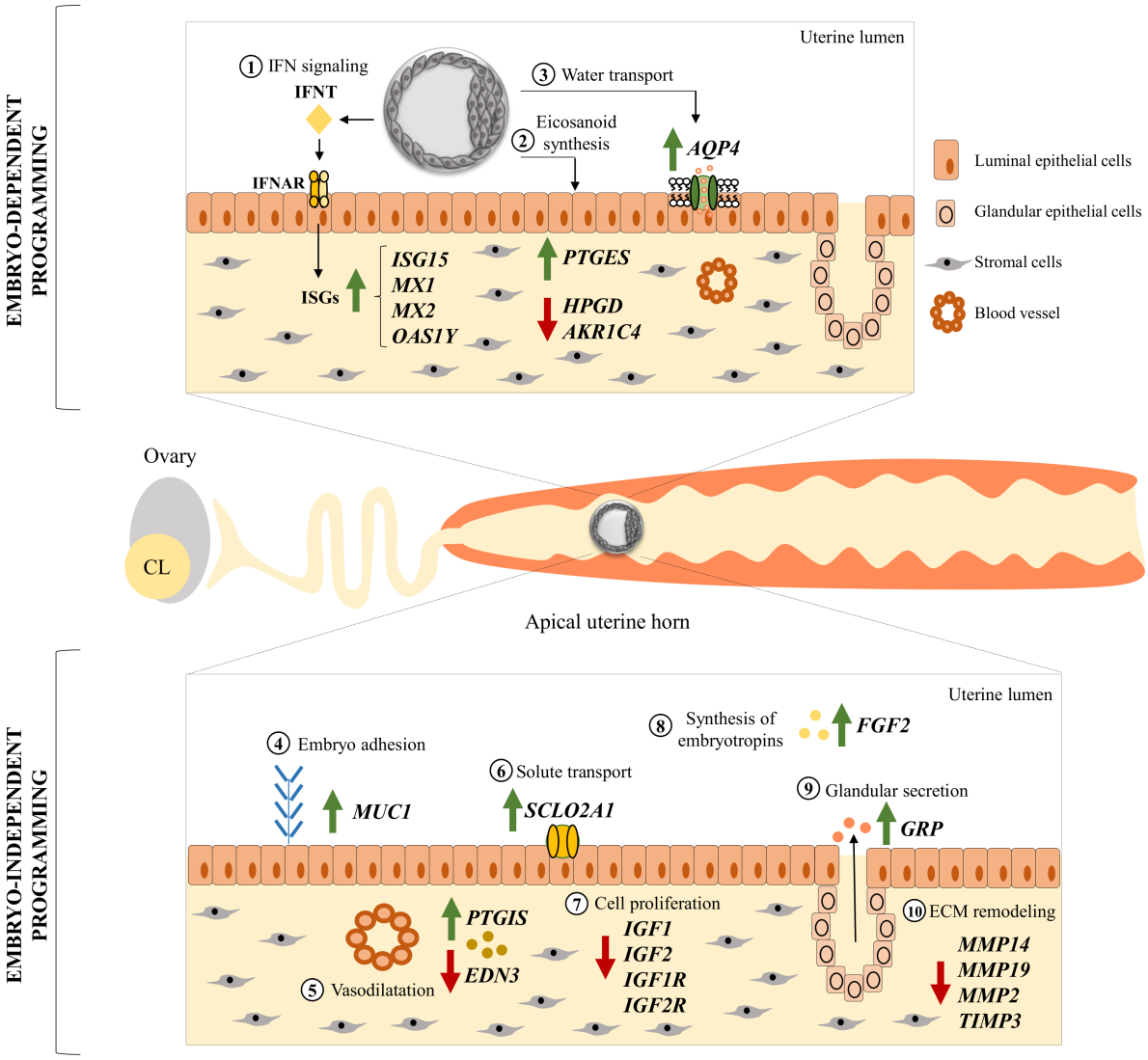

Figure 9. A working model integrating embryo-dependent (top panel) and -independent (bottom panel) programming of endometrial function 7 days after estrus. Numbers 1 to 9 represent processes and associated key genes whose transcription was modulated in the UTJ and/or apical portion of the uterine horn compared to the medial and posterior portions. Changes in transcript abundance are irrespective of cell type, since they were measured on whole endometrium homogenates. *Embryo-dependent signaling:* (1) Interferon-tau (IFNτ) secreted by the embryo affects the endometrium in a paracrine manner, regulating the transcription of interferon-stimulated genes (*ISG15, MX1, MX2* and *OAS1Y*); (2) embryo-induced regulation of eicosanoid metabolism genes favor a greater PGE2:PGF2α ratio; (3) embryo-induced regulation of *AQP4* transcripts indicates an increased water transport to the portion of the horn containing the embryo. *Embryo-independent signaling:* (4) upregulation of the anti-adhesive *MUC1* stimulates transit of the embryo from the UTJ to the more caudal regions of the uterine horn; (5) upregulation of vasodilatation-related gene (*PTGIS*) and downregulation of vasoconstriction-related gene (*EDN3*) indicate greater blood flow to the apical regions of the horn; (6) increase of solute transport (*SLCO2A1*); (7) downregulation of genes associated with cellular proliferation (*IGF1*, *IGF2*, *IGF1R* and *IGF2R*), suggests a change in tissue function to promote (8) synthesis of embryotropins (*FGF2*) and (9) secretion, which is supported by upregulation of glandular secretions-related gene (*GRP*); (10) decrease of extracellular matrix remodeling (*MMP14*, *MMP19*, *MMP2* and *TIMP3*). Collectively, at the transcriptional level, changes are consistent with an endometrial phenotype that is more receptive to the embryo in the apical portion of the uterine horn compared to the medial and posterior portions.

2.6 ACKNOWLEDGMENTS

The authors thank the Administration of the Fernando Costa campus of the University of São Paulo and Ourofino Saúde Animal for providing the animals and the products for pharmacological manipulation of estrous cycle, respectively. We are also thankful to staff of the FMVZ-USP campus Pirassununga, namely MI Silva, RR Santos, MR França, ML Oliveira, A Gonella-Diaza, BP Mello, K Ribeiro, KM Lemes, CMB Membrive, ECC Celeghini and RP Arruda for technical support. Also, PHM Rodrigues and CG de Lima for statistical assistance.

2.7 REFERENCES

Araújo ER, Sponchiado M, Pugliesi G, Van Hoeck V, Mesquita FS, Membrive CMB, *et al*. Spatio-specific regulation of endocrine-responsive gene transcription by periovulatory endocrine profiles in the bovine reproductive tract. Reproduction, Fertility and Development. 2015.

Arosh JA, Banu SK, McCracken JA. Novel concepts on the role of prostaglandins on luteal maintenance and maternal recognition and establishment of pregnancy in ruminants. Journal of dairy science. 2016.

Austin KJ, Ward SK, Teixeira MG, Dean VC, Moore DW, Hansen TR. Ubiquitin cross-reactive protein is released by the bovine uterus in response to interferon during early pregnancy. Biology of reproduction. 1996;54(3):600-6.

Bauersachs S, Ulbrich SE, Gross K, Schmidt SEM, Meyer HHD, Einspanier R, Wenigerkind H, Vermehren M, Blum H, Sinowatz F, Wolf E. Gene expression profiling of bovine endometrium during the estrous cycle: detection of molecular pathways involved in functional changes. Journal of Molecular Endocrinology. 2005;34(3):889-908.

Bazer FW, Wu G, Johnson GA, Kim J, Song G. Uterine histotroph and conceptus development: select nutrients and secreted phosphoprotein 1 affect mechanistic target of rapamycin cell signaling in ewes. Biology of reproduction. 2011;85(6):1094-107.

Beal WE, Hinshaw RH, Whitman SS. Evaluating embryo freezing method and the site of embryo deposition on pregnancy rate in bovine embryo transfer. Theriogenology. 1998;49(1):241.

Beltman ME, Forde N, Furney P, Carter F, Roche JF, Lonergan P, *et al*. Characterization of endometrial gene expression and metabolic parameters in beef heifers yielding viable or non-viable embryos on Day 7 after insemination. Reproduction, Fertility and Development. 2010;22(6):987-99.

Bowen JA, Bazer FW, Burghardt RC. Spatial and temporal analyses of integrin and Muc-1 expression in porcine uterine epithelium and trophectoderm *in vitro*. Biology of reproduction. 1997;56(2):409-15.

Cameron IT, Bacon CR, Collett GP, Davenport AP. Endothelin expression in the uterus. The Journal of steroid biochemistry and molecular biology. 1995;53(1):209-14.

Cameron IT, Plumpton C, Champeney R, Van Papendorp C, Ashby MJ, Davenport AP. Identification of endothelin-1, endothelin-2 and endothelin-3 in human endometrium. Journal of reproduction and fertility. 1993;98(1):251-5.

Correia-Álvarez E, Gómez E, Martín D, Carrocera S, Pérez S, Otero J, Peynot N, Giraud-Delville C, Caamaño JN, Sandra O, Duranthon V, Muñuz M. Expression and localization of interleukin 1 beta and interleukin 1 receptor (type I) in the bovine endometrium and embryo. Journal of reproductive immunology. 20015;110:1-13.

Diskin MG, Sreenan JM. Fertilization and embryonic mortality rates in beef heifers after artificial insemination. Journal of reproduction and fertility. 1980;59(2):463-8.

Dorniak P, Bazer FW, Spencer TE. Prostaglandins regulate conceptus elongation and mediate effects of interferon tau on the ovine uterine endometrium. Biology of reproduction. 2011;84(6):1119-27.

Arosh JA, Banu SK, Kimmins S, Chapdelaine P, Maclaren LA, Fortier MA. Effect of interferon-τ on prostaglandin biosynthesis, transport, and signaling at the time of maternal recognition of pregnancy in cattle: evidence of polycrine actions of prostaglandin E2. Endocrinology. 2004;145(11):5280-93.

Dyce KM, Wensing CJG, Sack WO. Tratado de anatomia veterinária: Elsevier Brasil; 2004.

Emond V, Fortier MA, Murphy BD, Lambert RD. Prostaglandin E2 regulates both interleukin-2 and granulocyte-macrophage colony-stimulating factor gene expression in bovine lymphocytes. Biology of reproduction. 1998;58(1):143-51.

Farin CE, Imakawa K, Roberts RM. In situ localization of mRNA for the interferon, ovine trophoblast protein-1, during early embryonic development of the sheep. Molecular Endocrinology. 1989;3(7):1099-107.

Forde N, Carter F, Fair T, Crowe MA, Evans ACO, Spencer TE, *et al*. Progesterone-regulated changes in endometrial gene expression contribute to advanced conceptus development in cattle. Biology of Reproduction. 2009;81(4):784-94.

Forde N, Carter F, Spencer TE, Bazer FW, Sandra O, Mansouri-Attia N, *et al*. Conceptus-induced changes in the endometrial transcriptome: how soon does the cow know she is pregnant? Biology of Reproduction. 2011;85(1):144-56.

Forde N, Spencer TE, Bazer FW, Song G, Roche JF, Lonergan P. Effect of pregnancy and progesterone concentration on expression of genes encoding for transporters or secreted proteins in the bovine endometrium. Physiological genomics. 2010;41(1):53-62.

Guillomot M, Flechon JE, Wintenberger-Torres S. Conceptus attachment in the ewe: an ultrastructural study. Placenta. 1981;2(2):169-81.

Guillomot M. Cellular interactions during implantation in domestic ruminants. Journal of reproduction and fertility Supplement. 1994;49:39-51.

Guillomot M. Changes in extracellular matrix components and cytokeratins in the endometrium during goat implantation. Placenta. 1999;20(4):339-345.

Hardy K, Spanos S. Growth factor expression and function in the human and mouse preimplantation embryo. Journal of Endocrinology. 2002;172(2):221-36.

Heald PJ. Changes in ornithine decarboxylase during early implantation in the rat. Biology of Reproduction. 1979;20(5):1195–1199.

Hook SJ, Hafez ESE. A comparative anatomical study of the mammalian uterotubal junction. Journal of morphology. 1968;125(2):159-84.

Kane MT, Morgan PM, Coonan C. Peptide growth factors and preimplantation development. Human Reproduction Update. 1997;3(2):137-57.

Kubisch HM, Larson MA, Roberts RM. Relationship between age of blastocyst formation and interferon-τ secretion by *in vitro*–derived bovine embryos. Molecular reproduction and development. 1998;49(3):254-60.

Lonergan P, Rizos D, Gutierrez-Adan A, Moreira PM, Pintado B, De La Fuente J, *et al*. Temporal divergence in the pattern of messenger RNA expression in bovine embryos cultured from the zygote to blastocyst stage *in vitro* or *in vivo*. Biology of Reproduction. 2003;69(4):1424-31.

Magness RR, Huie JM, Hoyer GL, Huecksteadt TP, Reynolds LP, Seperich GJ, *et al*. Effect of chronic ipsilateral or contralateral intrauterine infusion of prostaglandin E 2 (PGE 2) on luteal function of unilaterally ovariectomized ewes. Prostaglandins and medicine. 1981;6(4):389-401.

Mansouri-Attia N, Aubert J, Reinaud P, Giraud-Delville C, Taghouti G, Galio L, Evertis RE, Degrelle S, Richard C, Hue I, Yang X, Tian C, Lewin HA, Renard JP, Sandra O. Gene expression profiles of bovine caruncular and intercaruncular endometrium at implantation. Physiological genomics. 2009;39(1):14-27.

Mesquita FS, Ramos RS, Pugliesi G, Andrade SCS, Van Hoeck V, Langbeen A, *et al*. The receptive endometrial transcriptomic signature indicates an earlier shift from proliferation to metabolism at early diestrus in the cow. Biology of reproduction. 2015:biolreprod-115.

Michael DD, Alvarez IM, Ocon OM, Powell AM, Talbot NC, Johnson SE, *et al*. Fibroblast growth factor-2 is expressed by the bovine uterus and stimulates interferon-τ production in bovine trophectoderm. Endocrinology. 2006;147(7):3571-9.

Newcomb R, Christie WB, Rowson LEA. Fetal survival rate after the surgical transfer of two bovine embryos. Journal of reproduction and fertility. 1980;59(1):31-6.

Parent M, Madore E, MacLaren LA, Fortier MA. 15-Hydroxyprostaglandin dehydrogenase in the bovine endometrium during the estrous cycle and early pregnancy. Reproduction. 2006;131(3):573-82.

Pfarrer C, Hirsch P, Guillomot M, Leiser R. Interaction of Integrin Receptors with Extracellular Matrix is involved in trophoblast giant cell migration in bovine placentomes. Placenta. 2003;24(6), 588-597.

Pope WF, Maurer RR, Stormshak F. Distribution of progesterone in the uterus, broad ligament, and uterine arteries of beef cows. The Anatomical Record. 1982;203(2):245-9.

Pugliesi G, Santos FB, Lopes E, Nogueira É, Maio JRG, Binelli M. Improved fertility in suckled beef cows ovulating large follicles or supplemented with long-acting progesterone after timed-AI. Theriogenology. 2016;85(7):1239-48.

Ramos RS, Oliveira ML, Izaguirry AP, Vargas LM, Soares MB, Mesquita FS, *et al*. The periovulatory endocrine milieu affects the uterine redox environment in beef cows. Reproductive Biology and Endocrinology. 2015;13(1):39.

Robinson RS, Fray MD, Wathes DC, Lamming GE, Mann GE. *In vivo* expression of interferon tau mRNA by the embryonic trophoblast and uterine concentrations of interferon tau protein during early pregnancy in the cow. Molecular reproduction and development. 2006;73(4):470-4.

Salamonsen LA, Edgell T, Rombauts LJF, Stephens AN, Robertson DM, Rainczuk A, Nie G, Hannan NJ. Proteomics of the human endometrium and uterine fluid: a pathway to biomarker discovery. Fertility and Sterility. 2013.

Scenna FN, Edwards JL, Rohrbach NR, Hockett ME, Saxton AM, Schrick FN. Detrimental effects of prostaglandin F 2α on preimplantation bovine embryos. Prostaglandins & other lipid mediators. 2004;73(3):215-26.

Scolari SC, Pugliesi G, Strefezzi RF, Andrade SC, Coutinho LL, Binelli M. Dynamic remodeling of endometrial extracellular matrix regulates embryo receptivity in cattle.

Seals RC, Lemaster JW, Hopkins FM, Schrick FN. Effects of elevated concentrations of prostaglandin F 2α on pregnancy rates in progestogen supplemented cattle. Prostaglandins & other lipid mediators. 1998;56(5):377-89.

Spencer TE, Forde N, Dorniak P, Hansen TR, Romero JJ, Lonergan P. Conceptus-derived prostaglandins regulate gene expression in the endometrium prior to pregnancy recognition in ruminants. Reproduction. 2013;146(4):377-387.

Spencer TE, Hansen TR. Implantation and establishment of pregnancy in ruminants. Regulation of Implantation and Establishment of Pregnancy in Mammals: Springer; 2015. p. 105-35.

Spencer TE, Johnson GA, Bazer FW, Burghardt RC. Fetal-maternal interactions during the establishment of pregnancy in ruminants. Society of Reproduction and Fertility supplement. 2007;(64):379-96.

Surveyor GA, Gendler SJ, Pemberton L, Das SK, Chakraborty I, Julian J, *et al*. Expression and steroid hormonal control of Muc-1 in the mouse uterus. Endocrinology. 1995;136(8):3639-47.

Thatcher WW, Guzeloglu A, Mattos R, Binelli M, Hansen TR, Pru JK. Uterine-conceptus interactions and reproductive failure in cattle. Theriogenology. 2001;56(9):1435-50.

Vandesompele J, De Preter K, Pattyn F, Poppe B, Van Roy N, De Paepe A, *et al*. Accurate normalization of real-time quantitative RT-PCR data by geometric averaging of multiple internal control genes. Genome biology. 2002;3(7):research0034.

Wolf E, Arnold GJ, Bauersachs S, Beier HM, Blum H, Einspanier R, *et al*. Embryo-Maternal Communication in Bovine–Strategies for Deciphering a Complex Cross-Talk. Reproduction in Domestic Animals. 2003;38(4):276-89.

Wrobel K-H, Kujat R, Fehle G. The bovine tubouterine junction: general organization and surface morphology. Cell and tissue research. 1993;271(2):227-39.

Wydooghe E, Vandaele L, Heras S, De Sutter P, Deforce D, Peelman L, *et al*. Autocrine embryotropins revisited: how do embryos communicate with each other *in vitro* when cultured in groups? Biological Reviews. 2015.

Zhu C; Jiang Z; Bazer FW; Johnson GA; Burghardt RC; Wu G. Aquaporins in the female reproductive system of mammals. Frontiers in Bioscience (Landmark edition). 2014;20:838-871

CHAPTER 3

THE PRE-HATCHING BOVINE EMBRYO TRANSFORMS THE UTERINE LUMINAL METABOLITE COMPOSITION *IN VIVO*

M. Sponchiado[1,2], A. M. Gonella-Diaza[1,3], C. C. Rocha[1], E. G. Lo Turco[4], G. Pugliesi[1], J. L. M. R. Leroy[2], M. Binelli[1,5]

1 Department of Animal Reproduction, School of Veterinary Medicine and Animal Science, University of São Paulo, Pirassununga-SP, Brazil

2 Gamete Research Centre, Faculty of Biomedical, Pharmaceutical and Veterinary Sciences, University of Antwerp, Antwerp, Belgium

3 North Florida Research and Education Center, Institute of Food and Agricultural Sciences, University of Florida, Marianna, FL, USA

4 Human Reproduction Section, Division of Urology, Department of Surgery, São Paulo Federal University, Sao Paulo-SP, Brazil

5 Department of Animal Sciences, University of Florida, Gainesville, FL, USA

SUBMITTED, APRIL 2019

3 THE PRE-HATCHING BOVINE EMBRYO TRANSFORMS THE UTERINE LUMINAL METABOLITE COMPOSITION *IN VIVO*

3.1 ABSTRACT

In cattle, conceptus development after elongation relies on well-characterized, paracrine interactions with the hosting maternal reproductive tract. However, it was unrecognized previously that the pre-hatching, pre-implantation bovine embryo also engages in biochemical signaling with the maternal uterus. Our recent work showed that the embryo modified the endometrial transcriptome *in vivo*. Here, we hypothesized that the embryo modulates the biochemical composition of the uterine luminal fluid (ULF) in the most cranial portion of the uterine horn ipsilateral to the corpus luteum. Endometrial samples and ULF were collected post-mortem from sham-inseminated cows and from cows inseminated and detected pregnant 7 days after estrus. We used quantitative mass spectrometry to demonstrate that the pre-hatching embryo changes ULF composition *in vivo*. Embryo-induced modulation included an increase in concentrations of lipoxygenase-derived metabolites [12(S)-HETE, 15(S)-HETE] and a decrease in the concentrations of amino acids (glycine), biogenic amines (sarcosine), acylcarnitines and phospholipids. The changed composition of the ULF could be due to secretion or depletion of specific molecules, executed by either the embryo or the endometrium, but initiated by signals coming from the embryo. This study provides the basis for further understanding embryo-initiated modulation of the uterine milieu. Early embryonic signaling may be necessary to guarantee optimal development and successful establishment of pregnancy in cattle.

3.2 INTRODUCTION

In cattle, the embryo transits from the oviduct to the uterine lumen and remains loosely attached during the 20-days pre-implantation period. This is a critical window for pregnancy wherein as much as 40% of embryos die (Diskin *et al*., 2011). After implantation, embryo mortality decreases as hemotrophic nutrition is accomplished through placentation. Causes of mortality that occur before implantation are likely associated with disruptions on the complex biochemical interactions that take place between the developing conceptus (embryo and associated membranes) and the endometrium. Interactions between the endometrium and the conceptus occur through the exchange of secretions from both units into the uterine lumen. Secretions that originate from the endometrium are called the histotroph. The histotroph is composed of hormone-mediated, selective transudation of plasma components and release of locally *de novo* synthesized molecules that reach the uterine lumen through excretion from endometrial glands and transport across the epithelium lining the endometrium (Roberts & Bazer, 1988). The arrival of the embryo into the uterus adds molecular complexity to this scenario, as the conceptus releases additional molecules into the uterine luminal fluid (ULF). Moreover, molecules originating from each unit have the potential to influence the function of each other. The classical example is the effect of conceptus derived interferon-tau that inhibits prominent pulses of prostaglandin-F2alpha from the endometrium in cattle (Arosh *et al*., 2016). Furthermore, both the conceptus and the endometrium likely utilize molecules present in the ULF to support cellular proliferation and function. Finally, it is expected that both maternal and embryonic influences on the uterine environment composition change as the pregnancy progresses towards implantation. In summary, the biochemical composition of the ULF dynamically reflects the contributions and the consumption of molecules by both the maternal and the embryonic units during the pre-implantation window.

Exposure to histotroph is a prerequisite for development of the embryo after the hatched blastocyst stage *in vivo*. Indeed, efforts to artificially induce elongation of bovine conceptuses *in vitro* have been unsuccessful (Brandao *et al*., 2004; Alexopoulos *et al*., 2006). Furthermore, perturbations of histotroph composition prior to embryo transfer severely impaired embryo survival and pregnancy establishment in cattle (Martins *et al*., 2018). However, specific luminal metabolite requirements of the earliest phase of embryo development in the uterus are unknown. Nature and concentration of specific molecules likely reflect the changing requirements of the developing embryo in response to a changing

nutrient supply during its migration from the oviduct to the uterus and, subsequently, along the uterine lumen.

Exposure of the endometrium to ULF conditioned by the elongated conceptus is required for the maintenance of pregnancy (Knickerbocker *et al*., 1986). Conceptus-originated molecules, such as interferon-tau and prostaglandins, re-program function of endometrial cells from luteolytic to pregnancy-supporting. However, the influence of the pre-elongation embryo on endometrial function is poorly understood. *In vitro* studies have shown that pre-implantation embryos release a variety of biochemical signals, referred to as embryotropins (Wydooghe *et al.,* 2015), that act in concert to support embryonic development. The paracrine effects of embryo-derived molecules on the maternal tissue is expected to be limited to the immediate embryo surroundings. This may be attributed to the capacity of synthesis, secretion and diffusion of signaling molecules by the early-embryo, which is expected to be proportional to its cellular machinery (˜100 cells at the blastocyst stage). Notwithstanding, we reported previously that the endometrial abundance of specific transcripts was altered by the presence of a day 7-embryo in a spatial-specific manner (Sponchiado *et al*., 2017). The most pronounced effects were found in the cranial region of the uterine horn ipsilateral to the corpus luteum (CL), where the embryos were located on day 7. The main pathways changed by the embryo included type I interferon-response and genes associated to the prostaglandin metabolism. In agreement, recent *in vitro* studies showed that early bovine embryos were able to modulate gene expression of co-cultured endometrial (Talukder *et al*., 2017; Gomez *et al*., 2018; Passaro *et al*., 2018), oviductal (Maillo *et al*., 2015), luteal (Bridi *et al*., 2018) and immune cells (Talukder *et al*., 2017, 2018; Rashid *et al*., 2018). However, a critical unanswered question is whether the female tract has the ability to respond to pre-hatching embryo-derived signals beyond the transcription level, to change its transport and secretory functions and ultimately change the composition of the uterine microenvironment.

We hypothesized that the presence of an embryo modulates the biochemical composition of the ULF in the cranial region of the ipsilateral uterine horn. The aim was to assess a spatially-defined region of the uterine luminal environment, at a time-point coinciding with the apical location of the embryo, to compare the concentration of selected metabolites in ULF between pregnant and sham-inseminated cows. More specifically, we aimed to measure the absolute concentrations of targeted metabolites based on their possible role on early pregnancy biology. The analytes panel included amino acids, biogenic amines, acylcarnitines, lipids, hexoses, and eicosanoids and oxidation products of polyunsaturated

fatty acids. Transcripts analyses were performed on endometrial samples to link the findings at the ULF level to the surrounding endometrial tissue.

3.3 MATERIAL AND METHODS

All experimental procedures were performed in accordance with ethical principles in animal research. Protocol was approved by the Ethics and Animal Handling Committee of the School of Veterinary Medicine and Animal Science of the University of São Paulo (CEUA-FMVZ/USP, n3167260815).

3.3.1 Experimental design

The experimental design aimed to generate a group of pregnant and a group of non-inseminated cows 7 days after estrus as previously described in Sponchiado *et al*. (2017). Thirty-six reproductively normal, cycling, non-lactating, multiparous Nelore (*Bos taurus indicus*) cows were used in this study. Animals were maintained under grazing conditions, supplemented with concentrate, chopped sugarcane, and minerals to fulfil their maintenance requirements. Animals had free access to water. Briefly, estrous cycles were synchronized by i.m. administrations of 500 μg sodium cloprostenol ($PGF_{2\alpha}$ analogue; Ourofino Saúde Animal, Cravinhos, São Paulo, Brazil) and 2 mg estradiol benzoate (Ourofino Saúde Animal), followed by insertion of an intravaginal P4-releasing device (1 g; Ourofino Saúde Animal). Eight days apart, the P4-releasing device was withdrawn, animals received an i.m. administration of 500 μg sodium cloprostenol and an Estrotect (Rockway, Inc. Spring Valley, WI, USA) heat detector patch. Between 48 and 84 h after P4-device removal, cows were checked for signs of estrus activity twice a day. Only animals detected in estrus were maintained in the experiment. On day zero (D0 = estrus), cows were randomly assigned to the experimental groups: (i) Pregnant group (Preg; n = 16), cows were intracervically inseminated 12 h after estrus, with frozen-thawed commercial semen of a proven fertility bull; or (ii) Control group (Con; n = 8), cows were sham-inseminated with semen extender. On D7, all animals were slaughtered.

Transrectal B-mode ultrasonography (7.5-MHz transducer) exams were conducted at 5 time points: at the time of P4-releasing device insertion and removal to measure follicles and to check the presence of a CL; on D0 and D1 to measure the size of the preovulatory follicle and to confirm ovulation. The side of the preovulatory follicles were recorded. On D7, CL

area and the first-wave largest follicle diameter were evaluated. As expected, pre-ovulatory follicle and first-wave largest follicle diameters (on D7) did not differ between the two groups, nor the CL area and plasma P4 concentrations (on D7), as reported previously (Sponchiado *et al*., 2017).

3.3.2 Uterine flushing and endometrial sample collection

Animals were slaughtered by conventional captive bolt stunning followed by jugular exsanguination. The reproductive tracts were collected and transported on ice to the laboratory within 10 min. The uteri were trimmed free of adjacent tissues and processed to ULF and endometrial samples collection, as described previously (Sponchiado *et al*., 2017) and illustrated in Figure 1. Briefly, the uterine horn ipsilateral to the ovary containing the CL was isolated. Starting from the utero-tubal junction (UTJ), locking tweezers were clamped every 8 cm to delimit the anterior, medial and posterior uterine thirds. Each portion was individually flushed by injecting ice-cold PBS into the cranial extremity and collecting the ULF at the caudal end in a petri dish. The anterior, medial and posterior thirds were flushed with 3, 5 and 6 mL of PBS, respectively. Pregnancy status of the inseminated cows was confirmed by visualization of an embryo in the ULF under a stereomicroscope. All embryos found (n = 10 out of 16) were in the ULF recovered exclusively from the ipsilateral anterior third, and were at the expected developmental stage (compact morula or early blastocyst). Only inseminated cows from which an embryo was recovered were kept in the analyses. Uterine flushings were clarified by centrifugation at 1,000 x g for 10 min at 4 ºC. The supernatant was gradually transferred into cryotubes, snap frozen and stored at −80 °C until analysis.

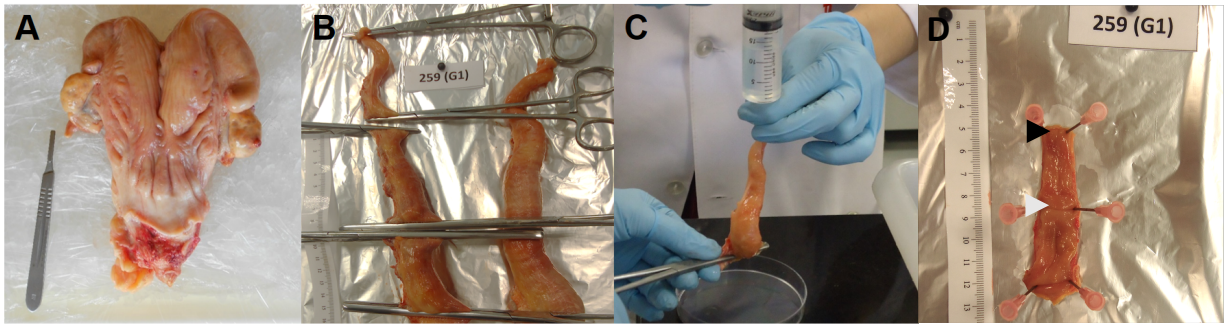

Figure 1. Diagram of sample collection procedure. (A) After slaughter, reproductive tracts were trimmed free of connective tissues; (B) The uterine horn ipsilateral to the corpus luteum was isolated. Starting from the utero-tubal junction (UTJ), locking tweezers were positioned every 8 cm to clamp the anterior, medial and posterior uterine thirds. (C) Ipsilateral anterior thirds were individually flushed by injecting 3 mL of PBS into the UTJ edge. (D) Intercaruncular endometrial samples were dissected from the UTJ (black arrow) and from the lengthwise intermediate region (white arrow) of the third, at the mesometrial side.

For endometrial samples collection, the ipsilateral anterior third was opened longitudinally along the mesometrial line. The endometrial side was exposed and photographed for further surface area measurements. Intercaruncular endometrial fragments were dissected from the uterotubal junction (UTJ) and from the lengthwise intermediate region of the third, at the mesometrial side (Fig. 1). Tissue samples were transferred to cryotubes, snap frozen and stored at –80 ºC until further processing.

3.3.3 Targeted metabolomic measurements

We applied a targeted, quantitative metabolomics approach to analyze ULF samples (Con = 8; Preg = 10) from the anterior ipsilateral uterine third by using the AbsoluteIDQ p180, and Eicosanoid & Oxidized lipids mass spectrometry-based assays (Biocrates Life Sciences AG, Innsbruck, Austria). These validated, targeted assays enabled the simultaneous identification and quantification of up to 205 endogenous metabolites from seven analytic groups including 21 amino acids, 21 biogenic amines, 40 acylcarnitines, 90 glycerophospholipids, 15 sphingolipids, sum of hexoses, and 17 eicosanoids and oxidation products of polyunsaturated fatty acids. The assay procedure and metabolite nomenclature have been described in detail (Römisch-Margl *et al*., 2012). Briefly, the measurements were carried out in a 96-well plate with seven calibration standards and three quality control samples included. Amino acids and biogenic amines were analyzed by UPLC (Waters ACQUITY UPLC, Waters Corporation, USA) system coupled with Xevo tandem quadrupole (TQ; Waters Corporation) and Xevo TQ-S mass spectrometers in positive mode. Acylcarnitines, glycerophospholipids, and sphingolipids were quantified by Waters tandem quadrupole mass spectrometers (Xevo TQ and Xevo TQ-S MS) by flow injection analysis (FIA) in positive mode, whereas hexoses were analyzed using a subsequent acquisition in negative mode. Detection and quantification of the analytes was achieved using internal standards in multiple reaction monitoring (MRM) mode. Calculation of the metabolite concentrations analyzed by FIA (acylcarnitines, glycerophospholipids, sphingolipids, and hexoses) was performed using Met*IDQ* software (Version 5– 4-8-DB100-Boron-2607, Biocrates Life Sciences AG). Analysis of peaks obtained by UPLC (amino acids and biogenic amines) was performed using TargetLynx Application Manager, and the results were imported into Met*IDQ* software for further processing.

Eicosanoids and related compounds were detected by Biocrates triple quadrupole MS-based platform in negative multiple-reaction monitoring detection mode as per a method

reported previously (Unterwurzacher *et al*., 2008). Oxidized polyunsaturated fatty acids were extracted from ULF samples by methanolic protein precipitating process. Analysis was performed by HPLC MS/MS on a Sciex 5500 QTRAP™ (AP Sciex, Darmstadt, Germany) instrument. Metabolites were quantified by comparison to structurally similar molecules labelled with stable isotopes added to the samples in defined concentrations as internal standards in MRM mode.

3.3.4 Metabolites panel

Throughout the article, amino acids are abbreviated based on their international notation. Acylcarnitines (Cx:y) are notated according to the fatty acid that is bound. Glycerophospholipids (sn) are classified according to the presence of ether (alkyl) or ester (acyl) residues attached to the glycerol moiety. The prefix 'lyso' denotes a single fatty acid or fatty alcohol bond on the sn-1 position of the glycerol moiety, as denoted by a single letter (acyl, a; alkyl, e). Two letters (diacyl, aa; acyl-alkyl, ae) means that the sn-1 and sn-2 positions on the glycerol moiety are each bound to a fatty acid or fatty alcohol residue. Sphingomyelins (SM) and hydroxysphingomyelins (SM-OH) are abbreviated based on the lipid chain composition (x:y). Biochemical name, abbreviation and PubChem CID of metabolites are listed in Supplemental Table S3 by class.

In addition to individual metabolite assessment, groups of metabolites were computed by sums or ratios of the amounts of analytes belonging to certain families or chemical structures to provide detailed insight into a wide range of functions. Details of ratios calculated and functional groups are provided in Supplementary Table S4.

3.3.5 Total RNA isolation and transcript abundance analysis

Using a stainless-steel apparatus, frozen endometrial fragments (~40 mg) were mechanically minced. Immediately after, the macerate was homogenized with lysis buffer from PureLink® RNA mini kit (Ambion, Life Technologies, Carlsbad, California, USA), following manufacturer's guidelines. The homogenate was passed ten times through a 21-ga needle accoupled to a 3 mL syringe to maximize lysis. Cell debris were removed by centrifugation at 12,000 g for 1 min at 4 ºC. Subsequentially, the supernatant was loaded in RNeasy columns for further RNA isolation. Final RNA was eluted with 30 µL diethyl pyrocarbonate (DEPC)-treated water. Total RNA yield and purity were evaluated using

NanoVue Plus Spectrophotometer (GE Healthcare, UK) by the absorbance at 260 nm and the 260/280 nm ratio, respectively.

Samples of RNA (400 ng) were subjected to treatment with DNase I Amplification Grade (Thermo Fisher Scientific) as per manufacturer's instructions. Total RNA was reverse transcribed using Oligo(dT)12-18 Primers (Invitrogen) and dNTP Mix (Thermo Fisher Scientific). Samples were incubated at 65 °C for 5 min. First strand cDNA was synthesized adding the SuperScript IV Reverse Transcriptase (Thermo Fisher Scientific) to the RNA-primer mix, followed by incubation at 55 °C for 10 min and inactivation at 80 °C for 10 min. cDNA samples were stored at −20 °C.

The abundance of specific transcripts was determined by Real-Time PCR. Optimized primers were designed based on GenBank Ref-Seq (*Bos taurus*) mRNA sequences. Only primer pairs with an efficiency ranging from 90 to 110% were used. Primers assay efficiency was calculated based on the slope obtained from a standard curve (5-point serial dilution). Primers details are presented on Supplementary Table S5. Reactions were performed in triplicates, in 96-well plates (Life Technologies), in a final volume of 20 µL. PCR amplification was carried out using the Step One Plus (Applied Biosystems, MA, USA) thermal cycler, using Power SYBR Green PCR Master Mix (Life Technologies). Cycling conditions were as follows. Initial denaturation was performed at 95 ºC for 10 min, followed by 40 cycles of denaturation at 95 ºC for 15 s and annealing reaction at 60 ºC for 60 s. Melting curve analyses (from 60 to 95 ºC) was performed to evaluate the amplification product. Negative controls (DEPC water replacing cDNA) were included in every run. Cycle thresholds (Cts) were determined using the LinReg PCR software as described by Ruijter *et al.* (2009). Target genes Ct values were normalized by the geometric mean of reference genes actin beta (*ACTB*), peptidylprolyl isomerase A (*PPIA*), and glyceraldehyde-3-phosphate dehydrogenase (*GAPDH*) transcript abundance values using the equation described by Pfaffl (Pfaffl, 2001).

3.3.6 Data preparation: Endometrial area measurements and normalization

To circumvent possible inaccuracies resulting from the flushing procedure due to different size of the uterine thirds between cows, we normalized the metabolite concentration values to the respective endometrial area. Endometrial area was measured with Image J 1.50i (National Institutes of Health, USA; http://rsb.info.nih.gov/ij/) software with the polygon

selections. Prior to statistical analysis, metabolite concentration (nmol) values were adjusted by endometrial area (cm^2) of the uterine third and are expressed as $nmol/cm^2$.

3.3.7 Bioinformatics and statistical analyses

For statistical analyses, only metabolites with more than 70% of their concentration values in the dynamic range were considered. Metabolic pathways and Multivariate data analysis were carried-out using the web-based metabolomic data processing tool MetaboAnalyst 4.0 (Xia & Wishart, 2016). Metabolite concentrations were Pareto scaled and the method K-Nearest Neighbours was used to impute the missing values to generate the heatmap, sparse partial least squares-discriminate (sPLS-DA) and Metabolite Sets Enrichment analyses. Heatmap was set considering P-values between the two groups and the Ward's methodology as clustering algorithm. For biological interpretation of the metabolite dataset, we mapped the quantified metabolites to the KEGG pathway database (Kyoto Encyclopedia of Genes and Genomes; www. genome.jp/kegg/). Metabolite Sets Enrichment Analysis was conducted on metabolite data mapped according to Human Metabolome Database (HMDB).

Univariate data analyses were carried-out using SAS software v. 9.3 (SAS Inst. Inc., Cary, NC, USA). Normal distribution and homogeneity of variances were ensured by Shapiro-Wilk and Welch's test, respectively. Variables presenting heterogeneity of variances were transformed using natural logarithm. Concentrations and relative mRNA abundance were analyzed for the main effect of group (Con *vs.* Preg) by two-tailed one-way ANOVA. To further validate the statistical significance, metabolite concentration results were subjected to False Discovery Rate (FDR) correction for multiple comparisons. The Q-value for FDR controlling procedure was set to 0.25 (Reiner *et al*., 2003). Statistical significance was stated at $P \leq 0.05$, and a probability of $0.05 < P \leq 0.10$ indicates a trend towards significance. Results are presented as means ± SEM.

3.4 RESULTS

3.4.1 Metabolite profiling of ULF between Pregnant vs. Control cows

Targeted MS metabolomics was used to address the influence of one pre-hatching embryo on metabolite composition of ULF recovered from the ipsilateral anterior third on day 7 after estrus. Of the 205 metabolites quantified, 167 were included in the analyses.

Metabolites that were not detected in more than 30% of samples of both experimental groups were excluded from analyses.

3.4.1.1 Multivariate analyses: Discriminant metabolomic signatures in the ULF from Control vs. Pregnant cows

The heatmap shown in Fig. 2A revealed that: (i) the metabolomic profile of Preg cows is associated with an overall decrease of metabolite concentrations in the ULF compared to the Con group, and (ii) the clustering was affected mainly by compounds belonging to phospholipids, eicosanoids, acylcarnitines, amino acids and biogenic amines classes.

Metabolite Sets Enrichment Analysis was performed to determine, within the specific classes of metabolites measured, which biologically meaningful pathways were overrepresented. The dataset was mainly enriched for molecules involved in lipid and amino acid metabolism. The three top-score enrichment category were, in order of decreasing significance, (i) arachidonic acid metabolism; (ii) alpha linolenic acid and linoleic acid metabolism; and (iii) glycine, serine and threonine metabolism (Fig. 2B).

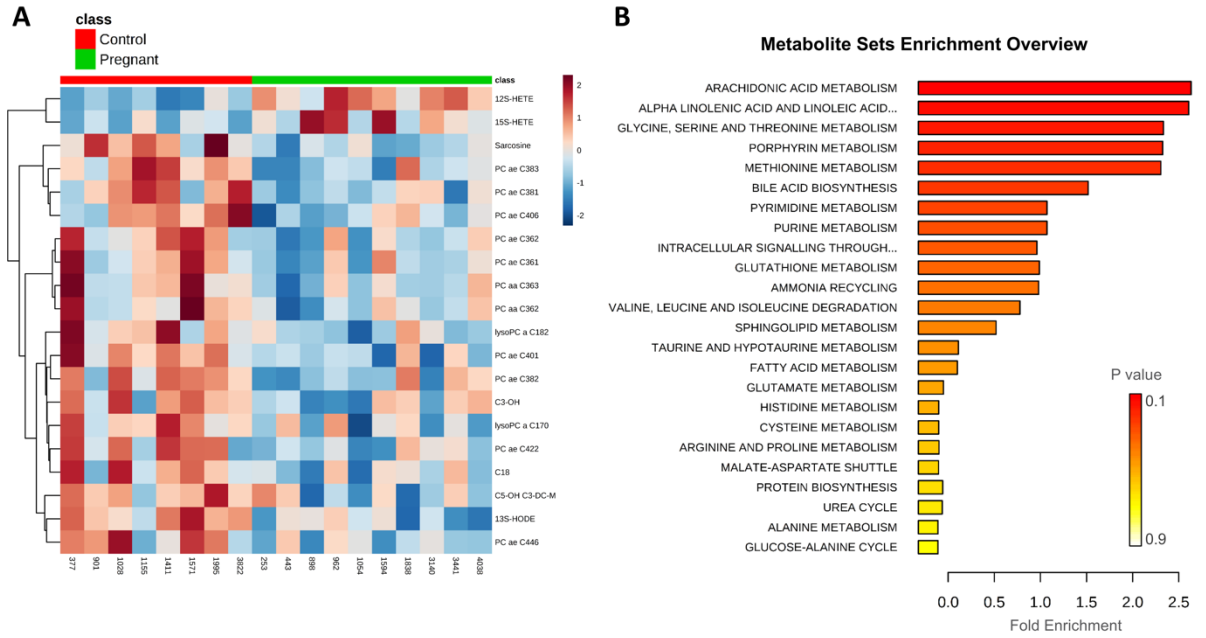

Figure 2. (A) Heatmap depicting the top 20 metabolites differently abundant between Pregnant and Control ULF samples based on *P*-values. (B) Quantitative Enrichment Analysis highlighted the metabolic pathways that were enriched in the Pregnant compared to the Control group, using the MetaboAnalyst 4.0 functional interpretation tools. The horizontal bars summarize the main metabolite sets identified in this analysis; the bars are colored based on their P values and the length is based on the -fold enrichment.

Ortho PLS-DA performed on the metabolomics data revealed a clear discrimination between Preg and Con ULF profiles (Fig. 3), with the following parameters: $R^2X = 0.114$, $R^2Y = 0.544$, and $Q^2 = 0.348$. All metabolites that passed quality control were included in this analysis. The top-seven most discriminant metabolites contributing to this model were: 12(S)-HETE, 15(S)-HETE, PC ae C42:5, DHA, LysoPC a C26:0, arachidonic acid (AA) and PGF_{2a}.

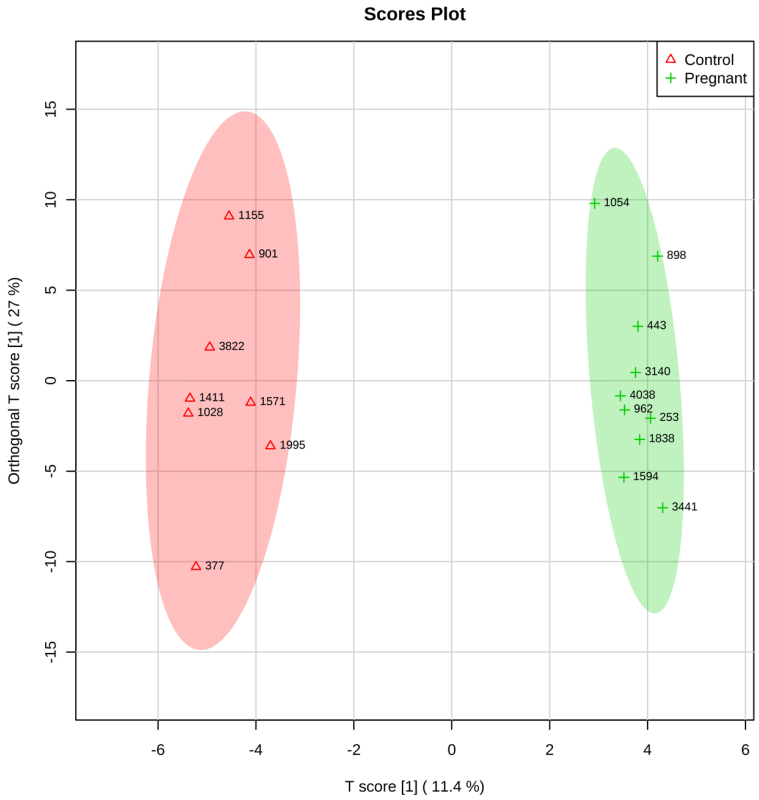

Figure 3. Ortho PLS-DA scatter plot depicting different ULF metabolomic profiles between Control and Pregnant cows on day 7 after oestrus. Each dot in the plot represents an animal according to the metabolite profile and groups are identified with ring ellipses corresponding to 95% confidence intervals.

3.4.1.2 Univariate analyses

We examined differences in concentrations of single analytes and groups of analytes of a common biochemical classification between the two experimental groups. Univariate analysis followed by FDR correction showed that, out of 167 metabolites that passed quality control, 22 (approximately 13%) showed significantly different concentrations ($P \leq 0.05$; FDR corrected) between Con versus Preg cows. Remarkably, only two of these 22 metabolites were found in significantly increased concentration in ULF of Preg cows. Comparisons between the abundances of each metabolite according to pregnancy status are presented in Supplementary Tables S4 through S7 and Figures 4 to 7, according to biochemical classification.

3.4.1.3 Recoverable amounts of amino acids and biogenic amines in ULF

Concentrations of individual amino acids and biogenic amines according to group are presented in full on Supplemental Table S6. The non-essential amino acid glutamate was the most abundant in the uterine flushings (5323 nmol/cm^2 of endometrial area) from both Con and Preg cows, followed by glycine (4293 nmol/cm^2) and alanine (1182 nmol/cm^2). Regarding the biogenic amines, taurine was the most prevalent (3705 nmol/cm^2), followed by sarcosine (407 nmol/cm^2) and putrescine (323 nmol/cm^2). Total recoverable amounts of amino acids and biogenic amines (Table 1) were similar between ULF of Con and Preg cows. Of the amino acids and biogenic amines quantified, only glycine (0.7-fold; $P \leq 0.05$) and sarcosine (0.6-fold; $P \leq 0.01$), respectively, showed significantly decreased concentration in the ULF of Preg compared to Con cows, as shown in Figure 4. Interestingly, glycine and sarcosine are both part of the glycine, serine and threonine metabolism pathway. Sums of small neutral and osmotic-stress protection amino acids were lower ($P \leq 0.05$) 0.74 and 0.75-fold, respectively, in the Preg group compared to the controls.

Table 1. Sums and ratios of amino acids (AA) and biogenic amines (BA) concentrations in uterine luminal fluid from Control (Con) and Pregnant (Preg) cows. Values are expressed as nmol/cm^2 of endometrial area; mean ± SEM. Metabolite groups definitions are on Supplementary Table S4.

Metabolite groups	**Group**		**P value[a]**	**Log2 Fold-change[b]**
	Con (n = 8)	**Preg (n = 10)**		
Total AA	19325.27 ± 1563.99	17447.25 ± 1895.85	0.36	-0.15
Non-essential AA	18861.09 ± 1469.75	17136.99 ± 1859.45	0.37	-0.14
Acidic AA	6766.67 ± 720.65	6154.43 ± 578.02	0.51	-0.14
Small Neutral AA	10951.75 ± 903.36	8130.94 ± 655.04	0.02	-0.43
Osmotic-stress protection AA	11807.05 ± 940.68	8808.92 ± 710.92	0.02	-0.42
Glucogenic AA	6538.66 ± 630.91	5201.54 ± 661.67	0.17	-0.32
Glutathione precursors AA	11229.58 ± 997.77	9936.98 ± 996.13	0.39	-0.18
Total BA	5342.97 ± 442.49	4989.55 ± 675.82	0.70	-0.10
Spermidine/Putrescine[c]	0.18 ± 0.04	0.17 ± 0.02	0.83	-0.09
Spermine/Spermidine[d]	0.78 ± 0.16	0.57 ± 0.11	0.30	-0.43

Groups of metabolites in bold were different between Con and Preg.
[a]Statistical analyses were carried out by one-way ANOVA.
[b]Data are represented as fold-change of the metabolite concentration between Preg and Con groups.
[c]Ratio of Spermidine to Putrescine was calculated to access the activity of Spermidine synthase.
[d]Ratio of Spermine to Spermidine was calculated to access the activity of Spermine synthase.

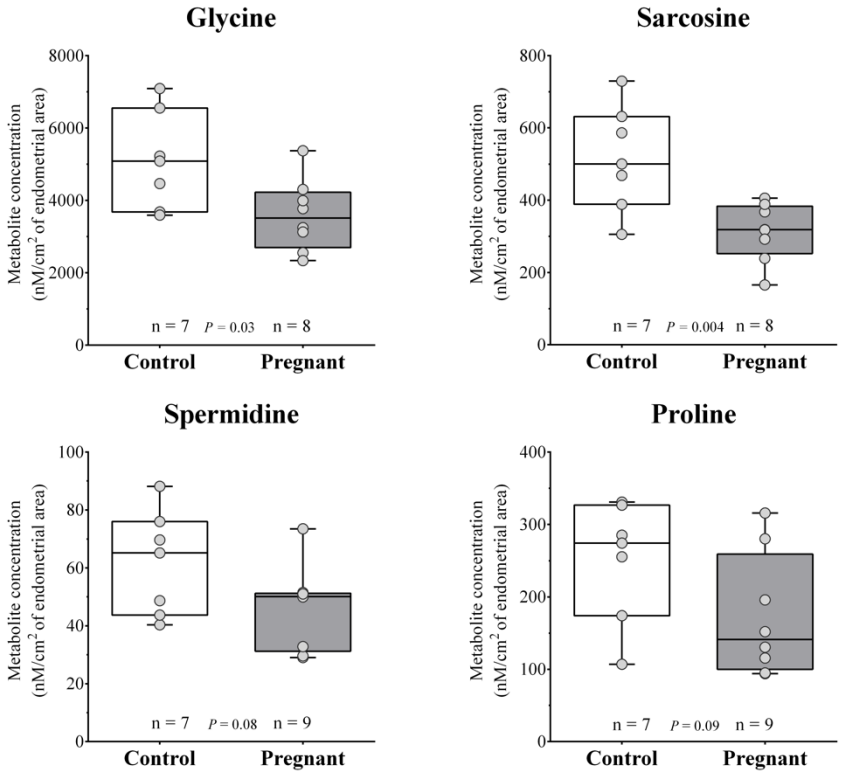

Figure 4. Box and whisker plots of amino acids and biogenic amines that show significant ($P \leq 0.05$) or approaching ($P \leq 0.1$) difference between Control and Pregnant uterine luminal fluids.

3.4.1.4 Recoverable amounts of Acylcarnitines in ULF

Concentrations of individual acylcarnitines according to group are presented in full on Supplemental Table S7. Short-chain acylcarnitines were the most abundant in ULF, followed by medium- and long-chain acylcarnitines (Table 2). Three acylcarnitines [Hydroxypropionylcarnitine (C3-OH), hydroxyisovalerylcarnitine (C5-OH), and hydroxyhexadecanolycarnitine (C16-OH)] of the 40 identified were found to be in significantly lower concentrations in the ULF from Preg cows (Fig. 5). Remarkably, all three metabolites that were different between the study groups were acylcarnitine esters derived from hydroxylated acids.

Table 2. Sums and ratios of carnitine and acylcarnitines (AC) concentrations in uterine luminal fluid from Control (Con) and Pregnant (Preg) cows. Acylcarnitines were categorized in esters derived from dicarboxylic acids (DC), esters derived from hydroxylated acids (OH), total short-chain acylcarnitines, total medium-chain acylcarnitines and total long-chain acylcarnitines. Values are expressed as nmol/cm^2 of endometrial area; mean ± SEM. Metabolite groups definitions are on Supplementary Table S4.

Metabolite groups	Group		P value[a]	Log2 Fold-change[b]
	Con (n = 8)	Preg (n = 10)		
Total Recoverable Amounts of AC	239.56 ± 37.22	221.77 ± 25.88	0.69	-0.10
Total short-chain AC	75.86 ± 9.22	74.46 ± 9.22	0.92	-0.03
Total medium-chain AC	15.07 ± 1.23	13.43 ± 0.63	0.23	-0.17
Total long-chain AC	5.44 ± 0.52	4.80 ± 0.43	0.35	-0.18
Acylcarnitine/Free carnitine	0.68 ± 0.07	0.57 ± 0.04	0.22	-0.25
Total short-chain AC/Free carnitine	0.70 ± 0.07	0.64 ± 0.06	0.55	-0.14
CPT-I([C16+C18]/C0)	0.046 ± 0.004	0.040 ± 0.004	0.32	-0.22
Total Esters derived from DC/Total AC	0.032 ± 0.003	0.031 ± 0.003	0.84	-0.04
Esters derived from HO	4.69 ± 0.33	4.25 ± 0.29	0.33	-0.14
Esters derived from DC	6.98 ± 0.43	6.37 ± 0.32	0.25	-0.14

[a]Statistical analyses were carried out by one-way ANOVA.
[b]Data are represented as fold-change of the metabolite concentration between Preg and Con groups.

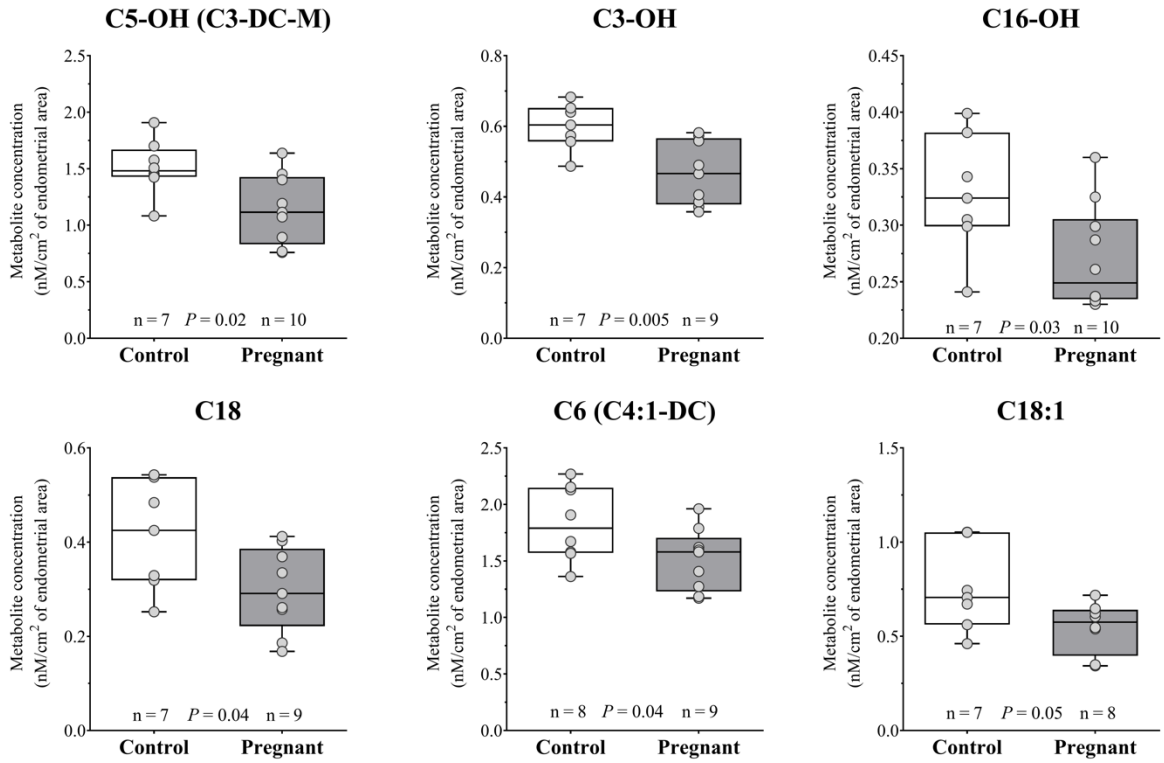

Figure 5. Box and whisker plots of acylcarnitines that show significant ($P \leq 0.05$) or approaching ($P \leq 0.1$) difference between Control and Pregnant uterine luminal fluids.

3.4.1.5 Recoverable amounts of Phosphatidylcholines and Lysophosphatidylcholines in ULF

Concentrations of individual phospholipids according to group are presented in full on Supplementary Table S8. LysoPC a C14:0 was the most abundant phosphatidylcholine measured (243 nmol/cm^2). Lysophosphatidylcholines represent 58% (Table 3) of the total phosphatidylcholines recovered in the ULFs. Total abundance of phosphatidylcholines (calculated by the sum of lyso-, diacyl- and acyl-alkyl-phosphatidylcholines; Table 3) was similar between ULF of Con and Preg cows. Total diacyl-phosphatidylcholines (P = 0.08) and polyunsaturated glycerophosphocholines (PUFA; P = 0.07) concentrations approached a significant reduction in the Preg group (Table 3). The ratio between PUFA and saturated (SFA) phosphatidylcholines showed a significant decrease in the Preg ULF samples (Table 3). This indicated that the activity of fatty acid desaturases of the endometrium might also be altered by pregnancy. There were 14 phosphatidylcholines identified with decreased concentration in the Preg group compared to its counterparts (Fig. 6), comprising 2 lyso-, 3 diacyl- and 9 acyl-alkyl-phosphatidylcholines. Interestingly, from the metabolites in different concentrations between groups, LysoPC a C18:2 and the diacyl-phosphatidylcholines (PC aa C36:0, PC aa 36:3, PC aa 36:5 and PC ae 36:2) are composed by one or two chains of stearic acid, a saturated fatty acid with an 18-carbon chain.

Table 3. Sums and ratios of Phospholipids concentrations in uterine luminal fluid from Control (Con) and Pregnant (Preg) cows. Phospholipids were grouped in Phosphatidylcholines (PC) and Lysophosphatidylcholines (LysoPC), diacyl- (PC aa) or acyl-alkyl- (PC ae) phosphatidylcholines, saturated (SFA), monounsaturated (MUFA) and polyunsaturated (PUFA) glycerophosphocholines. Values are expressed as nmol/cm^2 of endometrial area; mean ± SEM. Metabolite groups definitions are on Supplementary Table S4.

Metabolite groups	**Group**		**P value[a]**	**Log2 Fold-change[b]**
	Con (n = 8)	**Preg (n = 10)**		
Total recoverable amounts of phospholipids	478.90 ± 37.61	429.32 ± 20.76	0.23	-0.15
Total recoverable amounts of LysoPC	297.98 ± 22.49	280.51 ± 13.05	0.49	-0.09
Total recoverable amounts of PC	182.30 ± 16.40	148.81 ± 9.81	0.08	-0.29
Total LysoPC/Total PC[c]	1.66 ± 0.13	1.92 ± 0.08	0.10	0.21
Total PC aa	108.42 ± 12.35	83.71 ± 7.22	0.08	-0.38
Total PC ae	73.88 ± 5.56	65.10 ± 3.13	0.16	-0.18
Total MUFA (PC)	41.44 ± 6.16	30.18 ± 3.57	0.11	-0.45
Total PUFA (PC)	84.33 ± 7.74	67.26 ± 4.87	0.07	-0.32
Total SFA (PC)	56.53 ± 4.45	51.37 ± 2.41	0.29	-0.14
MUFA (PC)/SFA (PC)[d]	0.74 ± 0.10	0.59 ± 0.06	0.20	-0.34
PUFA (PC)/MUFA (PC)[d]	2.19 ± 0.13	2.33 ± 0.12	0.45	0.08
PUFA (PC)/SFA (PC)[d]	1.42 ± 0.08	1.24 ± 0.03	0.04	-0.20

Groups of metabolites in bold were different between Con and Preg group.
[a]Statistical analyses were carried out by one-way ANOVA.
[b]Data are represented as fold-change of the metabolite concentration between Preg and Con groups.
[c]Ratio of LysoPC to PC is an indicator of phospholipase activity.
[d]Ratios of MUFA to SFA, PUFA to MUFA, and PUFA to SFA were measures of the activity of fatty acid desaturases.

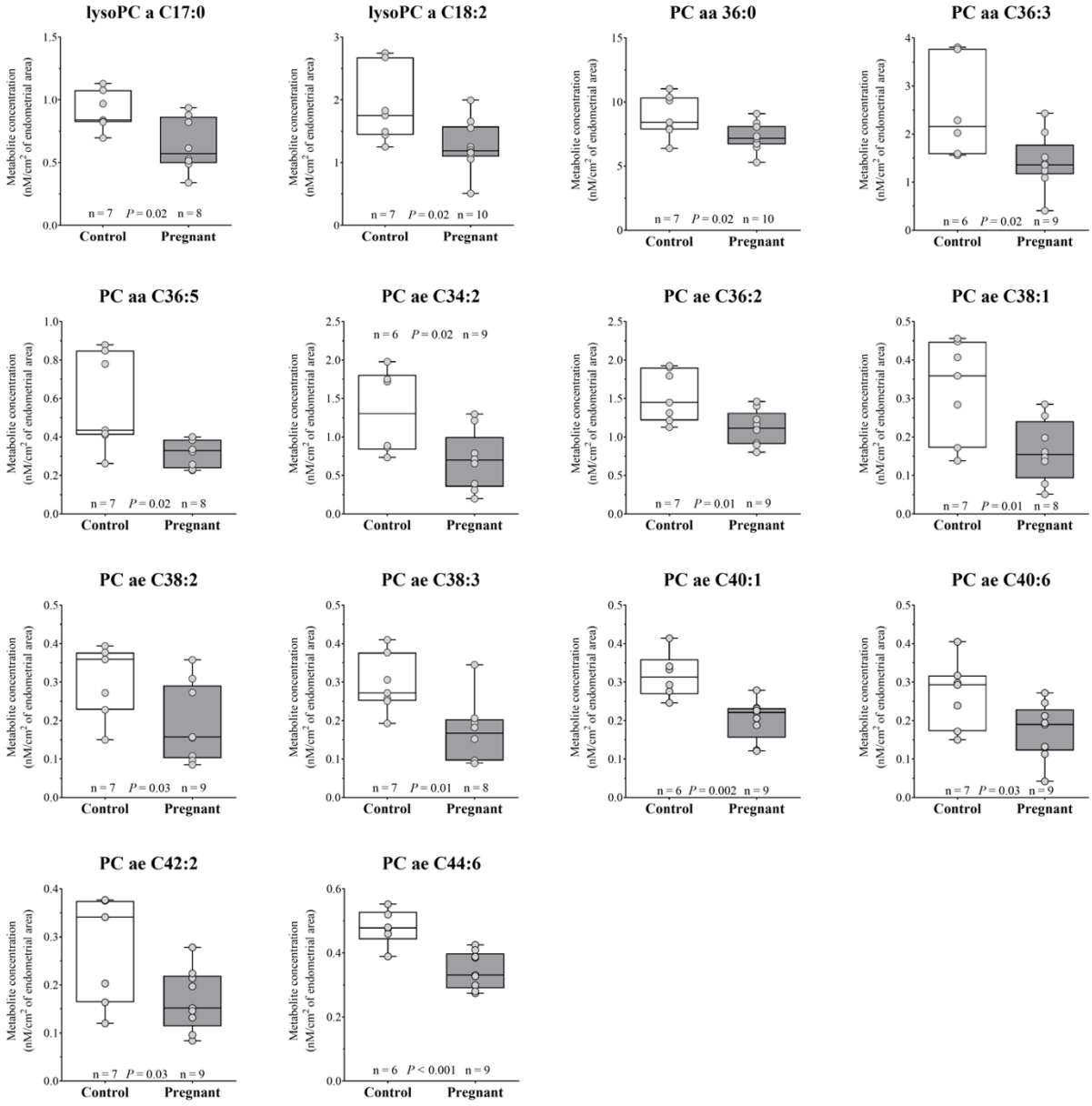

Figure 6. Box and whisker plots of phospholipids that show significant ($P \leq 0.05$) difference between Control and Pregnant uterine luminal fluids.

3.4.1.6 Recoverable amounts of sphingolipids in ULF

Concentrations of individual sphingolipids according to group are presented in full on Supplemental Table S9. We detected six species of sphingomyelins (C16:0, C16:1, C18:0, C18:1, C24:0 and C24:1) and four species of hydroxysphingomyelins (C16:1, C22:1, C22:2 and C24:1) in ULF obtained from both groups. Sphingomyelin C16:0 was the most abundant in the uterine flushings (19.84 nmol/cm^2 of endometrial area). There was no difference in the concentration of any sphingolipid between Con and Preg cows. However, the total

recoverable amount of hydroxysphingomyelins tended to be lower (0.67-fold; $P \leq 0.1$; Table 4) in the Preg ULF samples.

Table 4. Sums and ratios of Sphingolipids concentrations in uterine luminal fluid from Control (Con) and Pregnant (Preg) cows. Metabolites were grouped in sphingomyelins (SM) and hydroxysphingomyelins (SM-OH) and according to the unsaturation. Values are expressed as nmol/cm^2 of endometrial area; mean ± SEM. Metabolite groups definitions are on Supplementary Table S4.

Metabolite groups	Group		P value[a]	Log2 Fold-change[b]
	Con (n = 8)	Preg (n = 10)		
Total SM	36.87 ± 6.50	28.84 ± 4.49	0.31	-0.36
Total SM-OH	4.76 ± 0.85	3.18 ± 0.43	0.09	-0.58
Ratio SM/SM-OH	7.85 ± 0.39	9.02 ± 0.51	0.13	0.20
Total unsaturated SM	5.40 ± 0.96	4.31 ± 0.68	0.36	-0.32
Total saturated SM	31.47 ± 5.55	24.53 ± 3.85	0.31	-0.36

Group of metabolites in bold tended to be different between Con and Preg group.
aStatistical analyses were carried out by one-way ANOVA.
bData are represented as fold-change of the metabolite concentration between Preg and Con groups.

3.4.1.7 Recoverable amounts of hexoses in ULF

In this study, hexoses were the most abundant metabolite class identified in the ULF (334,474.62 nmol/cm^2 of endometrial area). There was no difference in hexoses concentration between Con and Preg ULF samples (Supplemental Table S10).

3.4.1.8 Recoverable amounts of eicosanoids and oxidation products of polyunsaturated fatty acids in ULF

Eicosanoid and oxidation products of polyunsaturated fatty acids profiling in ULF from Con and Preg cows is presented in Tables 5 and 6. Arachidonic acid, an omega-6 fatty acid, was the most abundant polyunsaturated fatty acid in uterine flushings from both Con and Preg groups, followed by Docosahexaenoic acid, an omega-3 fatty acid. Multiple cyclooxygenase, lipoxygenase, and cytochrome P450 metabolite products were identified. Regarding cyclooxygenase metabolite products, only $PGF_{2\alpha}$ and PGI_2 (inferred from measurement of 6-keto-Prostaglandin F1alpha) were detected in the ULF samples, while PGE_2, PGD_2, PGEM and TXB_2 were below the limit of detection. Univariate analysis revealed a main effect of group between Con and Preg ULF for lipoxygenase metabolite products, 12(S)-HETE, 15(S)-HETE and 13(S)-HODE, wherein 12(S)-HETE and 15(S)-HETE were 2.54 and 2.84-folds greater in the Preg ULF, respectively. However, 13(S)-HODE was 0.46-fold in lower concentration in ULF from the Preg group. Regarding

cyclooxygenase metabolite products, $PGF_{2\alpha}$ concentration tended to be higher (1.18-fold) in the Preg group.

Table 5. Eicosanoids and oxidation products of polyunsaturated fatty acids concentration in uterine luminal fluid from Control (Con) and Pregnant (Preg) cows. Values are expressed as nmol/cm^2 of endometrial area; mean ± SEM. Biochemical name, abbreviation and PubChem CID of metabolites are listed in Supplemental Table S3 by class.

Metabolites	Group		P value	FDR significance[a]	Log2 Fold-change[b]
	Con (n = 8)	Preg (n = 10)			
Arachidonic acid	12.95 ± 1.81	18.27 ± 0.90	0.18	n.s.	0.50
Docosahexaenoic acid (DHA)	2.58 ± 0.25	3.47 ± 0.11	0.06	n.s.	0.43
13(S)-HODE[c]	0.14 ± 0.02	0.06 ± 0.004	0.009	*	-1.12
12(S)-HETE[c]	0.06 ± 0.006	0.15 ± 0.003	0.0001	**	1.34
15(S)-HETE[c]	0.013 ± 0.005	0.038 ± 0.003	0.02	*	1.51
6-keto-Prostaglandin F1alpha (PGI_2)[d]	0.08 ± 0.01	0.09 ± 0.002	0.74	n.s.	0.06
Prostaglandin F2alpha ($PGF_{2\alpha}$)[d]	0.07 ± 0.004	0.09 ± 0.001	0.04	n.s.	0.24

Metabolites in bold were different between Con and Preg group by ANOVA followed by FDR correction.
[a]Statistical analyses were carried out by one-way ANOVA followed by FDR correction for multiple comparisons. Magnitude of effect is indicated by: ** $P \leq 0.01$; * $P \leq 0.05$; n.s. $P > 0.05$.
[b]Data are represented as fold-change of the metabolite concentration between Preg and Con groups.
[c]Lipoxygenase metabolite products.
[d]Cyclooxygenase metabolite products.

Table 6. Sums of eicosanoids and oxidation products of polyunsaturated fatty acids concentrations in uterine luminal fluid from Control (Con) and Pregnant (Preg) cows. Metabolites were grouped according to it derivation from the cycloxygenase (COX) and lipoxygenase (LOX) pathways. Values are expressed as nmol/cm^2 of endometrial area; mean ± SEM. Metabolite groups definitions are on Supplementary Table S4.

Metabolite groups	Group		P value[a]	Log2 Fold-change[b]
	Con (n = 8)	Preg (n = 10)		
COX pathway	0.152 ± 0.009	0.167 ± 0.007	0.20	0.14
LOX pathway	0.224 ± 0.041	0.225 ± 0.031	0.98	0.00

[a]Statistical analyses were carried out by one-way ANOVA.
[b]Data are represented as fold-change of the metabolite concentration between Preg and Con groups.

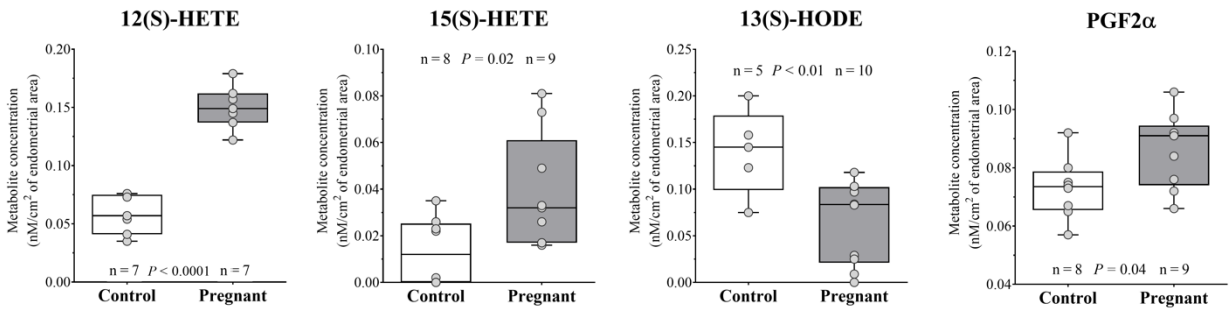

Figure 7. Box and whisker plots of eicosanoids and oxidation products of polyunsaturated fatty acids that show significant ($P \leq 0.05$) difference between Control and Pregnant uterine luminal fluids.

3.4.2 Transcript abundance on endometrial samples

Because of the significantly greater abundance of lipoxygenase-related metabolites in ULF from pregnant cows, we measured the abundance of transcripts coding for Lipoxygenase enzymes (*ALOX5, ALOX5AP, ALOX15B* and *ALOX12*), and lipoxygenase metabolite targets (*PPARG*, *RXRA* and *LPL*) in endometrial samples by Real Time PCR. Additionally, because of the lower abundance of glycine in the ULF from pregnant cows, we measured the abundance of a Glycine Transporter (*SLC6A9*) mRNA. Transcripts for *ALOX12* and *ALOX15B* were respectively 2.56-folds up-regulated and 0.54-fold down-regulated in the UTJ from Pregnant animals (Fig. 8). All the Lipoxygenases addressed in this study were similar between groups in the endometrium collected from the intermediate region of the anterior third. However, a downregulation of *SLC6A9* (a Glycine transporter; 0.76-fold) transcripts was found in the Preg endometrial tissue in the intermediate region, suggesting an embryo-modulated, endometrial response that was consistent with the lower Glycine concentration in the ULF. Transcripts for *PPARG* and *RXRA* were detected in endometrial tissue, as expected, but there was no effect of group on mRNA abundance of *PPARG* and *RXRA* in neither the UTJ or the intermediate anterior third endometrial samples. Similarly, mRNA abundance of *LPL*, a target-gene of PPARG-RXRA complex activation was not affected by group.

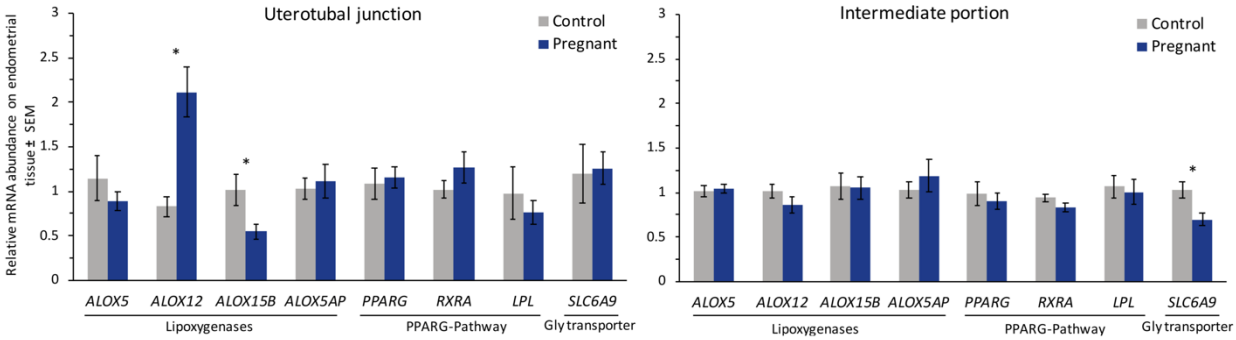

Figure 8. Relative mRNA abundance of Lipoxygenases, PPARG-pathway associated genes and Glycine Transporter in Control and Pregnant endometrial samples dissected from the uterotubal junction and the lengthwise intermediate portion of the anterior third of the ipsilateral uterine horn. Data are shown as arbitrary units; mean ± SEM.

3.5 DISCUSSION

Accumulating evidence supports the idea that the early bovine embryo is more than a passive passenger through the maternal reproductive tract. Embryo-induced effects, at transcriptional level, on oviductal (Maillo *et al*., 2015), endometrial (Sponchiado *et al*., 2017;

Talukder *et al*., 2017; Gomez *et al*., 2018; Passaro *et al*., 2018), luteal (Bridi *et al*., 2018) and immune (Talukder *et al*., 2018; Rashid *et al*., 2018) cells have been reported. In the present study, we further advanced the understanding of the embryo effects in early pregnancy. We demonstrated for the first time that the pre-hatching embryo changes the uterine microenvironment as early as day 7 after estrus *in vivo*. In the present study, we had the unique opportunity to collect ULF from the anterior third of the uterine horn. Consequently, metabolite concentrations measured represent the local concentrations. This is critical because due to the cranial-most localization of the embryo at day 7, it is possible that a greater magnitude of effects of the embryo were manifest in its closest proximity. Such modulation included changes in concentrations of lipoxygenase-derived metabolites, amino acids, biogenic amines, acylcarnitines and phospholipids. The changed composition of the ULF could be due to secretion or depletion of specific molecules, executed by either the embryo or the endometrium, but initiated by signals coming from the embryo. Another major contribution of our study is the expanded inventory and absolute quantification of naturally occurring compounds on ULF. This is important, because most published metabolomics-based investigations are either restricted to one class of analytes and only relative abundances are reported.

Multivariate analyses showed a clear separation between animals pertaining to the two experimental groups. This indicates that the pre-hatching embryo changes the global ULF metabolome profile *in vivo*. Eicosanoids and oxidation products of polyunsaturated fatty acids was the main biochemical class contributing to the discriminant model. Univariate analyses revealed 22 metabolites displaying different concentrations between Preg and Con ULF samples after FDR correction. If all comparisons showing $P \leq 0.05$ were considered regardless of FDR correction, we would have detected 33 analytes with different abundances between Preg and controls. Out of the 22 metabolites showing different concentrations among the two experimental groups, 20 were in lower concentration in the ULF recovered from Pregnant animals. *In vivo*, the ULF composition is modulated by both the endometrial and embryonic units, as well as their molecular interactions. Lower concentrations of metabolites in ULF samples could be attributed to at least four possibilities: (1) a hypermetabolic state of the endometrium, that resulted in increased consumption of substrates by the endometrial tissue with a consequent reduced transport towards the lumen; (2) an overall down-regulation of transport activity in the endometrial epithelia; (3) an increased resorption of metabolites from the uterine lumen towards the lining endometrial epithelium; (4) intake of compounds present in the uterine fluid by the embryo; or combinations of the above. Validation of such

hypothetical mechanisms requires further investigation. Most pregnancy-induced differences were found in eicosanoids, amino acids, biogenic amines, acylcarnitines and phospholipid classes.

The pre-hatching embryo modulates the eicosanoid metabolism in the uterine lumen. Pregnant animals presented greater concentrations of 12(S)-HETE and 15(S)-HETE, but decreased amounts of 13(S)-HODE. These metabolites are products of the oxidative metabolism of arachidonic and linoleic acids generated by the lipoxygenases (LOX) enzymes. Biological activities of lipoxygenase-products include neovascularization and vasodilatation, regulation of inflammatory response and immune function, control of oxidative stress and lipid metabolism (Singh & Rao, 2018). Synthesis of lipoxygenase products by uterine tissues and their role on early embryo development have not been studied extensively. In mice, it has been shown that complete blockade of uterine 12/15-LOX activity by a specific inhibitor reduced uterine levels of arachidonic acid metabolites and impaired implantation by 80% compared to untreated controls (Li *et al*., 2004). In cattle, Ribeiro *et al*., (2016) have shown that the ULF recovered from pregnant dairy cows had increased amounts of 15(S)-HETE compared to their non-pregnant counterparts on day 15. In the present study, we showed for the first time that presence of the pre-implantation embryo is capable of modulating the abundance of lipoxygenase-derived metabolites in the uterine lumen. This entices us to speculate that such metabolites may induce changes in function of target tissues, such as the embryo and the endometrium.

We next explored whether changes in the ULF abundance of lipoxygenase-derived metabolites were associated with changes in LOX transcript abundance in the endometrium. Endometrial abundances of *ALOX12* and *ALOX15B* transcripts were respectively up- and downregulated in the UTJ of Preg vs. Con animals. In our previous study, we demonstrated that the main effects of the D7 embryo on the endometrial transcriptome were mainly in the UTJ (Sponchiado *et al*., 2017). Our findings are consistent with those from a recent study comparing the transcriptome response of the endometrium to pregnancy between high fertile- and subfertile-classified heifers (Moraes *et al*., 2018). In that study, the pregnant endometrium displayed an up-regulated expression of *ALOX5AP* and *ALOX12*, and a down-regulation in the expression of *ALOX15* and *ALOX15B* compared to non-pregnant endometrium on day 17 (Moraes *et al*., 2018). Moreover, an upregulation of *ALOX5AP* was detected on endometrial tissue of pregnant heifers on day 16 of pregnancy compared to non-pregnant endometrium (Forde *et al*., 2011). Taken together, these studies prompt to the idea that embryo/conceptus-derived signals are capable to modulate the endometrial expression of

lipoxygenases and, ultimately, affect the lipoxygenase-derived concentration in the ULF. Studies are needed to elucidate the mechanisms of regulation and potential roles of Lipoxygenase-derived metabolites, as well as their associated signaling systems, in the endometrium and in the embryo during early pregnancy.

We subsequently investigated whether the changed abundance of lipoxygenase-derived metabolites influenced PPARγ signaling in the endometrium. Both 12(S)-HETE and 15(S)-HETE have been shown to be endogenous ligands/activators of PPARγ transcription factor *in vivo* (Li *et al*., 2004) and *in vitro* (Huang *et al*., 1999). In the report by Li *et al*. (2004), the impaired implantation in mice pre-treated with 12/15-LOX inhibitor was restored by the administration of rosiglitazone, a PPARγ agonist. In the present paper, we initially confirmed the expression of *PPARG* and *RXRA* mRNA in the endometrium on day 7. Next, we examined the endometrial abundance of *LPL* mRNA, a PPARγ target-gene, but failed to detect a difference in the abundance of that transcript between Preg and Con samples. This suggests a lack of regulation of this system by the embryo at this stage of pregnancy.

The pre-hatching embryo decreases abundance of specific amino acids and biogenic amines in the uterine lumen. Of the amino acids and biogenic amines quantified, glycine and sarcosine were present in significantly reduced concentrations in the ULF of Preg cows. We also verified that the sum of small neutral and osmotic-stress protection amino acids was lower in Preg compared to the Con group. This may seem at odds with evidence in the literature that amino acids are increased in the uterine lumen in cattle (Groebner *et al*., 2011; Forde *et al*., 2014) and sheep (Gao *et al*., 2009) during the peri-implantation period which is mediated via upregulation of amino acid transporters in the endometrium. However, compared with previous work, the present samples were collected approximately one week earlier in gestation. Interestingly, glycine and sarcosine are both part of the glycine, serine and threonine metabolism pathway. Sarcosine is an intermediate and byproduct in glycine synthesis and degradation. Glycine is inter-convertible to Serine and Alanine and is furthermore necessary for protein and DNA synthesis (i.e., for cell proliferation), also acts as an intracellular regulator and as an organic osmolyte (Steves *et al*., 2003). Brison *et al*. (2004) found that Glycine is less abundant in the culture medium of human embryos that resulted in successful IVF pregnancies. Regarding the mediated transport of Glycine to the uterine lumen, Hugentobler *et al*. (2007) have shown that ULF concentration of glycine on day 6 of the estrous cycle was greater and not correlated to its concentration in blood plasma. This pattern indicates that glycine is actively transported by the endometrial epithelia towards the uterine lumen. In the present study, we detected a downregulation of *SLC6A9* (Glycine

transporter, also known as *GLYT1*) transcript in the Preg endometrial tissue, suggesting an endometrial origin of regulation that was consistent with the lower Glycine concentration in the ULF. Mechanisms by which the embryo regulates this process are currently unknown.

Presence of a day-7 embryo decreases the concentration of acylcarnitines and phospholipids in the ULF. Acylcarnitines are key molecules enrolled in fatty acids transport and energy metabolism. Notably, three acylcarnitines (C3-OH, C5-OH and C16-OH), that were found in different concentrations between groups, are esters derived from hydroxylated acids. Hydroxylated acylcarnitine status is an important indicator of lipid metabolism by the fatty acid omega-oxidation pathway and may represent an important biomarker of fatty acid metabolism (Su *et al*., 2005). Phospholipids are important structural components of plasma lipoproteins and cell membranes, and have important roles in the regulation of cell function and signaling (Edidin, 2003). The ratio between PUFA and SFA showed to be decreased in Preg ULF samples. This finding indicates that the activity of fatty acid desaturases between Con and Preg endometria may be altered. Decreased levels of phospholipids in biological fluids might be attributable to enhanced cell membrane synthesis in the lining cellular compartments (Santos & Schulz, 2012). Differences in lipid profile in the endometrium at late diestrus between pregnant and nonpregnant ewes (Meyer *et al*., 1997), and between gravid and nongravid horns of pregnant cows (Meyer *et al*., 2011) have been reported before. In our study, we showed that both LysoPC a C17:0 and LysoPC a C20:3 fatty acids were significantly lower in abundance in ULF recovered from Preg compared to Con cows. It is possible that these lipids were partially retained by the lining endometrium. Meier *et al*. (2009) have shown that endometrial tissue from pregnant cows displayed greater concentrations of C17:0 and C20:3 fatty acids compared to their cyclic counterparts on day 17 after estrus. The C20:3 fatty acid acts as precursors for prostaglandin synthesis (Leaver & Poyser, 1981). Additionally, the total recoverable amount of hydroxysphingomyelins tended to be greater in the Con ULF samples. Stimulated synthesis of sphingolipids is related to a pro-apoptotic status of endometrium in women (Knific *et al*., 2018). At the present time, we can only speculate on the functional relevance and regulation of changes in the abundance of specific lipids. Much more research is needed on the topic of lipid biology of pregnancy.

In conclusion, we produced evidence to sustain the view that the bovine embryo modulates the biochemical composition of the uterine microenvironment as early as day 7 *in vivo*. Such modulation seems to be local and includes changes in concentrations of lipoxygenase-derived metabolites, amino acids, biogenic amines, acylcarnitines and phospholipids (Fig. 9). Although the endometrial or embryonic origin of the modulated

biochemical processes can only be speculated, it is clear that regulation is complex and interactive. Intensity and extent of embryo signaling capacity is expected to increase dynamically throughout the window of pre-implantation development, in order to cover its changing needs. Altogether, the data of our *in vivo* model highlighted key pathways involved in early embryo-induced alteration in the luminal uterine metabolome. Of particular interest, the products of the lipoxygenase-pathway seem to play an important role in early pregnancy. This novel finding warrants further investigation.

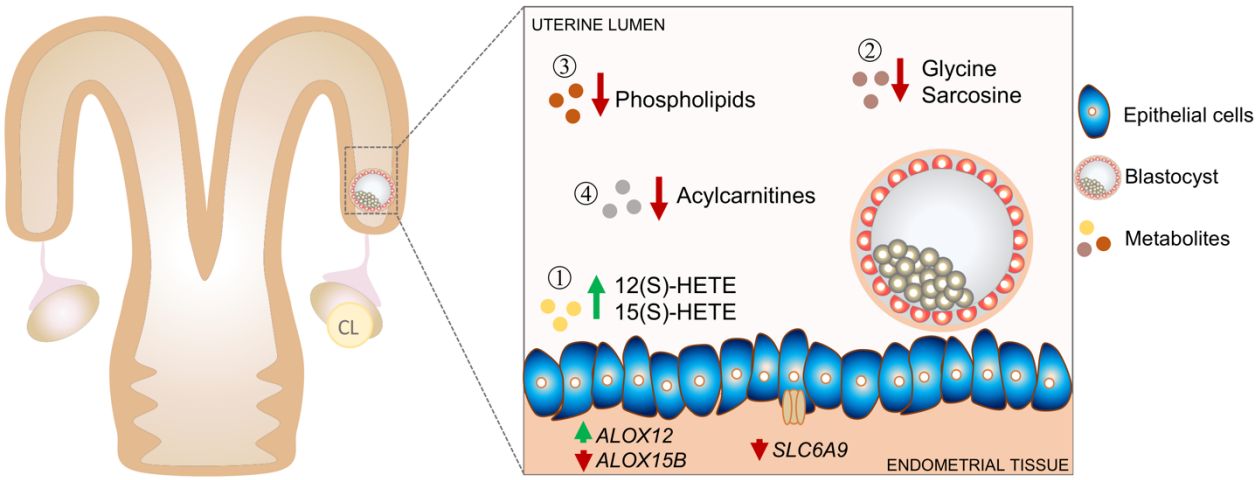

Figure 9. Summary and integration of the main results. Metabolomic measurements reveal an overall decrease on substrate concentration in uterine luminal fluid recovered from pregnant (Preg) compared to control cyclic (Con) cows on day 7 post estrus. (1) Concentration of two metabolites 12(S)-HETE and 15(S)-HETE, associated to the Lipoxygenases pathway, were significantly greater in the Preg group. Transcripts for lipoxygenases were up- (*ALOX12*) and downregulated (*ALOX15B*) in the uterotubal junction of Preg animals, suggesting an endometrial origin of regulation of Lipoxygenases-derived metabolites in ULF. (2) Glycine and sarcosine were significantly lower in abundance in ULF recovered from Preg compared to Con cows. A downregulation of *SLC6A9* (a Glycine transporter) transcripts was found in the Preg endometrial tissue, that was consistent with the lower Glycine concentration in ULF. Exposure to a day 7 embryo modulates the concentration of (3) phospholipids and (4) acylcarnitines concentration in ULF. We propose that metabolite composition of the ULF changes in response to a pre-hatching embryo *in vivo*.

3.6 ACKNOWLEDGEMENTS

This study was funded in part by Conselho Nacional de Desenvolvimento Científico e Tecnológico (CNPq) and by Fundação de Amparo à Pesquisa do Estado de São Paulo (FAPESP; Grant Number 2011/03226-4). MS was partly supported by the Coordenação de Aperfeiçoamento de Pessoal de Nível Superior - Brasil (CAPES; Finance Code 88881.132730/2016-01) and by the Special Research Fund (Uantwerpen, 2018) joint-PhD program. The authors thank the Administration of the Fernando Costa campus (University of

São Paulo) for providing the animals, and the technical assistance of FMVZ-USP staff and students to collect samples.

3.7 AUTHOR CONTRIBUTIONS

MS conceived the study, performed statistical analysis and wrote the manuscript. AMG-D assisted with sample processing and data analysis. CCR performed PCR analysis. EGLT contributed with mass spectrometric measurements and provided expertise in metabolomic data analysis and interpretation. GP and JLMRL contributed with critical review of the manuscript. MB is the PI of the project, provided the financial support, expertise in experimental design, analysis and corrected the manuscript. All authors reviewed and approved the manuscript.

3.8 COMPETING INTERESTS

The authors declare no competing interests.

3.9 REFERENCES

Alexopoulos, N. I., Vajta, G., Maddox-Hyttel, P., French, A. J. & Trounson, A. O. Stereomicroscopic and histological examination of bovine embryos following extended *in vitro* culture. *Reprod. Fert. Develop*. **17**, 799-808 (2006).

Arosh, J. A., Banu, S. K. & McCracken, J. A. Novel concepts on the role of prostaglandins on luteal maintenance and maternal recognition and establishment of pregnancy in ruminants. *J. dairy sci*. **99**, 5926-40 (2016).

Brandao, D. O., *et al*. Post hatching development: a novel system for extended *in vitro* culture of bovine embryos. *Biol. Reprod*. **71**, 2048-55 (2004).

Bridi, A., *et al*. Parthenogenetic bovine embryos secrete type I interferon capable of stimulating ISG15 in luteal cell culture. *Anim. Reprod*. **15**, 1268-77 (2018).

Brison, D. R., *et al.* Identification of viable embryos in IVF by non-invasive measurement of amino acid turnover. *Human reprod*. **19**, 2319-24 (2004).

Diskin, M. G., Parr, M. H. & Morris, D. G. Embryo death in cattle: an update. *Reprod. Fert. Develop.* **24**, 244-51 (2011).

Edidin, M. Lipids on the frontier: a century of cell-membrane bilayers. *Nature Reviews Mol. Cell Biol.* **4**, 414 (2003).

Forde, N., *et al.* Amino acids in the uterine luminal fluid reflects the temporal changes in transporter expression in the endometrium and conceptus during early pregnancy in cattle. *PLoS One*. **9**, e100010 (2014).

Forde, N., *et al.* Conceptus-induced changes in the endometrial transcriptome: how soon does the cow know she is pregnant? *Biol. Reprod*. **85**, 144-56 (2011).

Gao, H., *et al*. Select Nutrients in the Ovine Uterine Lumen. I. Amino Acids, Glucose, and Ions in Uterine Lumenal Flushings of Cyclic and Pregnant Ewes1. *Biol. Reprod*. **80**, 86-93 (2009).

Gómez, E., *et al*. *In vitro* cultured bovine endometrial cells recognize embryonic sex. *Theriogenology*. **108**, 176-84 (2018).

Groebner, A. E., *et al.* Increase of essential amino acids in the bovine uterine lumen during preimplantation development. *Reproduction*. **141**, 685-95 (2011).

Huang, J. T., *et al.* Interleukin-4-dependent production of PPAR-γ ligands in macrophages by 12/15-lipoxygenase. *Nature*. **400**, 378 (1999).

Hugentobler, S. A., *et al*. Amino acids in oviduct and uterine fluid and blood plasma during the estrous cycle in the bovine. *Mol. Reprod. dev*. **74**, 445-54 (2007).

Knickerbocker, J. J., *et al*. Proteins secreted by day-16 to-18 bovine conceptuses extend corpus luteum function in cows. *J. reprod. fert*. **77**, 381-91 (1986).

Knific, T., *et al*. Models including plasma levels of sphingomyelins and phosphatidylcholines as diagnostic and prognostic biomarkers of endometrial cancer. *J. steroid biochem. mol. biol*. **178**, 312-21 (2018).

Leaver, H. A. & Poyser, N. L. Distribution of arachidonic acid and other fatty acids in the lipids of guinea-pig uterus and plasma in relation to uterine prostaglandin synthesis. *J. reprod. fert*. **61**, 325-33 (1981).

Li, Q., Cheon, *et al.* A novel pathway involving progesterone receptor, 12/15-lipoxygenase-derived eicosanoids, and peroxisome proliferator-activated receptor γ regulates implantation in mice. *J. Biol. Chem.* **279**, 11570-81 (2004).

Maillo, V., *et al*. Oviduct-Embryo Interactions in Cattle: Two-Way Traffic or a One-Way Street? *Biol. Reprod*. **92**, 1-8. doi: 10.1095/biolreprod.115.127969 (2015).

Martins, T., *et al.* Perturbations in the uterine luminal fluid composition are detrimental to pregnancy establishment in cattle. *J. anim. sci. biotechno*. **9**, 70 (2018).

Meier, S., *et al*. Genetic strain and reproductive status affect endometrial fatty acid concentrations. *J. dairy sci*. **92**, 3723-30 (2009).

Meier, S., Trewhella, M. A., Fairclough, R. J. & Jenkin, G. Changes in uterine endometrial phospholipids and fatty acids throughout the oestrous cycle and early pregnancy in the ewe. *Prostaglandins, leukotrienes and essential fatty acids.* **57**, 341-9 (1997).

Meier, S., Walker, C. G., Mitchell, M. D., Littlejohn, M. D. & Roche, J. R. Modification of endometrial fatty acid concentrations by the pre-implantation conceptus in pasture-fed dairy cows. *J. dairy res*. **78**, 263-9 (2011).

Moraes, J. G. N, *et al*. Uterine influences on conceptus development in fertility-classified animals. *PNAS*. **115**, 1749-1758 (2018).

Passaro, C., *et al*. Blastocyst-induced changes in the bovine endometrial transcriptome. *Reproduction*. **156**, 219-29 (2018).

Pfaffl, M. W. A new mathematical model for relative quantification in real-time RT–PCR. *Nucleic acids res*. **29**, e45-e (2001).

Rashid, M. B., *et al*. Evidence that interferon-tau secreted from Day-7 embryo *in vivo* generates anti-inflammatory immune response in the bovine uterus. *Biochem Biophys Res Commun*. **500**, 879-84 (2018).

Reiner, A., Yekutieli, D. & Benjamini, Y. Identifying differentially expressed genes using false discovery rate controlling procedures. *Bioinformatics*. **19**, 368-75 (2003).

Ribeiro, E. S., *et al*. Biology of Preimplantation Conceptus at the Onset of Elongation in Dairy Cows. *Biol. Reprod*. **94**, 97-1 (2016).

Roberts, R. M. & Bazer, F. W. The functions of uterine secretions. *J. reprod. fert.* **82**, 875-92 (1988).

Römisch-Margl, W., *et al.* Procedure for tissue sample preparation and metabolite extraction for high-throughput targeted metabolomics. *Metabolomics*. **8**, 133-42 (2012).

Ruijter, J. M., *et al*. Amplification efficiency: linking baseline and bias in the analysis of quantitative PCR data. *Nucleic acids res*. **37**, e45-e (2009).

Santos, C. R. & Schulze, A. Lipid metabolism in cancer. *The FEBS J.* **279**, 2610-23 (2012).

Singh, N. K. & Rao, G. N. Emerging role of 12/15-Lipoxygenase (ALOX15) in human pathologies. *Progress in lipid res.* (2018).

Sponchiado M., *et al*. Pre-hatching embryo-dependent and-independent programming of endometrial function in cattle. *PloS one*. **12**, e0175954 (2017).

Steeves, C. L., *et al*. The glycine neurotransmitter transporter GLYT1 is an organic osmolyte transporter regulating cell volume in cleavage-stage embryos. *PNAS*. **100**, 13982-7 (2003).

Su, X., Han, X., Mancuso, D. J., Abendschein, D. R. & Gross, R. W. Accumulation of long-chain acylcarnitine and 3-hydroxy acylcarnitine molecular species in diabetic myocardium: identification of alterations in mitochondrial fatty acid processing in diabetic myocardium by shotgun lipidomics. *Biochemistry*. **44**, 5234-45 (2005).

Talukder, A. K., *et al.* Bovine embryo induces an anti-inflammatory response in uterine epithelial cells and immune cells *in vitro*: possible involvement of interferon tau as an intermediator. *J. Reprod. Develop.* **63**, 425-34 (2017).

Talukder, A. K., *et al*. Oviduct epithelium induces interferon-tau in bovine Day-4 embryos, which generates an anti-inflammatory response in immune cells. *Sci Rep*. **8**, 7850 (2018).

Unterwurzacher, I., Koal, T., Bonn, G. K., Weinberger, K. M. & Ramsay, S. L. Rapid sample preparation and simultaneous quantitation of prostaglandins and lipoxygenase derived fatty acid metabolites by liquid chromatography-mass spectrometry from small sample volumes. *Clin. Chem. Lab. Med*. **46**, 1589-97 (2008).

Wydooghe, E., *et al*. Autocrine embryotropins revisited: how do embryos communicate with each other *in vitro* when cultured in groups? *Biol. Rev*. **92**, 505-20 (2015).

Xia, J. & Wishart, D. S. Using MetaboAnalyst 3.0 for comprehensive metabolomics data analysis. *Curr. protocols in bioinformatics.* **55**, 14-10 (2016).

CHAPTER 4

THE BOVINE EMBRYO-ENDOMETRIUM INTERACTOME DECIPHERED *IN VITRO*

M. Sponchiado[1,2,3], W. F. A. Marei[1], G. T. S. Beemster[4], P. E. J. Bols[1], M. Binelli[2,3], J. L. M. R. Leroy[1*]

1 Gamete Research Centre, Department of Veterinary Sciences, Faculty of Biomedical, Pharmaceutical and Veterinary Sciences, University of Antwerp, 2610 Wilrijk, Belgium

2 Department of Animal Reproduction, School of Veterinary Medicine and Animal Science, University of São Paulo, 13635-900 Pirassununga-SP, Brazil

3 Department of Animal Sciences, University of Florida, 32611-0910 Gainesville, FL, USA

4 Laboratory for Integrated Plant Physiology Research (IMPRES), Department of Biology, University of Antwerp, 2020 Antwerp, Belgium

IN PREPARATION, MAY 2019

4 THE BOVINE EMBRYO-ENDOMETRIUM INTERACTOME DECIPHERED *IN VITRO*

4.1 ABSTRACT

In cattle, pregnancy establishment is ultimately dependent upon fine-tuned cellular and molecular interactions between a competent embryo and a receptive endometrium. Current understanding of the factors and mechanisms involved in the complex embryo-maternal interactome is limited. It is unknown, for example, whether a physical contact between the embryo and the endometrial epithelia is needed to elicit changes in both embryonic and maternal units. We hypothesized that nature and intensity of embryo-induced changes on endometrial transcriptome depend on a juxtaposition between the embryos and the endometrium. Hereto, we used an *in vitro* approach to decipher the very local embryo-endometrial interface for embryo-induced changes on the bovine endometrial epithelial cells (BEEC) transcriptome. *In vitro*-produced day-5.5 morulae were cultured in the absence of endometrial cells (NoBEEC group), juxtapositioned on top of BEECs (Juxt), or in transwells (Non-juxt), for 48 h. An extra group of BEEC cultured in the absence of embryos (NoEmbryos) was included. At BEEC transcriptome level, NoEmbryos versus Juxt comparison yield 1,797 DEGs. Interestingly, transcriptome changes were rather limited between NoEmbryos versus Non-juxt, with 230 genes being differentially regulated. Interferon-mediated pathways were enriched in either Juxt and Non-Juxt. Biological processes exclusively enriched in Non-juxt versus Juxt comparison include regulation of cell cycle, estrogen biosynthesis, mitochondrial dysfunction and pregnenolone biosynthesis. Co-culture with BEEC improved blastocyst rates on day 7.5, regardless of Juxt or Non-juxt conditions. In conclusion, nature and intensity of embryo-induced effects on bovine endometrium varies according to physical proximity of the embryos.

4.2 INTRODUCTION

Fundamentally, a successful pregnancy depends on the quality of the blastocyst and on a receptive endometrium. Moreover, tightly coordinated cellular and molecular interactions between the competent embryo and the receptive endometrium need to be established to safeguard the pregnancy in eutherian mammals. Disturbances in this complex communication can result in early embryonic losses and, therefore, subfertility. This is of special importance in cattle, since up to 40% of pregnancies fail within the first three weeks of pregnancy (Diskin *et al*., 201; Diskin *et al*., 2016).

The concept of embryo-maternal interactome implies dynamic processes precisely coordinated by both the maternal and the embryonic unit. In the cow, it is expected that the developing embryo starts to interact with the endometrium around day 5 post-fertilization when the zona pellucida-enclosed morula enters into the uterus (Guillomot *et al*., 1994). The embryo *in uterus* is tightly surrounded by the endometrial luminal epithelium (Wolf *et al*., 2003), however, until day 20, there is no anatomical union between the conceptus (embryo and associate membranes) and the endometrium. Thus, signaling molecules are understood to play an important role in the early embryo-maternal communication in cattle. The actions of those molecules can be directed from the embryo towards the maternal tissue, and vice-versa, in a paracrine or a juxtacrine fashion. One well known example of paracrine signaling is the embryo-produced Interferon-tau (IFNτ) which is released into the uterine lumen and acts in the endometrium to abrogate the luteolytic cascade (Bazer *et al*., 1997). Effects of the embryo on the adjacent endometrial cells are poorly defined.

Regarding this dialogue, it is well conceived that a successful embryo maintains basic tools for its own development, given the fact that the bovine embryo can thrive successfully up until the blastocyst stage *in vitro*, independently of exposure to the maternal reproductive tract. However, it is clear that the maternal genital tract, including the uterus itself, exerts considerable control over the ability of a conceptus to develop. For example, several studies have demonstrated that *in vivo* cultured embryos differ to their *in vitro* produced counterparts in terms of developmental competence, morphology, metabolism, gene expression profile, and cryotolerance (reviewed by Rizos *et al*., 2017). Moreover, exposure to the uterine environment at the post-hatching stage is a prerequisite for embryo elongation, given that elongation of bovine conceptuses do not occur *in vitro* (Brandao *et al*., 2004).

On the maternal side, it is well established that the maternal reproductive tract function is primarily controlled by ovarian steroids. Estradiol and progesterone, from pre-

ovulatory follicles and corpus luteum (CL), exert classical endocrine control of morphological and functional changes in the endometrium that affect embryo development and pregnancy success (Carter *et al*., 2008; Forde *et al*., 2009; Mesquita *et al*., 2015). Although the classical endocrine regulation of endometrial function has been extensively investigated, the programming of endometrial function exerted by the embryo has not been interrogated to the same extent.

In this regard, it has been shown that the endometrium senses the embryo quality (Macklon & Brosens, 2014). For example, the bovine endometrial transcriptome changes when exposed to *in vitro*- versus *in vivo*-produced embryos (Mansouri-Attia *et al*., 2009), and when exposed to standard *in vitro*-produced versus cloned embryos (Bauersachs *et al*., 2009). In fact, accumulating evidence supports the idea that the early embryo is more than a passenger throughout the uterine lumen and that it has the capacity to elicit changes from the endometrium. We have shown that the endometrial transcriptome responds locally to a pre-hatching embryo presence as early as day 7 *in vivo* (Sponchiado *et al*., 2017). Other *in vitro* studies have shown that early embryos modulate the abundance of specific transcripts in endometrial epithelial cells (Talukder *et al*., 2017; Gómez *et al*., 2018). Specific pathways modulated by the embryo include transcripts for interferon stimulated genes (ISGs) and prostaglandin metabolism. The question still remains whether the endometrial responses of the juxtacrine differs of the non-juxtacrine fashion. We hypothesized that nature and intensity of embryo-induced changes on endometrial transcriptome depend on physical proximity between the embryos and the endometrium. Therefore, we aimed to interrogate the unique embryo-maternal interface for embryo-induced changes on the endometrial epithelial cells transcriptome. A second aim was to investigate the effects of co-culture with endometrial cells on embryo development from morula to blastocyst stage. Hereto, we used an *in vitro* co-culture system of embryos juxtapositioned to bovine endometrial epithelial cells (BEECs) to elucidate basic mechanisms involved in the early embryo-maternal interactome. Non-juxtacrine condition was accomplished by using a transwell insert. The importance of physical proximity between the embryos and the endometrial cells was investigated in terms of embryonic development and BEEC transcriptome profiles.

4.3 MATERIAL AND METHODS

Chemicals used to prepare cell and embryo culture medium were purchased from Life Technologies (Thermo Fisher Scientific, Waltham, USA) or from Sigma Chemical Co. (St Louis, MO, USA), unless otherwise stated.

4.3.1 Overview of experimental model

For the purpose of this study, we established a straight forward bovine endometrial epithelial cell (BEEC)-embryo coculture as a research model to investigate the very early embryo-maternal interactions *in vitro*. An overview of the experimental procedures used in the present study is given in Figure 1. In addition to the experimental set up, a characterization regarding cell-origin markers and functional key transcripts in the cell model was performed for validation purposes.

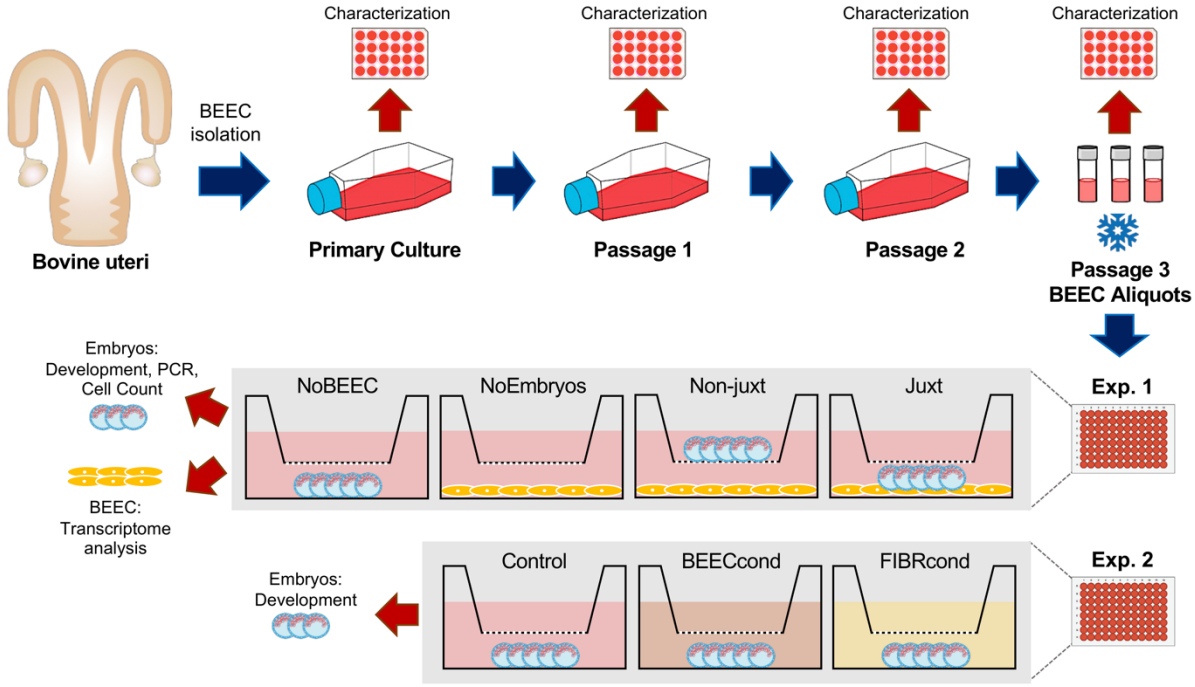

Figure 1. Schematic overview of experimental model. Bovine endometrial epithelial cells (BEECs) were isolated from uteri *ex vivo*, pooled, and used for the primary culture. BEECs were cultured until passage 3, when assigned to experimental conditions (Experiment 1 and 2). For means of characterization, cells from each passage were simultaneously cultured in 24-well plates for further PCR analyses. At passage 2, BEECs were then frozen-and-thawed to be co-cultured with embryos (Experiment 1), or to generate BEEC-conditioned medium (Experiment 2), in a manner that in all replicates, aliquots containing cells originated from the same bunch were applied. Detailed descriptions of procedures and outcomes for each step are given in the next sections.

4.3.2 Experiment One

In this experiment, we compared the effects of juxtaposition versus non-juxtaposition between embryos from morula to blastocyst stage and endometrial cells on BEEC transcriptome and embryo development. Embryos were co-cultured with BEEC monolayers from day 5.5 p.i. (post insemination) until day 7.5 p.i. The timing of exposure of the endometrial cells to embryos (i. e. day 5.5 p.i.) coincides with the embryo's arrival into the uterus *in vivo* in the cow (Bazer *et al*., 1991). Juxtacrine interaction was accomplished by placing 15 embryos directly on top of BEEC monolayers. Non-juxtacrine interaction was accomplished by placing 15 embryos in a 96-well cell-culture insert (IncuCyte® by Sartorius, USA). The insert membrane avoided the direct physical contact between the embryos and the endometrial monolayer. Additionally, the low pore density (<2% of the surface area; 8.0 µm pore size) of the insert membrane limited the diffusion of secreted signaling molecules between the upper (containing the embryos) and the basal (containing the BEEC monolayer) compartments. This feature was desirable because a dilution factor is expected to occur in non-adjacent, paracrine signaling *in vivo*. The distance between the basal plate and the insert is 1.425 mm.

In vitro produced day-5.5 morulae and early blastocysts were selected under stereomicroscope and transferred towards the 96-well ClearView reservoir plate containing 90% confluent, untreated BEEC monolayers according to the treatments: (i) **NoBEEC**: groups of 15±1 morulae/early blastocysts, without BEECs; (ii) **Juxt**: groups of 15±1 morulae/young blastocysts placed directly on top of a BEEC monolayer; (iii) **Non-juxt**: groups of 15±1 morulae/young blastocysts on cell culture transwells, without contact with the BEEC monolayer; or (iv) **NoEmbryos**: BEECs in the absence of embryos (Figure 1). Embryos were transferred using mouth-controlled, fine pore glass capillaries to minimize the volume of media transferred to the wells. Embryos/cell cultures (for all the experimental conditions) were conducted in 150 µL of SOF medium supplemented with 5% of fetal bovine serum (FBS), for 48 h (from day 5.5 p.i. until day 7.5 p.i.) in humified atmosphere of 5% CO_2 and 20% O_2 at 38.5 °C. On day 7.5, embryos and BEEC monolayers were evaluated and processed as described below. Experiment was performed in 6 replicates and 2 to 4 wells of each condition were included in each replicate.

4.3.2.1 Sample evaluation and processing

On day 7.5, embryo developmental stages were recorded and expressed as a proportion of total number of morulae assigned initially to the treatments. All morphological

assessments were conducted using an inverted Olympus CKX41 microscope (Olympus, Belgium). Blastocysts were either fixed in paraformaldehyde for immunostaining or snap frozen. Embryos were fixed in 4-well plates containing 500 µL of buffered 4% paraformaldehyde for 30 min at room temperature, and stored in PBS-PVP 1% at 4 °C. Groups of 5 embryos were washed in PBS-PVP 1%, snap frozen in (RNase/DNase free) microtubes and stored at –80 °C. BEEC monolayers were detached and retrieved by trypsinization. Briefly, cell monolayers were washed with pre-warmed PBS (Ca^{2+} Mg^{2+} free) to remove serum traces and detached cells. Cells were then incubated with 100 µL of pre-warmed TrypLE express (Thermo Fisher Scientific) for 6 min at 38.5°C. The reaction was stopped by adding 200 µL of PBS (Ca^{2+} Mg^{2+} free) to the wells. Trypsin-BEECs mixtures were transferred towards 1.5 mL (RNase/DNase free) microtubes and centrifuged at 200 x g for 10 min at 24 °C. The supernatants were carefully removed, cell pellets were snap frozen and stored at –80 °C for further processing.

4.3.3 Experiment Two

In this experiment, we aimed to isolate potential non-specific embryo supportive effects elicited by BEECs on embryo development. By using conditioned medium from mice fibroblasts, we tested whether heterologous, unspecific feeder cells could also affect embryo development. Secondly, by using conditioned medium from BEECs, we eliminated the potential effect of a reduced O_2 tension caused by the BEEC monolayer that may had favored embryo development in experiment 1. Therefore, *in vitro* produced day-5.5 morulae/early blastocysts were cultured with fresh conditioned medium from BEECs and mice fibroblasts as described below. Experiment was performed in 5 replicates and 2 to 5 wells of each condition were included in each replicate.

4.3.3.1 Conditioned medium preparation and treatments

DMEM/F12-based culture medium of BEEC and mice fibroblast subconfluent monolayers was replaced by SOF medium supplemented with 5% of FBS. Additional wells containing only SOF-5% FBS medium were included. After 24 h, the spent/control medium from 6 wells per condition were collected, pooled and centrifuged at 200 x g for 5 min at 24 °C to remove cell debris. After 30 min of equilibration in the incubator, 150 µL of BEEC- and fibroblasts-conditioned medium were distributed in 0.1% gelatin-coated 96-well ClearView

Reservoir Plate (IncuCyte® by Sartorius). Subsequently, groups of 15±1 day-5.5 morulae/early blastocysts were assigned to the following treatments: (i) **Control**: Culture medium (SOF-5% FBS); (ii) **BEECcond**: BEEC-conditioned SOF-5% FBS medium; or (iii) **FIBRcond:** fibroblast-conditioned SOF-5% FBS medium. Embryos were transferred using mouth-controlled fine pore glass capillaries to minimize the volume of media transferred to the wells. *In vitro* embryo culture was conducted in humified atmosphere at 38.5 °C in 5% CO_2 and 20% O_2 from day 5.5 until day 7.5 p.i.. The medium was replaced with freshly prepared conditioned (or control) medium in 50% of the volume after 24 h. On day 7.5, embryos were scored according to their developmental stages.

4.3.4 Isolation and culture of bovine endometrial epithelial cells (BEECs)

4.3.4.1 Cell collection and primary culture

Reproductive tracts at early luteal phase of the estrous cycle were collected from *Bos taurus* beef cows at a local slaughterhouse, inspected for absence of reproductive abnormalities or disorders, and transported to the laboratory at 30 °C. Four uteri were trimmed free of surrounding tissues and externally decontaminated with 70% ethanol. The uterine horns ipsilateral to the ovary containing the corpus hemorragicus were longitudinally opened at the mesometrial insertion with decontaminated scissors and then, the endometrial luminal surface was carefully scraped with sterile glass slides. Cells collected from the four uteri were pooled in equilibrated, pre-warmed cell culture medium. The cell culture medium consisted of DMEM/F-12 phenol red-free medium (Product number 11039-021; Gibco, Thermo Fisher Scientific) supplemented with 10% FBS (Product number F9665, Sigma-Aldrich), 2% Penicillin/Streptomycin, and 1% Fungizone. The cell suspension was centrifuged at 200 x g for 5 min at 24 °C, the supernatant was discarded and erythrocytes were subsequently lysed by incubation with a hyper-osmotic Lysis buffer (1 mM EDTA disodium salt, 150 mM NH_4CL and 100 mM $NaHCO_3$) for 1 min. The resulting cell pellet was resuspended in pre-warmed culture medium and centrifuged. After two washing steps, cells were plated in 25 cm^2 culture flasks at a density of 1 x 10^6 cells/mL and pre-incubated in humidified atmosphere of 5% CO_2 at 38.5 °C for 1 h 30 min. The pre-incubation step aimed to remove the contaminating non-epithelial cells. The supernatant containing non-attached, epithelial cells was transferred towards fresh 25 cm^2 culture flasks and maintained in humidified atmosphere of 5% CO_2 at 38.5 °C. After the adhesion process started, culture

medium was changed every 48 h. Flasks were checked daily for signs of contamination and to visually estimate the monolayer's confluence by inverted light microscopy.

4.3.4.2 Subculture and freezing procedure

Cells were subcultured when primary monolayers reached 95% of confluence. Monolayers were washed once with PBS (Ca^{2+} Mg^{2+} free; Gibco) to remove residual serum. Cells were then trypsinized (TrypLE Express; Gibco, Thermo Fisher Scientific) for 6 min, retrieved and centrifuged at 200 x g for 5 min at 25 °C. Cell count and viability were determined in a Bürker Counting Chamber (W. Schreck, Hofheim, Germany) by trypan blue exclusion test. BEECs were seeded at a density of 1 x 10^6 viable cells/flask into fresh 75 cm^2 culture flasks and cultured as described for primary culture. When 95% of confluence was reached, BEEC monolayers were washed with PBS (Ca^{2+} Mg^{2+} free) and trypsinized as described previously. BEECs at passage 2 were plated at a density of 1.5 x 10^6 viable cells/flask into fresh 75 cm^2 culture flasks. BEEC culture was conducted as described for primary culture. Subconfluent (90%) monolayers were then washed with PBS (Ca^{2+} Mg^{2+} free) and trypsinized as described previously. The resulting cell pellet was diluted in cryopreservation medium at a concentration of 1 x 10^6 viable cells/mL. The cryopreservation medium was based on DMEM/F-12 phenol red free medium supplemented with 15% FBS, 10% DMSO (Invitrogen, Thermo Fisher Scientific), 2% Penicillin/Streptomycin, and 1% Fungizone. Cryovials containing BEECs were placed in a freezing container (Nalgene® Cryo, Thermo Fisher Scientific) and kept at −80 °C overnight, afterward, stored in liquid nitrogen. Experiments 1 and 2 were performed using BEECs at passage 3 thawed from the same batch.

4.3.4.3 BEEC cell line characterization

BEEC cultures were conducted in 24-well plates in order to evaluate the presence of epithelial and mesenchymal cell markers and abundance of functional key transcripts from primary culture to passage 3. Cells were seeded at a density of 3 x 10^4 viable cells/well into 24-well plates for further trypsinization and retrieval for gene expression analysis, or on sterile glass coverslips for further fixation and immunostaining analysis. Cell cultures were conducted as described before (please check *Cell collection and primary culture*, and *Subculture and freezing procedures* sections). Subconfluent BEEC monolayers were washed twice with PBS (Ca^{2+} Mg^{2+} free). Monolayers grown on coverslips were fixed in buffered 4%

paraformaldehyde for 30 min at room temperature, washed twice with ice-cold PBS and stored at 4 °C for further immunostaining analysis (see below). The remaining wells containing cells were trypsinized for 6 min, retrieved and centrifuged at 200 x g for 5 min at 25 °C. Cell pellets were snap frozen and kept at −80 °C for further processing.

4.3.4.4 BEEC assignment to treatments (Experiments 1 and 2)

Vials containing BEECs at passage 3 were thawed and seeded in 0.1% gelatin-coated 96-well ClearView Reservoir Plate (IncuCyte® by Sartorius) at a density of 1.5 x 10^4 cells/well. Cells were maintained in DMEM/F-12 phenol red free medium supplemented with 10% FBS, 2% Penicillin/Streptomycin, and 1% Fungizone, in humidified atmosphere of 5% CO_2 at 38.5 °C. The medium was changed every 48 h. Approximately 90 h hours after plating, monolayers at 90% confluency were subjected to treatments as described previously for Experiments 1 and 2.

4.3.5 *In vitro* embryo production

Bovine embryos were *in vitro* produced as previously described (Marei *et al.*, 2019) with minor modifications. Briefly, ovaries were collected at a local slaughterhouse and transported within 1 h of slaughter to the laboratory. Antral follicles with a diameter of 3-8 mm were aspirated. Immature, unexpanded cumulus-oocytes complexes (COCs) were matured *in vitro* (day −1) in groups of 50±5 COCs in 4-well plates (Nunc, Langenselbold, Germany) containing 500 µL of maturation medium per well for 24 h in humidified atmosphere with 5% CO_2 at 38.5 °C. Matured COCs were then co-incubated in groups of 100±10 with spermatozoa at a final concentration of 10^6 sperm cells/mL for 22 h in 500 µL of fertilization medium in humidified atmosphere of 5% CO_2 at 38.5 °C (day 0). For all replicates, thawed semen from the same batch of a proven fertility bull was used following selection of motile spermatozoa by centrifugation on a discontinuous 45%-90% Percoll (Amersham Biosciences, Little Chalfont, UK) gradient. Finally, denuded presumptive zygotes were cultured (day 1) in groups of 25±2 in 75 µL basic synthetic oviductal fluid (SOF) culture medium supplemented with 5% FBS and 50 mg/mL gentamycin. Embryo culture was carried out in half-area 96-well plates under controlled atmosphere of 5% CO_2, 5% O_2, 90% N_2 at 38.5 °C until day 5.5 p.i.

4.3.6 Immunofluorescence

4.3.6.1 BEEC

Samples were fixed in buffered 4% paraformaldehyde for 30 min at room temperature and kept at 4 °C immerged in PBS-PVP. Coverslips were transferred towards a new 24-well plate and BEEC monolayers were permeabilized with 500 µL of PBS containing 1% Triton X-100 and 0.05% Tween-20 for 30 min at room temperature. Monolayers were washed 3 times in wash solution that consisted in 0.5% BSA and 0.05% Tween-20 in PBS. Next, samples were blocked in PBS containing 2% BSA and 0.05% Tween-20, for 45 min at room temperature, then incubated with primary antibodies overnight at 4 °C. Primary antibodies used in the present study were anti-Cytokeratin mouse monoclonal antibody (1:100 in blocking solution; M3515, Dako, CA, USA), and anti-Vimentin rabbit polyclonal antibody (1:100 in blocking solution; ab45939, Abcam, MA, USA). Negative control coverslips were incubated with an equivalent mixture of normal mouse and rabbit IgGs. Monolayers were washed in wash solution and subsequently incubated with the secondary antibodies Texas Red-labeled goat anti-mouse (1:200 in blocking solution; Life Technologies) and FITC-labeled goat anti-rabbit (1:200 in blocking solution; Novex, Life Technologies) for 1 h at 4 °C. Nuclei were counterstained in Hoechst 33342 (30 µg/mL in PBS-PVP 1%) for 10 min at room temperature. Thereafter, coverslips were mounted on glass slides in droplets of 1% DABCO. Images were captured under a fluorescence microscope IX71 (Olympus) and CellSens software with DAPI filter (excitation/emission: 360–370/420–460 nm for Hoechst stained nuclei), FITC filter (460–490/520–540 nm for Vimentin), and RITC filter (510–550/>570 nm for Cytokeratin-positive cells).

4.3.6.2 Embryos

Day 7.5 embryos (n = 91) beyond normal blastocyst stage were differentially stained to count the cells in the inner cell mass (ICM) and trophectoderm (TE) using an immunofluorescence method adapted from Wydooghe *et al*. (2011). Briefly, embryos were permeabilized in 0.1% Triton X-100 and 0.05% Tween-20 in PBS at 4 °C overnight. To avoid any non-specific binding, embryos were incubated in blocking solution (10% normal goat serum in 0.05% Tween-20 in PBS) for 2 h at 4 °C. Blastocysts were incubated overnight at 4 °C in primary antibody solution containing a 1:1 mixture of mouse anti-caudal type

homeobox 2 (CDX2) antibody (ready to use; BioGenex, San Ramon, USA). Negative control embryos were incubated with normal mouse IgG at the same concentration as the primary antibody. All embryos were washed in PBS-PVP 1% and subsequently incubated with the secondary antibody Texas Red-labeled goat anti-mouse (1:200 in blocking solution; Life Technologies) for 4 h at 4 °C. Nuclei were counterstained in Hoechst 33342 (30 µg/mL in PBS-PVP 1%) for 10 min at room temperature. Blastocysts were mounted onto glass slides in droplets of 1% DABCO and covered with coverslips. Images were captured under a fluorescence microscope IX71 (Olympus) and CellSens software with DAPI filter (excitation/emission: 360–370/420–460 nm for Hoechst stained total cells) and RITC filter (510–550/>570 nm for CDX2-positive TE cells).

4.3.7 Total RNA isolation and cDNA synthesis

4.3.7.1 BEEC (Experiment 1)

Total RNA was extracted using the PicoPure RNA Isolation Kit (Thermo Fisher) as per manufacturer's instructions with minor modifications. Briefly, BEEC samples were subjected to cell lysis in 50 µL of Extraction Buffer for 30 min at 42 ºC. Lysates were added 70% ethanol and loaded into pre-conditioned purification columns and centrifuged for 2 min at 100 g, immediately followed by centrifugation at 12,000 g for 1 min to remove flowthrough. Membranes were subjected to On-column DNase treatment (RNase-Free DNase Set; Qiagen) at room temperature for 15 min according to the standard protocol. After subsequent wash steps, the membrane-bound RNA was eluted in 16 µL of the Elution Buffer provided. Total RNA yield and purity (260/280 nm ratio) were verified by NanoDrop (Thermo Fisher Scientific) spectrophotometer analysis. RNA integrity was assessed using automated capillary gel electrophoresis on a Bioanalyzer 2100 (Agilent Genomics, Dublin, Ireland) with RNA 6000 Nano Lab-chips according to manufacturer's instructions. Absorbance ratios (28S/18S) and RNA integrity values recorded for all RNA samples extracted ranged between 2.0 and 2.6, and 8.5 and 10.0, respectively. The isolated RNA samples were stored at –80 °C until RNA sequencing.

4.3.7.2 Embryos (Experiment 1)

Pools of 15 embryos (developmental stages were distributed equally among samples) were subjected to total RNA isolation using the PicoPure RNA Isolation Kit (Thermo Fisher) as described for BEEC samples. Concentration and purity (260/280 nm ratio) of total RNA in extracts were evaluated by NanoDrop (Thermo Fisher Scientific) spectrophotometer analysis. Total RNA (50 ng) was reverse transcribed using the Sensiscript RT kit (Qiagen) according to manufacturer's instructions with minor modifications. The master mix was composed by the Sensiscript Reverse Transcriptase and the buffer RT supplied in the kit, supplemented with Recombinant RNasin RNase inhibitor (Promega), Oligo-dT (Promega) and Random (Promega) primers at a final concentration of 1 µM and 10 µM, respectively, and dNTP mix (Promega) at final concentration of 0.5 mM/each dNTP. Samples were incubated in a thermocycler at 37 ℃ for 1 h and stored at −20℃ until further analyses.

4.3.7.3 BEEC (Cell line characterization)

Total RNA was isolated using Trizol Reagent (Invitrogen, Thermo Fisher Scientific, CA, USA) in accordance with manufacturer's guidelines. Samples were lysed in 200 µL of Trizol and placed at room temperature for 5 min. Subsequently, 128 µL chloroform were added and samples centrifuged at 10,000 g for 15 min at 4 ºC for phase separation. The aqueous phase was transferred towards a new microtube and 400 µL isopropanol were added, for RNA precipitation. At this step, samples were stored overnight at –80 °C to maximize RNA harvest. Samples were centrifuged at 10,000 g for 12 min at 4 ºC. The RNA precipitate was resuspended in 400 µL of 75% ethanol, followed by centrifugation at 10,000 g for 8 min at 4 ºC. Air-dried RNA pellets were resuspended in 10 µL of DEPC water and, subsequently, incubated at 55 ºC for 10 min. Extracts containing RNA were kept at –80 °C until use. Total RNA yield and purity (260/280 nm ratio) were evaluated by NanoDrop (Thermo Fisher Scientific) spectrophotometer analysis. Samples of RNA (1 µg) were treated with DNase I (Promega) according to the standard protocol. Total RNA was reverse transcribed using the High Capacity cDNA Reverse Transcription kit (Invitrogen) according to the manufacturer's instructions. First strand cDNA was synthesized using random hexamers and by incubation at 25℃ for 10 min, followed by incubation at 37℃ for 2 h and reverse-transcriptase inactivation at 85℃ for 5 min. The cDNA was stored at −20℃ until further analyses.

4.3.8 Real Time PCR

Relative abundance of transcripts was analyzed by Real Time PCR. Transcripts analyzed in BEEC samples included cell origin markers (*KRT18* and *VIM*), and key gene associated with endometrial function (*ESR1*, *IFNAR1* and *PTGS2*). Specific pairs of primers were designed based on the *Bos taurus* GenBank Ref-Seq mRNA. Transcripts analyzed in day-7.5 embryos included a marker for trophoblast cells (*CDX2*), interferon-tau (*IFNT2*), and a gene associated with apoptosis (*BAX2*). Reactions were carried out in duplicates in 96-well plates (Bio-Rad Laboratories) sealed with Microseal B PCR plate sealing film (Bio-Rad Laboratories) using the CFX Connect Real-Time PCR detection system (Bio-Rad Laboratories B.V., Netherlands). The PCR reactions were conducted in a final volume of 16 µL, consisting of 8 µL of SsoAdvanced Universal Sybr Green supermix (Bio-Rad Laboratories), 0.4 µL of forward and reverse primers, and 4 µL of cDNA template. Negative control reactions (DEPC-treated water replacing template cDNA) were included in every run. The program consisted of an initial denaturation step at 95℃ for 15 min, followed by 40 cycles each of 30 seconds at 95℃, annealing at 59-61℃ for 30 seconds, and extension at 72 ℃ for 20 seconds. After a final extension step of 72 ℃ for 5 min, melting curves were plotted by stepwise increases in the temperature from 50 to 95℃. The annealing temperature was optimized for each primer assay. Relative abundances were obtained after normalization of the target genes Cq (Crossing Point) values by the geometric mean of the reference genes Cq values according to the mathematical model described by Pfaffl (2001). *PPIA*, *GAPDH* and *ACTB* were used as reference genes for BEEC samples, while *H2AFZ*, *GAPDH* and *RN18S1* were used for embryos. Primers details are provided in Supplementary Table S11.

4.3.9 RNA-sequencing

Five BEEC samples (Experiment 1) per experimental group were selected for transcriptome analysis. Each sample consisted of a BEEC monolayer retrieved from an individual well. Samples were chosen based on these criteria: (i) samples from the Juxt and Non-juxt groups having embryos developed to similar blastocyst rates and stages; and (ii) samples pertaining to the same replicates. Blastocyst developmental rates for each sample addressed for RNAseq analysis are given in Supplementary Table S12.

Poly-A containing mRNA molecules were purified from total RNA using oligo(dT)-attached magnetic beads and fragmented into small pieces using divalent cations under elevated temperature. First-strand cDNA was synthetized using random hexamer-primed reverse transcription, followed by a second-strand cDNA synthesis using DNA Polymerase I

and RNase H. The synthesized cDNA was subjected to end-repair and 3' adenylation. Adapters were ligated to the ends of 3' adenylated cDNA fragments. cDNA fragments with adapters from previous step were amplified by PCR. The resulting PCR products were purified with Agencourt AMPure XP Beads (Beckman Coulter, Beverly, MA, US), and dissolved in buffer EB. Double stranded PCR products were heat-denatured and circularized by the splint oligo sequence. Single stranded circular DNAs (ssCir DNA) were used for PE100 strand-specific library construction and validation on the Bioanalyzer 2100 (Agilent Genomics). The library was amplified with phi29 and DNA nanoballs (DNBs) were generated with ssCir DNA by rolling circle replication (RCR) to intensify the fluorescent signals during the sequencing process. The DNBs were loaded into the patterned nanoarray and pair-end reads of 100 bp were read on the BGISEQ-500 (Cambridge, MA, US) platform for subsequent data analysis.

4.3.10 Statistical Analyses and Bioinformatics

Statistical analyses were carried out in SAS 9.4 software. Discrete variables (blastocyst rates and the proportion of blastocysts reaching the expanded-stage or beyond) were analyzed by PROC GLIMMIX using binomial distribution. Replicates were included as random effects in the model. When different, means across treatments were compared by DIFF adjusted by Tukey-Kramer test. Continuous variables (PCR data, cell count and ICM:TE ratio) were checked for normality of residues and homogeneity of variances by Shapiro-Wilk and Welch's test, respectively. Variables were transformed by log or root square when necessary to accomplish assumptions. Effects of treatments were determined using PROC MIXED by analysis of variance considering Type III sums of squares. When different, means across treatments were compared using DIFF adjusted by Tukey-Kramer test. A probability of $P \leq 0.05$ indicates a significant difference, and a probability of $P > 0.05$ to $P \leq 0.1$ indicates a tendency. Data are presented as mean ± SEM, unless otherwise indicated.

Transcriptome analysis was performed in Galaxy (https://usegalaxy.org). Quality control was performed by FastQC (version 0.71). Paired reads were mapped to the Bos taurus reference genome (UMD 3.1) using HISAT2 (version 2.1.0), after which the counts per gene model was performed with FeatureCounts (version 1.6.2). Expression values were normalized and global and pairwise statistics were performed using DESeq2 (version 1.18.1) using false discovery rate (FDR)-corrected P values.

Canonical pathways of the DEGs was performed using Core Analyses in Ingenuity® Pathway Analysis (IPA, QIAGEN bioinformatics). For that, a cutoff of DEGs with Fold Change ≥ 1.5 and adjusted P value ≤ 0.05 was applied. A detailed description of the IPA analysis is available on the manufacturer's homepage (https://www.qiagenbioinformatics.com/products/features/). Heat map was generated with Morpheus software (https://software.broadinstitute.org/morpheus/).

4.4 RESULTS

4.4.1 Characterization of bovine endometrial epithelial cells

During primary culture, isolated BEECs attached to the plastic surface of culture dishes and exhibited a mixture of round, spindle and elongated morphologies (data not shown). However, after the first passage, monolayers consisted of a homogeneous population of epithelial-like adherent cells, and that feature remained constant after two subsequent passages.

For means of characterization, the abundance of transcripts for cell-origin and relevant functional markers were addressed by real time PCR in the BEECs from the primary culture and the 3 first passages. Gene expression data revealed a 6-fold increased ($P < 0.001$, Fig. 2) abundance of *VIM* mRNA from primary culture to passage 1, that remained constant until passage 3; however, abundance of transcripts for keratin 18 (*KRT18*), estrogen receptor alpha (*ESR1*), prostaglandin-endoperoxide synthase 2 (*PTGS2*), and interferon alpha and beta receptor subunit 1 (*IFNAR1*) remained similar among primary culture and first passages, suggesting that the cells conserved these functional characteristics (Fig. 2). Immunofluorescence staining revealed that the BEECs co-express cytokeratin, a typical cytoplasmic marker for epithelial origin, together with vimentin, a marker of mesenchymal-derived cells (Fig. 3). Taken together, these results indicate that our cell line, despite its dedifferentiated status, constitutes a physiologically relevant model to answer the hypotheses raised in this study.

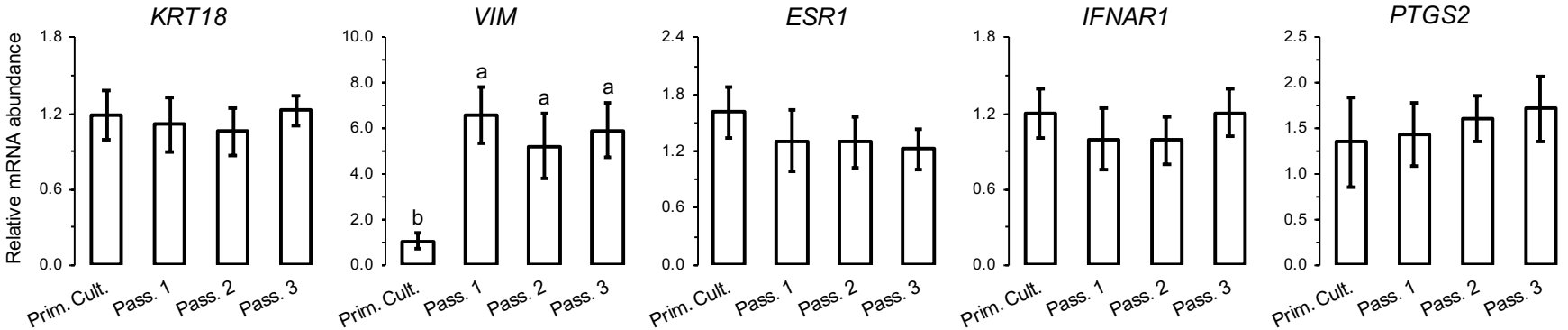

Figure 2. Relative mRNA abundance of keratin 18 (KRT18), vimentin (VIM), estrogen receptor alpha (ESR1), prostaglandin-endoperoxide synthase 2 (PTGS2), and interferon alpha and beta receptor subunit 1 (IFNAR1) on bovine endometrial epithelial cells at primary culture and first three passages. Data are shown as arbitrary units; mean ± SEM. a,b Statistically significant difference in mRNA abundance ($P \leq 0.05$, $n = 8$).

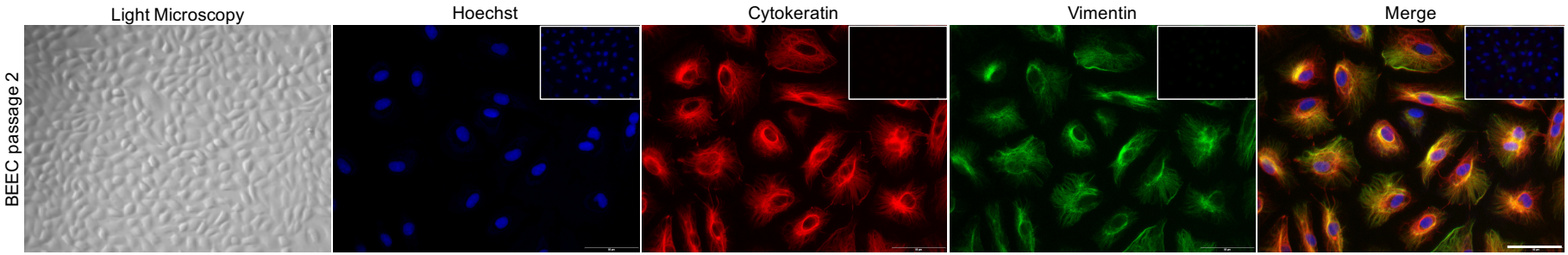

Figure 3. Morphology of bovine endometrial epithelial cells (BEEC) at passage 2. Light microscopy images were acquired with x10 magnification. Immunofluorescence staining for an epidermal stem cell marker (cytokeratin, in red) and a stromal cell marker (vimentin, in green). The endometrial cells were positive for both markers. Scale bar = 50 µm. Negative controls were incubated with an equivalent mixture of normal mouse and rabbit IgGs instead of primary antibodies (top right inserts).

4.4.2 Embryo-induced effects on bovine endometrial epithelial cells transcriptome

Five samples of BEECs from NoEmbryos, Juxt and Non-juxt groups were analyzed (criteria applied to select samples for transcriptome analysis are described in *RNA-sequencing* section). After mapped to the *Bos taurus* reference genome (assembly UMD3.1) and filtering, a total of 19,996 genes were used to identify differentially expressed genes [DEGs; false discovery rate (FDR), *P*adj ≤ 0.05]. A list of DEGs (*P*adj ≤ 0.05) is provided on Supplementary Datasets S13-S15 along with their respective mean normalized counts per group, Log fold-changes, and adjusted *P* values. A total of 1,797 (*P*adj ≤ 0.05; Fig. 4) genes were differentially expressed in the Juxt group compared to their NoEmbryos counterparts. Whereas, only 230 DEGs were found between Non-juxt compared to the NoEmbryos group (Fig. 4). Notably, from those 230 DEGs, a subset of 225 genes was found to be also differentially expressed in the Juxt versus NoEmbryos comparison, as represented in Figure 4. These 225 overlapping DEGs, therefore, represent the embryo-induced effects on BEEC transcriptome irrespective to juxtaposition.

4.4.2.1 Pathways impacted by embryo presence

Many of the 225 genes commonly responsive to embryo presence, regardless of Juxt or Non-juxt condition, were classical type I interferon stimulated genes (ISGs; Fig. 4 and 5). The 5 most up-regulated genes triggered by the embryo included *MX1* (192-fold), *OAS1X* (135-fold), *IFIT1* (123-fold), *OAS1Y* (73-fold), and *IFI27* (86-fold). Presence of embryos also modulated transcription of genes other than interferon-mediated signaling, as for example mRNA abundances for transporters including solute carrier family (*SLC*) 25, member 28 (*SLC25A28*), *SLC25A15*, and *SLC25A30* was increased in the Juxt and Non-Juxt groups compared to the NoEmbryos control. IPA analysis of the DEGs (Padj < 0.05; Cutoff fold-change >1.5) yield in the Non-juxt versus NoEmbryos comparison identified 125 enriched biological processes. As expected, the top canonical pathways revealed in this functional analysis are mostly related to interferon-mediated immune responses pathways (e.g. Interferon Signaling, Activation of IRF by Cytosolic Pattern Recognition Receptors, Antigen Presentation Pathway, and Role of PKR in Interferon Induction and Antiviral Response pathway; Fig. 6). Additional relevant pathways identified include Retinoic acid Mediated

Apoptosis Signaling, Protein Ubiquitination Pathway, Prolactin Signaling and Prostanoid Biosynthesis (Fig. 6).

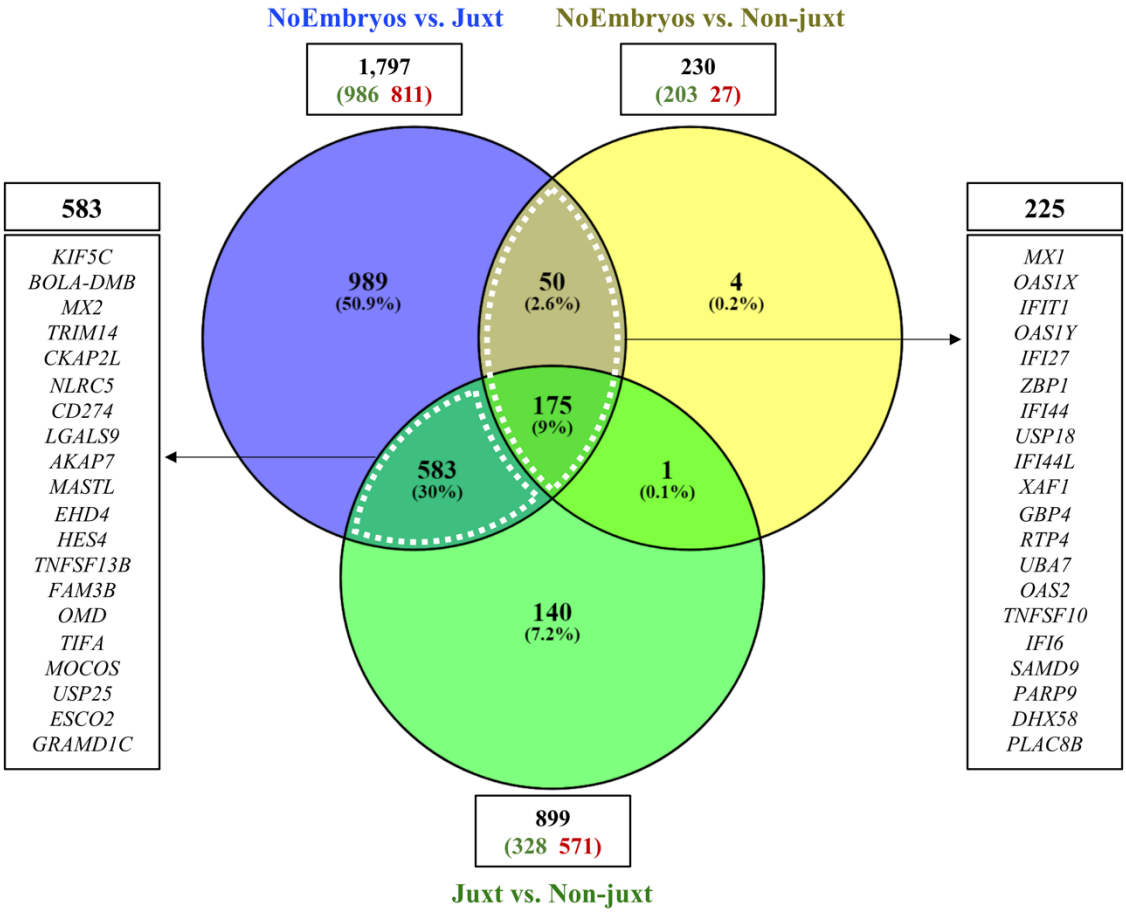

Figure 4. Venn diagram of RNAseq data from bovine endometrial epithelial cells (BEEC; n=5/group) exposed to none (NoEmbryos), juxtapositioned (Juxt) or without contact (Non-juxt) day-5.5 morulae/early blastocysts for 48 h. Differentially expressed genes (DEGs) were selected using adjusted P values (FDR ≤ 0.05). The number of up- and downregulated genes are shown in green and red, respectively. Embryo-induced effects regardless of juxtaposition are represented by the overlapping 225 DEGs yield in the NoEmbryos vs. Juxt, and NoEmbryos vs. Non-juxt comparisons. Effect of embryos juxtaposition on endometrial transcriptome is represented by the intersected 583 DEGs yield in the NoEmbryos vs. Juxt, and Juxt vs. Non-juxt comparisons. Top-20 DEGs for each dataset are shown. See Supplemental Datasets S13-S15 for a complete list of DEGs.

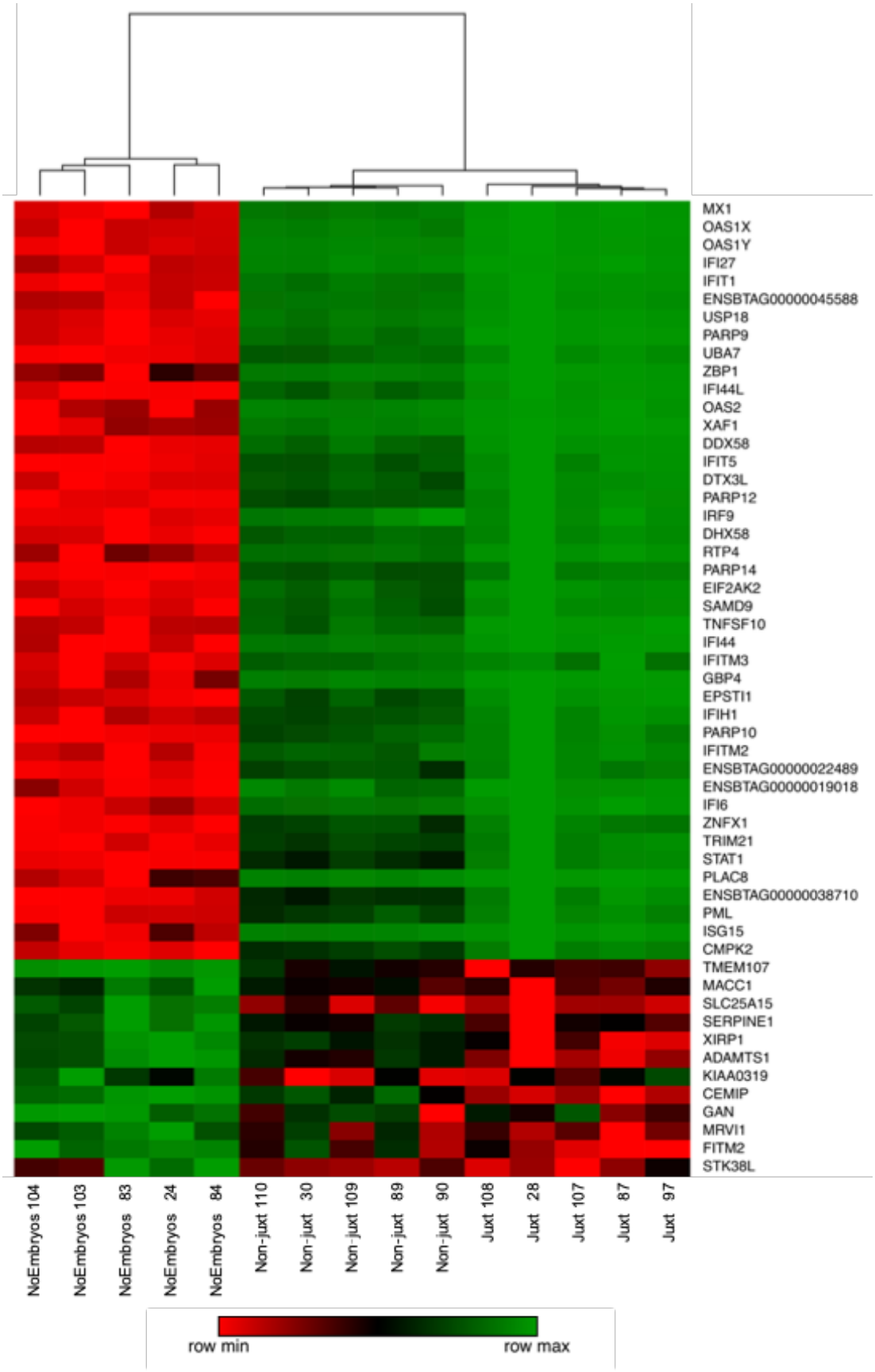

Figure 5. Heat map depicts the top differentially up- and downregulated genes among the three groups. Reads count data were log2 transformed and scaled to each row. Samples were clustered by Euclidean distances and are represented in each column.

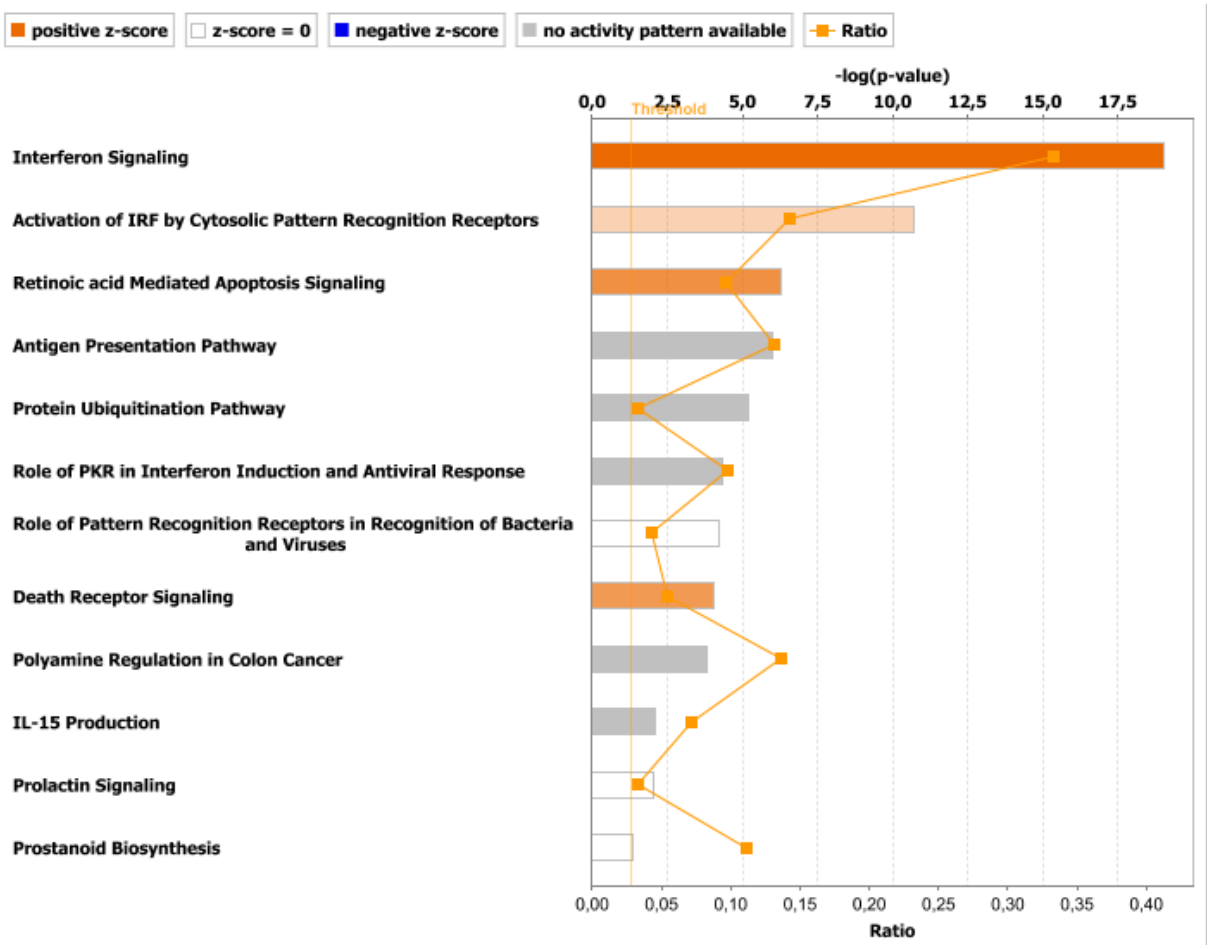

Figure 6. Overview of canonical pathways returned by Ingenuity Pathway Analysis (IPA) analysis of differentially expressed genes (DEGs; *P*adj ≤ 0.05; Cutoff fold-change >1.5) between NoEmbryos versus Non-juxt groups. The charts (y-axis) represent the top significantly enriched canonical pathways. The upper x-axis shows the −log of the value calculated based on Fisher's exact test. The ratio (bottom x-axis) represented by the orange points is calculated based on the numbers of genes in a given pathway divided by the number of genes pertaining to that pathway. Straight orange vertical line represents the threshold for significance (by default). Canonical pathways shown were selected based on their biological significance.

4.4.2.2 Pathways impacted by juxtaposition with embryos

The comparison between Juxt versus Non-juxt yielded 899 DEGs with 583 (~65%) genes commonly changed in the NoEmbryos versus Juxt comparison (Fig. 4). Effect of embryo juxtaposition on endometrial transcriptome was accessed by these intersected 583 DEGs. The top-5 DEGs include kinesin family member 5C (*KIF5C*), major histocompatibility complex, class II, DM beta (*BOLA-DMB*), *MX2*, tripartite motif containing 14 (*TRIM14*), and cytoskeleton associated protein 2 like (*CKAP2L*). IPA analysis produced 229 enriched biological processes in the Juxt versus Non-juxt comparison. In addition to changes in interferon-mediated immune responses canonical pathways, other pathways identified included: regulation of cell cycle (e.g. Mitotic Roles of Polo-like Kinase, Cell Cycle: G2/M DNA Damage Checkpoint regulation, Cyclins and Cell Cycle Regulation, and Estrogen-

mediated S-phase Entry), mitochondrial metabolism (e.g. Oxidative Phosphorylation, Sirtuin Signaling Pathway, and Mitochondrial Dysfunction), and pregnenolone biosynthesis. An overview of canonical pathways impacted by juxtaposition between embryos and the BEEC monolayer is provided in Figure 7 and 8.

Figure 7. Overview of canonical pathways returned by Ingenuity Pathway Analysis (IPA) analysis of differentially expressed genes (DEGs; *P*adj ≤ 0.05; Cutoff fold-change >1.5) between Juxt versus Non-juxt groups. The charts (y-axis) represent the top significantly enriched canonical pathways. The upper x-axis shows the −log of the value calculated based on Fisher's exact test. The ratio (bottom x-axis) represented by the orange points is calculated based on the numbers of genes in a given pathway divided by the number of genes pertaining to that pathway. Straight orange vertical line represents the threshold for significance (by default). Canonical pathways shown were selected based on their biological significance.

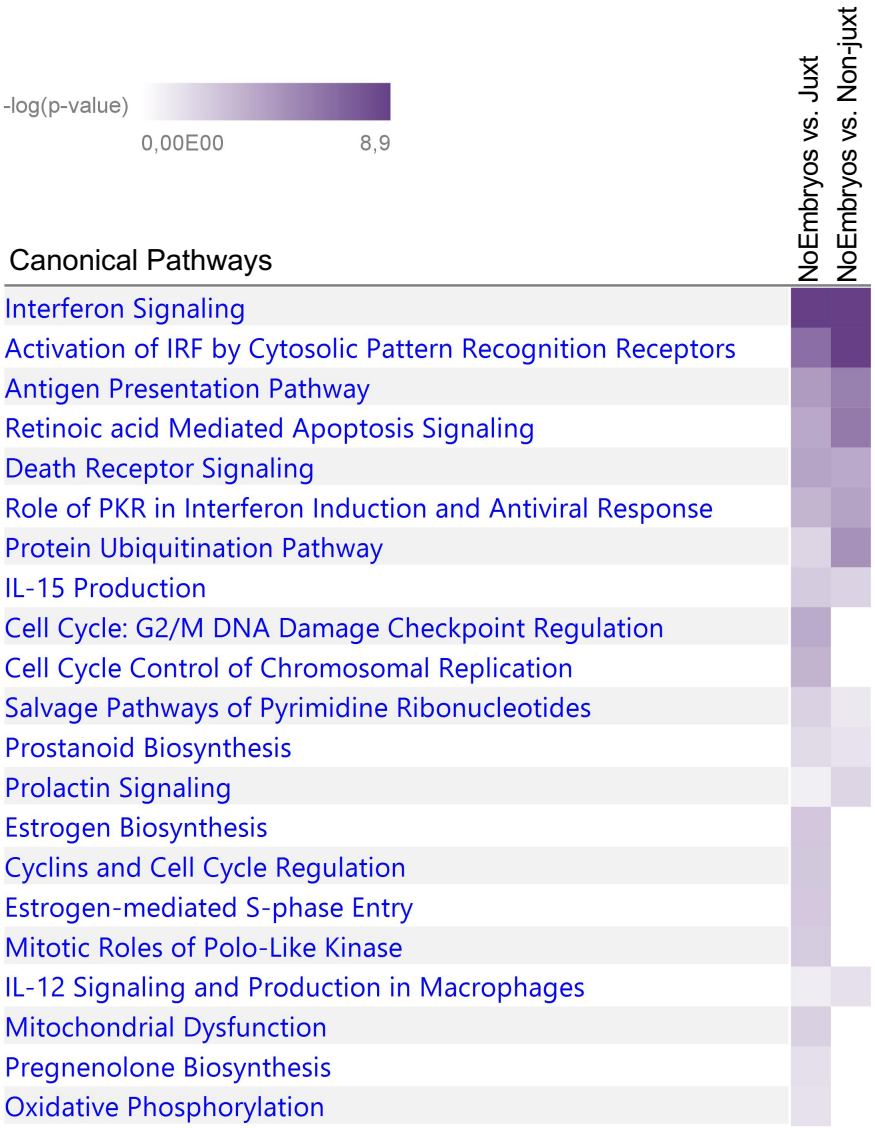

Figure 8. Heatmap analysis depicting IPA canonical pathways significantly modulated by embryos when juxtapositioned (Juxt) or without contact (Non-juxt) with a BEEC monolayer compared to the NoEmbryos control group. P-value scores indicate the significance of the pathway's association with the dataset and are represented by purple scale.

4.4.2.3 Ingenuity Upstream Regulator Analysis

To gain insights on the possible molecules triggering the transcriptome differences observed between Juxt versus Non-juxt conditions, upstream regulator analysis of DEGs (Padj < 0.05, Cutoff fold-change >1.5) was performed in IPA software. The top 20 potential upstream regulators based on DEGs yield in the Juxt versus Non-juxt comparison are shown in Table 1. Results confirmed type I interferon-signaling as an important upstream regulator eliciting differences between Juxt versus Non-juxt transcriptome profiles. Interestingly, other potential upstream regulators include PTGER4 (prostaglandin E receptor 4) and PRL

(prolactin) being activated, and NKX2-3 (NK2 Homeobox 3) and CDKN1A (Cyclin Dependent Kinase Inhibitor 1A) being inhibited in the Juxt group.

Table 1. Top 20 upstream regulators predicted based on the differentially expressed genes (DEGs) yield by transcriptome analysis between Juxt vs. Non-juxt groups. Analysis was performed in IPA software.

Upstream Regulator	Molecule Type	Predicted Activation State	Activation z-score	P-value of overlap
IRF7	transcription regulator	Activated	6.319	4.2×10^{-44}
Interferon alpha	group	Activated	5.905	1.34×10^{-39}
IFNL1	cytokine	Activated	4.853	5.73×10^{-37}
IFNA2	cytokine	Activated	5.836	1.51×10^{-33}
PTGER2	G-protein coupled receptor	Activated	5.282	1.28×10^{-30}
Ifnar	group	Activated	5.066	5.83×10^{-29}
MAPK1	kinase	Inhibited	-5.330	6.3×10^{-28}
dextran sulfate	chemical drug			1.01×10^{-27}
NKX2-3	transcription regulator	Inhibited	-4.700	2.63 x 10-^{27}
IRF1	transcription regulator	Activated	4.864	8.63×10^{-27}
CDKN1A	kinase	Inhibited	-3.337	6.13×10^{-26}
PRL	cytokine	Activated	5.719	5.81×10^{-25}
IRF3	transcription regulator	Activated	4.923	7.7×10^{-25}
IFN Beta	group	Activated	4.751	3.65×10^{-24}
STAT3	transcription regulator		0.203	1.8×10^{-23}
STAT1	transcription regulator	Activated	4.430	1.25×10^{-22}
TRIM24	transcription regulator	Inhibited	-4.626	2.95×10^{-22}
IFNB1	cytokine	Activated	5.059	3.1×10^{-22}
calcitriol	chemical drug	Inhibited	-4.611	4.06×10^{-21}
IL1RN	cytokine	Inhibited	-3.683	4.46×10^{-21}

4.4.3 Effect of co-culture on embryo development

In vitro produced day 5.5 morulae were cultured for 48 h in SOF-5% FBS in the absence of BEEC (NoBEEC), juxtapositioned on top of subconfluent BEEC monolayers (Juxt), or on transwells, without direct contact with BEEC (Non-juxt). Co-culture with BEEC significantly increased blastocyst rates on day 7.5, regardless of Juxt or Non-juxt condition (Table 2). Additionally, the proportion of blastocyst that reached the expanded, hatching or hatched stages was significantly greater ($P \leq 0.05$) or tented ($P \leq 0.1$) to be greater in the Non-juxt and Juxt groups, respectively, compared to the NoBEEC control. Although the average counts of total cells on day-7.5 blastocysts were similar across treatments, there was an increase on the ICM/TE ratio in blastocysts from Juxt (Table 2). This difference in blastomere cell fate, however, did not impact the abundance of *CDX2* mRNA between the three culture conditions (Fig. 9). Surprisingly, Non-juxt embryos presented a 4-fold increased abundance of

transcripts for *IFNT2* compared to the Juxt group. The Non-juxt condition also increased the abundance of mRNA for *BAX*, an apoptosis-related gene, compared to the NoBEEC and Juxt groups (Fig. 9).

Table 2. Effects of co-culture with bovine endometrial epithelial cells (BEEC) on embryo development. On day 5.5, groups of 15±1 untreated morulae/early blastocysts were cultured in SOF-based medium in the absence of BEEC (NoBEEC), juxtapositioned on top of subconfluent BEEC monolayers (Juxt), or on transwells, without contact with BEEC (Non-juxt). On day 7.5, embryonic development was evaluated. Embryos were evaluated for total cell counting and trophectoderm (TE) or Inner Cells Mass (ICM) differential immunostaining.

Day-5.5 morulae* assigned to treatments	640/1970 (32.5%)		
Variables	**Groups**		
	NoBEEC	**Juxt**	**Non-juxt**
Day-7.5 blastocysts**	109/205 (53.2%)^{b}	147/225 (65.3%)^{a}	134/210 (63.8%)^{a}
Expanded, hatching or hatched blastocysts***	50/109 (45.9%)^{b,Y}	88/147 (59.9%)^{a,X}	88/134 (65.7%)^{a}
Total cell counts (mean ± SEM)	111.08 ± 6.07	125.36 ± 5.16	117.86 ± 5.75
ICM:TE ratio (mean ± SEM)	0.36 ± 0.031^{b}	0.47 ± 0.027^{a}	0.36 ± 0.029^{b}

*From total oocytes
**From cultured morulae
***From total blastocysts
Within rows, values with different superscript letters differ significantly (a, b; $P \leq 0.05$) or tend to differ (X, Y; $P < 0.1$)

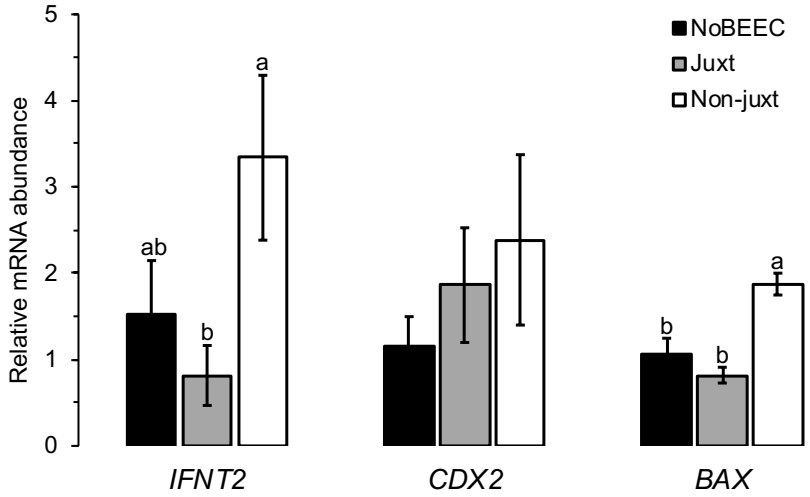

Figure 9. Relative mRNA abundance of interferon-tau (*IFNT2*), caudal type homeobox 2 (*CDX2*), and BCL2 associated X, apoptosis regulator (*BAX*) on day 7.5 blastocysts co-cultured with bovine endometrial epithelial cells (BEEC). Each sample consists of a pool of 15 embryos (n = 4-5). Data are shown as arbitrary units; mean ± SEM. ^{a,b} Statistically significant difference in mRNA abundance ($P \leq 0.05$).

4.4.4 Specificity of bovine endometrial epithelial cells (BEEC)-induced effects on embryo development

In the second experiment, *in vitro*-derived day 5.5 morulae/early blastocysts were cultured in SOF-based medium (Control), or in SOF medium conditioned by BEEC (BEECcond), or by fibroblasts (FIBRcond). On day 7.5, the number of morulae that became blastocysts was significantly greater in the BEECcond compared to the Control or to the FIBRcond groups (Table 3). However, there was no effect of BEECcond condition on the proportion of blastocysts that reached or surpassed the expanded-stage.

Table 3. Specificity of bovine endometrial epithelial cells (BEEC)-driven effects on embryo development on day 7.5. On day 5.5, groups of 15±1 untreated morulae/early blastocysts were cultured in SOF-based medium (Control), in BEEC-conditioned SOF medium (BEECcond), or in fibroblast-conditioned SOF medium (FIBRcond). On day 7.5, embryonic developmental rates were recorded.

Day-5.5 morulae* assigned to treatments	821/2320 (35.4%)		
Variables	**Groups**		
	Control	**BEECcond**	**FIBRcond**
Day-7.5 blastocysts**	178/315 (56.5%)[b]	234/328 (71.3%)[a]	100/178 (56.2%)[b]
Expanded, hatching or hatched blastocysts***	104/178 (58.4%)	143/234 (61.1%)	52/100 (52.0%)

*From total oocytes
**From cultured morulae
***From total blastocysts
Within rows, values with different superscript letters differ significantly (a, b; $P < 0.001$)

4.5 DISCUSSION

In cattle, there is limited information on the role of the pre-elongation embryo in programming the maternal reproductive tract function. Recent discoveries indicated that the endometrium transcriptome is locally changed by the presence of the embryo as early as day 7 *in vivo* (Sponchiado *et al*., 2017). Other *in vitro* studies have confirmed that endometrial cells are responsive to embryo-presence (Talukder *et al*., 2017; Gómez *et al*., 2018; Passaro *et al*., 2018). A critical question in this scenario is whether physical proximity of the embryo to the endometrium is necessary to elicit changes on its transcriptome. Alternatively, embryo secretions could act on the surrounding tissues in a classical paracrine manner. Here, by using an explorative approach based on an *in vitro* co-culture system, we were able to address the very local embryo-endometrial interface for embryo-induced changes in endometrial cell transcriptome. Embryos were co-cultured in juxtaposition or without contact with BEEC monolayers for 48 h and the magnitude of effects at the level of the embryo and the BEEC was investigated. It was shown that the embryo development supportive effects of the BEEC cells do not depend on an embryo-BEEC juxtaposition. Nonetheless, our results indicate that

intensity and nature of embryo-induced changes on endometrial epithelial cells transcriptome depended on the physical proximity between embryos and the BEEC monolayer.

We stablished an endometrial epithelial cell line in a manner that in every replicate, aliquots containing cells originated from the same pool were applied. Regarding the biological accuracy of our *in vitro* model, the co-expression of cytokeratin and vimentin in our BEEC line is in line with previous reports describing the expression of vimentin by cytokeratin-positive epithelial cells maintained in culture (Wang *et al*., 2000; Zeiler *et al*., 2007; Li *et al*., 2016) via a process described as epithelial-mesenchymal transition (Kalluri & Weinberg, 2009). However, even after three passages the BEECs displayed no changes on abundance of transcripts for epithelial-cell origin (*KRT18*) and functional markers (*ESR1*, *IFNAR1* and *PTGS2*) rendering our BEEC line valid to address the aims of the study.

By means of RNAseq, we further advanced the understanding on the embryo-endometrial interactome looking at the endometrial-response to the presence of peri-hatching embryos. Juxtaposition between embryos and BEECs elicited substantial changes on BEEC transcriptome, as seen by the high number of DEGs (1,797) yield in the NoEmbryos versus Juxt comparison. Interestingly, transcriptome changes were rather limited between NoEmbryos versus Non-juxt, with only 230 genes being differentially expressed between the two groups. Of note, out of these 230 genes, 225 also had their transcription regulated when embryos were juxtapositioned to the BEECs (Fig. 4). Thus, this group of 225 genes, differentially expressed in both Juxt and Non-juxt groups compared to the NoEmbryos control, likely represent the embryo specific paracrine stimulus exerted on the endometrial monolayer.

Interferon-tau seems to be the key player in the embryo-maternal communication. Most differentially expressed genes were related to classical type I interferon-mediated signaling, regardless of Juxt or Non-juxt condition. Notably, some transcripts for classical ISGs (*MX1*, *OAS1X*, *IFIT1*) showed dramatic fold changes (>100) in our study. There is no consensus about when does the bovine embryo start to produce IFNτ. It has been shown, for example, that bovine blastocysts express and release IFNT into the culture medium (Hernandez-Ledezma *et al*., 1993). More recently, expression of IFNT at protein level by bovine *in vitro*-produced morulae has been reported (Talukder *et al*., 2018). Here, we demonstrated that *in vitro*-produced day 7.5 bovine embryos present transcripts for *IFNT2,* as well as, that the BEECs used in our model present mRNA for interferon alpha and beta receptor subunit 1 (*IFNAR1*). Early embryo-induced changes in the abundance of ISGs, have been reported in the endometrium *in vivo* (Sponchiado *et al*., 2017), and in endometrial

(Talukder *et al*., 2017; Passaro *et al*., 2018) and immune cells (Talukder *et al*., 2018) *in vitro*. Other studies later on pregnancy also reported major changes on endometrial transcriptome between pregnant and cyclic cows being induced by IFNT (Bauersachs *et al*., 2006; Klein *et al*., 2006; Forde *et al*., 2011; Sánchez *et al*., 2019). Although IFNT has been extensively studied based on its ability to mediate pregnancy recognition in ruminants, its potential role in embryo development prior to the pregnancy recognition window is still not completely understood. For instance, it has been shown that deletion of Isg15 results in 50% pregnancy loss before placentation in mice (Ashley *et al*., 2010). However, a remaining open question is whether and to which extent classical ISGs have a biological role in programming the endometrium towards a more supportive status for the development of the bovine embryo in the context of early pregnancy (Pestka, 2007).

The exploratory nature of our approach enabled us to further advance the understanding on the potential pathways changed by the embryo at the embryo-endometrial interface in addition to the previously reported type I interferon-mediated signaling. We showed, for example, that presence of embryos increased mRNA abundance for transporters including members of the SLC family 25 (*SLC25A28*, *SLC25A15*, and *SLC25A30*). SLC25 transporters compose a large family of nuclear-encoded membrane-embedded proteins that promote solute transport across the inner mitochondrial membrane. They have been implicated as being responsible for the transport and utilization of glutamate (Palmieri, 2008), and decreases in the levels of these members of the SLC family may affect nutrient transport and utilization in the endometrium.

Intensity and nature of embryo-induced changes on endometrial transcriptome largely depend on juxtaposition between embryos and the BEEC monolayer. Differences in quantity and quality of embryo-induced effects on BEEC transcriptome due to a juxtaposition between the embryos and the endometrial cells might be attributed to three possibilities. One mechanism includes a **diffusion gradient** of embryo-derived signals when embryos were placed on transwell inserts, leading to a less pronounced endometrial response to embryo-derived soluble factors, as for example IFNτ. In this regard, our data showed an up-regulation of ISGs in the Juxt compared to the Non-juxt BEECs. Also, the upstream regulator analysis predicted the interferon-signaling system as a potential candidate of factors depicting transcriptional changes triggered by the juxtapositioned embryos on BEECs (Table 1). Another possibility comprises signaling triggered by **physical contact** between the embryos and the BEEC monolayer. Some of the top DEGs between Juxt versus Non-juxt provide evidence for a local immune response due to juxtaposition of embryos, as for example the up-

regulation of *BOLA-DMB* transcripts in the Juxt BEECs. The bovine leucocyte antigen (BoLA) system refers to the major histocompatibility complex (MHC) of cattle, which initiates an adaptive immune response to specific pathogens. *BOLA-DMB* pertains to the subclass IIb and is involved in antigen processing and transport (Ellis, 2004). The endometrial epithelial BoLA system may play an important role on immune recognition and tolerance of the semi-allogenic embryo within the uterine lumen. It is known, however, that there is no intimate contact (i.e., tissue adhesion) between the pre-implantation, non-invasive embryo and the lining endometrial epithelium in the bovine species (Bazer *et al*., 1991). It is noteworthy that in this study, at the end of the co-culture period (day 7.5 p.i.), most embryos were still enclosed in the zona pellucida. It is important to point out that the proportion of hatching and hatched blastocysts was similar between Juxt and Non-juxt conditions. Specifically, for the samples that were analyzed by RNAseq, the proportion of hatching and hatched blastocysts on day 7.5 was 17.3% (13/75) and 16% (12/75) for Juxt and Non-juxt, respectively (Supplementary Table S12). Direct cell-to-cell contact at the pre-hatching stage might be provided by membrane extensions through the zona pellucida (Allen & Wright Jr, 1984) and trophectoderm projections (Gonzales *et al*., 1996). Furthermore, it has been described that the zona pellucida could also contribute with binding sites and local release of signaling molecules (i.e. growth factors and cytokines) towards the endometrial cells (Denker, 2000; Herrler *et al*., 2002). Relatively little work has been done on the mechanisms underpinning a possible juxtracrine communication at the embryo-maternal interface prior to zona-hatching in monotocous mammals. A third possible explanation is that embryos juxtapositioned to the BEEC monolayer have **distinguished capacities to produce and/or release signaling molecules** in turn. In the present study, no difference was observed between embryos derived from Juxt versus Non-juxt conditions in terms of blastocyst development on day 7.5 p.i.. However, the embryo-BEEC juxtaposition did impact on resulting blastocysts' cell commitment as seen by the increased ICM:TE ratio in the Juxt group, as well as on the abundance of transcripts for *IFNT2* that was 4-fold greater in the Non-juxt embryos compared to the Juxt counterparts. Thus, it is also reasonable to expect that the co-culture conditions affected the signaling capacity of those embryos. Although our experimental set-up does not allow us to distinguish these three possibilities, we speculate that differences on BEEC response to Juxt versus Non-Juxt embryos likely reflect a combination of the above-mentioned mechanisms.

Interestingly, embryos juxtapositioned to the BEEC monolayer up-regulated transcription for genes related to cell cycle control and mitotic spindle formation, as for

example *PCNA*, *CKAP2L*, *KIF5C*, *KIFC1*, and *MASTL*. In fact, IPA analysis showed an enrichment for cell cycle-related pathways (e.g. Mitotic Roles of Polo-like Kinase, Cell Cycle: G2/M DNA Damage Checkpoint regulation, Cyclins and Cell Cycle Regulation, and Estrogen-mediated S-phase Entry) in the Juxt group (Fig. 7). Noteworthy, other genes associated with cell-cell adhesion and cytoskeleton were also regulated in the Juxt BEECs, including *XIRP1*, *AKAP7*, *ANXA1*, *AIDA*, and *CKAP2*. Further *in vivo* studies are necessary to address whether the endometrial epithelia changes its proliferation rate and/or its cell morphology in response to the local contact with the embryo/conceptus.

Co-culture with BEEC stimulates embryo development from morula to blastocyst stage. In the present study, morulae/early blastocysts were exposed to BEEC monolayers only on day 5.5 post fertilization to mimic the timing of embryo arrival into the uterus *in vivo* in the cow. In fact, many studies report that embryos at early developmental stages benefit from co-culture with endometrial cells in several species including bovine (Voelkel *et al*.,, 1985), human (Rubio *et al*., 2000), mice (Kauma & Matt, 1995; Lai *et al*., 1996) and porcine (Allen & Wright Jr, 1984). Although the specific mechanisms by which endometrial cells influence early embryo development remain to be elucidated, they may include five putative mechanisms: (i) **release of embryotrophic factors** into the culture medium, such as nutrients and substrates, including specific glycoproteins, amino acids, pyruvate, cytokines and growth factors (Kurachi *et al*., 1994; Kauma & Matt, 1995; Lim & Hansel, 1996); (ii) **reducing the concentration of embryo-suppressive components** from the culture medium, such as glucose or heavy metals; (iii) **stabilization of medium physicochemical conditions,** such as pH and osmolarity. Given that embryos-BEECs co-cultures and embryos (alone) cultures were conducted at 20% O_2, which is suboptimal for early embryo development, there is also a fourth possible mechanism that includes (iv) **protection from oxidative stress insults**. The cell monolayer could reduce the O_2 tension of the embryo microenvironment in culture and, therefore, benefit embryo development in a non-specific manner (Nagao *et al*., 1994); or (v) a combination of several of these mechanisms. The first three mechanisms are experimentally difficult to be distinguished, however, in our second experiment, we circumvent the potential effect of a reduced O_2 tension caused by feeder cell monolayers on embryo development by using conditioned medium.

Our results have shown that in fact the medium conditioned by BEECs had a significant positive effect on the proportion of morulae reaching the blastocyst stage compared to the Control (SOF) group, similar to what was observed in the first experiment. The specificity of the embryo supportive capacity of BEECs can be questioned by the fact that

numerous investigations have demonstrated an improvement in development when embryos were *in vitro* co-cultured with non-endometrial homologous somatic cells, such as oviductal cells (Eyestone, 1987; Thibodeaux *et al*., 1992), luteal cells (Maruri *et al*., 2018), granulosa cells (Freeman *et al*., 1995; Malekshah *et al*., 2006) or even in co-culture systems with stem cells, such as adipose tissue-derived mesenchymal cells (Miranda *et al*., 2016). It has been also shown that co-culture with heterologous somatic cells, as for example BRL (buffalo rat liver) cells and Vero (green monkey kidney epithelial) cells, efficiently improve the development of mouse, bovine and human embryos (Ouhibi *et al*., 1990; Reed *et al*., 1996; Menck *et al*., 1997; Duszewska *et al*., 2000; Kattal *et al*., 2008). Taken together, these results suggest a non-specific role of bovine endometrial cells, or even homologous cells, on embryo development in co-culture systems. Hereto, we challenged the specificity of the embryo supportive capacity of BEECs by using medium conditioned by heterologous unspecific feeder cells. The mice fibroblast-conditioned medium had no effect on embryo development compared to the Control. These observations suggest that bovine endometrial cells, and perhaps other reproductive tract cells, may provide a relatively specific stimulus for continued development of early embryos in co-culture.

Although the beneficial role of co-culture on embryo development does not seem to be dependent on a juxtaposition with the BEEC monolayer, the embryo-BEEC contact did affect the cell commitment of the resulting blastocysts, as seen by the increased ICM:TE ratio in the Juxt group. In mouse, it has been shown that cell-to-cell interaction can influence the lineage specification of embryonic blastomeres (Lorthongpanich *et al*., 2012). The greater ICM:TE ratio in Juxt derived blastocysts, however, did not impact on transcripts abundance of *CDX2*, a marker for trophectoderm cells. This could be explained by the fact that only embryos at normal blastocyst stage or beyond were evaluated for differential immunostaining, whereas embryos at all developmental stages (i.e. from morula to hatched blastocyst) were included in gene expression analyses. Additionally, day-7.5 blastocysts that were juxtapositioned to the BEEC monolayer displayed decreased abundances of *IFNT2* and *BAX* mRNA compared to Non-juxt embryos. It has been demonstrated that the attachment of trophectoderm to the uterine epithelium results in a decrease in IFNT expression during the implantation period in cattle (Ezashi & Imakawa, 2017). Also Sakurai *et al*. (2012) reported that co-culture with endometrial epithelial cells resulted in decreased *IFNT2* mRNA abundance in bovine trophoblast cells spheroids. The mechanisms by which the embryo-endometrium juxtaposition during the peri-hatching period could trigger to different patterns in IFNT expression warrants further investigation.

It should be pointed out that, in this study, 15 embryos were co-cultured with the BEEC monolayers. One could argue that this stimulus is though not representative for the physiological *in vivo* condition in the cow, as a monovulatory species. Experiment 1 was designed as an explorative approach for *in vitro* assessment of the embryo-maternal interface. As such, in order to maximize the embryo-BEEC physical contact zone and the stimulus promoted by the early embryo, multiple embryos were co-cultured with the BEEC monolayers. The multiple embryos co-culture strategy was also meant to minimize the individual influence of the quality of the embryo on endometrial response between samples and treatments. Extra attention was paid to select the BEEC samples that were analyzed by RNAseq. As show in Supplementary Table S12, BEEC samples that were co-cultured with embryos at similar developmental stages among the experimental groups were selected.

Collectively, our data provided new insights into the complex embryo-maternal interactome during the very early steps in pregnancy in cattle. We were able to demonstrate for the first time that day-7.5 bovine embryos change the endometrial epithelial cell global transcriptome. Highlighted pathways modulated by embryos presence included type I interferon signaling, regulation of cell cycle, prolactin signaling and prostanoid biosynthesis. Moreover, we can conclude that nature and magnitude of embryo-induced effects are influenced by physical proximity between endometrial cells and embryos. On the embryonic side, the co-culture system applied in this study improved bovine embryonic development from morula to blastocyst stage. This support seems to be BEEC specific and does not rely on a juxtaposition between the embryo and the BEEC monolayer. Nonetheless, juxtaposition with BEECs altered day-7.5 blastocysts' cell fate and *IFNT2* transcripts abundance. Nature of interactions between the lining endometrial epithelium and the non-invasive, pre-implantation embryo warrants further investigation.

4.6 ACKNOWLEDGEMENTS

The outstanding technical assistance of Gamete Research Centre staff and students to generate the embryos is gratefully acknowledged. The authors acknowledge Jens Slootmans for the assistance in performing RNA isolation and PCR analysis.

4.7 DECLARATION OF INTEREST

The authors declare no competing interests.

4.8 REFERENCES

Allen, R. L.; wright Jr, R. W. *In vitro* development of porcine embryos in coculture with endometrial cell monolayers or culture supernatants. **Journal of animal science,** v. 59, n. 6, p. 1657-1661, 1984.

Ashley, R. L. *et al*. Deletion of the Isg15 gene results in up-regulation of decidual cell survival genes and down-regulation of adhesion genes: implication for regulation by IL-1β. **Endocrinology,** v. 151, n. 9, p. 4527-4536, 2010.

Bauersachs, S. *et al*. Embryo-induced transcriptome changes in bovine endometrium reveal species-specific and common molecular markers of uterine receptivity. **Reproduction,** v. 132, n. 2, p. 319-331, 2006.

Bauersachs, S. *et al*. The endometrium responds differently to cloned versus fertilized embryos. **Proceedings of the National Academy of Sciences,** v. 106, n. 14, p. 5681-5686, 2009.

Bazer, F. W.; spencer, T. E.; ott, T. L. Interferon tau: a novel pregnancy recognition signal. **American Journal of Reproductive Immunology,** v. 37, n. 6, p. 412-420,

Bazer, F. W. *et al*. Physiological mechanisms of pregnancy recognition in ruminants. **Journal of reproduction and fertility,** v. 43, p. 39-47, 1991.

Brandao, D. O. *et al*. Post hatching development: a novel system for extended *in vitro* culture of bovine embryos. **Biology of Reproduction,** v. 71, n. 6, p. 2048-2055, 2004.

Carter, F. *et al*. Effect of increasing progesterone concentration from Day 3 of pregnancy on subsequent embryo survival and development in beef heifers. **Reproduction, Fertility and Development,** v. 20, n. 3, p. 368-375, 2008.

Denker, H. W. Structural dynamics and function of early embryonic coats. **Cells Tissues Organs,** v. 166, n. 2, p. 180-207, 2000.

Diskin, M. G.; parr, M. H.; morris, D. G. Embryo death in cattle: an update. **Reproduction, Fertility and Development,** v. 24, n. 1, p. 244-251, 2011.

Diskin, M. G. *et al*. Pregnancy losses in cattle: potential for improvement. **Reproduction, Fertility and Development,** v. 28, n. 2, p. 83-93, 2016.

Duszewska, A. M. *et al*. Development of bovine embryos on Vero/BRL cell monolayers (mixed co-culture). **Theriogenology,** v. 54, n. 8, p. 1239-1247, 2000.

Ellis, S. The cattle major histocompatibility complex: is it unique? **Veterinary immunology and immunopathology,** v. 102, n. 1-2, p. 1-8, 2004.

Eyestone, W. H. Coculture of early bovine embryos with oviductal epithelium. **Theriogenology,** v. 27, p. 228, 1987.

Ezashi, T.; Imakawa, K. Transcriptional control of IFNT expression. **Reproduction,** v. 154, n. 5, p. 21-31, 2017.

Forde, N. *et al*. Progesterone-regulated changes in endometrial gene expression contribute to advanced conceptus development in cattle. **Biology of Reproduction,** v. 81, n. 4, p. 784-794, 2009.

Forde, N. *et al*. Conceptus-induced changes in the endometrial transcriptome: how soon does the cow know she is pregnant? **Biology of Reproduction,** v. 85, n. 1, p. 144-156, 2011.

Freeman, M. R.; Whitworth, C. M.; Hill, G. A. Granulosa cell co-culture enhances human embryo development and pregnancy rate following *in vitro* fertilization. **Human reproduction,** v. 10, n. 2, p. 408-414, 1995.

Gonzales, D. S. *et al*. Implantation: Trophectoderm projections: a potential means for locomotion, attachment and implantation of bovine, equine and human blastocysts. **Human reproduction,** v. 11, n. 12, p. 2739-2745, 1996.

Guillomot, M. Cellular interactions during implantation in domestic ruminants. **Journal of reproduction and fertility,** v. 49, p. 39-51, 1994.

Gómez, E. *et al*. *In vitro* cultured bovine endometrial cells recognize embryonic sex. **Theriogenology,** v. 108, p. 176-184, 2018.

Hernandez-Ledezma, J. J. *et al*. Expression of bovine trophoblast interferons by *in vitro*-derived blastocysts is correlated with their morphological quality and stage of development. **Molecular reproduction and development,** v. 36, n. 1, p. 1-6, 1993.

Herrler, A.; Von Wolff, M.; Beier, H. Proteins in the extraembryonic matrix of preimplantation rabbit embryos. **Anatomy and embryology,** v. 206, n. 1-2, p. 49-55, 2002.

Kalluri, R.; Weinberg, R. A. The basics of epithelial-mesenchymal transition. **The Journal of clinical investigation,** v. 119, n. 6, p. 1420-1428, 2009.

Kattal, N.; Cohen, J.; Barmat, L. I. Role of coculture in human *in vitro* fertilization: a meta-analysis. **Fertility and sterility,** v. 90, n. 4, p. 1069-1076, 2008.

Kauma, S. W.; Matt, D. W. Coculture cells that express leukemia inhibitory factor (LIF) enhance mouse blastocyst development *in vitro*. **Journal of assisted reproduction and genetics,** v. 12, n. 2, p. 153-156, 1995.

Klein, C. *et al*. Monozygotic twin model reveals novel embryo-induced transcriptome changes of bovine endometrium in the preattachment period. **Biology of Reproduction,** v. 74, n. 2, p. 253-264, 2006.

Kurachi, H. *et al*. Expression of epidermal growth factor and transforming growth factor-alpha in fallopian tube epithelium and their role in embryogenesis. **Hormone Research in Paediatrics,** v. 41, n. Suppl. 1, p. 48-54, 1994.

Lai, Y. M. *et al*. Insulin-like growth factor-binding proteins produced by Vero cells, human oviductal cells and human endometrial cells, and the role of insulin-like growth factor-binding protein-3 in mouse embryo co-culture systems. **Human Reproduction,** v. 11, n. 6, p. 1281-1286, 1996.

Li, X. *et al*. The bovine endometrial epithelial cells promote the differentiation of trophoblast stem-like cells to binucleate trophoblast cells. **Cytotechnology,** v. 68, n. 6, p. 2687-2698, 2016.

Lim, J. M.; Hansel, W. Roles of growth factors in the development of bovine embryos fertilized *in vitro* and cultured singly in a defined medium. **Reproduction, fertility and development,** v. 8, n. 8, p. 1199-1205, 1996.

Lorthongpanich, C. *et al*. Developmental fate and lineage commitment of singled mouse blastomeres. **Development,** v. 139, n. 20, p. 3722-3731, 2012.

Macklon, N. S.; Brosens, J. J. The human endometrium as a sensor of embryo quality. **Biology of reproduction,** v. 91, n. 4, p. 98-1, 2014.

Malekshah, A. K.; Moghaddam, A. E.; Daraka, S. M. Comparison of conditioned medium and direct co-culture of human granulosa cells on mouse embryo development. **Indian Journal of Experimental Biology,** v. 44, n. 3, p. 189-192, 2006.

Mansouri-Attia, N. *et al*. Endometrium as an early sensor of *in vitro* embryo manipulation technologies. **Proceedings of the National Academy of Sciences,** v. 106, n. 14, p. 5687-5692, 2009.

Marei, W. F. A. *et al*. Proteomic changes in oocytes after *in vitro* maturation in lipotoxic conditions are different from those in cumulus cells. **Scientific reports,** v. 9, n. 1, p. 3673, 2019.

Maruri, A. *et al*. Embryotrophic effect of a short-term embryo coculture with bovine luteal cells. **Theriogenology,** v. 119, p. 143-149, 2018.

Menck, M. C. *et al*. Beneficial effects of Vero cells for developing IVF bovine eggs in two different coculture systems. **Reproduction Nutrition Development,** v. 37, n. 2, p. 141-150, 1997.

Mesquita, F. S. *et al*. The receptive endometrial transcriptomic signature indicates an earlier shift from proliferation to metabolism at early diestrus in the cow. **Biology of reproduction**, v. 93, n. 2, p. 52-64, 2015.

Miranda, M. S. *et al*. Increasing of blastocyst rate and gene expression in co-culture of bovine embryos with adult adipose tissue-derived mesenchymal stem cells. **Journal of assisted reproduction and genetics,** v. 33, n. 10, p. 1395-1403, 2016.

Nagao, Y. *et al*. Effects of oxygen concentration and oviductal epithelial tissue on the development of *in vitro* matured and fertilized bovine oocytes cultured in protein-free medium. **Theriogenology,** v. 41, n. 3, p. 681-687, 1994.

Ouhibi, N. *et al*. Co-culture of 1-cell mouse embryos on different cell supports. **Human Reproduction,** v. 5, n. 6, p. 737-743, 1990.

Palmieri, F. Diseases caused by defects of mitochondrial carriers: a review. **Biochimica et Biophysica Acta (BBA)-Bioenergetics,** v. 1777, n. 7-8, p. 564-578, 2008.

Passaro, C. *et al*. Blastocyst-induced changes in the bovine endometrial transcriptome. **Reproduction,** v. 156, n. 3, p. 219-229, 2018.

Pestka, S. The interferons: 50 years after their discovery, there is much more to learn. **Journal of Biological Chemistry,** v. 282, n. 28, p. 20047-20051, 2007.

Pfaffl, M. W. A new mathematical model for relative quantification in real-time RT–PCR. **Nucleic acids research,** v. 29, n. 9, p. e45, 2001.

Reed, W. A. *et al*. Culture of *in vitro* fertilized bovine embryos with bovine oviductal epithelial cells, buffalo rat liver (BRL) cells, or BRL-cell-conditioned medium. **Theriogenology,** v. 45, n. 2, p. 439-449, 1996.

Rubio, C. *et al*. Clinical experience employing co-culture of human embryos with autologous human endometrial epithelial cells. **Human reproduction,** v. 15, p. 31-38, 2000.

Sakurai, T. *et al*. Coculture system that mimics *in vivo* attachment processes in bovine trophoblast cells. **Biology of reproduction,** v. 87, n. 3, p. 1-11, 2012.

Sakurai, T. *et al*. Down-regulation of interferon tau gene transcription with a transcription factor, EOMES. **Molecular reproduction and development,** v. 80, n. 5, p. 371-383, 2013.

Sponchiado, M. *et al*. Pre-hatching embryo-dependent and-independent programming of endometrial function in cattle. **PloS one,** v. 12, n. 4, p. e0175954, 2017.

Sánchez, J. M. *et al*. Bovine endometrium responds differentially to age-matched short and long conceptuses. **Biology of Reproduction**, 2019.

Talukder, A. K. *et al*. Bovine embryo induces an anti-inflammatory response in uterine epithelial cells and immune cells *in vitro*: possible involvement of interferon tau as an intermediator. **Journal of Reproduction and Development,** v. 63, n. 4, p. 425-434, 2017.

Talukder, A. K. *et al*. Oviduct epithelium induces interferon-tau in bovine Day-4 embryos, which generates an anti-inflammatory response in immune cells. **Scientific reports,** v. 8, n. 1, p. 1-13, 2018.

Thibodeaux, J. K. *et al*. Evaluating an *in vitro* culture system of bovine uterine and oviduct epithelial cells for subsequent embryo co-culture. **Reproduction, fertility and development,** v. 4, n. 5, p. 573-583, 1992.

Voelkel, S. A. *et al*. Use of a uterine-cell monolayer culture system for micromanipulated bovine embryos. **Theriogenology,** v. 24, n. 3, p. 271-281, 1985.

Wang, G. *et al*. Isolation, immortalization, and initial characterization of uterine cell lines: An *in vitro* model system for the procine uterus. ***In Vitro*** **Cellular & Developmental Biology-Animal,** v. 36, n. 10, p. 650-656, 2000.

Wolf, E. *et al*. Embryo-Maternal Communication in Bovine–Strategies for Deciphering a Complex Cross-Talk. **Reproduction in Domestic Animals,** v. 38, n. 4, p. 276-289, 2003.

Wydooghe, E. *et al*. Differential apoptotic staining of mammalian blastocysts based on double immunofluorescent CDX2 and active caspase-3 staining. **Analytical biochemistry,** v. 416, n. 2, p. 228-230, 2011.

Zeiler, M. *et al*. Development of an *in vitro* model for bovine placentation: a comparison of the *in vivo* and *in vitro* expression of integrins and components of extracellular matrix in bovine placental cells. **Cells Tissues Organs,** v. 186, n. 4, p. 229-242, 2007.

CHAPTER 5

GENERAL DISCUSSION

5 GENERAL DISCUSSION

The purpose of this chapter is to discuss the general findings arising from this Thesis and how they extend the current knowledge of embryo-maternal communication in cattle. **The existence of a complex embryo-maternal interactome between a pre-elongating embryo and the endometrium provided the theoretical basis for the present research Thesis.** Focus was given on the effects of the embryo on programming the endometrial function during early gestation in cattle. Throughout this Thesis, evidences of embryo-induced changes at transcriptional level in the endometrium *in vivo* (**Chapter 2**), in the uterine microenvironment metabolome composition *in vivo* (**Chapter 3**), and in the global transcriptome of endometrial epithelial cells *in vitro* (**Chapter 4**) were provided. The explorative nature of the three studies has led us to **accept the overarching hypothesis of this Thesis that bovine embryos modulate the endometrial function as early as day 7 of pregnancy**. Herein, this general discussion will first integrate the data obtained from the *in vivo* (endometrial gene expression and uterine luminal fluid metabolome) and the *in vitro* (endometrial cells transcriptome) models; secondly, factors that may contribute to the embryo-endometrial interactome and the relevance of this cross-talk for pregnancy establishment in cattle will be discussed. Based on these findings, insights for future studies and implications will be provided.

5.1 AN OVERVIEW OF THE MAIN FINDINGS OF THIS THESIS

Owing to its untraceable effects within a relatively large uterine lumen, the 120-200 μm in diameter, pre-elongation bovine embryo had been historically considered to be no more than a passenger during its journey throughout the maternal reproductive tract. In the past years, accumulating evidence suggested that the early bovine embryo engages in biochemical signaling with the maternal uterus. This Thesis attempted to characterize and provide insights into the embryo-induced changes in the endometrium during early gestation in cattle. To that end, *in vivo* and *in vitro* experimental approaches associated with state-of-the-art omics technologies were applied to test central and specific hypotheses.

In **Chapter 2,** spatially defined regions of the ipsilateral uterine horn were compared between pregnant and cyclic cows to demonstrated that a day-7 embryo is able to locally regulate transcription of key-genes associated with endometrial function *in vivo*. Out of 86

genes that were evaluated by PCR using a microfluidic platform, 12 transcripts had their abundance modulated in the Pregnant endometrium. Embryo-induced effects included **classical interferon-stimulated genes** (ISGs; *ISG15*, *MX1*, *MX2*, *OAS1Y*), and genes related to **prostaglandin biosynthesis** (*PTGES*, *HPGD*, *AKR1C4*), cell-cell adhesion (*ITGAV*, *ITGB1*), polyamine regulation (*AMD1*), and solute and water transport (*AQP4, SLC1A4*). Stimulation of ISGs expression in the pregnant endometrium was attributed to a release of interferon-tau (IFNτ) by the early embryo. A major finding of this study was that changes triggered by the presence of the embryo were mainly in the most cranial portions (uterotubal junction and anterior third) of the uterine horn ipsilateral to the ovary containing the CL, where the embryos were located (Sponchiado *et al.*, 2017).To the best of knowledge, that was the first report of embryo-induced changes on the bovine endometrium, at transcriptional level, *in vivo*.

In **Chapter 3**, we further advanced the understanding on embryo-effects during early pregnancy. Analyses of the metabolite composition of the uterine luminal fluid (ULF) collected from the anterior third of the uterine horn ipsilateral to the CL were carried out to answer whether the presence of the embryo elicits changes in the uterine microenvironment composition *in vivo*. Embryo-induced modulation included an overall decrease in ULF concentrations of amino acids, biogenic amines, acylcarnitines and phospholipids, and an increase in concentrations of **eicosanoids and oxidation products of polyunsaturated fatty acids**. It was noteworthy that two eicosanoids derived from the lipoxygenase pathway, 12(S)-HETE and 15(S)-HETE, were in greater concentrations in the ULF recovered from pregnant animals. Transcripts for *ALOX12* and *ALOX15B* were respectively up- and down-regulated in the endometrial tissue of Pregnant animals. It was further investigated whether the changed amounts of lipoxygenase-derived metabolites influenced PPARγ (peroxisome proliferator-activated receptor gamma)-RXR (retinoid X receptor) signaling in the endometrium, but no difference was verified in the endometrial abundance of transcripts for *LPL*, a PPARγ-RXR target gene, between pregnant and cyclic cows.

Next in **Chapter 4**, by means of an *in vitro* model, the embryo-endometrial interface was probed for embryo-induced changes on endometrial cells and the possible modes of inter-tissue molecular communication. Day-5.5 morulae were co-cultured in juxtaposition or in cell culture inserts that prevented direct contact with bovine endometrial epithelial cells (BEECs) for 48 h. The magnitude of effects at the level of the embryos and the BEECs was investigated. Juxtaposition between embryos and the BEEC monolayer altered transcription of 1,797 genes compared to BEECs that were not exposed to embryos (control group).

Interestingly, embryo-induced changes on endometrial transcriptome were rather limited when embryos were not juxtapositioned to the BEEC monolayer. There were 230 genes differentially expressed in relation to BEECs cultured in the absence of embryos, indicating that nature and intensity of embryo-induced changes on bovine endometrial epithelial cell transcriptome *in vitro* depend upon a juxtaposition between embryonic and maternal units. Pathways modulated by presence of embryos included interferon-mediated immune responses, cell cycle regulation and apoptosis, prolactin signaling, and prostanoid biosynthesis. Moreover, it was verified that co-culture with BEECs improves blastocyst rates on day 7.5, irrespective of juxtaposition to the cell monolayer.

Both the *in vivo* and the *in vitro* studies revealed local effects of the embryo to program endometrial function. This is important because the dynamics of intrauterine migration of the pre-implantation embryo remains poorly known in cattle. Nonetheless, it is known that, unlike other species, the bovine embryo does not have an active migration capacity (like equine embryos, that have an acellular glycoprotein capsule, or swine embryos, that produce estrogens, for example). Additionally, anatomy and position of the bovine uterine horns do not seem to favor the process of intrauterine migration of the embryo along the longitudinal axis. Furthermore, the viscous nature of the luminal film makes the uterine microenvironment difficult for the embryo to migrate. Indeed, according to Wolf *et al.* (2003), the bovine embryo is surrounded tightly by the endometrium through a thin fluid layer stabilized by glycoproteins. In our first study (Chapter 2), all embryos were found in the most cranial third of the ipsilateral uterine horn on day 7 post estrus, and this is in agreement with another study that reported that day-8 embryos were located at the tip of the uterine horn, close to the UTJ, in inseminated beef cows (Diskin e Sreenan, 1980), suggesting that the pre-hatching bovine embryo does migrate actively along the uterine horn. Thus, it is presumed that the early embryo could benefit from a local change on the endometrial function. Although the technical approaches to better define this process are challenging, further studies are needed on this topic. In addition, intensity and extent of embryo signaling capacity is expected to increase throughout the window of pre-implantation development as the conceptus develops, in order to supply its changing needs.

Collectively, the studies carried out in this Thesis provided evidences that early bovine embryos are able to change the endometrial function as early as day 7. The functional relevance of embryo-dependent programming of endometrial function to pregnancy establishment can be questioned because day-7 bovine blastocysts are routinely transferred to the uterus of non-pregnant synchronized recipients which, up to that stage, have not seen an

embryo and can establish a pregnancy successfully. Taken to its extreme, it has been shown to be possible to establish a pregnancy in cattle by transferring embryos up to the time when the luteolytic mechanisms would normally be initiated (around day 16) (Betteridge *et al.*, 1980). Indeed, the reproductive tract does not absolutely require exposure to the embryo during that early phase in pregnancy in order for pregnancy to be established. However, pregnancy rates in commercial embryo transfer operations average on 40-45% (Hasler *et al.*, 1995; Pontes *et al.*, 2009; Randi *et al.*, 2016). This contrasts with pregnancy rates to artificial insemination, which are commonly 50-55%, indicating that lack of exposure of the reproductive tract to the embryo during the first week of pregnancy may be implied as a contributing factor to reduced pregnancy success after o embryo transfer. In addition, it has been reported that magnification of embryonic signals by simultaneous transfer of trophoblast vesicles with one blastocyst on day 7 increases pregnancy rates from 43% (control group) to 73% (cotransfer group) in cattle (Heyman *et al.*, 1987). Thus, it is proposed that exposure to the early embryo fine-tunes endometrial function to support subsequent pregnancy events.

From the results obtained in in the *in vivo* and in the *in vitro* studies, it became evident the importance of interferon-mediated signaling and eicosanoids pathways as major players in the embryo-maternal communication. Some aspects regarding these two pathways are discussed below.

5.2 CANDIDATE PATHWAYS

5.2.1 Interferon-mediated signaling

The findings of this Thesis underline the importance of IFNτ as an early embryo-derived pregnancy recognition signal. In addition to the well-conceived antiluteolytic effects, IFNτ acts in a paracrine manner on the endometrium to induce or enhance expression of ISGs that are hypothesized to regulate uterine receptivity and conceptus elongation (Bazer *et al.*; Brooks *et al.*, 2014; Hansen *et al.*, 2017). Other recent studies have shown that the early bovine embryos were able to stimulate ISGs expression in co-cultured endometrial (Talukder *et al.*, 2017; Gómez *et al.*, 2018; Passaro *et al.*, 2018), luteal (Bridi *et al.*, 2018) and immune cells (Rashid *et al.*, 2018; Talukder *et al.*, 2018) *in vitro*, due to release of interferon-tau (IFNτ). Remarkably, a 268-fold increased expression of *MX1* was found in BEECs in the presence of day-7.5 embryos (Chapter 4).

It is possible that factors other than IFNτ could also trigger type I interferon-responses in endometrial cells, as for example prostaglandins (Spencer *et al.*, 2013) or other type I interferons, such as interferon alpha and beta (Platanias, 2005). In the study conducted by Rashid *et al*. (2018), authors stimulated peripheral blood mononuclear cells (PBMCs) *in vitro* with uterine flushings collected from day-7 pregnant (donor) or non-pregnant cows. Treatment with uterine flushings from pregnant donors down-regulated pro-inflammatory cytokines (*TNFA*, *IL1B*) and up-regulated transcription of anti-inflammatory cytokines (*IL10*) and ISGs (*ISG15*, *OAS1*) compared with uterine flushings from non-pregnant cows. Moreover, addition of a specific anti-bovine IFNτ antibody to the uterine flushings inhibited the effects on PBMCs, indicating that IFNτ is a major factor triggering such responses.

Early embryonic losses and pregnancy failure may be attributed to insufficient secretion of IFNτ by the embryo/conceptus. However, accumulating literature supports the idea that embryonic IFNτ expression levels are not necessarily correlated with developmental competence. Kubisch *et al*. (1998) observed a negative relationship between early IFNτ production and developmental competence. For instance, it has been reported that *in vitro*-cultured blastocysts display greater abundance of transcripts for IFNτ compared with those cultured *in vivo* (Wrenzycki *et al.*, 2001; Lonergan *et al.*, 2003). Interestingly, it was found that embryos co-cultured, but not in direct contact with endometrial cells presented a 4-fold increased abundance of IFNτ mRNA compared to those embryos cultured in juxtaposition with cells (Chapter 4). The amount of IFNτ produced is also related to the sex of the embryo. Larson *et al*. (2001) showed that female blastocysts produce twice as much IFNτ as males. In this respect, it has been reported that bovine female conceptuses elongate more compared to their male counterparts and that this difference in growth rate leads to an increased release of IFNτ by the female conceptus later in pregnancy. However, regardless of the distinct capacity to produce and release IFNτ, both female or male conceptuses are able to establish and maintain pregnancy at similar rates. Altogether, these data indicate that, even though IFNτ is critical for the establishment of pregnancy, greater amounts of conceptus-released IFNτ does not warrant greater rates of embryonic survival. This leads to the assumption that early embryo-derived signals other than IFNτ may be involved in the embryo-maternal dialogue in cattle. Indeed, from an evolutionary point of view, it is unlikely that establishment of pregnancy relies on a single molecule synthesized by the embryo. The studies presented in this Thesis indicated alternative systems that might also play a role in the embryo-maternal communication, such as eicosanoid signaling.

5.2.2 Eicosanoids

Eicosanoids undoubtedly play an important role in reproductive processes in cattle, including ovulation, conceptus elongation, maternal recognition of pregnancy and luteolysis (Brooks *et al.*, 2014). Free polyunsaturated fatty acids are oxidized to eicosanoids prominently via three pathways: the cyclooxygenase (COXs) pathway to produce prostanoids, the lipoxygenase (LOXs) pathway to produce hydroxyeicosatetraenoates (HETEs), and the leukotriene pathway via Cytochrome P450 microsome (CYPs) to generate epoxyeicosatrienoic acids. Among these subfamilies, the roles of prostanoids on coordinating reproductive events have been studied more extensively.

Prostaglandins are produced both by epithelial cells of the endometrium and trophectoderm cells of the elongating conceptus in ruminants (Lewis *et al.*, 1982; Charpigny *et al.*, 1997). In addition, prostaglandins are found in much greater concentrations in the uterine lumen of pregnant than cyclic or nonpregnant heifers by day 13 of pregnancy (Spencer *et al.*, 2013). Indeed, prostaglandins are essential for conceptus elongation in ruminants, as intrauterine infusions of a selective PTGS2 (a prostaglandin synthase) inhibitor prevented conceptus elongation in pregnant ewes (Dorniak *et al.*, 2011). In Chapter 2, transcripts related to prostaglandin biosynthesis were detected in different abundances in the endometrium of pregnant versus control animals. Specifically, upregulation of *PTGES* (prostaglandin E synthase), and downregulation of *AKR1C4* (catalyzes the conversion of PGH_2 to $PGF_{2\alpha}$,) and *HPGD* (catalyzes the catabolism of prostaglandins) in response to the embryo was suggestive of a shift towards a greater PGE_2/PGF_{2a} ratio in the pregnant endometrium. However, metabolomic analysis of ULF composition carried out in Chapter 3 could not confirm this presumption. Specifically, PGE_2 was under the limit of detection in the ULF and, contrary to our expectation, $PGF_{2\alpha}$ concentration tended to be greater in the ULF recovered from pregnant cows. Greater concentrations of $PGF_{2\alpha}$ in ULF in response to the embryo is consistent with other experiments conducted later in pregnancy. Ulbrich *et al.* (2009) reported increased concentrations of $PGF_{2\alpha}$ and its stable metabolite 15-keto $PGF_{2\alpha}$ (PGFM) in uterine flushings collected on days 15 and 18 of pregnancy in heifers, compared to their cyclic counterparts. Increased amounts of prostaglandins in ULF close to the implantation period has been suggested to emanate from the embryonic side (Ulbrich *et al.*, 2009; Spencer *et al.*, 2013), as elongating bovine conceptuses synthesize and secrete more prostaglandins than the surrounding endometrium (Lewis *et al.*, 1982). However, Gómez *et al.*, (2015) found that blood $PGF_{2\alpha}$ concentrations were significantly increased in pregnant

cows on day 8, irrespective of the presence of a single or multiple embryos, suggesting that the effect on $PGF_{2\alpha}$ concentrations could be due to an early endometrial response.

Concerning *PTGES* mRNA abundance in the endometrium being modulated by the early embryo, other *in vitro* studies have shown that presence of bovine embryos increases expression of *PTGES* in endometrial (Talukder *et al.*, 2017) and immune cells (Talukder *et al.*, 2018). Talukder *et al.* (2017) also reported increased concentrations of PGE_2 in the culture media when bovine endometrial cells were co-cultured with day-7 embryos. Contrary to our results obtained *in vivo*, *PTGES* expression seemed to be down-regulated in BEECs exposed to day-7.5 embryos in our *in vitro* study (Chapter 4). This and other discrepancies were found between the *in vivo* and the *in vitro* results and possible explanations are discussed in the next sections.

Contrary to prostaglandins, the role of lipoxygenase-derived metabolites during early gestation has not been explored extensively. Presence of an embryo changed concentrations of hydroxyeicosatetraenoates in the ULF (Chapter 3). Specifically, 12(S)-HETE and 15(S)-HETE were in greater concentrations in the pregnant ULF, whereas a decreased amount of 13(S)-HODE was verified. Metabolites present in the ULF can arise from either the endometrium or from the embryo, but it is challenging to distinguish embryonic from the endometrial contributions. Distinct concentrations of lipoxygenase-derived metabolites in the ULF were associated with increased and decreased abundances of *ALOX12* and *ALOX15B* mRNA, respectively, in the pregnant UTJ, suggesting an endometrial origin of regulation (Chapter 3). In Chapter 4, co-culture with embryos down-regulated the expression of *ALOX12E* in BEECs. As discussed in Chapter 3, these findings support the idea that bovine embryos modulate the lipoxygenase pathway. Roles of lipoxygenase-derived metabolites on embryo development and establishment of pregnancy warrant further investigation.

5.3 THE UTERINE LUMINAL FLUID TO MEET THE EMBRYONIC NEEDS

The endometrial exchange of molecules into the uterine lumen represents the ultimate maternal influence to the developing pre-implantation embryo. Despite its importance on conceptus elongation and survival, there is limited information on the biochemical composition of the uterine fluid in cattle. In this regard, a major contribution of the quantitative measurement of metabolite concentrations carried out in Chapter 3 is the expanded inventory of naturally occurring compounds in ULF samples collected post-

mortem. This is important, because most published metabolomics-based investigations are either restricted to one class of analytes and only relative abundances are reported.

Intriguingly, quantification of metabolites in ULF between pregnant versus non-pregnant cows showed that presence of an embryo diminishes concentrations of amino acids, biogenic amines, phospholipids and acylcarnitines. In the *in vivo* condition, the ULF composition is modulated by both the endometrial and embryonic units, as well as their molecular interactions. As discussed in Chapter 3, possible explanations for lower concentrations of these compounds in the pregnant uterine lumen include: (i) an increased consumption of substrates by the endometrium; (ii) an overall down-regulation of transport activity in the endometrial epithelia; (iii) an increased resorption of metabolites from the uterine lumen towards the lining endometrial epithelium; or (iv) intake of substrates present in the uterine fluid by the embryo. Although the experimental set-up used in the study does not allow to distinguish these factors, it is speculated that the changes ULF composition likely reflect the combination of the above. Interestingly, results from the *in vivo* (Chapter 2) and the *in vitro* (Chapter 4) studies showed that bovine embryos are able to modulate the transcription of genes associated with active transport of molecules in the endometrium. Figure 1 provides an overview of the ULF metabolites and endometrial transcripts found to be modulated by the embryo. Specifically, transporters of macromolecules, such as amino acids, lipids and carbohydrates, were mainly down-regulated in the presence of the embryo, whereas the majority of mitochondrial carriers (SLC25 family) and antigen transporters was up-regulated by the embryo (Fig. 1).

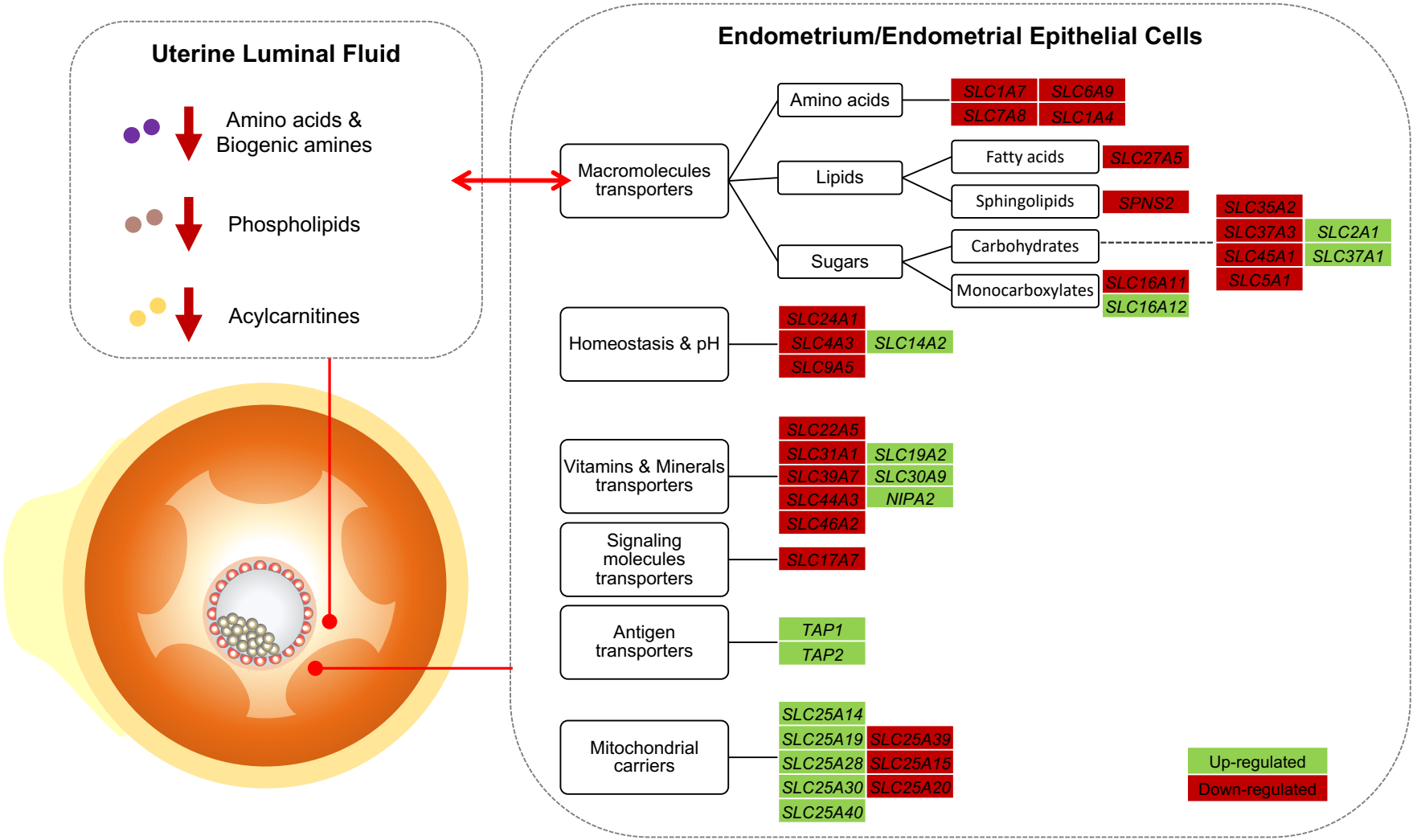

Figure 1. Overview of embryo-induced changes in metabolite concentrations in the uterine luminal fluid (Chapter 3), and abundances of transcripts for transporters in endometrial tissue (*in vivo* study; Chapter 2) or endometrial epithelial cells (*in vitro* study; Chapter 4). Solute Carriers (SLCs) were grouped according to their subfamilies. TAP (Transporter associated with antigen processing). SPNS (Sphingolipid Transporter). NIPA (Magnesium transporter).

A major down-regulation of transporters was consistent with lower metabolite concentrations in the ULF of pregnant animals. This may be against the paradigm that metabolites, especially amino acids, are present in higher concentrations in the pregnant uterine lumen in cattle (Groebner *et al.*, 2011; Forde *et al.*, 2014) and sheep (Gao *et al.*, 2009), which is mediated via upregulation of transporters in the endometrium. It is worth noticing that the aforementioned studies were performed later in pregnancy, around the pregnancy recognition window, when an elongated conceptus is present in the uterus. In the *in vivo* study presented in this Thesis, ULF samples were collected approximately one week earlier in gestation, when a pre-hatching embryo was present in the pregnant uterus. At this point, the nutrient demands of the embryo are quantitatively small (Leese *et al.*, 2008) and, perhaps, metabolites that compose the ULF do not need to be in abundant concentrations to cover the embryonic needs. For instance, essential amino acids were in much lower concentrations in ULF, irrespective of pregnancy status, compared to non-essential amino acids (Chapter 3). Only two (threonine and leucine) of the essential amino acids (lysine, methionine, threonine, tryptophan, isoleucine, leucine, histidine, phenylalanine and valine) were detected. While only tyrosine was not detected within non-essential amino acids (alanine, aspartate, asparagine, glutamate, cysteine, glycine, glutamine, proline, serine and tyrosine). This is in agreement with Elhassan *et al*. (2001), where authors found that non-essential amino acids represent more than 60% of the total concentration of amino acids in the bovine uterus on day 7. Supplementation of essential and non-essential amino acids in culture medium for *in vitro* production of bovine embryos is a common practice and contrasts with the relatively poor *in vivo* uterine environment. Specific luminal metabolite requirements of the earliest phases of embryo development in the uterus are currently unknown. It is proposed that embryonic needs are qualitatively specific rather than quantitively inclined during the first week of gestation.

5.4 APPROACHING THE EMBRYO-MATERNAL INTERFACE: *IN VIVO* VERSUS *IN VITRO* MODELS

Discrepancies found between the *in vivo* and *in vitro* results reported in this Thesis deserve discussion (summarized in Table 1). In the *in vivo* model, the gene expression data were obtained from intercaruncular endometrial tissue, whereas those in the *in vitro* study were from an endometrial epithelial cell line. The endometrium is composed of a mixture of luminal and glandular epithelial cells, stromal cells, as well as endothelial and immune cells.

In this respect, it is reasonable to assume that different cells types present distinct capacities and mechanisms to respond to external signals. It should also be pointed out that in the *in vivo* environment, the endometrial function is under control of a number of systems/factors, in particular, sex steroid hormones. Even though pregnant and control cows presented similar ovarian morphologies and sex steroid endocrine profiles in Chapter 2, it is expected that ovarian hormones have an impact on the endometrial responsiveness to embryo-derived signals. This is a major limitation of hormone-free *in vitro* systems, such as used in Chapter 4. Other remarkable difference between the two experimental models used in this Thesis is that in the *in vivo* study, changes in endometrial transcriptome were caused by a single *in vivo*-generated embryo, whereas changes in the *in vitro* study were triggered by 15 *in vitro*-generated embryos. In this regard, Mansouri-Attia *et al*. (2009) showed that the endometrium responds differently to *in vivo* versus *in vitro* embryos. Furthermore, cells cultured *in vitro* do not necessarily mirror their *in vivo* morphological and functional features. In fact, it was shown that the BEECs used in the *in vitro* model underwent an epithelial-mesenchymal transition, as seen by the co-expression of Cytokeratin and Vimentin (Chapter 4). However, evidences were provided that, despite their dedifferentiated status, the cells preserved functional features linked to their *in vivo* physiology, as for example expression of sex steroid hormones receptors. These limitations do not detract from our findings, as all conclusions drawn were carefully considered but require further substantiation. Even though *in vitro* models present such restraints, they still offer the advantage of surrounding the very local embryo-maternal interface and, therefore, serve as a useful tool to provide first basic insights into the complex embryo-maternal interactome. Development of more *in vivo*-like embryo/endometrial co-culture models will, indisputably, advance our understanding of early embryo-maternal communication.

Table 1. Comparison of results obtained in the *in vivo* versus the *in vitro* study. Green arrows indicate that presence of embryos up-regulated expression of a given gene in the endometrium *in vivo* (Chapter 2) or in bovine endometrial epithelial cells (BEECs) *in vitro* (Chapter 4) compared to the control (no embryo) group; red arrows indicate a down-regulation; Equal signs depict that no changes were observed.

Gene	Endometrium *(In vivo)*	BEECs *(In vitro)*
ISG15	↑	↑
MX1	↑	↑
MX2	↑	↑
OAS1Y	↑	↑
PTGES	↑	↓
AQP4	↑	No reads*
ITGAV	↑	↓
SLC1A4	↓	No reads*
AKR1C4	↓	=
AMD1	↓	=
HPGD	↓	=
ITGB1	↓	=

*No reads were retrieved by RNA-sequencing.

5.5 BACK TO THE ENDOMETRIUM: IS THERE A GOOD/COMPETENT EMBRYO FOR A NON-RESPONSIVE ENDOMETRIUM?

The results discussed in the present Thesis provided novel information on the embryo-maternal communication with emphasis in the embryo-dependent programming of endometrial function. The concept of effective communication implies an origin, a signaling agent, and an ultimate recipient that is able to decode the message. The ability of cells to respond to inducers, normally reflects the presence of cognate receptors and downstream signal transducers to modulate transcription and, ultimately, cell function. The target cells, in turn, can become inductive and trigger neighboring cells via new signals, thus generating sequential inductive events and amplifying the initial stimulus. In that regard, not only insufficient release of factors by the embryo, but also inadequate reaction of the endometrium to embryo-derived signals, can cause early embryonic loss and pregnancy failure. It is surprising that very little is currently known about the endometrial expression pattern of receptors for type 1 interferons (IFNAR1 and IFNAR2), for example, and the regulatory factors involved. It is of paramount importance to understand not only how the embryo

communicates with the endometrium, but also how the endometrium is programmed to respond to the embryo-derived signals.

5.6 THE BICORNUATE BOVINE UTERUS AS A COMPARTMENTALIZED STRUCTURE

Another major contribution of this Thesis is that remarkable regional differences in transcript abundances were detected along the uterine horn ipsilateral to the CL (Chapter 2), in addition to the well characterized functional differences between ipsi and contralateral uterine horns (Araújo *et al.*, 2015). The functional spatial signature of the endometrium can be partially explained by vascular arrangements along the bovine uterine horns. Specifically, there is a preferential input of blood draining the ovaries to the cranial region of the uterus compared to the mid and posterior regions (Pope *et al.*, 1982). These findings should be considered when designing experiments that aim to collect and analyze endometrial and/or uterine luminal fluid samples. Specifically, one should keep in mind that specific regions of the uterus will need to be sampled depending on the specific hypothesis tested.

5.7 HYPOTHETICAL MODEL

Based on the results presented throughout this Thesis, the following hypothetical model of the embryo-endometrial interactome on day 7 of pregnancy in cattle is proposed (Fig. 2).

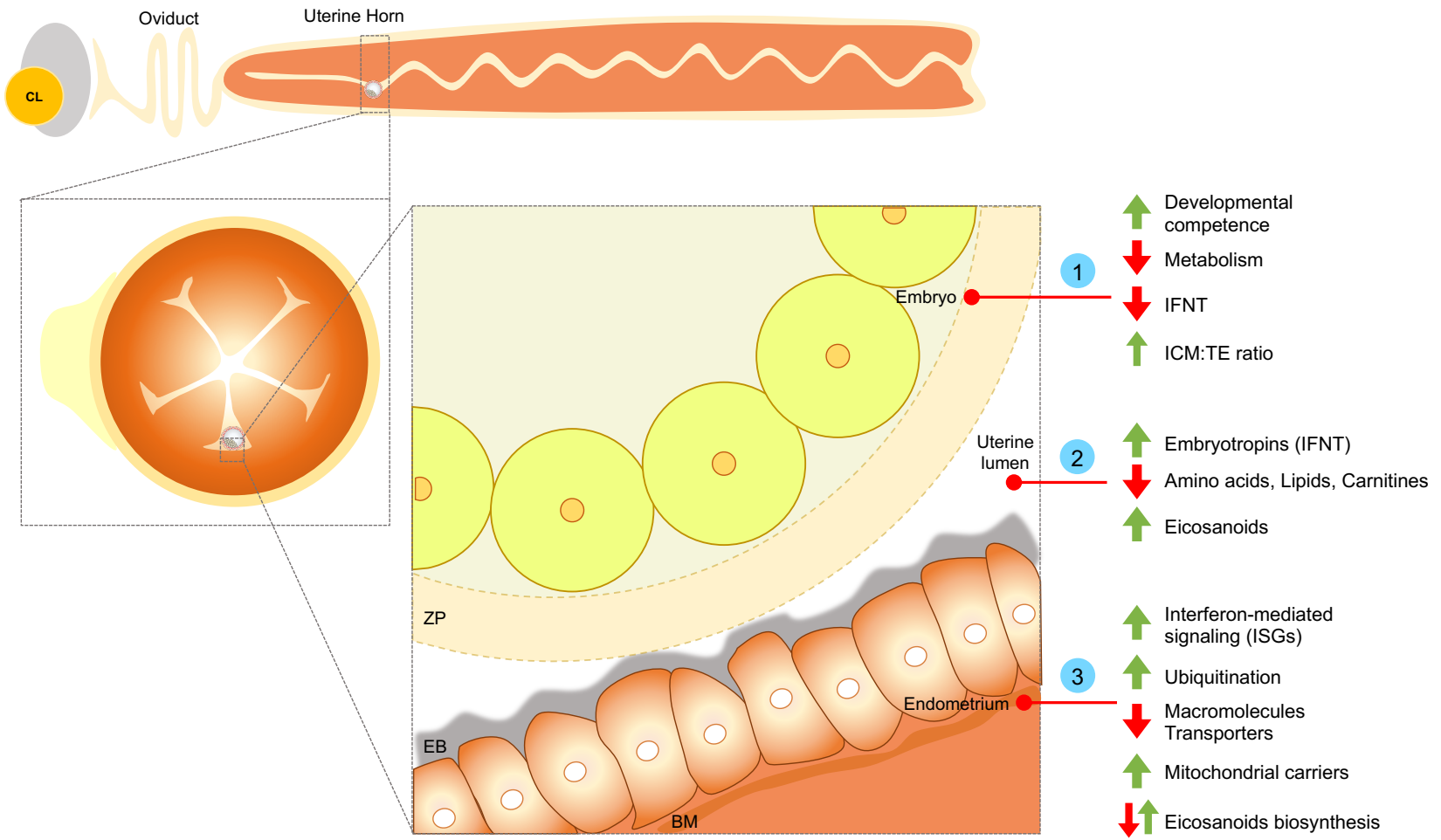

Figure 2. Hypothetical model of the embryo-endometrial interactome on day 7 of pregnancy in cattle. The embryo exerts local effects on the endometrium via juxtacrine and paracrine fashions. (1) **The embryo-endometrial interactome affects in the embryo:** embryos cultured *in vivo* are of superior quality of their *in vitro* counterparts indicating that the reproductive tract plays a role in embryo development. Embryos co-cultured *in vitro* contacting an endometrial epithelial cell monolayer display increased ICM:TE ratio and reduced abundance of transcripts for interferon-tau (IFNT). (2) **The embryo-endometrial interface represents a pool of stimulatory and response molecules, originated in the embryo and the endometrium:** the embryo releases signaling molecules, referred as to embryotropins, into the uterine lumen, as for example IFNT. Presence of the embryo leads to changes in the uterine luminal fluid composition, including an overall decrease in amino, acids, lipids and carnitines concentration, and an increase in metabolites of the eicosanoids pathway. Changes on the uterine luminal fluid composition might be a consequence of uptake and release of molecules by the embryo itself, and/or represent changes in the endometrial function initiated by the embryo. (3) **The embryo-endometrial interactome affects the endometrium:** embryo-induced effects on the endometrium include (i) stimulation of transcription of interferon stimulated genes (ISGs). Some ISGs are associated with ubiquitination pathways that might become up-regulated in the endometrium; (ii) decreased endometrial expression of transporters for macromolecules, and an increase in the expression of mitochondrial carriers; and (iii) modulation of eicosanoids synthesis by the endometrium. CL corpus luteum. ZP zona pellucida. EB endometrial biofilm. BM basal membrane.

5.8 FUTURE DIRECTIONS

This Thesis has identified a number of research needs. By using a combination of *in vivo* and *in vitro* models with state-of-the-art analytical tools, the early embryo-maternal interactome was explored. The findings presented hereby provide candidate systems that might be important for conditioning the uterine environment for conceptus development and represent starting points for interventional investigations, which are the logical next steps. Recent developments in genetic engineering (knock-out and knock-down models) associated with the well-established *in vitro* production of bovine embryos will facilitate the target validation of particular candidates. For instance, this Thesis identified interferon-mediated signaling and eicosanoids as important pathways intermediating the embryo-maternal cross-talk. Further research to understand the specific roles of these candidate molecules on programming the endometrium towards a more receptive status are needed. A potential scenario could be the temporary knock-down of IFNτ expression using RNA interference (RNAi) in day-7 *in vitro*-produced embryos followed by transfer to synchronized recipients to test whether and to which extent early embryo-derived IFNτ is required to establish pregnancy in cattle.

5.9 IMPLICATIONS

The results and insights generated in this Thesis are helpful for the determination of factors contributing to embryonic losses in cattle. Biotechnological applications in animal breeding could include strategies to either enhance embryonic pregnancy recognition signals or to select females according to markers of uterine responsiveness to embryo-derived signals. Alternatively, important mediating molecules could be generated as recombinant proteins and be transcervically administered into the uterus. Identification of genes, proteins, metabolites or systems that change in response to the embryo/conceptus can further serve as novel markers for early pregnancy diagnosis. For instance, ALOX12, one of the genes up-regulated in the endometrium in response to the embryo presence has been recently patented as one of the seven biomarkers used in a multiple pregnancy marker pattern (MPMP) for early detection of pregnancies on days 17-19 after insemination in lactating cows (Te Pas *et al*., 2019). Additionally, as a monovulatory species, signaling mechanisms identified in the

bovine can be used as a valuable indication for similar evaluations in other species, including the human.

5.10 REFERENCES

Araújo, E. R. *et al*. Spatio-specific regulation of endocrine-responsive gene transcription by periovulatory endocrine profiles in the bovine reproductive tract. **Reproduction, Fertility and Development**, v. 28, n. 10, p. 1533-1544, 2015.

Bazer, F. W.; Spencer, T. E.; Johnson, G. A. Interferons and uterine receptivity. **Seminars in reproductive medicine.** Thieme Medical Publishers, v. 27, n. 01, p. 90-102, 2009.

Betteridge, K. J. *et al*. Collection, description and transfer of embryos from cattle 10–16 days after oestrus. **Journal of reproduction and fertility,** v. 59, n. 1, p. 205-216, 1980.

Bridi, A. *et al*. Parthenogenetic bovine embryos secrete type I interferon capable of stimulating ISG15 in luteal cell culture. **Animal Reproduction (AR),** v. 15, n. 4, p. 1268-1277, 2018.

Brooks, K.; Burns, G.; Spencer, T. E. Conceptus elongation in ruminants: roles of progesterone, prostaglandin, interferon tau and cortisol. **Journal of animal science and biotechnology,** v. 5, n. 1, p. 53, 2014.

Charpigny, G. *et al*. Expression of cyclooxygenase-1 and-2 in ovine endometrium during the estrous cycle and early pregnancy. **Endocrinology,** v. 138, n. 5, p. 2163-2171, 1997.

Diskin, M. G.; Sreenan, J. M. Fertilization and embryonic mortality rates in beef heifers after artificial insemination. **Journal of reproduction and fertility,** v. 59, n. 2, p. 463-468, 1980.

Dorniak, P.; Bazer, F. W.; Spencer, T. E. Prostaglandins regulate conceptus elongation and mediate effects of interferon tau on the ovine uterine endometrium. **Biology of reproduction,** v. 84, n. 6, p. 1119-1127, 2011.

Elhassan, Y. M. *et al*. Amino acid concentrations in fluids from the bovine oviduct and uterus and in KSOM-based culture media. **Theriogenology,** v. 55, n. 9, p. 1907-1918, 2001.

Forde, N. *et al*. Amino acids in the uterine luminal fluid reflects the temporal changes in transporter expression in the endometrium and conceptus during early pregnancy in cattle. **PLoS One,** v. 9, n. 6, 2014.

Gao, H. *et al*. Select Nutrients in the Ovine Uterine Lumen. I. Amino Acids, Glucose, and Ions in Uterine Lumenal Flushings of Cyclic and Pregnant Ewes. **Biology of Reproduction,** v. 80, n. 1, p. 86-93, 2009.

Gomez, E. *et al*. PGF2α levels in Day 8 blood plasma are increased by the presence of one or more embryos in the uterus. **Animal,** v. 9, n. 8, p. 1355-1360, 2015.

Groebner, A. E. *et al*. Increase of essential amino acids in the bovine uterine lumen during preimplantation development. **Reproduction,** v. 141, n. 5, p. 685-695, 2011.

Gómez, E. *et al*. *In vitro* cultured bovine endometrial cells recognize embryonic sex. **Theriogenology,** v. 108, p. 176-184, 2018.

Hansen, T. R.; Sinedino, L. D. P.; Spencer, T. E. Paracrine and endocrine actions of interferon tau (IFNT). **Reproduction,** v. 154, n. 5, p. F45-F59, 2017.

Hasler, J. F. *et al*. Production, freezing and transfer of bovine IVF embryos and subsequent calving results. **Theriogenology,** v. 43, n. 1, p. 141-152, 1995.

Heyman, Y. *et al*. Improvement of survival rate of frozen cattle blastocysts after transfer with trophoblastic vesicles. **Theriogenology,** v. 27, n. 3, p. 477-484, 1987.

Kubisch, H. M.; Larson, M. A.; Roberts, R. M. Relationship between age of blastocyst formation and interferon-τ secretion by in vitro–derived bovine embryos. **Molecular reproduction and development,** v. 49, n. 3, p. 254-260, 1998.

Larson, M. A. *et al*. Sexual dimorphism among bovine embryos in their ability to make the transition to expanded blastocyst and in the expression of the signaling molecule IFN-τ. **Proceedings of the National Academy of Sciences,** v. 98, n. 17, p. 9677-9682, 2001.

Leese, H. J. *et al*. Metabolism of the viable mammalian embryo: quietness revisited. **Molecular human reproduction,** v. 14, n. 12, p. 667-672, 2008.

Lewis, G. S. *et al*. Metabolism of arachidonic acid in vitro by bovine blastocysts and endometrium. **Biology of Reproduction,** v. 27, n. 2, p. 431-439, 1982.

Lonergan, P. *et al*. Temporal divergence in the pattern of messenger RNA expression in bovine embryos cultured from the zygote to blastocyst stage in vitro or in vivo. **Biology of Reproduction,** v. 69, n. 4, p. 1424-1431, 2003.

Mansouri-Attia, N. *et al*. Endometrium as an early sensor of in vitro embryo manipulation technologies. **Proceedings of the National Academy of Sciences,** v. 106, n. 14, p. 5687-5692, 2009.

Passaro, C. *et al*. Blastocyst-induced changes in the bovine endometrial transcriptome. **Reproduction,** v. 156, n. 3, p. 219-229, 2018.

Platanias, L. C. Mechanisms of type-I-and type-II-interferon-mediated signalling. **Nature Reviews Immunology,** v. 5, n. 5, p. 375, 2005.

Pontes, J. H. F. *et al*. Comparison of embryo yield and pregnancy rate between in vivo and in vitro methods in the same Nelore (Bos indicus) donor cows. **Theriogenology,** v. 71, n. 4, p. 690-697, 2009.

Pope, W. F.; Maurer, R. R.; Stormshak, F. Distribution of progesterone in the uterus, broad ligament, and uterine arteries of beef cows. **The Anatomical Record,** v. 203, n. 2, p. 245-249, 1982.

Randi, F. *et al*. Asynchronous embryo transfer as a tool to understand embryo–uterine interaction in cattle: is a large conceptus a good thing? **Reproduction, Fertility and Development,** v. 28, n. 12, p. 1999-2006, 2016.

Rashid, M. B. *et al*. Evidence that interferon-tau secreted from Day-7 embryo in vivo generates anti-inflammatory immune response in the bovine uterus. **Biochemical and Biophysical Research Communications,** v. 500, n. 4, p. 879-884, 2018.

Spencer, T. E. *et al*. Conceptus-derived prostaglandins regulate gene expression in the endometrium prior to pregnancy recognition in ruminants. **Reproduction,** v. 146, n. 4, p. 377-387, 2013.

Sponchiado, M. *et al*. Pre-hatching embryo-dependent and-independent programming of endometrial function in cattle. **PloS one,** v. 12, n. 4, p. e0175954, 2017.

Talukder, A. K. *et al*. Bovine embryo induces an anti-inflammatory response in uterine epithelial cells and immune cells in vitro: possible involvement of interferon tau as an intermediator. **Journal of Reproduction and Development,** v. 63, n. 4, p. 425-434, 2017.

Talukder, A. K. *et al*. Oviduct epithelium induces interferon-tau in bovine Day-4 embryos, which generates an anti-inflammatory response in immune cells. **Scientific reports,** v. 8, n. 1, p. 7850, 2018.

Te Pas, M. F. W. *et al*. **Detection of proper insemination time by multiple pregnancy marker pattern (MPMP) recognition**: Google Patents 2019.

Ulbrich, S. E. *et al*. Quantitative characterization of prostaglandins in the uterus of early pregnant cattle. **Reproduction,** v. 138, n. 2, p. 371-382, 2009.

Wolf, E. *et al*. Embryo-Maternal Communication in Bovine–Strategies for Deciphering a Complex Cross-Talk. **Reproduction in Domestic Animals,** v. 38, n. 4, p. 276-289, 2003.

Wrenzycki, C. *et al*. Effects of culture system and protein supplementation on mRNA expression in pre-implantation bovine embryos. **Human Reproduction,** v. 16, n. 5, p. 893-901, 2001.

CHAPTER 6

CONCLUSIONS

6 CONCLUSIONS

In conclusion, the results presented in the course of this Thesis provide evidence of a complex embryo-maternal interactome between the pre-elongation embryo and the endometrium in cattle. Thus, the **overarching hypothesis that bovine embryos are able to modulate the endometrial function as early as day 7 of pregnancy was accepted.**

Specific hypotheses were tested in each of the three studies. In Chapter 2, an *in vivo* experiment was conducted to test the hypothesis that **exposure to an embryo changes the abundance of specific transcripts in the endometrial regions in closest proximity to the embryo in the pregnant uterine horn.** It was shown that transcription of specific genes was modulated in the endometrium in response to a day-7 embryo. Most effects detected were close to the location of the embryo into the uterine horn ipsilateral to the corpus luteum. In Chapter 3, it was hypothesized that **presence of the embryo modulates the biochemical composition of the uterine luminal fluid in the most cranial portion of the pregnant uterine horn.** Quantification of over 200 compounds showed that exposure to an embryo alters the metabolite composition of the uterine microenvironment. Finally, in Chapter 4, hypothesis was that **embryo-induced changes on endometrial transcriptome depend on physical proximity between the embryos and the endometrium.** By means of an *in vitro* model, it was shown that a juxtacrine relationship between embryos and bovine endometrial epithelial cells changes nature and intensity of embryo-induced effects on endometrial cells transcriptome. Co-culture conditions also impacted on embryonic developmental capacity, cell segregation and gene expression. Collectively, the findings discussed herein provide insights into the embryo-induced changes on the endometrial function during early gestation in cattle. Candidate systems that might be important for conditioning the uterine environment for conceptus development were provided and their biological relevance for the establishment of pregnancy warrants further investigation.

SUPPLEMENTARY TABLES AND DATASETS

Supplementary Table S1. Bovine specific oligonucleotide forward and reverse primer sequences (5'-3') and PCR product length. (Continued)

Symbol	Gene	GenBank number	Forward and Reverse sequences	Amplicon	Reference
Cell-cell adhesion					
FN1	fibronectin 1	NM_001163778.1	5' AGTACACAGTCAGTGTGGTTGCCT 3' AAACTTCAGGTTGGTTGGTGCAGG	101	Primer Express
ICAM1	intercellular adhesion molecule 1	NM_174348.2	5' AGACCCTGAAGTGCGAGGCT 3' TATTCTGGCCGTGGAGCACGTT	198	Primer Express
ICAM3	intercellular adhesion molecule 3	NM_174349.1	5' GAACCCGGTCACTATCAACATC 3' CTTGGCGTCAGGTGGTAAAT	124	Primer Express
ITFG3	family with sequence similarity 234 member A	NM_001075318.1	5' TGTGGAGGATCGATTACAATGC 3' CAGCACAGGAGAAGCTGGAAT	139	Primer Express
ITGAV	integrin subunit alpha V	NM_174367.1	5' TTTCAGGAGTTCCAAGAGCAGCGA 3' TGAAGAGAGGTGCGCCGATAAACA	183	Primer Express
ITGB1	integrin subunit beta 1	NM_174368.3	5' TCAGACTTCCGAATTGGGTTTG 3' AAATGGGCTCGTGCAGTTCT	118	Primer Express
LGALS1	lectin, galactoside-binding, soluble, 1	NM_175782.1	5' TCGTGGAGGTATGCATCTCCTT 3' TGAAGTCACCACCTGCAGACA	127	Primer Express
LGALS7B	lectin, galactoside-binding, soluble, 7B	XM_002694977.3	5' GCTTTAACGTCCCCCACAAG 3' CACCGCACAGCAGGTTCA	118	Primer Express
LGALS9	lectin, galactoside-binding, soluble, 9	NM_001039177.2	5' AGGCGGGAACAGGTTTGC 3' CCTCTCTGCTTCGTGTTGCA	118	Primer Express
MUC1	mucin 1	NM_174115.2	5' CAACCAGGGCAATGAGATAG 3' ACCATCAGCGGAGTTAGT	143	Primer Express
VIL1	villin 1	NM_001013591.1	5' GCTGCTCTACACCTACTTCATC 3' GATCTGGACCGGTTCATTGT	146	Primer Express
Eicosanoid metabolic process					
AKR1B1	aldo-keto reductase family 1, member B1	NM_001012519.1	5' ATACAAGCCGGCGGTTAAC 3' TGTCTGCAATCGCTTTGATC	188	Oliveira *et al*., 2015[1]
AKR1C4	aldo-keto reductase family 1, member C4	NM_181027.2	5' TCCTGTCCTGGGATTTGGAACCTT 3' ATCGGCAATCTTGCTTCGAATGGC	166	Oliveira *et al*., 2015[1]
HPGD	hydroxyprostaglandin dehydrogenase 15-(NAD)	NM_001034419.2	5' TGATCAGTGGAACCTACCTGG 3' TGAGATTAGCAGCCATCGC	183	Oliveira *et al*., 2015[1]

[1] Oliveira ML, D'Alexandri FL, Pugliesi G, Van Hoeck V, Mesquita FS, Membrive CMB, *et al*. Peri-ovulatory endocrine regulation of the prostanoid pathways in the bovine uterus at early dioestrus. Reproduction, Fertility and Development. 2015.

Symbol	Gene	GenBank number	Forward and Reverse sequences	Amplicon	Reference
PTGES	prostaglandin E synthase	NM_174443.2	5' GCTGCGGAAGAAGGCTTTTGCC 3' GGGCTCTGAGGCAGCGTTCC	101	Oliveira *et al*., 2015[1]
PTGES2	prostaglandin E synthase 2	NM_001166554.1	5' GTGGGCGGACGACTGGTTGG 3' CGGAGGTGGTGCCTGCGTTT	192	Oliveira *et al*., 2015[1]
PTGES3	prostaglandin E synthase 3	NM_001007806.2	5' CAGTCATGGCCAAGGTTAACAAA 3' ATCACCACCCATGTTGTTCATC	150	Oliveira *et al*., 2015[1]
PTGIS	prostaglandin I2 (prostacyclin) synthase	NM_174444.1	5' AAGATGGGAAGCGACTGAAG 3' ATCAGCTCCAGGTCAAACTG	136	Oliveira *et al*., 2015[1]
PTGS1	prostaglandin-endoperoxide synthase 1	NM_001105323.1	5' CACCCGCTCATGCCCGACTC 3' TTCCTACCCCCACCGATCCGG	155	Oliveira *et al.*, 2015[1]
PTGS2	prostaglandin-endoperoxide synthase 2	NM_174445.2	5' CCAGAGCTCTTCCTCCTGTG 3' GGCAAAGAATGCAAACATCA	161	Oliveira *et al*., 2015[1]
SLCO2A1	solute carrier organic anion transporter family member 2A1	NM_174829.3	5' TGTGGAGACGATGGGATTGA 3' GGGACACGGGCCTGTCTT	150	Oliveira *et al*., 2015[1]
Endogenous control					
ACTB	actin, beta	NM_173979.3	5' GGATGAGGCTCAGAGCAAGAGA 3' TCGTCCCAGTTGGTGACGAT	76	Araújo *et al*., 2015[2]
GAPDH	glyceraldehyde-3-phosphate dehydrogenase	NM_001034034.2	5' GCCATCAATGACCCCTTCAT 3' TGCCGTGGGTGGAATCA	68	Araújo *et al*., 2015[2]
PPIA	peptidylprolyl isomerase A	NM_178320.2	5' GCCATGGAGCGCTTTGG 3' CCACAGTCAGCAATGGTGATCT	63	Araújo *et al*., 2015[2]
Extracellular matrix assembly					
HAS3	hyaluronan synthase 3	NM_001192867.1	5' CTCATTGCCACGGTCATACA 3' AGGGAGTAGAGCGACATGAA	153	Primer Express
HMMR	hyaluronan mediated motility receptor	NM_001206621.1	5' TTGGAAAAAGAGATCCGGATTC 3' CCCTGACGGCAGCGTTTA	113	Primer Express
HYAL1	hyaluronoglucosaminidase 1	NM_001017941.1	5' AGACCAAGATAGCTGCATAAG 3' CTGTGACTGGATGCCTAAC	152	Primer Express

[1] Oliveira ML, D'Alexandri FL, Pugliesi G, Van Hoeck V, Mesquita FS, Membrive CMB, *et al*. Peri-ovulatory endocrine regulation of the prostanoid pathways in the bovine uterus at early dioestrus. Reproduction, Fertility and Development. 2015.

[2] Araújo ER, Sponchiado M, Pugliesi G, Van Hoeck V, Mesquita FS, Membrive CMB, *et al*. Spatio-specific regulation of endocrine-responsive gene transcription by periovulatory endocrine profiles in the bovine reproductive tract. Reproduction, Fertility and Development. 2015.

Symbol	Gene	GenBank number	Forward and Reverse sequences	Amplicon	Reference
HYAL2	hyaluronoglucosaminidase 2	NM_174347.2	5’ GTTGAGGTCTCCCGAAATG 3’ ACACGAAAGCTGACAAAGT	126	Primer Express
Extracellular matrix remodeling					
MMP14	matrix metallopeptidase 14	NM_174390.2	5’ GGATTGATGCTGCTCTCTTCT 3’ CCTTCCCAGACCTTGATGTT	131	Primer Express
MMP19	matrix metallopeptidase 19	NM_001075983.1	5’ TGCTGGGCCACTGGAGAA 3’ AGGTCAAGGGAGCCACATTG	130	Primer Express
MMP2	matrix metallopeptidase 2	NM_174745.2	5’ CCCAGACAGTGGATGATGC 3’ TTGTCCTTCCTCCCAGGGTC	159	Primer Express
TIMP2	TIMP metallopeptidase inhibitor 2	NM_174472.4	5’ TGCAGACATAGTGATCAGGGCCA 3’ AATCCGCTTGATGGGGTTGCCG	88	Primer Express
TIMP3	TIMP metallopeptidase inhibitor 3	NM_174473.4	5’ CCTTTGGCACGATGGTCTACA 3’ CTCGGCCTGTCAGCAGGTA	154	Primer Express
Growth factor signaling					
EDN3	endothelin 3	NM_001101979.1	5’ GTGTTAGCCTTGACCAAATGC 3’ GGAGTTGATGTAGAGACCAGTTT	157	Primer Express
EGFR	epidermal growth factor receptor	XM_592211.8	5’ ATGCTCTATGACCCTACCAC 3’ TTCCGTTACAAACTTTGCCA	132	Primer Express
FGF2	estrogen receptor 1	NM_174056.4	5’ AGCACTGGCACTACTACA 3’ AGCCAACTCCTAACATCCTA	141	Primer Express
FGFR2	fibroblast growth factor receptor 2	NM_001205310.1	5’ TTGACGTTGTTGAGCGATCAC 3’ GGCTGGGCATCGCTGTAC	119	Primer Express
FLT1	fms related tyrosine kinase 1	NM_001191132.3	5’ CCGAAAACTGAAAAGGTCGTCTT 3’ ACTTCATCCGGGTCCATGATAA	146	Primer Express
GRB7	growth factor receptor bound protein 7	NM_001046014.1	5’ TGCCCCCATGTCATAAAGGT 3’ CCCCCAGTTCTCGTCACTCA	133	Primer Express
IGF1	insulin like growth factor 1	NM_001077828.1	5’ CATCCTCCTCGCATCTCTTC 3’ CTCCAGCCTCCTCAGATCAC	239	Primer Express
IGF1R	insulin like growth factor 1 receptor	NM_001244612.1	5’ AGAGACATCTATGAGACGGAC 3’ CAGCTCAAACAGCATGTCAG	261	Primer Express
IGF2	insulin like growth factor 2	NM_174087.3	5’ GACCGCGGCTTCTACTTCAG 3’ AAGAACTTGCCCACGGGGTAT	203	Primer Express
IGF2R	insulin like growth factor 2 receptor	NM_174352.2	5’ AGAAAAGCGTGCACGTGCACTTGTC 3’ CGCCTACAGCGAGAAGGGCTTAGTCC	293	Primer Express

Symbol	Gene	GenBank number	Forward and Reverse sequences	Amplicon	Reference
IGFBP7	insulin like growth factor binding protein 7	NM_001102300.2	5' AAGGAAGATGCCGGAGAATATG 3' TTACAGCTCAGCACCTTCAC	130	Primer Express
KDR	kinase insert domain receptor	NM_001110000.1	5' AGACCGGCTGAAACTAGGTAAGC 3' CGTTGAGATGGTGGCCAATA	198	Primer Express
Interferon Signaling					
IFI6	interferon, alpha-inducible protein 6	NM_001075588.1	5' GGCGGTATCGCTCTTCCTATG 3' GCTCGAGTCGCTGTTTTCCT	98	Primer Express
IFNAR2	interferon (alpha, beta and omega) receptor 2	NM_174553.2	5' CTGGTCATTTGTATGGGCTCTTT 3' GTATCCCGGGACTGTCGAATT	128	Primer Express
IRF6	interferon regulatory factor 6	NM_001076934.1	5' GGTCTGCTCCTTGGGATGAG 3' ATGGGAGAACCATTGATGTTCAG	128	Primer Express
ISG15	ISG15 ubiquitin-like modifier	NM_174366.1	5' AGAGAGCCTGGCACCAGAAC 3' TTCTGGGCGATGAACTGCTT	130	Primer Express
MX1	MX dynamin-like GTPase 1	NM_173940.2	5' AGACGAGTGGAAAGGCAAAGTC 3' GATGGCAATCTGGGCTTCAC	98	Primer Express
MX2	MX dynamin-like GTPase 2	NM_173941.2	5' TCAGAGACGCCTCAGTCGAA 3' ACGTTTGCTGGTTTCCATGAA	109	Primer Express
OAS1Y	2',5'-oligoadenylate synthetase 1	NM_001040606.1	5' TAGGCCTGGAACATCAGGTC 3' TTTGGTCTGGCTGGATTACC	104	Primer Express
Oxidative Stress					
CAT	catalase	NM_001035386.2	5' CGCGCAGAAACCTGATGTC 3' GGAATTCTCTCCCGGTCAAAG	150	Ramos *et al*., 2015[3]
GPX4	glutathione peroxidase 4	NM_174770.3	5' TCACCAAGTTCCTCATTGACAAGA 3' TTCTCGGAACACAGGCAACA	150	Ramos *et al*., 2015[3]
SOD1	superoxide dismutase 1, soluble	NM_174615.2	5' GTTGGAGACCTGGGCAATGT 3' TCCACCCTCGCCCAAGTCAT	151	Ramos *et al*., 2015[3]
SOD2	superoxide dismutase 2, soluble	NM_201527.2	5' CCCATGAAGCCTTTCTAATCCTG 3' TTCAGAGGCGCTACTATTTCCTTC	307	Ramos *et al*., 2015[3]
Polyamine Regulation and proteolysis					

[3] Ramos RS, Oliveira ML, Izaguirry AP, Vargas LM, Soares MB, Mesquita FS, *et al*. The periovulatory endocrine milieu affects the uterine redox environment in beef cows. Reproductive Biology and Endocrinology. 2015;13(1):39.

Symbol	Gene	GenBank number	Forward and Reverse sequences	Amplicon	Reference
AMD1	adenosylmethionine decarboxylase 1	NM_173990.2	5' TGCTGGAGGTTTGGTTCTC 3' TCAAAAGTATGTCCCACTCGG	96	Ramos *et al*., 2014[4]
ODC1	ornithine decarboxylase 1	NM_174130.2	5' GTGAACCATGGAGTATATGGGTC 3' CTCATCTGGTTTGGGTCTCTTC	93	Ramos *et al*., 2014[4]
ANPEP	alanyl aminopeptidase, membrane	NM_001075144.1	5' ATCCGGATGCTCTCGAATTTC 3' TCTGATAGGCAAAGGTCTGCAA	82	Primer Express
EED	embryonic ectoderm development	NM_001040494.2	5' GAAATCCGGTTGTTGCAGTCTT 3' TGGCCAACATAGTGCTTTATGC	174	Primer Express
Secretory activity					
GRP	gastrin-releasing peptide	NM_001101239.1	5' GTGGGAAGAAGCGACAAGGA 3' TGCTGAGGACCTGTGTCTTTGA	148	Primer Express
LTF	lactotransferrin	NM_180998.2	5' CGTGGCAGTTGTCAAGAA 3' GCACAGCTCTGACTAAAGAA	169	Primer Express
MCOLN3	mucolipin 3	NM_001192367.1	5' ACCAGCATACATCTCCCTCT 3' TGGCAAGTTTCCAGGGTTT	124	Primer Express
PIP	prolactin-induced protein	NM_001080913.1	5' GCTGCCCTGCTTCTGATTCT 3' CCACGGTGGCCTCTTCACT	128	Primer Express
RBP4	retinol binding protein 4	NM_001040475.2	5' ACCTGCGCTGACAGCTACTCTT 3' CAGTAACCGTTGTGAGGGATCA	138	Primer Express
SCAMP1	secretory carrier membrane protein 1	NM_001076054.2	5' ACCCTTTCAAGGACCCATCAG 3' CAAGGCATGTTCCTTTGCAA	198	Primer Express
SCAMP2	secretory carrier membrane protein 2	NM_001102170.1	5' CATGTCGTCCTTTGACACCAA 3' TCGCTGCATTTGTCTCTGAGA	132	Primer Express
SCAMP3	secretory carrier membrane protein 3	NM_001035426.1	5' TGAAGCGGATCCACTCTTTGT 3' GCCCGGAAGGCATTTTCT	146	Primer Express
SERPINA14	serpin peptidase inhibitor, clade A (alpha-1 antiproteinase, antitrypsin), member 14	NM_174797.3	5' ATATCATCTTCTCCCCCATGG 3' GTGCACATCCAACAGTTTGG	123	Araújo *et al*., 2015[2]
SPP1	secreted phosphoprotein 1	NM_174187.2	5' TCCGCCCTTCCAGTTAAACC 3' TGTGGTGTTAGGAAAGTCTGCT	131	Primer Express

[4] Ramos RdS, Mesquita FS, D'Alexandri FL, Gonella-Diaza AM, Papa PdC, Binelli M. Regulation of the polyamine metabolic pathway in the endometrium of cows during early diestrus. Molecular reproduction and development. 2014;81(7):584-94.

[2] Araújo ER, Sponchiado M, Pugliesi G, Van Hoeck V, Mesquita FS, Membrive CMB, *et al*. Spatio-specific regulation of endocrine-responsive gene transcription by periovulatory endocrine profiles in the bovine reproductive tract. Reproduction, Fertility and Development. 2015.

Symbol	Gene	GenBank number	Forward and Reverse sequences	Amplicon	Reference
Sex steroid signaling					
ESR1	estrogen receptor 1	NM_001001443.1	5’ CAGGCACATGAGCAACAAAG 3’ TCCAGCAGCAGGTCGTAGAG	82	Primer Express
ESR2	estrogen receptor 2	NM_174051.3	5’ GTAGAGAGCCGCCATGAATAC 3’ CAATGGATGGCTAAAGGAGAGA	159	Primer Express
GPER	G protein-coupled estrogen receptor 1	XM_015469468.1	5’ CCTGTACACCATCTTCCTCTTC 3’ CGATGTCATAGTACTGCTCGTC	189	Primer Express
OXTR	oxytocin receptor	NM_174134.2	5’ AAGATGACCTTCATCGTCGTG 3’ CGTGAAGAGCATGTAGATCCAG	175	Primer Express
PAQR8	progestin and adipoQ receptor family member VIII	NM_001101135.1	5’ TGCCCCTGCTCGTCTATGTC 3’ CCCACGTAGTCCACGAAGTAGAA	121	Primer Express
PGR1	progesterone receptor isoform A	NM_001205356.1	5’ ACTACCTGAGGCCGGATT 3’ CCCTTCCATTGCCCTCTTAAA	163	Primer Express
PGRMC1	progesterone receptor membrane component 1	NM_001075133.1	5’ AGGGGCCGTATGGAGTCTTT 3’ CCACATGATGGTACTTGAAAGTGAA	172	Primer Express
PGRMC2	progesterone receptor membrane component 2	NM_001099060.1	5’ CAGGGGAAGAACCGTCAGAA 3’ ATGAAGCCCCACCAGACATT	282	Primer Express
Solute and water transport					
AQP1	aquaporin 1	NM_174702.3	5’ AACCCTGCCCGGTCCTT 3’ CGCGGTCTGTGAGGTCACT	149	Primer Express
AQP4	aquaporin 4	NM_181003.3	5’ GTGTCTGTTGCAGTGAGAT 3’ CAAAGGGACCTGGGATTTAG	157	Primer Express
CLDN10	claudin 10	NM_001014857.1	5’ AGCCTCACTCTGCCTAAT 3’ TTCTCTGCCGTGATACTTTG	134	Primer Express
SLC13A5	solute carrier family 13, member 5	NM_001191446.1	5’ GGAAGCAGATGGAGCCTTT 3’ ATCATGGAGGCAAAGATGGG	137	Primer Express
SLC1A4	solute carrier family 1, member 4	NM_001081577.1	5’ ATCTTGATAGGCGTGGTTTC 3’ GCAACACTGGTTCTCTCTATAA	132	França *et al*., 2015[5]
SLC2A1	solute carrier family 2, member 1	NM_174602.2	5’ ATCATCTTCACCGTGCTCCTGGTT 3’ TGTCACTTTGACTTGCTCCTCCC	127	França *et al*., 2015[5]

[5] França MR, Mesquita FS, Lopes E, Pugliesi G, Van Hoeck V, Chiaratti MR, *et al*. Modulation of periovulatory endocrine profiles in beef cows: consequences for endometrial glucose transporters and uterine fluid glucose levels. Domestic animal endocrinology. 2015;50:83-90.

Symbol	Gene	GenBank number	Forward and Reverse sequences	Amplicon	Reference
SLC5A6	solute carrier family 5, member 6	NM_001046219.2	5’ TCCCTCAGCACCATATCCTC 3’ CCAAGGCAGAAGAGTCCAAG	248	Primer Express
SLC7A8	solute carrier family 7, member 8	NM_001192889.2	5’ GAGATTGGATTGGTCAGTGG 3’ CTCCCACAACTGTGATAAG	156	Primer Express

Supplementary Table S2. Summary of regional effects in the transcripts abundance measured by Real Time PCR in the uterotubal junction (UTJ), anterior (IA), medial (IM) and posterior (IP) samples of the ipsilateral uterine horn. (Continued)

Gene	Overall effects			Inter-regions Comparisons					
	Group	Region	Group* Region	UTJ *vs.* IA	UTJ *vs.* IM	UTJ *vs.* IP	IA *vs.* IM	IA *vs.* IP	IM *vs.* IP
Cell-cell adhesion									
FN1	ns	**	ns	**	**	**	ns	ns	ns
ICAM1	ns	**	ns	**	**	**	**	**	×
ICAM3	ns	**	ns	**	**	**	ns	×	ns
ITFG3	ns	**	ns	**	**	**	ns	*	ns
LGALS1	ns	*	ns	ns	ns	ns	**	*	ns
LGALS7B	ns	*	ns	*	**	*	*	ns	ns
LGALS9	ns	*	ns	ns	**	**	ns	ns	ns
MUC1	ns	×	ns	*	*	*	×	*	ns
VIL1	ns	ns	ns	ns	ns	ns	ns	ns	ns
Eicosanoid metabolic process									
AKR1B1	ns	**	ns	**	**	**	*	ns	ns
PTGES2	ns	**	ns	**	**	**	ns	×	ns
PTGES3	ns	**	ns	**	**	×	ns	×	ns
PTGIS	ns	**	ns	**	**	**	×	×	ns
PTGS1	ns	**	ns	**	**	**	ns	ns	ns
PTGS2	ns	**	ns	**	×	**	**	ns	*
SLCO2A1	ns	**	ns	**	**	**	ns	ns	ns
Extracellular matrix assembly									
HAS3	ns	**	ns	**	**	**	ns	*	ns
HMMR	ns	**	ns	**	**	**	ns	ns	ns
HYAL1	ns	**	ns	**	**	**	ns	ns	ns
HYAL2	ns	**	ns	**	**	**	ns	ns	ns
Extracellular matrix remodeling									
MMP14	ns	**	ns	**	**	**	ns	ns	ns
MMP19	ns	**	ns	**	**	**	×	ns	ns
MMP2	ns	**	ns	**	**	**	×	ns	ns
TIMP2	ns	**	ns	**	**	**	ns	×	*
TIMP3	ns	**	ns	**	**	**	ns	ns	ns
Growth factor signaling									
EDN3	ns	**	ns	**	**	**	*	**	ns
EGFR	ns	*	ns	*	**	*	ns	ns	ns
FGF2	ns	*	ns	**	*	**	ns	ns	ns
FGFR2	ns	**	ns	**	**	**	*	×	ns
FLT1	ns	**	ns	**	**	**	**	ns	ns
GRB7	ns	**	ns	**	**	**	**	**	ns
IGF1	ns	**	ns	**	**	**	ns	ns	ns
IGF1R	ns	**	ns	**	**	**	ns	ns	ns
IGF2	ns	**	ns	*	**	**	×	ns	ns
IGF2R	ns	*	ns	**	*	**	ns	ns	ns
IGFBP7	ns	×	ns	ns	*	*	*	ns	ns

Gene	Overall effects			Inter-regions Comparisons					
	Group	Region	Group* Region	UTJ *vs.* IA	UTJ *vs.* IM	UTJ *vs.* IP	IA *vs.* IM	IA *vs.* IP	IM *vs.* IP
KDR	ns	**	ns	**	**	**	**	*	ns
Interferon Signaling									
IFI6	ns	**	ns	**	**	**	ns	ns	ns
IFNAR2	ns	*	ns	*	*	*	ns	ns	ns
IRF6	ns	**	ns	**	**	**	ns	ns	ns
Oxidative Stress									
CAT	ns	**	ns	**	**	*	ns	ns	ns
GPX4	ns	**	ns	**	**	**	ns	ns	ns
SOD1	ns	**	ns	**	**	**	ns	ns	ns
SOD2	ns	ns	ns	ns	ns	ns	ns	ns	ns
Polyamine regulation and proteolysis									
ODC1	ns	**	ns	**	**	**	ns	ns	ns
ANPEP	ns	**	ns	**	**	**	ns	ns	ns
EED	ns	**	ns	ns	ns	ns	ns	ns	ns
Secretory activity									
LTF	ns	ns	ns	ns	ns	ns	ns	ns	ns
MCOLN3	ns	**	ns	**	**	**	ns	*	ns
PIP	ns	ns	ns	ns	ns	ns	ns	ns	ns
RBP4	ns	**	ns	**	**	**	**	*	ns
SCAMP1	ns	*	ns	**	*	ns	ns	ns	ns
SCAMP2	ns	**	ns	**	**	**	*	**	ns
SCAMP3	ns	**	ns	**	**	**	×	ns	ns
SERPINA14	ns	*	ns	**	*	ns	ns	ns	ns
SPP1	ns	*	ns	*	ns	ns	×	×	ns
Sex steroid signaling									
ESR1	ns	**	ns	**	**	**	ns	ns	ns
ESR2	ns	**	ns	**	**	**	**	**	×
GPER	ns	×	ns	*	*	*	ns	ns	×
OXTR	ns	**	ns	**	**	**	*	*	×
PAQR8	ns	**	ns	**	**	**	ns	*	ns
PGR1	ns	×	ns	×	×	×	ns	ns	ns
PGRMC1	ns	**	ns	**	**	**	ns	ns	ns
PGRMC2	ns	ns	ns	ns	ns	ns	ns	ns	ns
Solute and water transport									
AQP1	ns	ns	ns	ns	ns	ns	ns	ns	ns
AQP4	ns	**	*	**	ns	ns	*	*	ns
CLDN10	ns	×	ns	ns	ns	ns	ns	ns	*
SLC13A5	ns	**	ns	**	**	**	ns	ns	ns
SLC1A4	ns	ns	×	ns	ns	×	ns	ns	ns
SLC2A1	ns	**	ns	**	**	**	*	**	ns
SLC5A6	ns	**	ns	**	**	**	ns	ns	ns
SLC7A8	ns	**	ns	**	**	*	ns	ns	ns

Magnitude of effect is indicated by: $**P \leq 0.01$; $*P \leq 0.05$; $^{\times}P \leq 0.1$; ns: not significant ($P > 0.1$).

Supplementary Table S3. Biochemical name, abbreviation and PubChem Compound ID of each metabolite quantified in uterine luminal fluid samples recovered from Control and Pregnant cows *post mortem*. (Continued)

Metabolite	Abbreviation	PubChem CID
Acylcarnitines		
Carnitine (free)	C0	2724480
Decanoylcarnitine [= Caprylcarnitine]	C10	10245190
Decenoylcarnitine	C10:1	53481651
Decadienoylcarnitine	C10:2	53481669
Dodecanoylcarnitine [= Laurylcarnitine]	C12	168381
Dodecanedioylcarnitine	C12-DC	53481673
Dodecenoylcarnitine	C12:1	53481671
Tetradecanoylcarnitine [= Myristylcarnitine]	C14	53477791
Tetradecenoylcarnitine [= Myristoleylcarnitine]	C14:1	22833575
Hydroxytetradecenoylcarnitine [= Hydroxymyristoleylcarnitine]	C14:1-OH	53481679
Tetradecadienoylcarnitine	C14:2	71464539
Hydroxytetradecadienoylcarnitine	C14:2-OH	71464482
Hexadecanoylcarnitine [= Palmitoylcarnitine]	C16	11953816
Hydroxyhexadecanolycarnitine [= Hydroxypalmitoylcarnitine]	C16-OH	24779579
Hexadecenoylcarnitine [= Palmitoleylcarnitine]	C16:1	53477817
Hydroxyhexadecenoylcarnitine [= Hydroxypalmitoleylcarnitine]	C16:1-OH	53481779
Hexadecadienoylcarnitine	C16:2	53481687
Hydroxyhexadecadienoylcarnitine	C16:2-OH	53481689
Octadecanoylcarnitine [= Stearylcarnitine]	C18	6426855
Octadecenoylcarnitine [= Oleylcarnitine]	C18:1	53477837
Hydroxyoctadecenoylcarnitine [= Hydroxyoleylcarnitine]	C18:1-OH	53481697
Octadecadienoylcarnitine [= Linoleylcarnitine]	C18:2	53477834
Acetylcarnitine	C2	1
Propionylcarnitine	C3	107738
Hydroxybutyrylcarnitine (Malonylcarnitine)	C3-DC (C4-OH)	22833583
Hydroxypropionylcarnitine	C3-OH	53481613
Propenoylcarnitine	C3:1	53481611
Butyrylcarnitine / Isobutyrylcarnitine	C4	439829
Butenoylcarnitine	C4:1	4151505
Isovalerylcarnitine / 2-Methylbutyrylcarnitine / Valerylcarnitine	C5	6426851
Glutarylcarnitine (Hydroxyhexanoylcarnitine [= Hydroxycaproylcarnitine])	C5-DC (C6-OH)	53481622
Methylglutarylcarnitine	C5-M-DC	128145
Hydroxyisovalerylcarnitine / Hydroxy-2-methylbutyryl / Hydroxyvalerylcarnitine (Methylmalonylcarnitine)	C5-OH (C3-DC-M)	53481628
Tiglylcarnitine / 3-Methyl-crotonylcarnitine	C5:1	22833596
Glutaconylcarnitine / Mesaconylcarnitine	C5:1-DC	53481620
Hexanoylcarnitine [= Caproylcarnitine] (Fumarylcarnitine)	C6 (C4:1-DC)	3246938
Hexenoylcarnitine	C6:1	53481638
Pimelylcarnitine	C7-DC	53481675
Octanoylcarnitine [= Caprylylcarnitine]	C8	11953814
Nonanoylcarnitine [= Pelargonylcarnitine]	C9	53481660
Amino Acids & Biogenic Amines		
Alanine	Ala	5950
Arginine	Arg	6322
Asparagine	Asn	6267

Metabolite	Abbreviation	PubChem CID
Aspartate	Asp	5960
Carnosine	Carnosine	439224
Citrulline	Cit	9750
Creatinine	Creatinine	588
Dopamin	Dopamine	681
Glutamine	Gln	5961
Glutamate	Glu	33032
Glycine	Gly	750
Histamine	Histamine	774
Leucine	Leu	6106
Proline	Pro	145742
Putrescine	Putrescine	1045
Sarcosine	Sarcosine	1088
Symmetric dimethylarginine	SDMA	169148
Serine	Ser	5951
Spermidine	Spermidine	1102
Spermine	Spermine	1103
trans-4-Hydroxyproline	t4-OH-Pro	5810
Taurine	Taurine	1123
Threonine	Thr	6288
Eicosanoids & Oxidation products of polyunsaturated fatty acids		
12(S)-hydroxy-5Z,8Z,10E,14Z-eicosatetraenoic acid	12S-HETE	5283155
13(S)-hydroxy-9Z,11E-octadecadienoic acid	13S-HODE	6443013
15(S)-hydroxy-5Z,8Z,11Z,13E-eicosatetraenoic acid	15S-HETE	5280724
6-keto-Prostaglandin F1alpha	6-keto-PGF1a	5280888
Arachidonic acid	AA	444899
Docosahexaenoic acid	DHA	445580
Prostaglandin F2alpha	PGF2a	5282415
Hexoses		
Hexoses	H1	.
Phosphatidylcholines		
Lysophosphatidylcholine with acyl residue C14:0	lysoPC a C14:0	460604
Lysophosphatidylcholine with acyl residue C16:0	lysoPC a C16:0	10917802
Lysophosphatidylcholine with acyl residue C16:1	lysoPC a C16:1	24779461
Lysophosphatidylcholine with acyl residue C17:0	lysoPC a C17:0	24779463
Lysophosphatidylcholine with acyl residue C18:0	lysoPC a C18:0	2733532
Lysophosphatidylcholine with acyl residue C18:1	lysoPC a C18:1	53480465
Lysophosphatidylcholine with acyl residue C18:2	lysoPC a C18:2	11005824
Lysophosphatidylcholine with acyl residue C20:3	lysoPC a C20:3	52924055
Lysophosphatidylcholine with acyl residue C20:4	lysoPC a C20:4	53480469
Lysophosphatidylcholine with acyl residue C24:0	lysoPC a C24:0	24779481
Lysophosphatidylcholine with acyl residue C26:0	lysoPC a C26:0	44340994
Lysophosphatidylcholine with acyl residue C26:1	lysoPC a C26:1	52925041
Lysophosphatidylcholine with acyl residue C28:0	lysoPC a C28:0	52924960
Lysophosphatidylcholine with acyl residue C28:1	lysoPC a C28:1	52923870
Phosphatidylcholine with diacyl residue sum C24:0	PC aa C24:0	6452499
Phosphatidylcholine with diacyl residue sum C26:0	PC aa C26:0	52924957

Metabolite	Abbreviation	PubChem CID
Phosphatidylcholine with diacyl residue sum C28:1	PC aa C28:1	52922210
Phosphatidylcholine with diacyl residue sum C30:0	PC aa C30:0	24778679
Phosphatidylcholine with diacyl residue sum C32:0	PC aa C32:0	131150
Phosphatidylcholine with diacyl residue sum C32:1	PC aa C32:1	24778618
Phosphatidylcholine with diacyl residue sum C32:2	PC aa C32:2	52922262
Phosphatidylcholine with diacyl residue sum C32:3	PC aa C32:3	52922763
Phosphatidylcholine with diacyl residue sum C34:1	PC aa C34:1	53478717
Phosphatidylcholine with diacyl residue sum C34:2	PC aa C34:2	53478719
Phosphatidylcholine with diacyl residue sum C34:3	PC aa C34:3	52922280
Phosphatidylcholine with diacyl residue sum C34:4	PC aa C34:4	52922891
Phosphatidylcholine with diacyl residue sum C36:0	PC aa C36:0	94190
Phosphatidylcholine with diacyl residue sum C36:1	PC aa C36:1	52922290
Phosphatidylcholine with diacyl residue sum C36:2	PC aa C36:2	15378085
Phosphatidylcholine with diacyl residue sum C36:3	PC aa C36:3	52922727
Phosphatidylcholine with diacyl residue sum C36:4	PC aa C36:4	53478831
Phosphatidylcholine with diacyl residue sum C36:5	PC aa C36:5	52922687
Phosphatidylcholine with diacyl residue sum C36:6	PC aa C36:6	53478633
Phosphatidylcholine with diacyl residue sum C38:0	PC aa C38:0	52923443
Phosphatidylcholine with diacyl residue sum C38:1	PC aa C38:1	53478731
Phosphatidylcholine with diacyl residue sum C38:3	PC aa C38:3	53478735
Phosphatidylcholine with diacyl residue sum C38:4	PC aa C38:4	53478701
Phosphatidylcholine with diacyl residue sum C38:5	PC aa C38:5	52923235
Phosphatidylcholine with diacyl residue sum C38:6	PC aa C38:6	24778898
Phosphatidylcholine with diacyl residue sum C40:1	PC aa C40:1	53479437
Phosphatidylcholine with diacyl residue sum C40:2	PC aa C40:2	53478745
Phosphatidylcholine with diacyl residue sum C40:3	PC aa C40:3	52923247
Phosphatidylcholine with diacyl residue sum C40:4	PC aa C40:4	53478881
Phosphatidylcholine with diacyl residue sum C40:6	PC aa C40:6	52922935
Phosphatidylcholine with diacyl residue sum C42:0	PC aa C42:0	24779162
Phosphatidylcholine with diacyl residue sum C42:1	PC aa C42:1	53479497
Phosphatidylcholine with diacyl residue sum C42:2	PC aa C42:2	52923201
Phosphatidylcholine with diacyl residue sum C42:4	PC aa C42:4	53478821
Phosphatidylcholine with diacyl residue sum C42:5	PC aa C42:5	52923265
Phosphatidylcholine with diacyl residue sum C42:6	PC aa C42:6	53479301
Phosphatidylcholine with acyl-alkyl residue sum C30:0	PC ae C30:0	24779275
Phosphatidylcholine with acyl-alkyl residue sum C30:1	PC ae C30:1	52923874
Phosphatidylcholine with acyl-alkyl residue sum C30:2	PC ae C30:2	53478639
Phosphatidylcholine with acyl-alkyl residue sum C32:1	PC ae C32:1	52923926
Phosphatidylcholine with acyl-alkyl residue sum C32:2	PC ae C32:2	52923928
Phosphatidylcholine with acyl-alkyl residue sum C34:0	PC ae C34:0	24779324
Phosphatidylcholine with acyl-alkyl residue sum C34:1	PC ae C34:1	53480705
Phosphatidylcholine with acyl-alkyl residue sum C34:2	PC ae C34:2	53478777
Phosphatidylcholine with acyl-alkyl residue sum C34:3	PC ae C34:3	24779386
Phosphatidylcholine with acyl-alkyl residue sum C36:0	PC ae C36:0	24779297
Phosphatidylcholine with acyl-alkyl residue sum C36:1	PC ae C36:1	53478887
Phosphatidylcholine with acyl-alkyl residue sum C36:2	PC ae C36:2	53478759
Phosphatidylcholine with acyl-alkyl residue sum C36:3	PC ae C36:3	53480743

Metabolite	Abbreviation	PubChem CID
Phosphatidylcholine with acyl-alkyl residue sum C36:4	PC ae C36:4	53478805
Phosphatidylcholine with acyl-alkyl residue sum C38:0	PC ae C38:0	24779329
Phosphatidylcholine with acyl-alkyl residue sum C38:1	PC ae C38:1	52923956
Phosphatidylcholine with acyl-alkyl residue sum C38:2	PC ae C38:2	53480811
Phosphatidylcholine with acyl-alkyl residue sum C38:3	PC ae C38:3	53478937
Phosphatidylcholine with acyl-alkyl residue sum C38:4	PC ae C38:4	53478939
Phosphatidylcholine with acyl-alkyl residue sum C38:5	PC ae C38:5	53480761
Phosphatidylcholine with acyl-alkyl residue sum C40:1	PC ae C40:1	53480717
Phosphatidylcholine with acyl-alkyl residue sum C40:2	PC ae C40:2	53480827
Phosphatidylcholine with acyl-alkyl residue sum C40:3	PC ae C40:3	53480829
Phosphatidylcholine with acyl-alkyl residue sum C40:4	PC ae C40:4	53479249
Phosphatidylcholine with acyl-alkyl residue sum C40:5	PC ae C40:5	53479269
Phosphatidylcholine with acyl-alkyl residue sum C40:6	PC ae C40:6	53480833
Phosphatidylcholine with acyl-alkyl residue sum C42:0	PC ae C42:0	24779354
Phosphatidylcholine with acyl-alkyl residue sum C42:1	PC ae C42:1	53480725
Phosphatidylcholine with acyl-alkyl residue sum C42:2	PC ae C42:2	53480841
Phosphatidylcholine with acyl-alkyl residue sum C42:3	PC ae C42:3	53480785
Phosphatidylcholine with acyl-alkyl residue sum C42:5	PC ae C42:5	6443119
Phosphatidylcholine with acyl-alkyl residue sum C44:3	PC ae C44:3	53481753
Phosphatidylcholine with acyl-alkyl residue sum C44:4	PC ae C44:4	53481761
Phosphatidylcholine with acyl-alkyl residue sum C44:5	PC ae C44:5	53481767
Phosphatidylcholine with acyl-alkyl residue sum C44:6	PC ae C44:6	53481755
Sphingomyelins		
Hydroxysphingomyelin with acyl residue sum C16:1	SM (OH) C16:1	53481780
Hydroxysphingomyelin with acyl residue sum C22:1	SM (OH) C22:1	53481785
Hydroxysphingomyelin with acyl residue sum C22:2	SM (OH) C22:2	53481787
Hydroxysphingomyelin with acyl residue sum C24:1	SM (OH) C24:1	53481791
Sphingomyelin with acyl residue sum C16:0	SM C16:0	5283590
Sphingomyelin with acyl residue sum C16:1	SM C16:1	53481781
Sphingomyelin with acyl residue sum C18:0	SM C18:0	5283588
Sphingomyelin with acyl residue sum C18:1	SM C18:1	6443882
Sphingomyelin with acyl residue sum C20:2	SM C20:2	44260124
Sphingomyelin with acyl residue sum C24:0	SM C24:0	5283595
Sphingomyelin with acyl residue sum C24:1	SM C24:1	44260126

Supplementary Table S4. Sums and ratios of metabolites quantified in bovine uterine luminal fluid samples, according to their biochemical classifications. Metabolites are categorized in amino acids (AA), biogenic amines (BA), acylcarnitines (AC), esters derived from dicarboxylic acids (DC), esters derived from hydroxylated acids (OH), Phosphatidylcholines (PC), Lysophosphatidylcholines (LysoPC), diacyl- (PC aa) or acyl-alkyl- (PC ae) phosphatidylcholines, saturated (SFA), monounsaturated (MUFA), polyunsaturated (PUFA) glycerophosphocholines, sphingomyelins (SM), hydroxysphingomyelins (SM-OH), and eicosanoids derived from the cycloxygenase (COX) and lipoxygenase (LOX) pathways. (Continued)

Biochemical classification	Calculations
Total AA	Sum of the concentrations of Ala, Arg, Asn, Asp, Cit, Gln, Glu, Gly, Leu, Pro, Ser, Thr and Taurine
Non-essential AA	Sum of the concentrations of Ala, Asn, Asp, Gln, Gly, Pro, Ser and Taurine
Acidic AA	Sum of the concentrations of Asp and Glu
Small Neutral AA	Sum of Ala, Asn, Gly, Ser, Thr and Taurine
Osmotic-stress protection AA	Sum of Ala, Gln, Gly, Pro and Taurine
Glucogenic AA	Sum of Ala, Gly and Ser
Glutathione precursors AA	Sum of Glu and Gly
Total BA	Sum of Carnosine, Creatinine, Dopamine, Histamine, Putrescine, Sarcosine, SDMA, Spermidine, Spermine and t4-OH-Pro
Spermidine/Putrescine	Ratio of Spermidine to Putrescine
Spermine/Spermidine	Ratio of Spermine to Spermidine
Total Recoverable Amounts of AC	Sum of the concentrations of all acylcarnitines
Total short-chain AC	Sum of the concentrations of C2, C3, C3:1, C4, C4:1, C5 and C5:1
Total medium-chain AC	Sum of the concentrations of C6:1, C8, C9, C10, C10:1, C10:2, C12 and C12:1
Total long-chain AC	Sum of the concentrations of C14, C14:1, C14:2, C16, C16:1, C16:2, C18, C18:1 and C18:2
Acylcarnitine/Free carnitine	Ratio of Carnitine (C2) to Free carnitine (C0)
Total short-chain AC/Free carnitine	Ratio of total short-chain acylcarnitine (AC) to Free carnitine (C0)
CPT-I([C16+C18]/C0)	Ratio of [C16, C16-OH, C16:1, C16:1-OH, C16:2, C16:2-OH, C18, C18:1, C18:1-OH, C18:2] to Free carnitine (C0)
Total Esters derived from DC/Total AC	Ratio of Esters derived from DC to total AC
Esters derived from HO	Sum of the concentrations of C3-OH, C5-OH(C3-DC-M), C14:1-OH, C14:2-OH, C16-OH, C16:1-OH, C16:2-OH and C18:1-OH
Esters derived from DC	Sum of C3-DC(C4-OH), C5-DC(C6-OH), C5-M-DC, C5:1-DC, C7-DC and C12-DC
Total recoverable amounts of phospholipids	Sum of all phospholipids
Total recoverable amounts of LysoPC	Sum of the concentrations of lysoPC a C14:0, lysoPC a C16:0, lysoPC a C16:1, lysoPC a C17:0, lysoPC a C18:0, lysoPC a C18:1, lysoPC a C18:2, lysoPC a C20:3, lysoPC a C20:4, lysoPC a C24:0, lysoPC a C26:0, lysoPC a C26:1, lysoPC a C28:0 and lysoPC a C28:1

Biochemical classification	Calculations
Total recoverable amounts of PC	Sum of the concentrations of PC aa C24:0, PC aa C26:0, PC aa C28:1, PC aa C30:0, PC aa C32:0, PC aa C32:1, PC aa C32:2, PC aa C32:3, PC aa C34:1, PC aa C34:2, PC aa C34:3, PC aa C34:4, PC aa C36:0, PC aa C36:1, PC aa C36:2, PC aa C36:3, PC aa C36:4, PC aa C36:5, PC aa C36:6, PC aa C38:0, PC aa C38:1, PC aa C38:3, PC aa C38:4, PC aa C38:5, PC aa C38:6, PC aa C40:1, PC aa C40:2, PC aa C40:3, PC aa C40:4, PC aa C40:6, PC aa C42:0, PC aa C42:1, PC aa C42:2, PC aa C42:4, PC aa C42:5, PC aa C42:6, PC ae C30:0, PC ae C30:1, PC ae C30:2, PC ae C32:1, PC ae C32:2, PC ae C34:0, PC ae C34:1, PC ae C34:2, PC ae C34:3, PC ae C36:0, PC ae C36:1, PC ae C36:2, PC ae C36:3, PC ae C36:4, PC ae C38:0, PC ae C38:1, PC ae C38:2, PC ae C38:3, PC ae C38:4, PC ae C38:5, PC ae C40:1, PC ae C40:2, PC ae C40:3, PC ae C40:4, PC ae C40:5, PC ae C40:6, PC ae C42:0, PC ae C42:1, PC ae C42:2, PC ae C42:3, PC ae C42:5, PC ae C44:3, PC ae C44:4, PC ae C44:5 and PC ae C44:6
Total LysoPC/Total PC[c]	Ratio of total LysoPC to total recoverable PC
Total PC aa	Sum of the concentrations of PC aa C24:0, PC aa C26:0, PC aa C28:1, PC aa C30:0, PC aa C32:0, PC aa C32:1, PC aa C32:2, PC aa C32:3, PC aa C34:1, PC aa C34:2, PC aa C34:3, PC aa C34:4, PC aa C36:0, PC aa C36:1, PC aa C36:2, PC aa C36:3, PC aa C36:4, PC aa C36:5, PC aa C36:6, PC aa C38:0, PC aa C38:1, PC aa C38:3, PC aa C38:4, PC aa C38:5, PC aa C38:6, PC aa C40:1, PC aa C40:2, PC aa C40:3, PC aa C40:4, PC aa C40:6, PC aa C42:0, PC aa C42:1, PC aa C42:2, PC aa C42:4, PC aa C42:5 and PC aa C42:6
Total PC ae	Sum of the concentrations of PC ae C30:0, PC ae C30:1, PC ae C30:2, PC ae C32:1, PC ae C32:2, PC ae C34:0, PC ae C34:1, PC ae C34:2, PC ae C34:3, PC ae C36:0, PC ae C36:1, PC ae C36:2, PC ae C36:3, PC ae C36:4, PC ae C38:0, PC ae C38:1, PC ae C38:2, PC ae C38:3, PC ae C38:4, PC ae C38:5, PC ae C40:1, PC ae C40:2, PC ae C40:3, PC ae C40:4, PC ae C40:5, PC ae C40:6, PC ae C42:0, PC ae C42:1, PC ae C42:2, PC ae C42:3, PC ae C42:5, PC ae C44:3, PC ae C44:4, PC ae C44:5 and PC ae C44:6
Total MUFA (PC)	Sum of the concentrations of PC aa C28:1, PC aa C32:1, PC aa C34:1, PC aa C36:1, PC aa C38;1, PC aa C40:1, PC aa C42:1, PC ae C30:1, PC ae C32:1, PC ae C34:1, PC ae C36:1, PC ae C38:1, PC ae C40:1 and PC ae C42:1
Total PUFA (PC)	Sum of the concentrations of PC aa C32:2, PC aa C32:3, PC aa C34:2, PC aa C 34:3, PC aa 34:4, PC aa C36:2, PC aa C36:3, PC aa C36:4, PC aa C36:5, PC aa C36:6, PC aa C38:3, PC aa C38:4, PC aa C38:5, PC aa C38:6, PC aa C40:2, PC aa C40:3, PC aa C40:4, PC aa C40:6, PC aa C42:2, PC aa C42:4, PC aa C42:5, PC aa C42:6, PC ae C30:2, PC ae C32:2, PC ae C34:2, PC ae C34:3, PC ae C36:2, PC ae C36:3, PC ae C36:4, PC ae C38:2, PC ae C38:3, PC ae C38:4, PC ae C38:5, PC ae C40:2, PC ae C40:3, PC ae C40:4, PC ae C40:5, PC ae C40:6, PC ae C42:2, PC ae C42:3, PC ae C42:5, PC ae C44:3, PC ae C44:4, PC ae C44:5 and PC ae C44:6
Total SFA (PC)	Sum of the concentrations of PC aa C24:0, PC aa C26:0, PC aa C30:0, PC aa C32:0, PC aa C36:0, PC aa C38:0, PC aa C42:0, PC ae C30:0, PC ae C34:0, PC ae C36:0, PC ae C38:0 and PC ae C42:0
MUFA (PC)/SFA (PC)[d]	Ratio of monounsaturated fatty acids (MUFA) to saturated fatty acids (SFA)
PUFA (PC)/MUFA (PC)[d]	Ratio of polyunsaturated fatty acids (PUFA) to monounsaturated fatty acids (MUFA)
PUFA (PC)/SFA (PC)[d]	Ratio of polyunsaturated fatty acids (PUFA) to saturated fatty acids (SFA)

Biochemical classification	Calculations
Total SM	Sum of all sphingomyelins (SM)
Total SM-OH	Sum of the concentrations of SM (OH) C16:1, SM (OH) C22:1, SM (OH) C22:2, SM (OH) C24:1
Ratio SM/SM-OH	Ratio of total recoverable sphingomyelins (SM) to hydroxysphingomyelins (SM-OH)
Total unsaturated SM	Sum of the concentrations of SM C16:1, SM C18:1 and SM C24:1
Total saturated SM	Sum of the concentrations of SM C16:0, SM C18:0 and SM C24:0
Hexoses	Sum of the concentrations of Glucose; Aldohexose; L-Allopyranose; D-Allose; D-Allopyranose; D-Allose; D-Altropyranose; D-Glucopyranose; alpha-D-Glucopyranose; beta-D-Glucopyranose; D-Mannopyranose; alpha-D; Mannopyranose; L-Gulopyranose; D-Gulopyranose; D-Idopyranose; Alpha-L-Galactopyranose; alpha-D-Galactopyranose; beta-D-Galactopyranose; D-Talose; D-Talopyranose; Ketohexose; D-Psicopyranose; L-Fructofuranose; D-Fructose; D-Fructofuranose; L-Sorbopyranose; D-Sorbopyranose; D-Tagatose; D-Tagatopyranose
COX pathway	Sum of the concentrations of 6-keto-PGF1a and PGF2a
LOX pathway	Sum of the concentrations of 12S-HETE, 15S-HETE and 13S-HODE

Supplementary Table S5. Bovine specific oligonucleotide forward and reverse primer sequences (5'-3') and PCR product length.

Gene symbol	Gene	GenBank accession	Forward and Reverse sequences	Amplicon size (bp)
ALOX5	arachidonate 5-lipoxygenase	NM_001192792.2	5' CAAGCAGCACAGACGCAAAGAACT 3'AAGTCCTTGTGGCATTTGGCATCG	108
ALOX5AP	arachidonate 5-lipoxygenase activating protein	NM_001076293	5' ACACTGCCAACCAGAACTGTGT 3' CTGCCTCACGAACAGGTACATC	125
ALOX12	arachidonate 12-lipoxygenase	NM_001192336.1	5' GTCCTAACCCAGCCATGTTT 3' GCCCAGTCAGTCTTCAGTTT	163
ALOX15B	arachidonate 15-lipoxygenase, type B	NM_001205703.1	5' TCTTCAAGCTGCTGATCCCTCACA 3' ATATCATCAGGCAGACACAGGGCA	187
SLC6A9	solute carrier family 6, member 9	NM_001242343.1	5' TGTTCAAAGGTGTGGGCTAC 3' GGCGTGTTCCAAGGGTTATT	151
LPL	lipoprotein lipase	NM_001075120.1	5' AACCGGACTCCAACGTCATC 3' TTCATCCGCCATCCAGTTC	128
PPARG	peroxisome proliferator activated receptor gamma	NM_181024.2	5' AAGCCCTTTGGTGACTTTATGG 3' GGCGGTCTCCACTGAGAATAAT	121
RXRA	retinoid X receptor alpha	NM_001304343.1	5' AAGATGCGGGACATGCAGAT 3' CAGCTTGGCGAACCTTCCT	189
ACTB	actin, beta	NM_173979.3	5' GGATGAGGCTCAGAGCAAGAGA 3' TCGTCCCAGTTGGTGACGAT	76
GAPDH	glyceraldehyde-3-phosphate dehydrogenase	NM_001034034.2	5' GCCATCAATGACCCCTTCAT 3' TGCCGTGGGTGGAATCA	68
PPIA	peptidylprolyl isomerase A	NM_178320.2	5' GCCATGGAGCGCTTTGG 3' CCACAGTCAGCAATGGTGATCT	63

Supplementary Table S6. Amino acids and biogenic amines concentration in uterine luminal fluid from Control (Con) and Pregnant (Preg) cows. Values are expressed as nmol/cm^2 of endometrial area; mean ± SEM.

Metabolite	Group		P value	FDR significance[a]	Log2 Fold-change[b]
	Con (n = 8)	Preg (n = 10)			
Amino acids					
Alanine	1236.58 ± 148.21	1143.85 ± 54.05	0.70	n.s.	-0.11
Arginine	39.02 ± 11.07	18.71 ± 2.36	0.14	n.s.	-1.06
Asparagine	74.30 ± 4.37	67.21 ± 2.38	0.47	n.s.	-0.14
Aspartate	636.89 ± 66.30	578.99 ± 27.41	0.61	n.s.	-0.14
Citrulline	33.57 ± 6.22	27.16 ± 1.95	0.48	n.s.	-0.31
Glutamate	5538.84 ± 367.80	5179.54 ± 142.01	0.56	n.s.	-0.10
Glutamine	1008.70 ± 123.14	1028.15 ± 43.33	0.92	n.s.	0.03
Glycine	5099.80 ± 506.62	3588.41 ± 123.76	0.03	*	-0.51
Leucine	69.83 ± 26.46	29.77 ± 4.47	0.16	n.s.	-1.22
Proline	250.44 ± 31.07	172.26 ± 10.60	0.09	n.s.	-0.54
Serine	202.29 ± 33.24	145.71 ± 10.96	0.25	n.s.	-0.47
Threonine	218.88 ± 23.40	211.43 ± 6.94	0.83	n.s.	-0.04
Biogenic amines					
Carnosine	51.65 ± 7.73	40.12 ± 1.73	0.23	n.s.	-0.36
Creatinine	156.23 ± 14.69	141.52 ± 5.20	0.55	n.s.	-0.14
Dopamine	2.52 ± 0.58	2.19 ± 0.10	0.60	n.s.	-0.20
Histamine	81.11 ± 21.16	45.23 ± 3.57	0.13	n.s.	-0.84
Putrescine	349.09 ± 52.27	304.01 ± 14.13	0.51	n.s.	-0.20
Sarcosine	515.78 ± 54.96	311.97 ± 10.02	0.005	**	-0.74
Spermidine	61.68 ± 6.78	46.43 ± 1.57	0.08	n.s.	-0.42
Spermine	44.96 ± 10.64	30.52 ± 2.29	0.26	n.s.	-0.56
SDMA	0.58 ± 0.18	0.66 ± 0.07	0.81	n.s.	0.16
Taurine	4074.73 ± 369.12	3418.52 ± 122.18	0.23	n.s.	-0.25
Trans-4-Hydroxyproline	46.59 ± 5.67	44.42 ± 2.03	0.81	n.s.	-0.07

Metabolites in bold were different between Con and Preg group by ANOVA followed by FDR correction.
[a]Statistical analyses were carried out by one-way ANOVA followed by FDR correction for multiple comparisons. Magnitude of effect is indicated by: ** $P \leq 0.01$; * $P \leq 0.05$; n.s. $P > 0.05$.
[b]Data are represented as fold-change of the metabolite concentration between Preg and Con groups.

Supplementary Table S7. Carnitine and acylcarnitines concentration in uterine luminal fluid from Control (Con) and Pregnant (Preg) cows. Values are expressed as nmol/cm^2 of endometrial area; mean ± SEM. (Continued)

Metabolite	Group		P value	FDR significance[a]	Log2 Fold-change[b]
	Con (n = 8)	Preg (n = 10)			
Carnitine free (C0)	99.14 ± 10.28	100.51 ± 4.03	0.93	n.s.	0.01
Short-chain acylcarnitine					
C2	63.18 ± 8.10	59.72 ± 2.51	0.76	n.s.	-0.07
C3	2.50 ± 0.28	2.50 ± 0.12	0.99	n.s.	0.00
C3:1	0.45 ± 0.03	0.39 ± 0.01	0.18	n.s.	-0.20
C4	7.61 ± 1.43	9.47 ± 0.60	0.61	n.s.	0.31
C4:1	0.81 ± 0.05	0.75 ± 0.02	0.40	n.s.	-0.12
C5	1.71 ± 0.18	1.67 ± 0.07	0.89	n.s.	-0.03
C5:1	1.14 ± 0.10	1.17 ± 0.03	0.85	n.s.	0.03
Medium-chain acylcarnitine					
C6	1.83 ± 0.12	1.51 ± 0.03	0.04	n.s.	-0.29
C6:1	0.91 ± 0.07	0.91 ± 0.02	0.97	n.s.	0.00
C8	2.70 ± 0.18	2.46 ± 0.05	0.30	n.s.	-0.14
C9	0.60 ± 0.05	0.58 ± 0.01	0.73	n.s.	-0.04
C10	2.41 ± 0.18	2.02 ± 0.03	0.06	n.s.	-0.25
C10:1	1.83 ± 0.17	1.72 ± 0.04	0.60	n.s.	-0.09
C10:2	0.81 ± 0.06	0.76 ± 0.01	0.48	n.s.	-0.09
C12	1.91 ± 0.12	1.88 ± 0.03	0.87	n.s.	-0.01
C12:1	1.59 ± 0.15	1.48 ± 0.03	0.50	n.s.	-0.10
Long-chain acylcarnitine					
C14	0.71 ± 0.07	0.63 ± 0.02	0.36	n.s.	-0.17
C14:1	0.20 ± 0.02	0.19 ± 0.01	0.61	n.s.	-0.10
C14:2	1.41 ± 0.08	1.36 ± 0.03	0.69	n.s.	-0.06
C16	0.44 ± 0.05	0.37 ± 0.01	0.21	n.s.	-0.23
C16:1	0.60 ± 0.05	0.51 ± 0.01	0.15	n.s.	-0.23
C16:2	0.26 ± 0.03	0.25 ± 0.01	0.89	n.s.	-0.03
C18	0.41 ± 0.04	0.30 ± 0.01	0.04	n.s.	-0.47
C18:1	0.75 ± 0.09	0.55 ± 0.02	0.05	n.s.	-0.45
C18:2	0.28 ± 0.03	0.29 ± 0.01	0.86	n.s.	0.04
Esters derived from dicarboxylic acids					
C3-DC	1.30 ± 0.10	1.22 ± 0.03	0.60	n.s.	-0.09
C5:1-DC	0.72 ± 0.05	0.63 ± 0.01	0.17	n.s.	-0.22
C5-DC	0.40 ± 0.02	0.38 ± 0.01	0.30	n.s.	-0.10
C5-M-DC	1.02 ± 0.09	0.95 ± 0.02	0.52	n.s.	-0.10
C7-DC	0.35 ± 0.02	0.32 ± 0.004	0.22	n.s.	-0.12

Metabolite	Group		P value	FDR significance[a]	Log2 Fold-change[b]
	Con (n = 8)	Preg (n = 10)			
C12-DC	3.02 ± 0.21	2.88 ± 0.04	0.56	n.s.	-0.06
Esters derived from hydroxylated acids					
C3-OH	0.60 ± 0.03	0.47 ± 0.01	0.005	**	-0.36
C5-OH	1.51 ± 0.08	1.14 ± 0.03	0.02	*	-0.40
C14:1-OH	0.32 ± 0.03	0.29 ± 0.01	0.30	n.s.	-0.17
C14:2-OH	0.37 ± 0.03	0.36 ± 0.01	0.79	n.s.	-0.04
C16-OH	0.33 ± 0.02	0.27 ± 0.004	0.03	*	-0.27
C16:1-OH	0.30 ± 0.02	0.26 ± 0.01	0.20	n.s.	-0.20
C16:2-OH	0.48 ± 0.04	0.54 ± 0.01	0.33	n.s.	0.16
C18:1-OH	0.63 ± 0.04	0.65 ± 0.01	0.73	n.s.	0.03

Metabolites in bold were different between Con and Preg group by ANOVA followed by FDR correction.
[a]Statistical analyses were carried out by one-way ANOVA followed by FDR correction for multiple comparisons. Magnitude of effect is indicated by: ** $P \leq 0.01$; * $P \leq 0.05$; n.s. $P > 0.05$.
[b]Data are represented as fold-change of the metabolite concentration between Preg and Con groups.

Supplementary Table S8. Phosphatidylcholines (PC) and Lysophosphatidylcholines (LysoPC) concentration in uterine luminal fluid from Control (Con) and Pregnant (Preg) cows. Values are expressed as nmol/cm^2 of endometrial area; mean ± SEM. (Continued)

Metabolite	Group		P value	FDR significance[a]	Log2 Fold-change[b]
	Con (n = 8)	Preg (n = 10)			
Lysophosphatidylcholines					
lysoPC a C14:0	241.28 ± 16.48	243.82 ± 3.64	0.90	n.s.	0.01
lysoPC a C16:0	3.77 ± 0.41	3.29 ± 0.12	0.42	n.s.	-0.20
lysoPC a C16:1	1.68 ± 0.09	1.88 ± 0.03	0.11	n.s.	0.16
lysoPC a C17:0	0.91 ± 0.06	0.64 ± 0.03	0.02	*	-0.49
lysoPC a C18:0	5.47 ± 0.15	5.56 ± 0.11	0.85	n.s.	0.03
lysoPC a C18:1	2.91 ± 0.32	3.02 ± 0.09	0.82	n.s.	0.06
lysoPC a C18:2	1.88 ± 0.23	1.27 ± 0.04	0.02	*	-0.58
lysoPC a C20:3	2.35 ± 0.26	1.73 ± 0.04	0.05	n.s.	-0.43
lysoPC a C20:4	0.47 ± 0.06	0.56 ± 0.02	0.35	n.s.	0.26
lysoPC a C24:0	15.11 ± 1.01	14.50 ± 0.18	0.59	n.s.	-0.06
lysoPC a C26:0	0.45 ± 0.05	0.57 ± 0.02	0.14	n.s.	0.33
lysoPC a C26:1	0.27 ± 0.05	0.30 ± 0.01	0.66	n.s.	0.15
lysoPC a C28:0	2.17 ± 0.17	2.13 ± 0.05	0.87	n.s.	-0.03
lysoPC a C28:1	0.46 ± 0.05	0.38 ± 0.03	0.41	n.s.	-0.27
Diacyl-phosphatidylcholines					
PC aa C24:0	0.54 ± 0.03	0.53 ± 0.01	0.74	n.s.	-0.03
PC aa C26:0	17.63 ± 1.28	16.65 ± 0.23	0.50	n.s.	-0.09
PC aa C28:1	0.39 ± 0.05	0.36 ± 0.01	0.51	n.s.	-0.14
PC aa C30:0	3.25 ± 0.23	2.99 ± 0.06	0.37	n.s.	-0.12
PC aa C32:0	1.58 ± 0.17	1.28 ± 0.05	0.27	n.s.	-0.30
PC aa C32:1	0.92 ± 0.18	0.66 ± 0.03	0.18	n.s.	-0.49
PC aa C32:2	0.98 ± 0.23	0.63 ± 0.04	0.19	n.s.	-0.62
PC aa C32:3	0.68 ± 0.18	0.32 ± 0.02	0.06	n.s.	-1.09
PC aa C34:1	15.79 ± 3.24	10.29 ± 0.49	0.11	n.s.	-0.62
PC aa C34:2	3.20 ± 0.48	2.07 ± 0.10	0.06	n.s.	-0.62
PC aa C34:3	0.80 ± 0.17	0.42 ± 0.02	0.04	n.s.	-0.92
PC aa C34:4	0.46 ± 0.11	0.25 ± 0.02	0.08	n.s.	-0.89
PC aa C36:0	8.89 ± 0.63	7.25 ± 0.11	0.02	*	-0.29
PC aa C36:1	8.12 ± 1.40	5.39 ± 0.21	0.07	n.s.	-0.60
PC aa C36:2	6.95 ± 1.01	4.54 ± 0.19	0.04	n.s.	-0.62
PC aa C36:3	2.51 ± 0.42	1.43 ± 0.06	0.02	*	-0.81
PC aa C36:4	1.87 ± 0.38	1.27 ± 0.07	0.16	n.s.	-0.56
PC aa C36:5	0.58 ± 0.09	0.32 ± 0.01	0.02	*	-0.86
PC aa C36:6	0.31 ± 0.09	0.21 ± 0.01	0.27	n.s.	-0.58

Metabolite	Group		P value	FDR significance[a]	Log2 Fold-change[b]
	Con (n = 8)	Preg (n = 10)			
PC aa C38:0	0.67 ± 0.09	0.60 ± 0.01	0.40	n.s.	-0.17
PC aa C38:1	0.43 ± 0.11	0.33 ± 0.02	0.37	n.s.	-0.40
PC aa C38:3	1.41 ± 0.30	0.77 ± 0.04	0.05	n.s.	-0.86
PC aa C38:4	2.27 ± 0.43	1.58 ± 0.07	0.12	n.s.	-0.51
PC aa C38:5	1.49 ± 0.29	1.17 ± 0.06	0.34	n.s.	-0.34
PC aa C38:6	0.71 ± 0.14	0.66 ± 0.03	0.76	n.s.	-0.10
PC aa C40:1	6.18 ± 0.41	6.35 ± 0.10	0.74	n.s.	0.04
PC aa C40:2	0.16 ± 0.03	0.16 ± 0.01	0.84	n.s.	0.06
PC aa C40:3	0.14 ± 0.03	0.10 ± 0.01	0.20	n.s.	-0.47
PC aa C40:4	0.60 ± 0.17	0.38 ± 0.02	0.22	n.s.	-0.69
PC aa C40:6	6.38 ± 0.49	5.90 ± 0.10	0.39	n.s.	-0.12
PC aa C42:0	0.87 ± 0.06	0.84 ± 0.02	0.79	n.s.	-0.04
PC aa C42:1	0.15 ± 0.03	0.17 ± 0.01	0.54	n.s.	0.20
PC aa C42:2	1.89 ± 0.13	1.63 ± 0.03	0.09	n.s.	-0.22
PC aa C42:4	0.22 ± 0.03	0.17 ± 0.01	0.14	n.s.	-0.38
PC aa C42:5	0.19 ± 0.05	0.15 ± 0.01	0.53	n.s.	-0.30
PC aa C42:6	1.93 ± 0.18	1.71 ± 0.04	0.34	n.s.	-0.17
Acyl-alkyl-phosphatidylcholines					
PC ae C30:0	1.91 ± 0.18	1.56 ± 0.03	0.10	n.s.	-0.29
PC ae C30:1	0.38 ± 0.12	0.24 ± 0.03	0.36	n.s.	-0.69
PC ae C30:2	7.21 ± 0.52	6.29 ± 0.09	0.12	n.s.	-0.20
PC ae C32:1	0.47 ± 0.14	0.36 ± 0.02	0.42	n.s.	-0.40
PC ae C32:2	0.58 ± 0.12	0.40 ± 0.02	0.15	n.s.	-0.54
PC ae C34:0	0.66 ± 0.12	0.58 ± 0.02	0.55	n.s.	-0.18
PC ae C34:1	1.85 ± 0.31	1.34 ± 0.07	0.19	n.s.	-0.47
PC ae C34:2	1.32 ± 0.22	0.70 ± 0.04	0.02	*	-0.92
PC ae C34:3	0.67 ± 0.13	0.38 ± 0.02	0.05	n.s.	-0.81
PC ae C36:0	3.15 ± 0.21	2.74 ± 0.05	0.13	n.s.	-0.20
PC ae C36:1	2.18 ± 0.31	1.47 ± 0.05	0.05	n.s.	-0.58
PC ae C36:2	1.53 ± 0.13	1.12 ± 0.02	0.01	*	-0.45
PC ae C36:3	0.31 ± 0.05	0.21 ± 0.01	0.16	n.s.	-0.56
PC ae C36:4	0.73 ± 0.10	0.54 ± 0.02	0.07	n.s.	-0.43
PC ae C38:0	1.94 ± 0.19	1.72 ± 0.03	0.29	n.s.	-0.17
PC ae C38:1	0.32 ± 0.05	0.16 ± 0.01	0.01	*	-0.97
PC ae C38:2	0.31 ± 0.03	0.19 ± 0.01	0.03	*	-0.69
PC ae C38:3	0.30 ± 0.03	0.17 ± 0.01	0.01	*	-0.79
PC ae C38:4	0.79 ± 0.08	0.60 ± 0.02	0.04	n.s.	-0.40

Metabolite	Group		P value	FDR significance[a]	Log2 Fold-change[b]
	Con (n = 8)	Preg (n = 10)			
PC ae C38:5	0.48 ± 0.10	0.28 ± 0.01	0.06	n.s.	-0.76
PC ae C40:1	0.32 ± 0.02	0.20 ± 0.01	0.002	**	-0.64
PC ae C40:2	0.15 ± 0.02	0.14 ± 0.00	0.80	n.s.	-0.06
PC ae C40:3	0.09 ± 0.04	0.09 ± 0.01	0.97	n.s.	0.01
PC ae C40:4	1.17 ± 0.11	0.98 ± 0.02	0.14	n.s.	-0.25
PC ae C40:5	0.18 ± 0.04	0.12 ± 0.01	0.21	n.s.	-0.56
PC ae C40:6	0.27 ± 0.03	0.17 ± 0.01	0.03	*	-0.64
PC ae C42:0	14.45 ± 0.85	14.32 ± 0.22	0.90	n.s.	-0.01
PC ae C42:1	1.41 ± 0.13	1.30 ± 0.03	0.49	n.s.	-0.12
PC ae C42:2	0.27 ± 0.04	0.17 ± 0.01	0.03	*	-0.69
PC ae C42:3	0.13 ± 0.02	0.09 ± 0.01	0.15	n.s.	-0.51
PC ae C42:5	20.61 ± 1.16	21.71 ± 0.28	0.46	n.s.	0.07
PC ae C44:3	0.57 ± 0.04	0.64 ± 0.01	0.21	n.s.	0.15
PC ae C44:4	1.91 ± 0.11	1.76 ± 0.03	0.28	n.s.	-0.12
PC ae C44:5	1.05 ± 0.08	0.97 ± 0.02	0.43	n.s.	-0.12
PC ae C44:6	0.48 ± 0.02	0.35 ± 0.01	0.003	**	-0.47

Metabolites in bold were different between Con and Preg group by ANOVA followed by FDR correction.

[a]Statistical analyses were carried out by one-way ANOVA followed by FDR correction for multiple comparisons. Magnitude of effect is indicated by: ** $P \leq 0.01$; * $P \leq 0.05$; n.s. $P > 0.05$.

[b]Data are represented as fold-change of the metabolite concentration between Preg and Con groups.

Supplementary Table S9. Sphingomyelins (SM) concentration in uterine luminal fluid from Control (Con) and Pregnant (Preg) cows. Values are expressed as nmol/cm^2 of endometrial area; mean ± SEM.

Metabolite	Group		P value	FDR significance[a]	Log2 Fold-change[b]
	Con (n = 8)	Preg (n = 10)			
Sphingomyelins					
SM C16:0	23.14 ± 4.25	17.86 ± 0.92	0.31	n.s.	-0.38
SM C16:1	1.23 ± 0.32	0.80 ± 0.04	0.17	n.s.	-0.62
SM C18:0	4.30 ± 0.83	3.17 ± 0.17	0.24	n.s.	-0.43
SM C18:1	0.70 ± 0.12	0.52 ± 0.03	0.27	n.s.	-0.42
SM C24:0	4.03 ± 0.55	2.76 ± 0.10	0.05	n.s.	-0.56
SM C24:1	3.47 ± 0.55	2.99 ± 0.15	0.53	n.s.	-0.22
Hydroxysphingomyelins					
SM(OH) C16:1	1.94 ± 0.24	1.28 ± 0.06	0.04	n.s.	-0.60
SM(OH) C22:1	2.10 ± 0.42	1.23 ± 0.06	0.06	n.s.	-0.76
SM(OH) C22:2	0.52 ± 0.18	0.38 ± 0.01	0.35	n.s.	-0.43
SM(OH) C24:1	0.33 ± 0.05	0.29 ± 0.02	0.62	n.s.	-0.18

[a]Statistical analyses were carried out by one-way ANOVA followed by FDR correction for multiple comparisons. Magnitude of effect is indicated by: ** $P \leq 0.01$; * $P \leq 0.05$; n.s. $P > 0.05$.
[b]Data are represented as fold-change of the metabolite concentration between Preg and Con groups.

Supplementary Table S10. Hexoses concentration in uterine luminal fluid from Control (Con) and Pregnant (Preg) cows. Values are expressed as nmol/cm^2 of endometrial area; mean ± SEM.

Metabolite	Group		P value	FDR significance[a]	Log2 Fold-change[b]
	Con (n = 8)	Preg (n = 10)			
Hexoses[c]	337,367.78 ± 20441.23	331,581.47 ± 5435.96	0.83	n.s.	-0.02

[a]Statistical analyses were carried out by one-way ANOVA followed by FDR correction for multiple comparisons. Magnitude of effect is indicated by: ** $P \leq 0.01$; * $P \leq 0.05$; n.s. $P > 0.05$.
[b]Data are represented as fold-change of the metabolite concentration between Preg and Con groups.
[c]Sum of the concentrations of the following hexoses: Glucose; Aldohexose; L-Allopyranose; D-Allose; D-Allopyranose; D-Allose; D-Altropyranose; D-Glucopyranose; alpha-D-Glucopyranose; beta-D-Glucopyranose; D-Mannopyranose; alpha-D; Mannopyranose; L-Gulopyranose; D-Gulopyranose; D-Idopyranose; Alpha-L-Galactopyranose; alpha-D-Galactopyranose; beta-D-Galactopyranose; D-Talose; D-Talopyranose; Ketohexose; D-Psicopyranose; L-Fructofuranose; D-Fructose; D-Fructofuranose; L-Sorbopyranose; D-Sorbopyranose; D-Tagatose; D-Tagatopyranose.

Supplementary Table S11. Primers used for Real Time PCR analysis in bovine endometrial epithelial cells and blastocysts.

Gene Symbol	Gene	GenBank accession	Sequence of forward and reverse primers	Amplicon (bp)	Reference
VIM	vimentin	NM_173969.3	F: TGCGCTCAAAGGGACTAACGA R: GTGACGAGCCATCTCTTCCT	145	
KRT18	keratin 18	NM_001192095.1	F: GAGGATTTCAGTCTTGGCGAC R: TCAGTGCCTCAGAACTTTGGT	132	
ESR1	estrogen receptor 1	NM_001001443.1	F: GCGGAATACGGAAAGACCGA R: TTGGCAGCTCTCATGTCTCC	112	
PTGS2	prostaglandin-endoperoxide synthase 2	NM_174445.2	F: CATGGGTGTGAAAGGGAGGAAA R: GTGCTGGGCAAAGAATGCAAA	127	
IFNAR1	interferon alpha and beta receptor subunit 1	NM_174552.2	F: CTTCAGATCGCAGGTCCAAA R: ATCCAAGGCAGGTCCAATG	126	
CDX2	caudal type homeobox 2	NM_001206299.1	F: GCCACCATGTACGTGAGCTAC R: ACATGGTATCCGCCGTAGTC	140	(Sakurai *et al.*, 2013)
BAX	BCL2 associated X, apoptosis regulator	NM_173894.1	F: AGCAGATCATGAAGACAGGG R: TCAGACACTCGCTCAGCTTC	141	
IFNT2	interferon tau	NM_001015511.4	F: CATCTTCCCCATGGCCTTCG R: TCATCTCAAAGTGAGTTCAG	206	(Sakurai *et al.*, 2013)
RN18S1	18S ribosomal RNA	XR_003033789.1	F: AGAAACGGCTACCACATCCA R: CACCAGACTTGCCCTCCA	167	
GAPDH	glyceraldehyde-3-phosphate dehydrogenase	NM_001034034.2	F: AGTTCAACGGCACAGTCAAGG R: CCCACTTGATGTTGGCAGGAT	99	
H2AFZ	H2A histone family, member Z	NM_174809.2	F: CGGAATTCGAAATGGCTGGC R: TCTTTCGATGCATTTCCTGCC	238	

Supplementary Table S12. Number of morulae, young (YB), normal (NB), expanded (EB), hatching (H*B) and hatched (HB) blastocysts on day 7.5 post insemination in bovine endometrial epithelial cells (BEEC) samples selected for transcriptomic analysis. Samples from 3 replicates were chosen together with their NoEmbryos (within replicate) counterparts.

Sample ID	Group	Replicate	Morulae (n)	YB (n)	NB (n)	EB (n)	H*B (n)	HB (n)	Total (n)	Blastocyst rate (%)
24	NoEmbryos	2	-	-	-	-	-	-	-	-
83	NoEmbryos	5	-	-	-	-	-	-	-	-
84	NoEmbryos	5	-	-	-	-	-	-	-	-
103	NoEmbryos	6	-	-	-	-	-	-	-	-
104	NoEmbryos	6	-	-	-	-	-	-	-	-
28	Juxt	2	3	1	3	5	2	1	15	80.00
97	Juxt	5	5	1	4	3	1	1	15	66.67
87	Juxt	5	2	1	2	7	2	1	15	86.67
107	Juxt	6	5	1	1	4	3	1	15	66.67
108	Juxt	6	3	0	2	9	0	1	15	80.00
30	Non-juxt	2	3	1	3	6	0	2	15	80.00
89	Non-juxt	5	5	2	1	4	2	1	15	66.67
90	Non-juxt	5	4	0	3	6	2	0	15	73.33
110	Non-juxt	6	4	0	2	8	0	1	15	73.33
109	Non-juxt	6	2	0	4	5	1	3	15	86.67

Supplementary Dataset S13. Gene ID, mean normalized counts per group, Log2 Fold-Change, and FDR adjusted P-Values for differentially expressed genes (DEGs) in BEECs between NoEmbryos versus Juxt conditions. (Continued)

GeneID	Gene	Mean Counts Juxt	Mean Counts NoEmbryos	Log2 Fold-Change	P-Value (FDR adj)
ENSBTAG00000034349	IFI44	1561.642	1.187	10.361	0
ENSBTAG00000014529	GBP4	869.347	1.707	8.992	0
ENSBTAG00000012406	ZBP1	3082.706	9.578	8.330	0
ENSBTAG00000030913	MX1	26814.051	100.966	8.053	0
ENSBTAG00000037527	OAS1X	8857.437	50.446	7.456	0
ENSBTAG00000007881	IFIT1	16307.409	96.570	7.400	0
ENSBTAG00000045588		4894.733	32.124	7.251	0
ENSBTAG00000011343	XAF1	1605.704	13.673	6.876	0
ENSBTAG00000003152	IFI27	17435.707	169.423	6.685	0
ENSBTAG00000032265	RTP4	1286.875	14.708	6.451	0
ENSBTAG00000014628	OAS2	883.092	10.187	6.438	0
ENSBTAG00000039861	OAS1Y	8768.631	102.107	6.424	0
ENSBTAG00000030932	IFI44L	4580.486	60.527	6.242	0
ENSBTAG00000016661	USP18	3803.554	73.030	5.703	0
ENSBTAG00000012335	UBA7	7138.319	169.368	5.397	0
ENSBTAG00000046580	DHX58	2444.223	81.267	4.911	0
ENSBTAG00000021791	PARP9	2845.556	133.619	4.413	0
ENSBTAG00000003366	DDX58	7544.599	357.543	4.399	0
ENSBTAG00000009933	DTX3L	3600.750	170.731	4.399	0
ENSBTAG00000016546	PARP12	3666.142	389.494	3.235	0
ENSBTAG00000017367	IFIT5	7797.873	1013.969	2.943	0
ENSBTAG00000018994	TNFSF10	1569.377	26.832	5.870	6.91E-288
ENSBTAG00000012894	SAMD9	2242.560	60.392	5.215	3.55E-287
ENSBTAG00000016656	PARP14	4250.004	395.511	3.426	1.1E-282
ENSBTAG00000008142	IFIH1	2965.725	109.727	4.756	7.8E-267
ENSBTAG00000008703	EIF2AK2	9469.259	1128.725	3.069	5.32E-262
ENSBTAG00000019054	EPSTI1	1879.235	162.935	3.528	6.49E-249
ENSBTAG00000007867	STAT1	10249.789	1854.287	2.467	1.9E-242
ENSBTAG00000005816	IRF9	2863.764	389.725	2.877	1.33E-216
ENSBTAG00000022489		12723.211	884.552	3.846	4.9E-214
ENSBTAG00000038710		2700.708	439.489	2.619	3.39E-204
ENSBTAG00000007554	IFI6	16397.473	56.043	8.193	2.83E-202
ENSBTAG00000013900	TRIM21	1278.781	192.324	2.733	2.82E-200
ENSBTAG00000009677	PARP10	3705.873	623.675	2.571	2.77E-196
ENSBTAG00000019979	CMPK2	1736.875	55.189	4.976	5.05E-189
ENSBTAG00000020166	ZNFX1	8076.849	865.448	3.222	4.74E-187
ENSBTAG00000017670		1074.593	94.936	3.501	2.55E-181
ENSBTAG00000019017	IFITM2	2765.574	201.706	3.777	7.21E-179
ENSBTAG00000019015	IFITM3	13750.853	2130.631	2.690	1.38E-171
ENSBTAG00000011511		499.736	12.355	5.338	1.17E-169
ENSBTAG00000031750	PLAC8	2014.683	3.372	9.223	2.48E-167
ENSBTAG00000015779	PML	4426.102	730.555	2.599	2.56E-156
ENSBTAG00000003719	TDRD7	1805.483	418.307	2.110	6.38E-153
ENSBTAG00000019018		2633.348	255.097	3.368	4.18E-145
ENSBTAG00000011936	ATP8B4	1348.566	94.728	3.831	5.18E-141
ENSBTAG00000007519	ADAR	4447.305	856.937	2.376	2.18E-139
ENSBTAG00000037465	TRIM34	916.245	148.748	2.623	1.29E-131
ENSBTAG00000015752		1235.108	248.890	2.311	7.8E-129
ENSBTAG00000009206	FOXS1	759.033	28.538	4.733	8.16E-125
ENSBTAG00000014707	ISG15	5149.006	12.447	8.692	4.41E-121
ENSBTAG00000001143		715.939	90.135	2.990	6.78E-118
ENSBTAG00000020538	HERC5	1774.309	238.285	2.896	7.64E-116
ENSBTAG00000012330	B2M	15246.081	3321.168	2.199	4.41E-108
ENSBTAG00000002416		415.702	9.182	5.501	1.12E-106
ENSBTAG00000031214		444.078	18.870	4.557	5.21E-105
ENSBTAG00000008909	PNPT1	3381.717	621.358	2.444	3.82E-104
ENSBTAG00000009664		875.319	161.302	2.440	1.18E-103
ENSBTAG00000014297	MOV10	2919.171	1290.466	1.178	7.23E-99
ENSBTAG00000001368	LGALS3BP	11621.324	3499.035	1.732	1.05E-92
ENSBTAG00000027317	RNF114	3268.460	1203.789	1.441	2.33E-89
ENSBTAG00000034918	IFIT2	2094.095	15.689	7.060	2.97E-88
ENSBTAG00000017040	LY6E	9861.644	1874.443	2.395	1.68E-84
ENSBTAG00000016061	RSAD2	6549.763	11.241	9.187	1.3E-79
ENSBTAG00000037702	SP140L	414.925	74.964	2.469	1.48E-79
ENSBTAG00000017091	CMTR1	2608.186	1105.439	1.238	1.49E-78
ENSBTAG00000011304	XRN2	3279.526	1457.992	1.170	4.23E-77

GeneID	Gene	Mean Counts Juxt	Mean Counts NoEmbryos	Log2 Fold-Change	P-Value (FDR adj)
ENSBTAG00000038536		1495.143	427.150	1.807	9.99E-77
ENSBTAG00000008021		317.376	0.357	9.798	5.97E-73
ENSBTAG00000009177	PLEKHA4	2484.335	615.534	2.013	3.47E-72
ENSBTAG00000020536	HERC6	11396.044	4476.249	1.348	9.14E-66
ENSBTAG00000018417	PSMF1	1987.983	592.847	1.746	9.29E-64
ENSBTAG00000037989		107.239	2.779	5.270	5.3E-63
ENSBTAG00000021452	TRANK1	11883.620	3814.284	1.639	1.41E-62
ENSBTAG00000003495	KDM7A	459.353	140.877	1.705	7.85E-60
ENSBTAG00000022227	PLSCR2	2929.016	1088.691	1.428	9.96E-60
ENSBTAG00000000312	GRINA	3012.301	1056.786	1.511	2.99E-58
ENSBTAG00000006801	TMEM106A	1580.922	498.763	1.664	7.88E-57
ENSBTAG00000015636	C7H19orf66	657.276	179.648	1.871	3.19E-55
ENSBTAG00000016217	RBM43	427.631	92.222	2.213	3.96E-54
ENSBTAG00000018523	TRIM38	769.223	284.272	1.436	3.79E-53
ENSBTAG00000039275	ERAP2	1362.611	489.910	1.476	1.43E-51
ENSBTAG00000032369	NMI	1198.171	436.399	1.457	8.71E-49
ENSBTAG00000005146		605.134	234.723	1.366	2.71E-48
ENSBTAG00000010166	MIC1	1938.144	868.490	1.158	3.89E-47
ENSBTAG00000020884	CASP4	2635.428	984.480	1.421	1.39E-46
ENSBTAG00000000892	CGAS	228.260	39.221	2.541	2.04E-46
ENSBTAG00000002435	PTPRE	2254.725	998.797	1.175	8.12E-44
ENSBTAG00000008707	SULT6B1	182.644	28.268	2.692	1.84E-43
ENSBTAG00000047367	CMTR2	700.412	187.306	1.903	1.15E-42
ENSBTAG00000005251		120.273	8.719	3.786	2.72E-42
ENSBTAG00000011876	MORC3	1004.592	463.800	1.115	7.03E-42
ENSBTAG00000016092	SPATS2L	2348.048	900.135	1.383	1.76E-41
ENSBTAG00000007431	CEMIP	6129.304	20631.006	-1.751	9.94E-41
ENSBTAG00000024272		108.653	2.457	5.466	1.16E-40
ENSBTAG00000021395	PSME1	1988.616	841.761	1.240	1.91E-40
ENSBTAG00000012989	UBE2L6	210.199	55.686	1.916	2.72E-40
ENSBTAG00000004679	WARS	7787.986	3326.253	1.227	3.08E-39
ENSBTAG00000003039	PSMB8	789.804	290.722	1.442	1E-38
ENSBTAG00000040244	APOL3	106.259	14.940	2.830	7.02E-37
ENSBTAG00000004380	STAT2	1561.471	757.656	1.043	1.2E-36
ENSBTAG00000018125	KIF5C	90.260	0.690	7.030	1.97E-36
ENSBTAG00000009768	IFIT3	1159.098	42.949	4.754	2.76E-36
ENSBTAG00000009183	SHISA5	1386.183	602.048	1.203	3.82E-36
ENSBTAG00000038625		62.843	2.722	4.529	5.32E-35
ENSBTAG00000019386	BOLA-NC1	312.768	134.287	1.220	4.53E-33
ENSBTAG00000007389	IFI35	445.308	135.695	1.714	1.97E-32
ENSBTAG00000002069	BOLA	2438.096	903.588	1.432	3.28E-32
ENSBTAG00000003639	ELMO2	2352.366	1328.510	0.824	5.15E-32
ENSBTAG00000021687	JADE2	338.870	115.694	1.550	2.56E-31
ENSBTAG00000038619		332.049	88.756	1.903	4.06E-30
ENSBTAG00000017002	RBCK1	1694.143	798.446	1.085	3.56E-29
ENSBTAG00000000990	PSMA2	1677.918	861.939	0.961	4.66E-29
ENSBTAG00000002691	ELMOD1	139.663	42.235	1.725	2.48E-28
ENSBTAG00000009091	RNASEL	199.494	59.651	1.742	3.9E-28
ENSBTAG00000000504	GTF2B	883.719	391.571	1.174	1.08E-27
ENSBTAG00000007077	ABHD1	236.838	76.869	1.623	7.04E-27
ENSBTAG00000019437		254.338	80.370	1.662	1.64E-26
ENSBTAG00000000706	ADAMTS1	1532.691	3634.067	-1.246	3.94E-26
ENSBTAG00000038233		33.628	0.171	7.619	3.51E-25
ENSBTAG00000003636	LIPA	1093.994	583.070	0.908	1.59E-24
ENSBTAG00000005814	PSME2	1050.465	447.587	1.231	1.88E-24
ENSBTAG00000001702	TMEM107	19.592	87.690	-2.162	5.44E-24
ENSBTAG00000003743		124.266	36.102	1.783	1E-23
ENSBTAG00000000995	FAM46A	165.225	67.021	1.302	1.85E-23
ENSBTAG00000015718	CASP8	955.840	472.571	1.016	1.95E-23
ENSBTAG00000015778	SASS6	460.259	199.622	1.205	1.15E-22
ENSBTAG00000016830	DAXX	2084.512	1102.913	0.918	1.32E-22
ENSBTAG00000013557	ERAP1	832.224	427.429	0.961	1.81E-22
ENSBTAG00000002717	INA	246.398	78.394	1.652	2.06E-22
ENSBTAG00000019989	PXK	689.215	367.242	0.908	2.28E-22
ENSBTAG00000008744	PDK2	317.048	542.062	-0.774	6.32E-22
ENSBTAG00000007935	CALCOCO2	1537.218	907.108	0.761	3.28E-21
ENSBTAG00000004272	ISG12(B)	122.889	45.903	1.421	8.06E-21
ENSBTAG00000019314	USP25	1299.781	715.663	0.861	8.41E-21
ENSBTAG00000037533	C4A	4241.017	1679.501	1.336	8.83E-21
ENSBTAG00000015509	NAMPT	608.341	263.868	1.205	1.25E-20

GeneID	Gene	Mean Counts Juxt	Mean Counts NoEmbryos	Log2 Fold-Change	P-Value (FDR adj)
ENSBTAG00000012107	SLC25A28	1024.028	621.553	0.720	1.25E-20
ENSBTAG00000006697	RICTOR	1447.697	847.970	0.772	1.71E-20
ENSBTAG00000006633	IRF3	1811.001	1048.694	0.788	1.82E-20
ENSBTAG00000005815	RNF31	1103.597	695.120	0.667	4.36E-20
ENSBTAG00000009948	TRIM25	1560.343	573.782	1.443	5.46E-20
ENSBTAG00000008953	TAP1	679.302	252.853	1.426	5.46E-20
ENSBTAG00000003381	PAPD7	1129.642	697.396	0.696	2.87E-19
ENSBTAG00000000806	ATAD1	1626.014	883.208	0.881	6.46E-19
ENSBTAG00000005454	FUT10	377.083	209.223	0.850	9.37E-19
ENSBTAG00000000204	TMEM268	438.629	262.802	0.739	1.17E-18
ENSBTAG00000008471	MX2	1678.997	0.677	11.275	1.73E-18
ENSBTAG00000025762	CNP	1751.194	1100.743	0.670	1.88E-18
ENSBTAG00000019614	FAM76A	364.278	217.992	0.741	2.75E-18
ENSBTAG00000009132	TMPRSS2	93.999	0.157	9.230	5.89E-18
ENSBTAG00000012451	BOLA-DMB	112.643	33.860	1.734	6.1E-18
ENSBTAG00000038938		32.573	1.609	4.339	8.17E-18
ENSBTAG00000024851	TRIM14	129.977	50.230	1.372	1.73E-17
ENSBTAG00000022590		1710.328	931.627	0.876	1.89E-17
ENSBTAG00000000639	APRT	1198.919	659.172	0.863	2.66E-17
ENSBTAG00000002271	CDADC1	541.191	255.334	1.084	5.61E-17
ENSBTAG00000016529	SLC25A30	905.424	530.864	0.770	6.04E-17
ENSBTAG00000046512	XIRP1	153.319	462.075	-1.592	8.35E-17
ENSBTAG00000006974	PLEKHA7	475.934	217.110	1.132	9.6E-17
ENSBTAG00000011467	BATF2	67.892	16.398	2.050	8.4E-16
ENSBTAG00000020116	JSP.1	186.444	59.309	1.652	9.96E-16
ENSBTAG00000008353	CDKN1A	4290.803	6758.760	-0.656	2.26E-15
ENSBTAG00000034519		321.198	149.504	1.103	4.78E-15
ENSBTAG00000007755	APOBEC3Z3	257.079	134.125	0.939	4.78E-15
ENSBTAG00000044019	KAT2A	891.805	585.304	0.608	4.78E-15
ENSBTAG00000021617	ZC3HAV1	2368.502	1481.788	0.677	6.27E-15
ENSBTAG00000008140	FAP	1083.360	1651.554	-0.608	6.92E-15
ENSBTAG00000005063	THEM6	57.252	13.153	2.122	8E-15
ENSBTAG00000003807	CNOT9	1063.386	734.357	0.534	1.36E-14
ENSBTAG00000002298	CKAP2L	238.629	104.292	1.194	2.79E-14
ENSBTAG00000015978	ANXA1	11737.549	7283.389	0.688	3.5E-14
ENSBTAG00000012252	MOCOS	333.278	173.965	0.938	5.28E-14
ENSBTAG00000007450	C2	4963.994	3438.165	0.530	7.84E-14
ENSBTAG00000031231	IRF1	381.583	133.792	1.512	9.02E-14
ENSBTAG00000006615	CASP7	139.553	69.117	1.014	1.22E-13
ENSBTAG00000020225	TBXAS1	33.344	3.428	3.282	2.76E-13
ENSBTAG00000004378	IL23A	360.071	187.775	0.939	6.95E-13
ENSBTAG00000008406	TREX1	256.216	86.732	1.563	1.01E-12
ENSBTAG00000000240	AKAP7	191.315	89.259	1.100	1.09E-12
ENSBTAG00000007593	AIDA	870.048	539.720	0.689	2.46E-12
ENSBTAG00000014099	YTHDC2	674.605	447.677	0.592	2.51E-12
ENSBTAG00000008682	TLR3	382.131	235.119	0.701	2.91E-12
ENSBTAG00000006846	LGALS9	16.982	0.181	6.554	3.55E-12
ENSBTAG00000004971	GRAMD1C	174.208	94.718	0.879	5.03E-12
ENSBTAG00000009681	PPP2R3C	366.950	203.921	0.848	5.96E-12
ENSBTAG00000005182	BoLA	742.735	381.015	0.963	6.26E-12
ENSBTAG00000013254	XPO1	2332.785	1365.661	0.772	6.62E-12
ENSBTAG00000018569	CUL4B	1446.186	876.910	0.722	8.01E-12
ENSBTAG00000043550	CYTB	43070.691	81020.654	-0.912	8.01E-12
ENSBTAG00000018065	YARS	1255.249	919.327	0.449	8.48E-12
ENSBTAG00000030921	FAM3B	14.805	0.000	#DIV/0!	8.71E-12
ENSBTAG00000001296	TMEM50A	2226.558	1497.692	0.572	1.4E-11
ENSBTAG00000000957	CDKN2AIP	469.864	266.062	0.820	1.57E-11
ENSBTAG00000004064	BPNT1	510.028	293.513	0.797	1.74E-11
ENSBTAG00000003038		1422.653	1009.831	0.494	1.81E-11
ENSBTAG00000002357	TICAM2	515.905	367.590	0.489	1.85E-11
ENSBTAG00000043577	ND4	60652.455	113333.649	-0.902	2.72E-11
ENSBTAG00000014728	TAPBPL	833.194	517.992	0.686	4.11E-11
ENSBTAG00000013405	FAM92A	378.702	589.667	-0.639	4.66E-11
ENSBTAG00000043559	ND4L	5703.555	9700.090	-0.766	4.7E-11
ENSBTAG00000021780	SCO1	868.594	612.312	0.504	4.87E-11
ENSBTAG00000006792	EHD4	450.694	209.011	1.109	7.12E-11
ENSBTAG00000010225	POLR2D	746.307	494.575	0.594	8.02E-11
ENSBTAG00000013191	AGRN	10743.235	5785.091	0.893	8.18E-11
ENSBTAG00000005066	HSPBAP1	353.621	178.886	0.983	1.92E-10
ENSBTAG00000003066	NSA2	691.629	998.431	-0.530	2.01E-10

GeneID	Gene	Mean Counts Juxt	Mean Counts NoEmbryos	Log2 Fold-Change	P-Value (FDR adj)
ENSBTAG00000006707	ACSL5	3775.635	3105.413	0.282	2.43E-10
ENSBTAG00000014705	HES4	19.245	0.334	5.849	2.48E-10
ENSBTAG00000018040	PSMB10	304.366	148.344	1.037	2.48E-10
ENSBTAG00000010170	MBTPS1	1570.326	2313.906	-0.559	2.95E-10
ENSBTAG00000020989	SUSD4	760.802	1080.769	-0.506	4.05E-10
ENSBTAG00000006751	PAPD4	784.695	477.899	0.715	4.41E-10
ENSBTAG00000003418	MSN	16395.903	21765.335	-0.409	4.87E-10
ENSBTAG00000019716	CXCL8	56.113	140.683	-1.326	4.91E-10
ENSBTAG00000009812	CXCL5	1096.475	2371.309	-1.113	4.98E-10
ENSBTAG00000011647	SLC25A15	209.097	326.537	-0.643	5.35E-10
ENSBTAG00000015046	MST1R	284.373	164.248	0.792	7.19E-10
ENSBTAG00000020030	FITM2	416.752	685.215	-0.717	8.25E-10
ENSBTAG00000016828	TAPBP	4892.096	3285.470	0.574	9.17E-10
ENSBTAG00000008954	PSMB9	143.893	45.959	1.647	9.94E-10
ENSBTAG00000004117	AZI2	1095.693	791.820	0.469	1.08E-09
ENSBTAG00000005413	NLRC5	88.595	30.628	1.532	1.6E-09
ENSBTAG00000007117	CTC1	623.650	414.151	0.591	1.68E-09
ENSBTAG00000003330	ATL3	2441.326	1570.974	0.636	1.72E-09
ENSBTAG00000014633	ABCD4	441.914	307.484	0.523	2.23E-09
ENSBTAG00000006587	ZNF367	178.631	105.950	0.754	3.01E-09
ENSBTAG00000020277	PPP2R1B	2729.518	3347.355	-0.294	3.21E-09
ENSBTAG00000006638	BCL2L12	979.512	647.752	0.597	3.32E-09
ENSBTAG00000018016	NUPR1	5549.053	3171.971	0.807	3.36E-09
ENSBTAG00000017271	MASTL	123.917	49.934	1.311	3.63E-09
ENSBTAG00000024492		32.047	9.030	1.827	4.09E-09
ENSBTAG00000010721	MCM3	708.627	462.396	0.616	5.57E-09
ENSBTAG00000011465	MYBPH	64.230	177.715	-1.468	5.71E-09
ENSBTAG00000000095	CD274	38.198	12.263	1.639	6.1E-09
ENSBTAG00000016254	HDAC5	1885.407	2821.843	-0.582	6.22E-09
ENSBTAG00000013855	ORMDL3	927.602	1710.794	-0.883	6.28E-09
ENSBTAG00000012519	XDH	2099.885	3530.303	-0.749	6.51E-09
ENSBTAG00000000555	ACO1	841.961	1092.564	-0.376	6.55E-09
ENSBTAG00000000988	BRCA2	599.601	412.683	0.539	7.2E-09
ENSBTAG00000001244	PLAT	2065.532	1594.893	0.373	8.54E-09
ENSBTAG00000013275	MAD2L2	366.575	207.848	0.819	8.6E-09
ENSBTAG00000004999	KIAA1551	8917.116	4660.505	0.936	9.76E-09
ENSBTAG00000027655	TIFA	84.290	37.727	1.160	9.8E-09
ENSBTAG00000002915	GPR63	96.951	38.430	1.335	1.04E-08
ENSBTAG00000023607	HACD2	783.100	516.749	0.600	1.19E-08
ENSBTAG00000011563		19.847	2.514	2.981	1.44E-08
ENSBTAG00000010517	EVPL	3184.623	4798.109	-0.591	1.51E-08
ENSBTAG00000016709	NT5C3A	505.499	307.470	0.717	1.59E-08
ENSBTAG00000002331	DLGAP5	174.747	92.789	0.913	1.61E-08
ENSBTAG00000000146	FARP1	831.676	1119.095	-0.428	0.000000017
ENSBTAG00000002605		237.163	145.333	0.707	2.02E-08
ENSBTAG00000019857	OTUD4	1639.126	1204.220	0.445	2.15E-08
ENSBTAG00000012314	LDLR	1609.169	1094.200	0.556	0.000000022
ENSBTAG00000000202	SLC25A19	309.260	172.046	0.846	2.22E-08
ENSBTAG00000021442	CRTAP	1407.045	1956.337	-0.475	2.49E-08
ENSBTAG00000044083	LIMK1	540.274	348.389	0.633	2.88E-08
ENSBTAG00000012673	CDK18	290.593	185.758	0.646	3.02E-08
ENSBTAG00000003751	MACC1	98.016	211.491	-1.109	3.08E-08
ENSBTAG00000016387	GDAP2	405.856	277.127	0.550	3.65E-08
ENSBTAG00000021177	ADAMTS14	185.693	347.383	-0.904	4.36E-08
ENSBTAG00000006551	ESCO2	120.894	56.860	1.088	4.79E-08
ENSBTAG00000007399	LAMP2	5727.543	4220.090	0.441	4.83E-08
ENSBTAG00000046450		226.685	347.956	-0.618	5.44E-08
ENSBTAG00000002747	ABCA5	208.856	329.755	-0.659	5.67E-08
ENSBTAG00000014465	SERPINE1	855.590	2053.723	-1.263	0.000000065
ENSBTAG00000015230	PLA2G12A	483.087	351.190	0.460	7.54E-08
ENSBTAG00000001637	FUNDC1	418.142	275.303	0.603	7.63E-08
ENSBTAG00000006851		148.422	72.784	1.028	7.82E-08
ENSBTAG00000012038	TRIM56	273.897	129.805	1.077	8.33E-08
ENSBTAG00000026025		86.457	42.230	1.034	8.88E-08
ENSBTAG00000012383	CHMP5	1115.295	743.565	0.585	9.36E-08
ENSBTAG00000009888	DRAM2	494.884	340.716	0.539	9.54E-08
ENSBTAG00000000087	HSD17B12	851.626	579.077	0.556	0.000000105
ENSBTAG00000012216	MLKL	193.767	111.388	0.799	0.000000106
ENSBTAG00000008733	MAGED1	3761.515	5017.856	-0.416	0.00000011
ENSBTAG00000043563	ND5	67997.442	108770.944	-0.678	0.000000122

GeneID	Gene	Mean Counts Juxt	Mean Counts NoEmbryos	Log2 Fold-Change	P-Value (FDR adj)
ENSBTAG00000019312	TFCP2	1188.793	876.458	0.440	0.000000123
ENSBTAG00000046699		29.925	6.285	2.251	0.000000133
ENSBTAG00000011421	CD37	122.400	196.125	-0.680	0.000000133
ENSBTAG00000011839	HMGCS1	931.626	624.454	0.577	0.000000134
ENSBTAG00000043546	ND6	22717.010	36208.075	-0.673	0.000000139
ENSBTAG00000012074	MYB	573.133	399.523	0.521	0.000000143
ENSBTAG00000037634		14.500	1.380	3.393	0.000000145
ENSBTAG00000019262	TOP2A	691.592	415.967	0.733	0.000000148
ENSBTAG00000008772	SMC2	543.067	345.743	0.651	0.000000157
ENSBTAG00000021474	GSDMD	323.781	196.595	0.720	0.000000161
ENSBTAG00000007937	PRIM2	323.625	211.513	0.614	0.000000173
ENSBTAG00000020054	TNFRSF21	5664.127	7527.520	-0.410	0.000000184
ENSBTAG00000009441	RBBP6	3128.478	2348.920	0.413	0.000000193
ENSBTAG00000011412	LAMB1	18128.820	23593.507	-0.380	0.000000194
ENSBTAG00000006864		211.503	84.919	1.317	0.000000206
ENSBTAG00000043568	ND3	12891.720	24294.892	-0.914	0.000000238
ENSBTAG00000010313	DDX52	589.948	435.242	0.439	0.000000251
ENSBTAG00000013929	RRAD	11.085	40.357	-1.864	0.000000266
ENSBTAG00000011986	PLSCR4	976.318	648.753	0.590	0.000000291
ENSBTAG00000024081	ECM2	2578.027	1641.780	0.651	0.000000301
ENSBTAG00000007494	SMARCA2	2097.148	2736.834	-0.384	0.000000307
ENSBTAG00000021102	GALM	1456.631	1045.512	0.478	0.000000335
ENSBTAG00000004943	CCNA2	269.535	142.402	0.920	0.000000348
ENSBTAG00000010532	KCTD11	452.112	739.968	-0.711	0.00000035
ENSBTAG00000001081	PALLD	1375.230	1929.076	-0.488	0.000000352
ENSBTAG00000007129	MRVI1	224.952	371.763	-0.725	0.000000352
ENSBTAG00000024539	SPSB1	1214.564	1838.604	-0.598	0.000000385
ENSBTAG00000020179	AAAS	185.724	298.025	-0.682	0.000000398
ENSBTAG00000011836	OMD	509.555	170.435	1.580	0.00000041
ENSBTAG00000009983	KIF23	387.787	209.538	0.888	0.00000041
ENSBTAG00000014744	TXNDC15	765.431	572.911	0.418	0.00000041
ENSBTAG00000016936	MISP3	94.766	167.186	-0.819	0.000000413
ENSBTAG00000004203	VPS33A	395.202	531.669	-0.428	0.000000427
ENSBTAG00000001992	CYP51A1	817.507	541.286	0.595	0.000000439
ENSBTAG00000001741	DLGAP4	1625.180	2236.503	-0.461	0.000000445
ENSBTAG00000009218	ANLN	1115.069	697.429	0.677	0.000000455
ENSBTAG00000008636	PDE4B	817.057	442.670	0.884	0.000000525
ENSBTAG00000019554	FBP2	143.232	220.939	-0.625	0.000000605
ENSBTAG00000004349	DAZAP2	4732.523	3626.226	0.384	0.000000658
ENSBTAG00000012219	CSPG4	455.364	810.817	-0.832	0.000000723
ENSBTAG00000015541	DLC1	2959.300	1985.847	0.576	0.000000745
ENSBTAG00000002586	TCF12	2067.782	1479.803	0.483	0.000000841
ENSBTAG00000011911		174.190	104.629	0.735	0.000000857
ENSBTAG00000006984	CD55	10979.372	7689.856	0.514	0.00000102
ENSBTAG00000016265	DNAJA1	1740.757	1255.802	0.471	0.00000114
ENSBTAG00000013160	GFRA4	587.407	875.354	-0.576	0.00000115
ENSBTAG00000007808	ANTXR1	2820.382	4172.943	-0.565	0.00000129
ENSBTAG00000008817	LAMA4	1112.201	1820.617	-0.711	0.00000136
ENSBTAG00000001182		9657.305	6856.998	0.494	0.00000138
ENSBTAG00000003963	FER1L5	137.572	222.776	-0.695	0.00000138
ENSBTAG00000013631	GLUL	5685.490	7356.075	-0.372	0.0000015
ENSBTAG00000001497	MRAS	1089.571	1627.059	-0.579	0.00000157
ENSBTAG00000021381	DAAM2	986.912	1352.451	-0.455	0.00000159
ENSBTAG00000002249	NAALADL1	88.833	145.405	-0.711	0.0000016
ENSBTAG00000018157	IFT172	462.924	625.690	-0.435	0.00000175
ENSBTAG00000019636	SCARA5	16.556	47.632	-1.525	0.00000176
ENSBTAG00000009522	EIF4E	862.772	636.346	0.439	0.00000195
ENSBTAG00000005915	SFMBT2	2944.820	2266.189	0.378	0.00000197
ENSBTAG00000015527	MYO1D	15525.541	20177.700	-0.378	0.000002
ENSBTAG00000015713	TLK2	777.544	596.679	0.382	0.00000201
ENSBTAG00000018240	CYP2S1	152.881	77.768	0.975	0.00000213
ENSBTAG00000012432	FDFT1	831.421	624.365	0.413	0.0000022
ENSBTAG00000015163	TM4SF1	2944.783	1968.032	0.581	0.00000229
ENSBTAG00000044066	CATSPERE	40.101	13.237	1.599	0.00000265
ENSBTAG00000018142	DTL	182.000	96.557	0.914	0.00000266
ENSBTAG00000007237	BUB1B	276.217	162.329	0.767	0.0000029
ENSBTAG00000001343	DEPDC1	116.417	56.237	1.050	0.00000293
ENSBTAG00000003089	RHPN2	816.855	584.515	0.483	0.00000301
ENSBTAG00000040584	DSC2	909.739	1228.783	-0.434	0.00000326
ENSBTAG00000012925	NCAPH	162.370	96.883	0.745	0.00000346

GeneID	Gene	Mean Counts Juxt	Mean Counts NoEmbryos	Log2 Fold-Change	P-Value (FDR adj)
ENSBTAG00000043584	ATP6	67089.976	98678.254	-0.557	0.00000353
ENSBTAG00000007181	KIFC3	592.534	405.757	0.546	0.00000355
ENSBTAG00000017446	E2F8	125.643	55.118	1.189	0.00000363
ENSBTAG00000033441	SHCBP1	109.141	57.479	0.925	0.00000377
ENSBTAG00000012397	DCK	277.562	177.199	0.647	0.00000378
ENSBTAG00000021162	CKAP2	1010.308	638.821	0.661	0.00000402
ENSBTAG00000024493	DHRS3	1293.329	2677.235	-1.050	0.00000409
ENSBTAG00000000828	CAPN6	131.521	220.316	-0.744	0.00000432
ENSBTAG00000027320	KCNB1	149.555	212.911	-0.510	0.00000437
ENSBTAG00000043558	ND1	47222.788	77672.689	-0.718	0.00000447
ENSBTAG00000016771	PLK2	947.086	1249.862	-0.400	0.00000477
ENSBTAG00000010002	IRF2	524.014	382.658	0.454	0.00000505
ENSBTAG00000003068	MSMO1	2284.990	1562.582	0.548	0.00000517
ENSBTAG00000013100	SPAG5	194.788	115.128	0.759	0.00000594
ENSBTAG00000013573	BIRC5	197.931	123.075	0.685	0.00000612
ENSBTAG00000019164	RHOBTB1	434.186	654.320	-0.592	0.00000616
ENSBTAG00000020647	RASL11B	154.679	304.301	-0.976	0.00000618
ENSBTAG00000003165	ADAMTS9	1799.940	2788.430	-0.632	0.00000679
ENSBTAG00000012443	DIAPH3	380.572	248.119	0.617	0.0000069
ENSBTAG00000039556	WIPI1	540.979	718.165	-0.409	0.00000711
ENSBTAG00000021957	LTBP2	36044.878	89857.535	-1.318	0.00000736
ENSBTAG00000013245	ITPR3	7702.084	6201.117	0.313	0.00000753
ENSBTAG00000015772	STOML1	150.858	98.787	0.611	0.0000076
ENSBTAG00000005862	SMC4	942.926	645.031	0.548	0.00000769
ENSBTAG00000035744	TRIM26	562.271	404.019	0.477	0.00000777
ENSBTAG00000014278	TBX2	96.005	167.141	-0.800	0.00000809
ENSBTAG00000008758	KIF20A	416.727	270.380	0.624	0.00000815
ENSBTAG00000004459	TMEM45A	138.066	199.198	-0.529	0.00000839
ENSBTAG00000024648		198.269	99.274	0.998	0.00000864
ENSBTAG00000003800	LRRC27	275.374	371.027	-0.430	0.00000882
ENSBTAG00000046324		3957.350	2927.964	0.435	0.00000893
ENSBTAG00000016501	ARHGAP1	4946.673	6205.103	-0.327	0.00000893
ENSBTAG00000003711	EPAS1	3782.739	5765.040	-0.608	0.00000912
ENSBTAG00000032515	PLA2R1	269.197	426.871	-0.665	0.00000946
ENSBTAG00000030435	PNRC2	4277.521	3073.324	0.477	0.00000956
ENSBTAG00000037456	AHDC1	1107.452	1505.061	-0.443	0.0000101
ENSBTAG00000017763	NFIL3	253.595	380.550	-0.586	0.0000101
ENSBTAG00000016131	NCAPG2	272.416	190.469	0.516	0.0000102
ENSBTAG00000010077	FANCD2	161.779	98.264	0.719	0.0000105
ENSBTAG00000015563	PDE12	175.724	114.615	0.617	0.0000105
ENSBTAG00000003733	TM4SF5	94.048	160.505	-0.771	0.0000105
ENSBTAG00000009617	SLC2A1	546.636	381.755	0.518	0.0000108
ENSBTAG00000012749	CUL7	3190.927	4014.686	-0.331	0.0000109
ENSBTAG00000010665	CBLN3	411.813	277.678	0.569	0.0000112
ENSBTAG00000002444		1462.307	914.057	0.678	0.0000116
ENSBTAG00000026437	ULBP3	54.019	28.999	0.897	0.0000117
ENSBTAG00000016043	GNB3	185.803	302.412	-0.703	0.0000119
ENSBTAG00000006836	FBXO33	647.932	439.478	0.560	0.000012
ENSBTAG00000027081	ATP10A	1021.037	788.313	0.373	0.0000122
ENSBTAG00000040193	COLQ	76.171	143.568	-0.914	0.0000137
ENSBTAG00000044079	SMIM4	102.493	179.196	-0.806	0.0000139
ENSBTAG00000024381	MAN1A1	2144.046	3274.527	-0.611	0.000014
ENSBTAG00000010671	GLI3	5291.947	8050.286	-0.605	0.0000154
ENSBTAG00000020070	ABCC3	329.255	448.415	-0.446	0.0000157
ENSBTAG00000008097	WNT2	1075.809	806.316	0.416	0.0000165
ENSBTAG00000014291	WNT2B	1646.634	1308.575	0.332	0.0000165
ENSBTAG00000003120	ZNF385B	73.894	144.086	-0.963	0.0000166
ENSBTAG00000005498	SQLE	957.491	666.752	0.522	0.0000174
ENSBTAG00000020975	SYNGAP1	394.426	547.952	-0.474	0.0000174
ENSBTAG00000005092	ROR2	111.529	178.995	-0.682	0.0000179
ENSBTAG00000002099	SLC14A2	35.568	14.125	1.332	0.000018
ENSBTAG00000004240	TMPO	1130.896	810.963	0.480	0.0000191
ENSBTAG00000047495	CD81	1880.296	1406.141	0.419	0.0000198
ENSBTAG00000018775	TPX2	503.391	315.490	0.674	0.0000199
ENSBTAG00000022004	FLNB	17651.854	25577.592	-0.535	0.0000207
ENSBTAG00000043560	COX3	94657.863	141400.482	-0.579	0.0000208
ENSBTAG00000016017	CCDC40	30.593	56.586	-0.887	0.0000208
ENSBTAG00000019461	NUMBL	449.525	603.447	-0.425	0.0000231
ENSBTAG00000037558	GRO1	86.821	166.180	-0.937	0.0000231
ENSBTAG00000021799	RCN3	1236.299	1752.449	-0.503	0.0000244

GeneID	Gene	Mean Counts Juxt	Mean Counts NoEmbryos	Log2 Fold-Change	P-Value (FDR adj)
ENSBTAG00000013949	AHCTF1	1298.390	1039.004	0.322	0.0000265
ENSBTAG00000006506	GIT2	1850.777	2363.401	-0.353	0.0000265
ENSBTAG00000006877	MMP16	182.634	274.910	-0.590	0.0000272
ENSBTAG00000006882	IQGAP3	377.637	256.869	0.556	0.0000281
ENSBTAG00000021069	PBK	134.525	73.551	0.871	0.0000291
ENSBTAG00000017488	KLF3	426.951	600.373	-0.492	0.0000291
ENSBTAG00000007429	SPNS2	192.457	277.906	-0.530	0.0000308
ENSBTAG00000047268	WT1	5577.288	6824.840	-0.291	0.0000313
ENSBTAG00000016726	KIF15	114.866	59.089	0.959	0.0000324
ENSBTAG00000015801	EFNB1	738.164	889.062	-0.268	0.0000335
ENSBTAG00000015582	HMOX1	1496.800	2195.957	-0.553	0.0000337
ENSBTAG00000009383	KIF11	321.099	196.880	0.706	0.0000356
ENSBTAG00000004333	COPA	5663.358	6661.901	-0.234	0.0000361
ENSBTAG00000016918	MYOF	6559.505	8030.271	-0.292	0.0000369
ENSBTAG00000016406	MCM10	274.943	190.922	0.526	0.0000375
ENSBTAG00000030557	LIN52	749.669	571.390	0.392	0.0000375
ENSBTAG00000006928	OAT	8732.094	6862.675	0.348	0.0000387
ENSBTAG00000015794	NES	803.424	1113.914	-0.471	0.0000399
ENSBTAG00000012854	GSDMB	179.706	434.516	-1.274	0.0000401
ENSBTAG00000018800	RPS4X	7841.905	10214.291	-0.381	0.000042
ENSBTAG00000014376	ANKRD13A	1111.095	1354.619	-0.286	0.000046
ENSBTAG00000021372		2472.505	1939.528	0.350	0.0000466
ENSBTAG00000020734	ARL6IP1	1002.566	707.993	0.502	0.0000475
ENSBTAG00000024909	H3F3B	3377.002	2716.019	0.314	0.0000475
ENSBTAG00000001631	KIFC1	315.153	221.146	0.511	0.0000477
ENSBTAG00000006225	RPA2	407.645	290.499	0.489	0.0000477
ENSBTAG00000020641	PSMA5	1733.585	1337.593	0.374	0.0000477
ENSBTAG00000010672	PCCA	611.940	795.318	-0.378	0.000048
ENSBTAG00000005456	TTK	104.787	60.442	0.794	0.000049
ENSBTAG00000020745	HIVEP3	228.336	397.023	-0.798	0.0000495
ENSBTAG00000006721	TWISTNB	539.172	421.859	0.354	0.0000497
ENSBTAG00000007356	ELF1	1135.104	899.756	0.335	0.0000504
ENSBTAG00000005110	CADPS2	104.040	55.751	0.900	0.0000509
ENSBTAG00000006482	PTCD3	714.464	563.042	0.344	0.0000509
ENSBTAG00000013225	NBN	899.268	639.859	0.491	0.000052
ENSBTAG00000002792	FUT11	431.907	551.416	-0.352	0.000052
ENSBTAG00000019166	NSMCE4A	353.772	257.494	0.458	0.0000538
ENSBTAG00000043564	ATP8	9128.072	13000.374	-0.510	0.0000566
ENSBTAG00000007836	PPA1	730.827	524.075	0.480	0.0000574
ENSBTAG00000023369	GRIN2D	118.909	173.799	-0.548	0.0000595
ENSBTAG00000015505	FADS2	551.239	400.177	0.462	0.0000596
ENSBTAG00000044192	MAF	584.315	930.887	-0.672	0.0000596
ENSBTAG00000015264	ITGAE	118.844	188.344	-0.664	0.0000599
ENSBTAG00000025219		28.337	8.573	1.725	0.0000603
ENSBTAG00000047161	ARSH	65.105	32.423	1.006	0.0000603
ENSBTAG00000002224	UHRF1	379.085	226.881	0.741	0.0000672
ENSBTAG00000016869	POLD3	364.564	264.138	0.465	0.0000685
ENSBTAG00000018548	INTS7	724.686	562.352	0.366	0.0000685
ENSBTAG00000024449	CENPF	631.739	416.614	0.601	0.0000688
ENSBTAG00000017133	GINS4	67.224	36.177	0.894	0.0000689
ENSBTAG00000014784	NT5DC2	579.274	782.500	-0.434	0.0000697
ENSBTAG00000011518	RARB	52.965	103.520	-0.967	0.0000739
ENSBTAG00000007397	FOLH1B	62.370	33.796	0.884	0.0000748
ENSBTAG00000038844	ANKRD35	83.872	48.057	0.803	0.0000748
ENSBTAG00000011484	ZDHHC3	898.146	731.729	0.296	0.0000754
ENSBTAG00000002826	CLSPN	129.653	70.395	0.881	0.0000763
ENSBTAG00000015172	MCM6	584.568	453.718	0.366	0.0000783
ENSBTAG00000012352	PARP16	975.348	788.503	0.307	0.0000783
ENSBTAG00000008436	CDC25B	173.839	107.931	0.688	0.000079
ENSBTAG00000048151	PRPF40A	1760.622	1407.485	0.323	0.000079
ENSBTAG00000021151	MYH10	9834.671	14364.128	-0.547	0.000079
ENSBTAG00000002615	LONRF3	568.671	324.179	0.811	0.0000805
ENSBTAG00000025826	SLC24A1	11.722	35.942	-1.616	0.0000805
ENSBTAG00000018643	PRC1	367.755	267.092	0.461	0.0000809
ENSBTAG00000039764	IER5	313.305	438.861	-0.486	0.0000815
ENSBTAG00000011146	RAB8B	856.977	617.641	0.472	0.0000816
ENSBTAG00000007840	HMGCR	708.283	511.612	0.469	0.0000839
ENSBTAG00000031849	TMEM119	55.410	98.227	-0.826	0.0000841
ENSBTAG00000008093	NACAD	739.825	989.772	-0.420	0.0000844
ENSBTAG00000020313	FNBP1	1243.773	1581.008	-0.346	0.0000867

GeneID	Gene	Mean Counts Juxt	Mean Counts NoEmbryos	Log2 Fold-Change	P-Value (FDR adj)
ENSBTAG00000023814	ECT2	290.639	170.621	0.768	0.000088
ENSBTAG00000001592	INSIG1	557.504	369.290	0.594	0.0000885
ENSBTAG00000005979	HELLS	282.481	177.143	0.673	0.0000899
ENSBTAG00000037746	SNRNP27	360.252	258.607	0.478	0.0000899
ENSBTAG00000012434	ENOX1	211.459	292.181	-0.466	0.0000919
ENSBTAG00000037996	ARMCX3	1122.063	1348.454	-0.265	0.0000928
ENSBTAG00000021176	CRISPLD2	1703.424	2198.601	-0.368	0.0000999
ENSBTAG00000014380	MCM2	901.795	626.083	0.526	0.000102279
ENSBTAG00000008139	HOXA3	879.363	1140.099	-0.375	0.000103517
ENSBTAG00000007639	SDAD1	715.922	573.428	0.320	0.000104603
ENSBTAG00000020837	ARHGEF16	117.259	75.900	0.628	0.000109363
ENSBTAG00000047461		85.435	132.895	-0.637	0.000109831
ENSBTAG00000016766	TMEM176B	67.303	117.027	-0.798	0.000110632
ENSBTAG00000020636	SYN3	7595.496	9090.337	-0.259	0.000112568
ENSBTAG00000040131	CD58	5745.834	4583.352	0.326	0.000113052
ENSBTAG00000001920	POLQ	59.202	30.677	0.948	0.000120153
ENSBTAG00000024726	HJURP	169.418	102.178	0.729	0.000133637
ENSBTAG00000019938	N4BP1	1230.755	769.859	0.677	0.000133637
ENSBTAG00000017644	KIF17	157.641	230.318	-0.547	0.000133745
ENSBTAG00000012225	KPNA2	720.285	511.110	0.495	0.000134205
ENSBTAG00000019794	SYPL1	1972.732	1552.513	0.346	0.000135369
ENSBTAG00000004339		40.171	19.835	1.018	0.00013666
ENSBTAG00000006921	ABCA6	163.701	236.673	-0.532	0.000136734
ENSBTAG00000032140	SBK1	174.226	235.704	-0.436	0.000137863
ENSBTAG00000002408	FHAD1	61.702	107.192	-0.797	0.000140689
ENSBTAG00000020992	RHBDL3	12.399	29.500	-1.251	0.000141156
ENSBTAG00000000647	SELENOO	609.900	826.029	-0.438	0.000143909
ENSBTAG00000035544	CYP46A1	39.635	71.815	-0.857	0.000143909
ENSBTAG00000014440	PSMA4	921.940	727.742	0.341	0.000144996
ENSBTAG00000033690	BARD1	72.328	40.923	0.822	0.000149579
ENSBTAG00000015304	ANXA9	41.561	67.653	-0.703	0.000150855
ENSBTAG00000004531	CCT4	2497.731	2072.511	0.269	0.000156938
ENSBTAG00000021497	CDH23	115.180	174.296	-0.598	0.000156938
ENSBTAG00000018566	SFRP5	253.951	589.176	-1.214	0.000158721
ENSBTAG00000010956	SCARB2	3622.600	2846.381	0.348	0.000163421
ENSBTAG00000021301	ACSF2	575.857	765.448	-0.411	0.000163527
ENSBTAG00000017289	MCF2L	432.646	339.163	0.351	0.000164238
ENSBTAG00000010692	SND1	4285.605	5168.818	-0.270	0.000177207
ENSBTAG00000033727	RBPMS	2198.232	2666.076	-0.278	0.00017878
ENSBTAG00000001694	TYRO3	3102.572	3889.614	-0.326	0.000179656
ENSBTAG00000015424	WDR12	592.506	471.897	0.328	0.000180096
ENSBTAG00000020931	CHN2	488.870	620.979	-0.345	0.000180486
ENSBTAG00000011824	OGN	1857.258	783.299	1.246	0.000187826
ENSBTAG00000011133	AP1S3	937.678	716.908	0.387	0.000187826
ENSBTAG00000002669	RASSF4	54.066	95.703	-0.824	0.000187826
ENSBTAG00000011779	MAL2	3106.394	2306.537	0.430	0.000188887
ENSBTAG00000021181	BUB1	384.950	275.160	0.484	0.000191332
ENSBTAG00000020780	SBNO2	1689.242	2138.271	-0.340	0.000191332
ENSBTAG00000012861	KIF4A	201.274	134.468	0.582	0.000195172
ENSBTAG00000007970	C1H3orf38	370.850	275.308	0.430	0.000195172
ENSBTAG00000008538	DNAI1	12.757	33.149	-1.378	0.000195172
ENSBTAG00000012774	RAB7B	219.105	294.287	-0.426	0.00019859
ENSBTAG00000014729	MRPL51	543.830	673.195	-0.308	0.000198617
ENSBTAG00000023610	U2AF1L4	298.986	215.348	0.473	0.000204859
ENSBTAG00000011115	CH25H	4.209	19.958	-2.245	0.000207206
ENSBTAG00000000767	DCP2	302.961	202.560	0.581	0.000207893
ENSBTAG00000018418	TMEM74B	11.250	1.872	2.587	0.000208417
ENSBTAG00000011934	PCK2	439.214	342.463	0.359	0.000213632
ENSBTAG00000016174	NCL	6512.279	5680.986	0.197	0.000213632
ENSBTAG00000015457	FGFR1	3283.241	4110.383	-0.324	0.000222797
ENSBTAG00000005708	KIF20B	237.848	153.074	0.636	0.000225819
ENSBTAG00000001173	PLXNA2	2548.058	3270.253	-0.360	0.000226809
ENSBTAG00000001100	IL22RA1	67.382	41.134	0.712	0.000227233
ENSBTAG00000003970	MITD1	150.043	98.285	0.610	0.000227998
ENSBTAG00000016095	PRICKLE3	343.018	229.222	0.582	0.000231382
ENSBTAG00000044006	GINS2	110.896	69.138	0.682	0.000234268
ENSBTAG00000014060	LSM6	570.493	435.455	0.390	0.000236403
ENSBTAG00000022382	TMEM218	203.878	271.229	-0.412	0.000251219
ENSBTAG00000005305	NTS	112.293	60.924	0.882	0.000252203
ENSBTAG00000001465	P2RY1	435.706	287.080	0.602	0.000252957

GeneID	Gene	Mean Counts Juxt	Mean Counts NoEmbryos	Log2 Fold-Change	P-Value (FDR adj)
ENSBTAG00000008934	ESPL1	210.391	138.723	0.601	0.000252957
ENSBTAG00000040422	UTP23	302.239	217.480	0.475	0.000257443
ENSBTAG00000009438	EPHA5	1073.591	1377.918	-0.360	0.000260276
ENSBTAG00000000025	RAB6A	2292.119	1952.813	0.231	0.000266659
ENSBTAG00000017448	EFEMP1	13655.592	10295.401	0.407	0.000271727
ENSBTAG00000012658	TMA16	616.765	464.827	0.408	0.000274342
ENSBTAG00000012671	TNIP1	979.072	1372.906	-0.488	0.000275902
ENSBTAG00000000042	PYCR1	1435.771	1968.324	-0.455	0.000281111
ENSBTAG00000007247	NUF2	178.894	108.081	0.727	0.000281646
ENSBTAG00000012046	JUNB	3153.365	4408.170	-0.483	0.00028578
ENSBTAG00000017739	TNK1	292.142	390.496	-0.419	0.000287074
ENSBTAG00000010774	NUSAP1	251.778	149.786	0.749	0.000289033
ENSBTAG00000045504		272.411	365.530	-0.424	0.0002926
ENSBTAG00000000991	MRPL32	329.758	237.628	0.473	0.000293204
ENSBTAG00000011340	NSL1	162.783	111.564	0.545	0.000295148
ENSBTAG00000009405	TRPC4	1219.357	1579.545	-0.373	0.000295148
ENSBTAG00000009047	YPEL3	1520.450	1941.802	-0.353	0.00030057
ENSBTAG00000003604	ADAMTSL4	399.362	588.634	-0.560	0.000302961
ENSBTAG00000011102	TPCN1	121.291	177.158	-0.547	0.000303056
ENSBTAG00000012464	AFAP1	385.087	501.413	-0.381	0.000308568
ENSBTAG00000018629	CWF19L2	453.252	333.800	0.441	0.00031006
ENSBTAG00000021506	ARL6IP5	2542.026	2004.412	0.343	0.000312804
ENSBTAG00000018186	PDXK	486.490	749.249	-0.623	0.000315404
ENSBTAG00000009430	MYRIP	7.636	23.815	-1.641	0.000315404
ENSBTAG00000026819	HDAC7	2697.285	3329.152	-0.304	0.000319198
ENSBTAG00000018223	CHI3L1	2539.725	3446.486	-0.440	0.000323054
ENSBTAG00000020379	AREL1	1174.127	1585.880	-0.434	0.000326225
ENSBTAG00000007740	MDK	123.135	81.283	0.599	0.000326651
ENSBTAG00000009552	ATP2B1	1386.472	1719.020	-0.310	0.000326651
ENSBTAG00000015894	WWOX	485.977	608.956	-0.325	0.000331865
ENSBTAG00000018010	ABCA4	491.851	687.412	-0.483	0.000338801
ENSBTAG00000002462	MRPL47	464.391	341.865	0.442	0.000348042
ENSBTAG00000005793	PEA15	15919.877	19046.749	-0.259	0.000349276
ENSBTAG00000018216	SKA1	71.408	34.360	1.055	0.000358444
ENSBTAG00000005934	TTYH3	1084.858	1431.247	-0.400	0.000358695
ENSBTAG00000015898	RABL3	278.954	197.495	0.498	0.00036253
ENSBTAG00000008167	TTC3	1809.059	2125.048	-0.232	0.00036396
ENSBTAG00000021741	RPS6KA2	106.928	157.740	-0.561	0.000367536
ENSBTAG00000005015	SFXN3	296.787	409.760	-0.465	0.000368804
ENSBTAG00000010659	CUX1	3197.711	4338.548	-0.440	0.0003693
ENSBTAG00000003314	SKA3	208.751	152.990	0.448	0.00038079
ENSBTAG00000011488	PRPF8	5602.034	7383.237	-0.398	0.000394009
ENSBTAG00000000781	HIP1	730.434	997.740	-0.450	0.000394767
ENSBTAG00000026971	CDCA5	97.532	54.602	0.837	0.000396408
ENSBTAG00000015266	SDHAF2	691.317	556.265	0.314	0.000397133
ENSBTAG00000012317	PNP	2165.482	2612.851	-0.271	0.000397817
ENSBTAG00000020407	MTSS1	381.174	580.172	-0.606	0.000409444
ENSBTAG00000017321	SUMO3	898.705	719.188	0.321	0.000413671
ENSBTAG00000000184	EIF2AK3	692.885	876.956	-0.340	0.000413671
ENSBTAG00000039462	PCLAF	123.318	67.005	0.880	0.000421061
ENSBTAG00000016378	LRP10	6218.733	5047.615	0.301	0.000421517
ENSBTAG00000010597	GGCT	99.561	61.063	0.705	0.00042507
ENSBTAG00000003791	LPAR3	443.775	628.894	-0.503	0.000428798
ENSBTAG00000011549	TRPC2	138.478	92.563	0.581	0.000431627
ENSBTAG00000007976	FAM3C	991.861	765.515	0.374	0.00043638
ENSBTAG00000015519	GFM2	482.914	390.993	0.305	0.000446177
ENSBTAG00000017533	LRRC1	813.568	659.928	0.302	0.000447034
ENSBTAG00000010007	MAPK13	206.786	281.678	-0.446	0.000449753
ENSBTAG00000019278	KNTC1	171.699	111.658	0.621	0.000453545
ENSBTAG00000005124	JADE3	1235.649	878.517	0.492	0.000455562
ENSBTAG00000003532	TLE4	726.719	599.527	0.278	0.00045942
ENSBTAG00000009717	FGL2	15.081	3.510	2.103	0.000471466
ENSBTAG00000001864	NR4A3	21.915	8.335	1.395	0.000474377
ENSBTAG00000006065	PCNA	653.698	435.354	0.586	0.000479731
ENSBTAG00000011187	FAM13A	527.371	412.412	0.355	0.000482284
ENSBTAG00000005825	NEIL3	43.829	22.327	0.973	0.000484016
ENSBTAG00000021680	SKA2	433.451	313.061	0.469	0.00048832
ENSBTAG00000013249	SALL2	193.740	264.963	-0.452	0.00048832
ENSBTAG00000000297	ZNF330	754.971	569.682	0.406	0.000494466
ENSBTAG00000007799	MTFR2	104.166	59.612	0.805	0.000499182

GeneID	Gene	Mean Counts Juxt	Mean Counts NoEmbryos	Log2 Fold-Change	P-Value (FDR adj)
ENSBTAG00000011528	SMIM11A	87.931	129.772	-0.562	0.000507264
ENSBTAG00000010164	ESPNL	282.471	211.516	0.417	0.000511605
ENSBTAG00000006378	RIPK1	632.570	512.294	0.304	0.000511605
ENSBTAG00000007303	RAD21	2480.193	1999.039	0.311	0.000517832
ENSBTAG00000008629	MTFR1	578.614	722.150	-0.320	0.000525463
ENSBTAG00000015318	NECTIN2	331.607	240.221	0.465	0.000537802
ENSBTAG00000007075		81.110	52.580	0.625	0.000543369
ENSBTAG00000021193	FBXO5	97.020	60.125	0.690	0.000552671
ENSBTAG00000019106	EIF1B	2081.685	2831.118	-0.444	0.000553014
ENSBTAG00000043553	GPX3	159.405	247.265	-0.633	0.000557579
ENSBTAG00000033160	FAM114A1	635.605	805.316	-0.341	0.000564491
ENSBTAG00000017329	GMNN	205.066	118.909	0.786	0.000566308
ENSBTAG00000017751	RGS9	126.408	173.425	-0.456	0.000566308
ENSBTAG00000018588	TMBIM6	9630.501	8253.477	0.223	0.00056656
ENSBTAG00000031461	SNX7	175.335	117.292	0.580	0.00056965
ENSBTAG00000009019	SH3PXD2B	289.628	410.354	-0.503	0.000578652
ENSBTAG00000031306	PLSCR1	24.850	11.332	1.133	0.000615471
ENSBTAG00000005786	ATXN3	251.016	178.321	0.493	0.000629835
ENSBTAG00000013676	DYNC2LI1	678.877	518.537	0.389	0.000641131
ENSBTAG00000008216	RRM2	853.998	462.692	0.884	0.000643201
ENSBTAG00000012927	ALDOA	5515.422	6864.785	-0.316	0.000643201
ENSBTAG00000021819	IFNAR1	838.407	1185.189	-0.499	0.000644554
ENSBTAG00000005607	ERCC6L	69.978	41.868	0.741	0.000646097
ENSBTAG00000007192	SIDT2	908.443	1128.178	-0.313	0.000662113
ENSBTAG00000005483	ESYT2	1417.130	1690.994	-0.255	0.000664783
ENSBTAG00000017750	RHBDD3	301.337	231.434	0.381	0.000666664
ENSBTAG00000048077	MAGED4B	777.263	1012.770	-0.382	0.000670575
ENSBTAG00000007362	XPC	2468.967	2878.697	-0.222	0.000689172
ENSBTAG00000039231	MTURN	2368.219	2972.486	-0.328	0.000706931
ENSBTAG00000021071	TRIM8	859.527	1186.012	-0.465	0.000706931
ENSBTAG00000021673	NDC80	146.975	87.323	0.751	0.000711982
ENSBTAG00000020525	SEC31A	4488.322	5122.393	-0.191	0.000711982
ENSBTAG00000013881	GJA4	4.100	17.688	-2.109	0.000712227
ENSBTAG00000012865	DEK	2713.344	2092.860	0.375	0.000718961
ENSBTAG00000011505	RABEP1	3175.901	2604.027	0.286	0.000718961
ENSBTAG00000018773	RND1	528.866	774.585	-0.551	0.000726311
ENSBTAG00000010726	F8	333.147	426.152	-0.355	0.000729827
ENSBTAG00000015105	HERPUD2	2054.853	1672.743	0.297	0.000739101
ENSBTAG00000005718	PLIN2	288.355	208.193	0.470	0.000756208
ENSBTAG00000008575	CGNL1	800.081	1112.577	-0.476	0.00076914
ENSBTAG00000005503	PRMT2	570.843	455.552	0.325	0.000771676
ENSBTAG00000003878	ZUP1	272.988	207.962	0.393	0.000771995
ENSBTAG00000015127	SDC4	2936.106	3974.236	-0.437	0.000773848
ENSBTAG00000012205	CPT1C	107.997	152.599	-0.499	0.000773848
ENSBTAG00000010981	CIB2	47.377	76.671	-0.695	0.000790434
ENSBTAG00000026375	RMI2	147.391	104.099	0.502	0.000790857
ENSBTAG00000046837	ZNF358	1241.778	1556.992	-0.326	0.000790857
ENSBTAG00000008567	DLEC1	159.259	215.479	-0.436	0.000798995
ENSBTAG00000003002	WDR75	960.069	788.829	0.283	0.000802462
ENSBTAG00000014091	ARHGEF3	626.325	465.951	0.427	0.000825905
ENSBTAG00000014382	KANK4	714.303	559.060	0.354	0.000826324
ENSBTAG00000019156	CCT2	2375.640	2044.605	0.216	0.00082779
ENSBTAG00000030523	ZPBP2	1.818	10.119	-2.477	0.00082779
ENSBTAG00000031001	MEGF8	1795.669	2224.553	-0.309	0.00083553
ENSBTAG00000010935	EML4	1824.273	1333.512	0.452	0.000835879
ENSBTAG00000021691	PSMD14	890.473	722.167	0.302	0.000841323
ENSBTAG00000016127	ELP	272.214	341.173	-0.326	0.000871511
ENSBTAG00000020371	ACOT8	251.184	325.223	-0.373	0.000871511
ENSBTAG00000000590	POLE	374.969	266.541	0.492	0.000876283
ENSBTAG00000008541	MGST1	247.282	177.208	0.481	0.000876283
ENSBTAG00000012206	SNX33	986.865	1468.017	-0.573	0.000876283
ENSBTAG00000001154	DGAT2	61.501	31.685	0.957	0.00088206
ENSBTAG00000010773	GNPAT	530.223	655.459	-0.306	0.000893485
ENSBTAG00000031435	SELENOT	1073.153	844.925	0.345	0.000903427
ENSBTAG00000018638	CC2D2A	338.092	426.385	-0.335	0.000914448
ENSBTAG00000013492	PRKAG3	19.488	5.575	1.806	0.000918774
ENSBTAG00000021514	DNPEP	792.920	612.263	0.373	0.000923026
ENSBTAG00000000660	FAM83D	117.981	72.112	0.710	0.000928758
ENSBTAG00000018003	ARHGEF25	243.189	322.619	-0.408	0.000928758
ENSBTAG00000013369	COL14A1	4072.608	5448.695	-0.420	0.000932178

GeneID	Gene	Mean Counts Juxt	Mean Counts NoEmbryos	Log2 Fold-Change	P-Value (FDR adj)
ENSBTAG00000002014	SNX1	1654.575	1441.836	0.199	0.000936638
ENSBTAG00000024869	CX3CL1	2.230	11.335	-2.346	0.000953956
ENSBTAG00000010334	SYTL3	12.358	35.731	-1.532	0.000979009
ENSBTAG00000012380	HK1	1551.203	1910.851	-0.301	0.000988317
ENSBTAG00000005495		499.415	627.852	-0.330	0.001005545
ENSBTAG00000001553	HNRNPA1	7567.400	6119.382	0.306	0.001019941
ENSBTAG00000004625	PYGB	304.534	400.703	-0.396	0.001049059
ENSBTAG00000011798	STK38L	1081.958	1453.449	-0.426	0.001049059
ENSBTAG00000009830	PLEKHB1	392.606	502.090	-0.355	0.001067681
ENSBTAG00000003259	TCERG1	1709.173	1344.805	0.346	0.001069021
ENSBTAG00000045794	STMP1	2149.610	2469.031	-0.200	0.001076592
ENSBTAG00000016282	EIF5	5583.709	4605.346	0.278	0.001076775
ENSBTAG00000013009	AURKA	171.715	121.888	0.494	0.001078346
ENSBTAG00000011916	USP8	2334.166	1975.491	0.241	0.001082334
ENSBTAG00000021582	NCAPG	272.708	175.062	0.639	0.001084614
ENSBTAG00000014239	CCNB1	185.744	114.001	0.704	0.001088052
ENSBTAG00000010457	NUAK1	215.494	341.947	-0.666	0.001088052
ENSBTAG00000021787	PAQR7	33.013	55.430	-0.748	0.001099077
ENSBTAG00000000803	ZNF667	179.863	238.339	-0.406	0.001117679
ENSBTAG00000004723	TEX2	1592.574	2216.367	-0.477	0.001129993
ENSBTAG00000013971	PI4KA	1695.111	2124.622	-0.326	0.001134709
ENSBTAG00000011405	CEP72	165.219	108.193	0.611	0.001176251
ENSBTAG00000009886	KDELR3	1432.533	1893.117	-0.402	0.001214727
ENSBTAG00000015604	ZNF385A	3862.529	4697.684	-0.282	0.001220687
ENSBTAG00000047697		129.647	83.415	0.636	0.001222237
ENSBTAG00000017021		245.589	164.595	0.577	0.00123248
ENSBTAG00000014367	PRKX	153.737	223.296	-0.538	0.001246376
ENSBTAG00000013475	TRAF3	312.791	415.916	-0.411	0.001265144
ENSBTAG00000019023	NANS	246.963	340.544	-0.464	0.001272176
ENSBTAG00000002573	UBA2	1626.140	1369.481	0.248	0.001276462
ENSBTAG00000024803	ENDOD1	821.637	652.349	0.333	0.001282057
ENSBTAG00000014246	CENPH	95.872	57.237	0.744	0.001312503
ENSBTAG00000016557	MTMR2	763.474	627.426	0.283	0.00132489
ENSBTAG00000037686	SRPX2	159.249	63.518	1.326	0.001351729
ENSBTAG00000014435	TCF19	113.946	66.592	0.775	0.001361624
ENSBTAG00000014262	BZW2	1221.921	987.148	0.308	0.001362562
ENSBTAG00000000668	SLC22A5	273.606	358.736	-0.391	0.001369955
ENSBTAG00000008192	PLPPR2	130.078	184.064	-0.501	0.001381095
ENSBTAG00000016155	GDPD3	64.086	93.909	-0.551	0.001410904
ENSBTAG00000001057	ARFGAP3	757.372	897.315	-0.245	0.001411527
ENSBTAG00000013699	TBC1D1	180.608	243.624	-0.432	0.001418361
ENSBTAG00000008827	SPOCK2	1715.856	2059.879	-0.264	0.001421166
ENSBTAG00000006823	CMYA5	51.306	83.958	-0.711	0.001432618
ENSBTAG00000005745	HPSE	1430.359	1036.216	0.465	0.001446327
ENSBTAG00000002613	MIS18BP1	327.889	225.165	0.542	0.001458615
ENSBTAG00000015931	TTC4	406.570	323.781	0.328	0.001463144
ENSBTAG00000020301	BLM	162.368	114.331	0.506	0.001490232
ENSBTAG00000002688	ATP1B1	7706.607	5989.580	0.364	0.001490232
ENSBTAG00000005269	CCNB2	115.084	71.485	0.687	0.001527412
ENSBTAG00000014626	RARS	1079.142	904.613	0.255	0.001529989
ENSBTAG00000017369	MAMDC2	323.498	472.417	-0.546	0.001529989
ENSBTAG00000016547	CEP57	362.986	284.796	0.350	0.001532925
ENSBTAG00000009396	EXO1	51.879	26.138	0.989	0.001538075
ENSBTAG00000001950	RDH11	996.294	677.442	0.556	0.00154942
ENSBTAG00000011149	SIGIRR	223.574	160.348	0.480	0.001564608
ENSBTAG00000015225	NUP58	1350.773	1113.847	0.278	0.001598587
ENSBTAG00000034442	LNP1	75.224	115.966	-0.624	0.001598587
ENSBTAG00000013259	POLR3A	995.604	852.108	0.225	0.001637097
ENSBTAG00000015369	MLLT11	130.555	181.079	-0.472	0.001654673
ENSBTAG00000008054	ZNF706	586.549	452.500	0.374	0.001656931
ENSBTAG00000044029	AVEN	686.072	570.891	0.265	0.00167192
ENSBTAG00000016969	ORC3	465.751	352.134	0.403	0.001672056
ENSBTAG00000005710	NCAM1	581.342	836.690	-0.525	0.001673329
ENSBTAG00000031962	RAB20	36.876	62.021	-0.750	0.001677173
ENSBTAG00000001938	CKS2	180.099	114.121	0.658	0.001719943
ENSBTAG00000021681	PRR11	64.241	34.733	0.887	0.00174945
ENSBTAG00000010357	ST6GAL1	176.274	252.425	-0.518	0.001766918
ENSBTAG00000004805	ITFG1	2138.667	1845.093	0.213	0.001768596
ENSBTAG00000020905	RPL11	7872.941	9252.874	-0.233	0.001777388
ENSBTAG00000001141	ADAM17	600.185	830.583	-0.469	0.001780875

GeneID	Gene	Mean Counts Juxt	Mean Counts NoEmbryos	Log2 Fold-Change	P-Value (FDR adj)
ENSBTAG00000008100	GOLGA7B	48.076	84.610	-0.816	0.001780875
ENSBTAG00000020059	GEN1	194.286	129.707	0.583	0.001789449
ENSBTAG00000018049	MKNK2	721.413	955.768	-0.406	0.001795892
ENSBTAG00000047379	CYP3A4	29.442	60.717	-1.044	0.001801172
ENSBTAG00000015016	CALCOCO1	4882.189	5743.161	-0.234	0.001811767
ENSBTAG00000019272	LPCAT2	332.034	240.708	0.464	0.001839966
ENSBTAG00000012139	SIX1	97.487	66.158	0.559	0.001850234
ENSBTAG00000018706	PCTP	263.550	195.993	0.427	0.001874189
ENSBTAG00000019246	SC5D	1276.550	1040.444	0.295	0.001874189
ENSBTAG00000001578	ADPGK	979.964	805.991	0.282	0.001888154
ENSBTAG00000016042	TM6SF2	19.215	7.065	1.443	0.001891823
ENSBTAG00000032521	PLEKHH2	1288.419	954.548	0.433	0.001909006
ENSBTAG00000005957	CSE1L	1825.256	1485.933	0.297	0.001922802
ENSBTAG00000018517	VLDLR	269.460	509.116	-0.918	0.00192817
ENSBTAG00000010230	CAPN1	1083.144	1311.137	-0.276	0.001930542
ENSBTAG00000000813	HOMER3	88.000	123.637	-0.491	0.001947945
ENSBTAG00000007121	TK1	284.599	205.189	0.472	0.001965482
ENSBTAG00000010945	SEC24B	1915.892	1536.482	0.318	0.001965482
ENSBTAG00000025809	ABHD8	524.904	704.650	-0.425	0.001965482
ENSBTAG00000021686	MELK	126.328	81.128	0.639	0.001968015
ENSBTAG00000007644	GNG7	449.610	560.433	-0.318	0.001969082
ENSBTAG00000016895	NIPA2	1151.215	930.063	0.308	0.001979536
ENSBTAG00000001193	UNC93B1	607.672	482.197	0.334	0.002049036
ENSBTAG00000013300	KCNMA1	56.517	92.798	-0.715	0.002049158
ENSBTAG00000015280	KIF2C	103.245	62.982	0.713	0.002059345
ENSBTAG00000026246	MOSPD3	393.251	485.615	-0.304	0.002059345
ENSBTAG00000043556	COX2	45293.065	63554.571	-0.489	0.002059345
ENSBTAG00000006037	WISP2	121.573	76.955	0.660	0.002083825
ENSBTAG00000007415	SLC7A8	1810.504	2139.159	-0.241	0.002097574
ENSBTAG00000015683	HSPA4	2332.000	1995.618	0.225	0.002114948
ENSBTAG00000033315	DNAJC1	370.818	271.921	0.448	0.002122913
ENSBTAG00000046325		237.945	169.993	0.485	0.002124231
ENSBTAG00000025450	SYNE2	1714.440	1338.041	0.358	0.002124231
ENSBTAG00000014326	CDCA8	118.419	74.156	0.675	0.002139329
ENSBTAG00000019604	VASP	2221.799	1921.441	0.210	0.002148577
ENSBTAG00000025136	MYOZ3	57.351	107.535	-0.907	0.002148577
ENSBTAG00000015595	MCM5	579.175	397.191	0.544	0.002155993
ENSBTAG00000005372	DLGAP1	182.177	250.961	-0.462	0.002155993
ENSBTAG00000003457	ATF5	829.006	1036.569	-0.322	0.002162267
ENSBTAG00000021768	CCNG2	251.614	333.645	-0.407	0.002176863
ENSBTAG00000047694	SERF2	3125.332	4275.651	-0.452	0.002186706
ENSBTAG00000037778	CXCL3	605.357	955.923	-0.659	0.002214516
ENSBTAG00000007513	PGAM5	711.571	596.955	0.253	0.002235776
ENSBTAG00000017037	PKN1	1064.386	1357.587	-0.351	0.002239355
ENSBTAG00000002260	NCAPD3	401.775	316.636	0.344	0.002241326
ENSBTAG00000020272	SIK2	3235.323	4197.878	-0.376	0.002259535
ENSBTAG00000018824	MIA3	3808.815	3347.454	0.186	0.002271152
ENSBTAG00000012350	MAT2B	907.304	731.309	0.311	0.002275347
ENSBTAG00000031797	MANF	502.555	357.464	0.491	0.002275721
ENSBTAG00000046750	B3GNT3	10.351	2.819	1.876	0.002295808
ENSBTAG00000009475	PLXDC2	8305.995	10802.278	-0.379	0.002295836
ENSBTAG00000002554	TCAF1	2298.097	2702.579	-0.234	0.002306257
ENSBTAG00000017599	NR2F1	1449.895	1228.546	0.239	0.002309789
ENSBTAG00000039529	BTBD19	232.355	295.208	-0.345	0.00231429
ENSBTAG00000015032	CD14	81.371	117.606	-0.531	0.002370735
ENSBTAG00000006015	POLH	506.786	405.734	0.321	0.002390603
ENSBTAG00000017845	BAG1	1102.637	918.561	0.264	0.002412459
ENSBTAG00000018650	HEPACAM	19.411	41.231	-1.087	0.002434604
ENSBTAG00000006835	MCAM	209.798	155.972	0.428	0.0024376
ENSBTAG00000009725	AOX1	760.143	567.535	0.422	0.0024376
ENSBTAG00000022890	MBP	2046.137	2543.275	-0.314	0.0024376
ENSBTAG00000013491	EML1	265.567	343.306	-0.370	0.002454158
ENSBTAG00000017616	ADSSL1	161.136	208.398	-0.371	0.002501027
ENSBTAG00000002922		296.195	431.923	-0.544	0.002501027
ENSBTAG00000021568	VWCE	71.025	100.266	-0.497	0.002528866
ENSBTAG00000010422	MDM2	1457.721	1881.299	-0.368	0.002600543
ENSBTAG00000003384	CEP162	229.317	179.048	0.357	0.002605688
ENSBTAG00000007773	VCAM1	57.428	106.905	-0.897	0.00264193
ENSBTAG00000004472	DYNLT1	456.565	357.984	0.351	0.002658409
ENSBTAG00000020311	USP20	860.647	1088.290	-0.339	0.002670077

GeneID	Gene	Mean Counts Juxt	Mean Counts NoEmbryos	Log2 Fold-Change	P-Value (FDR adj)
ENSBTAG00000008552	PLXNA3	886.580	1087.144	-0.294	0.002672402
ENSBTAG00000015101	HMGB2	447.220	316.887	0.497	0.002687182
ENSBTAG00000038865	TCEA3	9.663	22.544	-1.222	0.002711666
ENSBTAG00000013159	PHF11	1209.845	976.981	0.308	0.002730389
ENSBTAG00000015185	MRGPRF	131.293	212.213	-0.693	0.002739028
ENSBTAG00000019822	TPPP3	18.462	45.219	-1.292	0.002756493
ENSBTAG00000000877	ETFBKMT	201.166	128.553	0.646	0.002770184
ENSBTAG00000021707	MYBPC3	24.801	49.320	-0.992	0.002785748
ENSBTAG00000000064	FEN1	179.907	126.202	0.512	0.002844153
ENSBTAG00000012586	HSPD1	1598.558	1396.393	0.195	0.002844153
ENSBTAG00000015470	SYPL2	191.990	249.688	-0.379	0.002844153
ENSBTAG00000039129		349.175	268.636	0.378	0.002857797
ENSBTAG00000008295	ACTL6B	21.280	40.189	-0.917	0.002857797
ENSBTAG00000004085	ASF1B	93.449	54.380	0.781	0.002859772
ENSBTAG00000008579	RCC2	1494.491	1274.628	0.230	0.00286335
ENSBTAG00000010048	SPC25	51.925	26.731	0.958	0.002873439
ENSBTAG00000017557	QRSL1	421.542	334.264	0.335	0.002873869
ENSBTAG00000011044	TACC3	340.724	226.834	0.587	0.002942201
ENSBTAG00000001116	P4HA2	1912.902	2414.837	-0.336	0.00295384
ENSBTAG00000047345		364.174	284.438	0.357	0.002975843
ENSBTAG00000001745	LUM	6254.832	4654.962	0.426	0.002977779
ENSBTAG00000006063	TMEM230	705.040	569.981	0.307	0.002977779
ENSBTAG00000010321	TTC1	597.517	501.875	0.252	0.002977779
ENSBTAG00000003169	FBXO24	166.360	234.794	-0.497	0.002977779
ENSBTAG00000013745	ITGA5	1174.775	1526.977	-0.378	0.002978028
ENSBTAG00000000752	SGO1	73.688	43.827	0.750	0.002983976
ENSBTAG00000009051	MMP19	1620.872	1367.812	0.245	0.003012682
ENSBTAG00000020710	CENPQ	103.914	66.952	0.634	0.003035212
ENSBTAG00000032163	LTV1	818.789	622.424	0.396	0.003041016
ENSBTAG00000012516	SLC1A7	29.591	56.204	-0.925	0.003041016
ENSBTAG00000017580	RFX5	170.042	122.582	0.472	0.003066647
ENSBTAG00000034360	SERF1A	109.101	164.669	-0.594	0.003069979
ENSBTAG00000000021	WASHC3	875.172	1073.555	-0.295	0.003070455
ENSBTAG00000007447	NUDT4	1653.653	1395.646	0.245	0.003108386
ENSBTAG00000004354		138.340	189.198	-0.452	0.003108386
ENSBTAG00000012180	BMF	88.803	131.471	-0.566	0.003108386
ENSBTAG00000017280	C3	341306.533	438940.538	-0.363	0.003154944
ENSBTAG00000026977	PTPRQ	3616.261	4805.871	-0.410	0.003154944
ENSBTAG00000005129	CEP55	112.796	73.249	0.623	0.003206851
ENSBTAG00000016722	PGGHG	670.037	547.006	0.293	0.003282397
ENSBTAG00000014843	COPB2	2969.127	3377.094	-0.186	0.003297196
ENSBTAG00000020963	RASSF1	311.256	233.289	0.416	0.003350323
ENSBTAG00000013162	HSPA8	20422.727	17566.051	0.217	0.003367643
ENSBTAG00000021678	SLC31A1	2329.342	2747.071	-0.238	0.003367643
ENSBTAG00000012505	ARHGEF17	1200.296	1562.980	-0.381	0.003422352
ENSBTAG00000018497	CAVIN2	60.244	86.077	-0.515	0.003436984
ENSBTAG00000017165	MATN2	260.688	203.819	0.355	0.003473971
ENSBTAG00000002697	KCTD10	916.316	1124.762	-0.296	0.00347587
ENSBTAG00000014093	IDH2	247.573	323.761	-0.387	0.003495944
ENSBTAG00000020244	EFNA1	527.225	690.615	-0.389	0.00353829
ENSBTAG00000006255	MDM4	544.393	402.754	0.435	0.003540153
ENSBTAG00000018315	PELP1	2903.222	3925.083	-0.435	0.003540153
ENSBTAG00000008499	TROAP	193.916	122.788	0.659	0.003564633
ENSBTAG00000020551	ABCD1	262.972	203.599	0.369	0.003590176
ENSBTAG00000032534	RHOF	69.261	101.998	-0.558	0.003620062
ENSBTAG00000023780	SYCE1L	66.198	109.414	-0.725	0.003620547
ENSBTAG00000002027	FAM167B	93.639	129.926	-0.473	0.003624038
ENSBTAG00000011437		292.107	214.971	0.442	0.003627868
ENSBTAG00000017258	ACSL3	592.382	460.993	0.362	0.003639885
ENSBTAG00000017844	STIL	75.458	49.387	0.612	0.003677951
ENSBTAG00000009691	SH2B2	207.321	313.045	-0.595	0.003677951
ENSBTAG00000014230	VRK1	407.246	290.893	0.485	0.003680786
ENSBTAG00000015358	ALDOB	315.696	403.621	-0.354	0.003705639
ENSBTAG00000010276	RECQL4	86.711	45.311	0.936	0.003715356
ENSBTAG00000014820	OXA1L	1745.189	2093.613	-0.263	0.003764688
ENSBTAG00000001151	APLP1	490.188	614.965	-0.327	0.003777064
ENSBTAG00000012212	CYP26B1	42.113	22.050	0.933	0.003792582
ENSBTAG00000020873	MAT2A	3515.682	3020.200	0.219	0.003824043
ENSBTAG00000012467	MASP1	129.092	80.094	0.689	0.003876954
ENSBTAG00000018272	RERE	4416.755	5937.831	-0.427	0.003930851

GeneID	Gene	Mean Counts Juxt	Mean Counts NoEmbryos	Log2 Fold-Change	P-Value (FDR adj)
ENSBTAG00000003959	ARHGAP24	1334.301	1680.469	-0.333	0.004011901
ENSBTAG00000003191	FSCN1	5206.808	6578.522	-0.337	0.004014702
ENSBTAG00000012050	ORAI2	117.662	170.113	-0.532	0.004060883
ENSBTAG00000016838	SRPK1	1021.177	858.276	0.251	0.00408373
ENSBTAG00000018373	DPYSL2	1147.068	1373.007	-0.259	0.00410038
ENSBTAG00000006277	ENGASE	177.313	235.907	-0.412	0.004120579
ENSBTAG00000003192	TBC1D16	126.871	185.389	-0.547	0.00422576
ENSBTAG00000005564	PIAS1	1403.377	1195.281	0.232	0.004232361
ENSBTAG00000019526	CMTM6	2220.358	1924.007	0.207	0.004255846
ENSBTAG00000014694	JTB	320.104	397.792	-0.313	0.00433311
ENSBTAG00000004688	DHCR24	639.958	442.202	0.533	0.004372786
ENSBTAG00000008963	CIT	288.337	216.854	0.411	0.004398159
ENSBTAG00000022520	BRCA1	394.004	302.199	0.383	0.004449865
ENSBTAG00000010477	TTC21A	152.041	196.811	-0.372	0.004494018
ENSBTAG00000004490	TRIM31	45.716	67.456	-0.561	0.004494018
ENSBTAG00000036113	RSPH14	195.820	265.218	-0.438	0.004505133
ENSBTAG00000015346	NASP	871.459	690.243	0.336	0.004505344
ENSBTAG00000018112	TBL1X	1837.284	1515.596	0.278	0.004557227
ENSBTAG00000012444	ADAM12	861.907	1206.690	-0.485	0.004576957
ENSBTAG00000018383	ATAD5	146.309	95.422	0.617	0.004595389
ENSBTAG00000003553	ZFP36L2	1553.331	2053.844	-0.403	0.004595389
ENSBTAG00000021521	BFAR	1519.482	1330.446	0.192	0.004608242
ENSBTAG00000015052	PROX2	257.855	341.648	-0.406	0.004608883
ENSBTAG00000012674	CNKSR3	531.752	418.096	0.347	0.004616226
ENSBTAG00000018464	ZDHHC14	317.824	223.666	0.507	0.004620039
ENSBTAG00000005475	TCAF2	457.954	359.482	0.349	0.004620039
ENSBTAG00000039571	PROSER2	1109.721	903.246	0.297	0.004620039
ENSBTAG00000003208	RAB33B	396.469	332.748	0.253	0.004620039
ENSBTAG00000006838	AIFM1	596.470	502.692	0.247	0.004620039
ENSBTAG00000039958	GYS1	681.397	856.726	-0.330	0.004620039
ENSBTAG00000023963	RHBDD1	309.088	243.269	0.345	0.004623191
ENSBTAG00000018910	WDR6	1692.715	1923.502	-0.184	0.004640777
ENSBTAG00000013023	MAP4K4	1890.197	2466.646	-0.384	0.004640777
ENSBTAG00000000505	KYAT3	437.582	352.143	0.313	0.004643993
ENSBTAG00000040442		106.124	73.571	0.529	0.004666699
ENSBTAG00000013588	ZNF532	979.956	1145.955	-0.226	0.004678283
ENSBTAG00000008743	ALDH2	1242.582	1522.641	-0.293	0.004684857
ENSBTAG00000013614	TMEM38A	133.098	179.852	-0.434	0.004687425
ENSBTAG00000008607	ARID3A	232.888	305.072	-0.390	0.004689809
ENSBTAG00000026181	UGT1A1	41.949	21.572	0.959	0.004698918
ENSBTAG00000013953	CALD1	11860.736	13893.434	-0.228	0.004729201
ENSBTAG00000008306	MKRN1	657.281	777.699	-0.243	0.004739306
ENSBTAG00000011419	HSPA9	3331.138	2958.414	0.171	0.004759777
ENSBTAG00000019470	NEK6	760.091	887.419	-0.223	0.004830685
ENSBTAG00000000599	CCNI	3392.944	4031.923	-0.249	0.004859296
ENSBTAG00000009428	GAN	113.732	176.296	-0.632	0.004859296
ENSBTAG00000017964	LRRC51	174.214	219.960	-0.336	0.00486219
ENSBTAG00000021286	SLC37A1	77.776	52.798	0.559	0.004942695
ENSBTAG00000016137	ZNF608	56.320	89.682	-0.671	0.004948917
ENSBTAG00000019409	GNPTAB	1818.723	2196.901	-0.273	0.005009188
ENSBTAG00000047416	HEPH	299.912	223.269	0.426	0.005021926
ENSBTAG00000011514	MRPL44	255.783	200.157	0.354	0.005041586
ENSBTAG00000031609	THAP12	354.796	280.569	0.339	0.005085023
ENSBTAG00000008180	SPDL1	102.559	61.949	0.727	0.005085732
ENSBTAG00000017582	CHEK1	162.701	104.426	0.640	0.005186051
ENSBTAG00000032148	TMEM117	142.865	189.669	-0.409	0.005192286
ENSBTAG00000013885	ADSS	1066.691	796.124	0.422	0.005221139
ENSBTAG00000018823	GRN	3944.610	3233.006	0.287	0.005265347
ENSBTAG00000000738	DAPK1	2564.064	3166.604	-0.305	0.005265347
ENSBTAG00000043561	COX1	485698.972	608293.615	-0.325	0.005265347
ENSBTAG00000000163	DDIT4	222.722	406.722	-0.869	0.005294992
ENSBTAG00000000937	SSFA2	657.261	536.519	0.293	0.005339127
ENSBTAG00000014711	DBF4	149.952	103.598	0.534	0.005372639
ENSBTAG00000002714	GNAI1	1158.228	959.811	0.271	0.005390639
ENSBTAG00000013848	ADGRD1	1002.999	1313.442	-0.389	0.005390639
ENSBTAG00000002117	KIF18A	135.927	92.953	0.548	0.005401215
ENSBTAG00000037581	MZF1	791.640	921.631	-0.219	0.00541782
ENSBTAG00000015164	SLC27A5	12.022	26.043	-1.115	0.00541782
ENSBTAG00000018364	TMEM132A	831.995	1032.441	-0.311	0.005430181
ENSBTAG00000018348	CBLL1	548.579	442.064	0.311	0.005462349

GeneID	Gene	Mean Counts Juxt	Mean Counts NoEmbryos	Log2 Fold-Change	P-Value (FDR adj)
ENSBTAG00000003419	EAPP	396.411	496.536	-0.325	0.005462349
ENSBTAG00000001082	SH2D5	82.141	121.481	-0.565	0.0055128
ENSBTAG00000008453	LBR	169.862	131.213	0.372	0.005621154
ENSBTAG00000020221	WNT5A	2052.303	1636.123	0.327	0.005621154
ENSBTAG00000038500		55.454	33.904	0.710	0.005637762
ENSBTAG00000018447	RABGGTB	674.168	510.033	0.403	0.005646028
ENSBTAG00000010568	ZBED5	398.197	513.027	-0.366	0.005668317
ENSBTAG00000020100		168.227	112.950	0.575	0.00568687
ENSBTAG00000013548	GABRE	433.583	338.673	0.356	0.005688649
ENSBTAG00000016959	LAPTM4B	2268.916	1815.227	0.322	0.005688649
ENSBTAG00000023832	ADAM8	201.383	275.363	-0.451	0.005688649
ENSBTAG00000011317	GOLGA2	1393.526	1675.601	-0.266	0.005757669
ENSBTAG00000006642	PRKACA	388.459	485.166	-0.321	0.005757669
ENSBTAG00000021880	COQ8A	2888.500	2414.001	0.259	0.005817994
ENSBTAG00000007208	HDAC11	236.324	304.642	-0.366	0.00586717
ENSBTAG00000016836	PDK1	206.657	269.846	-0.385	0.005889512
ENSBTAG00000006052	PLCD3	428.367	521.888	-0.285	0.005906977
ENSBTAG00000033504	MAK16	400.922	315.323	0.346	0.00591888
ENSBTAG00000003836	ADAM19	367.833	462.655	-0.331	0.00591888
ENSBTAG00000018255	ACTN1	9386.654	11589.526	-0.304	0.005933096
ENSBTAG00000015781	TRMT13	611.115	470.221	0.378	0.005939819
ENSBTAG00000000679	PGM3	476.714	574.669	-0.270	0.005940368
ENSBTAG00000015743	GMPR	120.589	167.267	-0.472	0.005979711
ENSBTAG00000012784	RACGAP1	398.513	314.750	0.340	0.006062208
ENSBTAG00000014922	SHB	522.666	666.300	-0.350	0.006062208
ENSBTAG00000020959	SET	2138.509	1832.150	0.223	0.006076604
ENSBTAG00000001640	EPB41L1	687.681	834.195	-0.279	0.006077991
ENSBTAG00000003072	ACADVL	2143.012	2500.858	-0.223	0.00611519
ENSBTAG00000034385	GPR162	20.610	45.981	-1.158	0.006148531
ENSBTAG00000008320		233.389	294.196	-0.334	0.006176365
ENSBTAG00000010584	AP2S1	604.587	759.152	-0.328	0.006179672
ENSBTAG00000005356	ST5	3569.115	4306.995	-0.271	0.006248151
ENSBTAG00000017549	KITLG	721.792	479.684	0.589	0.006313354
ENSBTAG00000006695	VCPIP1	587.961	440.468	0.417	0.006313354
ENSBTAG00000005961	CDC42SE2	734.511	577.743	0.346	0.006313354
ENSBTAG00000003100	SMTN	1022.466	1251.350	-0.291	0.006372033
ENSBTAG00000021392	DCAF11	701.622	602.788	0.219	0.006382769
ENSBTAG00000020139	RPL7	8982.419	11191.122	-0.317	0.006496913
ENSBTAG00000022396	SAA3	9.447	28.460	-1.591	0.006526747
ENSBTAG00000008186	UBXN6	696.850	815.553	-0.227	0.006533497
ENSBTAG00000031572		297.526	376.644	-0.340	0.006533497
ENSBTAG00000014773	HMMR	250.977	189.826	0.403	0.00656159
ENSBTAG00000010890	PRMT5	1154.137	938.904	0.298	0.006578754
ENSBTAG00000000773	TTC9C	378.927	309.031	0.294	0.006626188
ENSBTAG00000003971	E2F1	115.581	73.397	0.655	0.006644922
ENSBTAG00000007061	PPP2R5B	374.075	469.349	-0.327	0.006655152
ENSBTAG00000007614	BBS4	843.484	699.192	0.271	0.006658858
ENSBTAG00000033453	MTCH1	4689.316	5347.294	-0.189	0.006658858
ENSBTAG00000020617	TSC2	2042.553	2529.677	-0.309	0.006685867
ENSBTAG00000009005	DUSP15	207.626	159.631	0.379	0.00669147
ENSBTAG00000000897	IQGAP2	112.310	146.357	-0.382	0.00669147
ENSBTAG00000000097	EFCAB14	1142.010	888.015	0.363	0.006772931
ENSBTAG00000000795	NMNAT2	355.814	437.229	-0.297	0.006772931
ENSBTAG00000003174	NDUFAF4	94.284	62.665	0.589	0.006796194
ENSBTAG00000009199	GLIS2	2753.426	3326.670	-0.273	0.006796194
ENSBTAG00000018725	FBLIM1	1650.184	2000.871	-0.278	0.00682744
ENSBTAG00000019081	COL7A1	232.539	303.651	-0.385	0.006831853
ENSBTAG00000016667	ZBTB46	315.626	392.904	-0.316	0.006893213
ENSBTAG00000014554	SNAI1	230.106	303.190	-0.398	0.006936048
ENSBTAG00000046358	PABPC1	19398.330	22599.133	-0.220	0.006936124
ENSBTAG00000012496	MTMR11	119.829	156.498	-0.385	0.00699081
ENSBTAG00000020238	RIMS1	95.506	64.922	0.557	0.006996868
ENSBTAG00000021808	CACNB3	1010.526	1237.460	-0.292	0.007012945
ENSBTAG00000043971	NOTCH3	60.286	40.311	0.581	0.007107115
ENSBTAG00000013111	RRM1	1107.220	923.159	0.262	0.007128055
ENSBTAG00000020791	RAPGEF1	749.865	963.823	-0.362	0.007244209
ENSBTAG00000048062	KDM6B	970.157	1197.898	-0.304	0.007254696
ENSBTAG00000003877	ZCCHC24	334.841	454.881	-0.442	0.007286042
ENSBTAG00000002356	RBM47	450.255	327.155	0.461	0.007302369
ENSBTAG00000031718	OGFR	627.098	486.550	0.366	0.007302369

GeneID	Gene	Mean Counts Juxt	Mean Counts NoEmbryos	Log2 Fold-Change	P-Value (FDR adj)
ENSBTAG00000024042	MORN2	108.263	153.728	-0.506	0.007327358
ENSBTAG00000019214	USP14	812.658	663.502	0.293	0.00742221
ENSBTAG00000010033		6.459	1.520	2.087	0.007523674
ENSBTAG00000003069	MAN1C1	53.154	87.894	-0.726	0.007541217
ENSBTAG00000011368	NOC3L	396.248	319.425	0.311	0.007566387
ENSBTAG00000018164	FNDC4	156.346	222.736	-0.511	0.007580053
ENSBTAG00000018658	TNRC6C	408.020	511.355	-0.326	0.007584066
ENSBTAG00000000848	SNRNP200	3879.047	4773.727	-0.299	0.007628403
ENSBTAG00000012919	MMP15	88.475	64.336	0.460	0.007642938
ENSBTAG00000006139	TRPM4	212.894	276.757	-0.378	0.007642938
ENSBTAG00000011847	ASPN	69.682	23.550	1.565	0.007727827
ENSBTAG00000002820	RBBP7	3013.112	2573.689	0.227	0.007776665
ENSBTAG00000001440	PMM2	859.792	1047.915	-0.285	0.007825272
ENSBTAG00000015198	DZIP1L	192.797	251.195	-0.382	0.00784549
ENSBTAG00000032951	ABHD17C	1194.789	1391.916	-0.220	0.007928548
ENSBTAG00000002050	COA7	68.839	45.369	0.602	0.007930197
ENSBTAG00000015875	FOXM1	98.523	65.315	0.593	0.007930197
ENSBTAG00000015311	PTPRR	638.081	505.792	0.335	0.007930197
ENSBTAG00000038523	ATP1A4	96.057	134.475	-0.485	0.008116558
ENSBTAG00000045604	TTC9	429.919	323.491	0.410	0.008124327
ENSBTAG00000014401	SORBS3	3007.241	3777.446	-0.329	0.008130649
ENSBTAG00000020939	PLAC9	29.886	49.746	-0.735	0.008203393
ENSBTAG00000018936	LSS	573.374	460.243	0.317	0.008211151
ENSBTAG00000016156	MAPK3	2162.188	2547.833	-0.237	0.008225823
ENSBTAG00000014355	MYCBPAP	162.692	206.137	-0.341	0.008253402
ENSBTAG00000008332	ENPEP	64.893	90.781	-0.484	0.008294405
ENSBTAG00000014730	NCAPD2	1069.760	874.358	0.291	0.008315814
ENSBTAG00000001835	GJA1	5882.295	4670.995	0.333	0.008349011
ENSBTAG00000048059	TMEM86A	658.679	536.034	0.297	0.008349011
ENSBTAG00000044175	CENPK	104.055	61.984	0.747	0.008389552
ENSBTAG00000013401	ARHGEF40	383.270	473.690	-0.306	0.008389552
ENSBTAG00000002515		98.681	134.372	-0.445	0.008389552
ENSBTAG00000025400	PARP4	1007.439	1204.640	-0.258	0.008407334
ENSBTAG00000015362	BMP7	1457.837	1200.767	0.280	0.008444408
ENSBTAG00000012987	ULK1	1874.571	2202.838	-0.233	0.008495907
ENSBTAG00000020223	CASQ1	87.823	128.454	-0.549	0.008522218
ENSBTAG00000018600	VGLL4	568.812	659.923	-0.214	0.008590975
ENSBTAG00000015444	LETM2	150.118	204.057	-0.443	0.008609415
ENSBTAG00000023429	PLS1	2931.503	2214.740	0.405	0.008671081
ENSBTAG00000004046	DTX4	31.853	52.459	-0.720	0.008739283
ENSBTAG00000004249	TANC2	253.125	334.996	-0.404	0.008803397
ENSBTAG00000009952	C2H2orf69	75.221	51.756	0.539	0.008939198
ENSBTAG00000005205	DSE	1986.238	1720.582	0.207	0.008939198
ENSBTAG00000002080	NOV	6244.156	4834.979	0.369	0.009081413
ENSBTAG00000021977	PRRC1	1024.917	1227.038	-0.260	0.009081413
ENSBTAG00000015912	DMKN	738.514	924.954	-0.325	0.009083206
ENSBTAG00000038480	FPGT	360.839	277.362	0.380	0.009112658
ENSBTAG00000019183	FUZ	195.266	259.932	-0.413	0.009147241
ENSBTAG00000005670	ARHGEF19	47.186	71.731	-0.604	0.009182977
ENSBTAG00000047389		823.350	962.357	-0.225	0.009183759
ENSBTAG00000007366	HAUS8	265.410	207.856	0.353	0.00919043
ENSBTAG00000012342	LIMA1	5008.675	5770.900	-0.204	0.009218767
ENSBTAG00000017460	PRORSD1	135.359	189.493	-0.485	0.009226946
ENSBTAG00000001146	HIVEP2	750.681	969.547	-0.369	0.009241104
ENSBTAG00000020999	DDB2	550.173	461.763	0.253	0.009271013
ENSBTAG00000005990	S1PR1	15.974	34.292	-1.102	0.009283874
ENSBTAG00000015593	KIAA0753	429.922	356.760	0.269	0.009402188
ENSBTAG00000018691	RHOU	313.432	248.573	0.334	0.009424302
ENSBTAG00000004051	SBDS	3025.110	2621.672	0.207	0.009424302
ENSBTAG00000014603	VAMP1	157.804	209.100	-0.406	0.009424302
ENSBTAG00000018189	CSTB	416.996	591.188	-0.504	0.009427441
ENSBTAG00000004177	TANC1	2123.756	2516.485	-0.245	0.009442888
ENSBTAG00000011899	USP4	1141.812	980.132	0.220	0.00948884
ENSBTAG00000003986	CXXC5	431.385	523.116	-0.278	0.009521855
ENSBTAG00000024815	ANKRD28	345.083	281.149	0.296	0.009644568
ENSBTAG00000005116	FKBP15	1268.766	1123.186	0.176	0.009644568
ENSBTAG00000007586	SYNJ2BP	630.742	524.935	0.265	0.009669798
ENSBTAG00000024476	CKS1B	206.760	146.970	0.492	0.009672952
ENSBTAG00000013112	C7H5orf15	1716.171	1414.944	0.278	0.009672952
ENSBTAG00000017816	FXYD1	11.292	29.420	-1.381	0.009672952

GeneID	Gene	Mean Counts Juxt	Mean Counts NoEmbryos	Log2 Fold-Change	P-Value (FDR adj)
ENSBTAG00000002534	EEF1E1	541.017	444.288	0.284	0.009695624
ENSBTAG00000010253	SYTL1	226.836	287.297	-0.341	0.009698311
ENSBTAG00000019674	CLIP3	736.728	930.871	-0.337	0.009783213
ENSBTAG00000046677	RTN4R	28.045	15.301	0.874	0.009830341
ENSBTAG00000009231	NSDHL	562.262	446.800	0.332	0.009830341
ENSBTAG00000012739	C1QBP	1059.083	862.922	0.296	0.009830341
ENSBTAG00000046841	IRF2BP2	932.402	1123.001	-0.268	0.009830341
ENSBTAG00000021864	TXNDC17	258.271	187.826	0.459	0.00991075
ENSBTAG00000020528	PCOLCE	197.812	253.514	-0.358	0.009925129
ENSBTAG00000001662	EHD3	1291.971	1539.438	-0.253	0.01009025
ENSBTAG00000009024	KCND1	41.029	61.171	-0.576	0.010276893
ENSBTAG00000001401	SLC45A1	2.118	10.112	-2.255	0.010287574
ENSBTAG00000008355	CPSF1	1307.820	1569.082	-0.263	0.010405235
ENSBTAG00000004476	ADHFE1	265.444	348.891	-0.394	0.010405235
ENSBTAG00000014762	ISG20	79.145	52.527	0.591	0.010405828
ENSBTAG00000043969	CALN1	11.617	26.663	-1.199	0.010407638
ENSBTAG00000031261	REPS2	28.524	45.318	-0.668	0.010414003
ENSBTAG00000036102		69.763	43.954	0.666	0.010444166
ENSBTAG00000016269	ME2	603.032	499.753	0.271	0.010455342
ENSBTAG00000021158	SATB1	687.739	577.189	0.253	0.010585577
ENSBTAG00000026613	MSTO1	185.198	230.394	-0.315	0.010637046
ENSBTAG00000004641	PLEKHA6	382.604	287.188	0.414	0.010696836
ENSBTAG00000001142	GNE	662.663	772.620	-0.221	0.010696836
ENSBTAG00000011463	MID1IP1	589.578	460.006	0.358	0.01069856
ENSBTAG00000007866	HS3ST3B1	16.282	33.398	-1.037	0.01074806
ENSBTAG00000040304	HTR3E	52.156	78.374	-0.588	0.010770781
ENSBTAG00000004906	CCNE2	140.832	100.796	0.483	0.010865387
ENSBTAG00000021217	COL11A1	2156.634	2891.013	-0.423	0.010865387
ENSBTAG00000047166	SH2D7	43.183	64.398	-0.577	0.010885473
ENSBTAG00000018560	DNAH3	356.246	429.560	-0.270	0.010920059
ENSBTAG00000001599	SV2A	31.001	46.695	-0.591	0.010933302
ENSBTAG00000000469	PPP2CA	2855.726	2393.681	0.255	0.011026081
ENSBTAG00000021091	ANKFY1	1479.373	1171.363	0.337	0.011057702
ENSBTAG00000006141	WDR93	27.031	43.896	-0.699	0.01107868
ENSBTAG00000014912	FMOD	7600.170	6226.929	0.288	0.011101536
ENSBTAG00000009014	UPK1B	25405.003	23259.275	0.127	0.011184626
ENSBTAG00000008133	ALKBH1	766.282	626.070	0.292	0.011290133
ENSBTAG00000016882	VPS26A	2016.894	1695.370	0.251	0.01129999
ENSBTAG00000007166	CAMKK1	118.097	155.408	-0.396	0.01129999
ENSBTAG00000007606	HNRNPU	5699.479	4865.669	0.228	0.011324984
ENSBTAG00000000057	THBS3	1242.212	960.398	0.371	0.011352811
ENSBTAG00000020399	RNF139	567.318	469.582	0.273	0.011352811
ENSBTAG00000006978	HSD17B4	967.829	1123.689	-0.215	0.011352811
ENSBTAG00000000281	MND1	65.782	40.856	0.687	0.011439174
ENSBTAG00000033669	IL17RC	942.806	790.719	0.254	0.011477515
ENSBTAG00000004912	ANKRD17	3457.217	2972.931	0.218	0.011520407
ENSBTAG00000006526	BCL2L1	696.812	814.653	-0.225	0.011539851
ENSBTAG00000045907	TNFSF13B	6.755	1.587	2.090	0.011551935
ENSBTAG00000014975	SLC4A3	250.915	321.349	-0.357	0.011629583
ENSBTAG00000007783	MYBL2	518.728	353.349	0.554	0.011648371
ENSBTAG00000018103	HMGB1	1317.658	1031.573	0.353	0.011651486
ENSBTAG00000007196	TAGLN	4568.766	6191.895	-0.439	0.011690418
ENSBTAG00000021172	IWS1	827.660	711.709	0.218	0.011701951
ENSBTAG00000010694	BICC1	4546.622	5812.476	-0.354	0.011710973
ENSBTAG00000017674	SCNN1D	63.354	87.484	-0.466	0.011731759
ENSBTAG00000004237	BTC	7.255	2.060	1.816	0.011791609
ENSBTAG00000017401	TBK1	492.430	393.565	0.323	0.011791609
ENSBTAG00000002921	RMDN3	354.399	289.920	0.290	0.011834036
ENSBTAG00000048271	MICAL3	921.929	1148.012	-0.316	0.011834036
ENSBTAG00000020344	SLC44A3	100.857	141.665	-0.490	0.011834036
ENSBTAG00000012944	USP35	136.157	175.111	-0.363	0.011838224
ENSBTAG00000015908	MBOAT7	1242.472	1052.855	0.239	0.011861313
ENSBTAG00000017721	METTL13	264.215	210.557	0.328	0.011862918
ENSBTAG00000015209	MXD4	746.909	909.595	-0.284	0.011870361
ENSBTAG00000009819	CDC20	152.154	104.616	0.540	0.011871166
ENSBTAG00000012738	ZNF827	237.766	307.566	-0.371	0.011904072
ENSBTAG00000016315	COTL1	3231.219	3930.197	-0.283	0.011969011
ENSBTAG00000008462	FAM43A	22.700	41.335	-0.865	0.011969011
ENSBTAG00000034626	FBXO16	86.894	62.688	0.471	0.012047191
ENSBTAG00000014156	AMN1	346.856	266.598	0.380	0.012058835

GeneID	Gene	Mean Counts Juxt	Mean Counts NoEmbryos	Log2 Fold-Change	P-Value (FDR adj)
ENSBTAG00000001250	TFAP2A	1554.195	1899.369	-0.289	0.01208764
ENSBTAG00000014224	IGSF9B	18.992	38.049	-1.002	0.012135048
ENSBTAG00000020533	FBXO34	435.668	533.473	-0.292	0.012217887
ENSBTAG00000004851	NCKAP5L	2001.616	2307.628	-0.205	0.012256718
ENSBTAG00000014824	MMP14	2064.189	2688.265	-0.381	0.012256718
ENSBTAG00000000562	TOMM20	1589.273	1310.284	0.278	0.01227391
ENSBTAG00000011125	MYO9B	1662.501	1901.221	-0.194	0.012306672
ENSBTAG00000015612	UTP6	1951.140	2294.316	-0.234	0.012313415
ENSBTAG00000007446	NGF	100.031	61.882	0.693	0.012320846
ENSBTAG00000044003	TEX10	759.535	659.714	0.203	0.012320846
ENSBTAG00000014588	RSL1D1	1618.583	1321.499	0.293	0.01247182
ENSBTAG00000002941	FES	261.972	208.469	0.330	0.012474888
ENSBTAG00000027431	ZNF226	588.585	510.410	0.206	0.012494973
ENSBTAG00000011458	CPXM1	417.021	343.886	0.278	0.012501783
ENSBTAG00000004021	CDK2	295.543	225.855	0.388	0.012753921
ENSBTAG00000039766	FBRSL1	1211.474	1404.511	-0.213	0.012796029
ENSBTAG00000021999	CPT1A	688.163	884.005	-0.361	0.012796029
ENSBTAG00000009294	DEGS2	15.592	35.712	-1.196	0.012796029
ENSBTAG00000019325	TRMT1	298.706	369.395	-0.306	0.012844404
ENSBTAG00000046013	SSLP1	34.494	20.296	0.765	0.012847439
ENSBTAG00000002211	MAPK8IP3	727.126	868.959	-0.257	0.012847439
ENSBTAG00000000283	CSF1	1194.382	1621.376	-0.441	0.012847439
ENSBTAG00000016263	SLC25A14	277.873	223.705	0.313	0.012864351
ENSBTAG00000031299	TTC17	938.101	826.248	0.183	0.012864351
ENSBTAG00000002823	MPZL1	2056.690	1834.469	0.165	0.012864351
ENSBTAG00000013253	THAP4	635.010	800.155	-0.333	0.012864351
ENSBTAG00000018810	THBS2	215.105	296.332	-0.462	0.012864351
ENSBTAG00000039335	ARRDC2	119.482	230.358	-0.947	0.012864351
ENSBTAG00000004315	HDLBP	5739.846	6748.233	-0.233	0.012997134
ENSBTAG00000015106	DSP	3018.424	2546.752	0.245	0.013011835
ENSBTAG00000033679	HLCS	500.065	571.039	-0.191	0.013018326
ENSBTAG00000032481	DAPL1	53.534	81.012	-0.598	0.013086151
ENSBTAG00000024097	MRPS15	290.739	384.632	-0.404	0.013104965
ENSBTAG00000016911	ARHGAP23	4086.895	5057.670	-0.307	0.013114526
ENSBTAG00000011532	MLLT6	2166.651	2769.533	-0.354	0.013133171
ENSBTAG00000030839	MUM1	657.324	761.665	-0.213	0.013271096
ENSBTAG00000000030	RDM1	62.054	39.181	0.663	0.013287432
ENSBTAG00000037968	PCDHGB2	11.106	22.644	-1.028	0.013303601
ENSBTAG00000012885	ACAT1	1154.260	977.570	0.240	0.013315536
ENSBTAG00000040555	FBXL19	488.210	597.221	-0.291	0.013379962
ENSBTAG00000030608	SWI5	307.948	382.581	-0.313	0.013379962
ENSBTAG00000014375	TMCC3	629.282	526.239	0.258	0.013419683
ENSBTAG00000024015	PTPRM	560.622	693.578	-0.307	0.013600172
ENSBTAG00000046166		25.959	42.282	-0.704	0.013654385
ENSBTAG00000008074	C1QTNF6	0.966	5.997	-2.634	0.013654385
ENSBTAG00000018385	DNAJC8	924.336	774.282	0.256	0.013711269
ENSBTAG00000004499	RGS3	237.571	330.464	-0.476	0.013721709
ENSBTAG00000001983	SMAGP	87.756	63.099	0.476	0.013744576
ENSBTAG00000005870	FANCL	571.905	455.594	0.328	0.013749675
ENSBTAG00000018622	PCBP4	1756.928	2023.440	-0.204	0.013756997
ENSBTAG00000006322	DENND5A	2929.689	3710.915	-0.341	0.013906183
ENSBTAG00000044129	ST6GALNAC6	558.248	443.560	0.332	0.013914155
ENSBTAG00000003826	SCN1B	128.631	183.771	-0.515	0.013914155
ENSBTAG00000013016	GNAI3	1500.055	1261.251	0.250	0.013944207
ENSBTAG00000008102	CRTAC1	70.914	112.069	-0.660	0.014075982
ENSBTAG00000030705	DACT3	38.836	60.112	-0.630	0.014084713
ENSBTAG00000000153	LRFN3	166.605	214.886	-0.367	0.014085084
ENSBTAG00000000099	CERS2	2206.184	1981.345	0.155	0.014094096
ENSBTAG00000008101	PCSK5	331.434	403.464	-0.284	0.014094096
ENSBTAG00000006837	UBA6	793.538	645.617	0.298	0.014245846
ENSBTAG00000020345	CNN3	3594.480	4130.589	-0.201	0.014304505
ENSBTAG00000020079	MAP3K4	1331.187	1558.331	-0.227	0.014353131
ENSBTAG00000017339	RUNX1T1	832.720	1019.587	-0.292	0.014386153
ENSBTAG00000018546	LRBA	543.812	697.414	-0.359	0.014400169
ENSBTAG00000040559		38.222	60.872	-0.671	0.014442575
ENSBTAG00000013612	MBLAC2	120.494	87.336	0.464	0.014472469
ENSBTAG00000019218	ATP6V0A1	883.686	1051.700	-0.251	0.014733111
ENSBTAG00000035782	METTL22	214.469	269.167	-0.328	0.014824132
ENSBTAG00000010109	CDK1	153.025	107.014	0.516	0.014914397
ENSBTAG00000019180	AP2A1	2193.978	2624.791	-0.259	0.014939687

GeneID	Gene	Mean Counts Juxt	Mean Counts NoEmbryos	Log2 Fold-Change	P-Value (FDR adj)
ENSBTAG00000019174	ZNF710	100.533	74.207	0.438	0.014941888
ENSBTAG00000016228	NMD3	730.157	611.220	0.257	0.014948127
ENSBTAG00000011338	NREP	118.708	83.624	0.505	0.014953956
ENSBTAG00000016896	HERPUD1	991.028	1213.571	-0.292	0.014974677
ENSBTAG00000014119	PRKCZ	400.141	472.555	-0.240	0.015048663
ENSBTAG00000004706	SUV39H1	185.709	142.889	0.378	0.015058942
ENSBTAG00000013726	RNPEP	999.018	795.878	0.328	0.01511659
ENSBTAG00000010402	MYH9	16468.629	21071.624	-0.356	0.01511659
ENSBTAG00000002084	UNC5C	2834.982	3483.869	-0.297	0.015133781
ENSBTAG00000019864	MAPK15	46.746	67.597	-0.532	0.015173948
ENSBTAG00000005340	SERGEF	171.193	214.729	-0.327	0.015209621
ENSBTAG00000010303	ICAM1	421.935	597.117	-0.501	0.015254362
ENSBTAG00000016194	FBXO32	246.668	342.885	-0.475	0.015272488
ENSBTAG00000040575	KCTD5	442.791	374.492	0.242	0.015293457
ENSBTAG00000000473	ATP10D	157.158	204.742	-0.382	0.015354475
ENSBTAG00000019929	ITGAV	2764.817	3752.984	-0.441	0.015363142
ENSBTAG00000047586	NPY1R	41.317	22.923	0.850	0.015386223
ENSBTAG00000014650	NFATC2IP	169.836	136.835	0.312	0.015386223
ENSBTAG00000011988	KIAA0100	881.540	1107.143	-0.329	0.015386223
ENSBTAG00000016413	DUSP26	14.735	28.776	-0.966	0.015386223
ENSBTAG00000005436	SHQ1	485.273	385.135	0.333	0.015497205
ENSBTAG00000001105	ANXA4	6275.909	5420.567	0.211	0.015497205
ENSBTAG00000016192	MDH1B	157.600	201.107	-0.352	0.015497205
ENSBTAG00000018196	WDR43	1308.064	1074.626	0.284	0.015700599
ENSBTAG00000016619	MIS18A	39.670	21.220	0.903	0.015994295
ENSBTAG00000008191	SLC39A7	1451.272	1702.754	-0.231	0.015994295
ENSBTAG00000000266	NAB1	1656.106	1365.120	0.279	0.01604397
ENSBTAG00000002690	BLZF1	559.330	472.065	0.245	0.01604397
ENSBTAG00000019120	WDHD1	285.823	204.267	0.485	0.016116344
ENSBTAG00000014551	TNFAIP8	126.955	92.682	0.454	0.01618841
ENSBTAG00000018732	HSPA12B	234.716	288.242	-0.296	0.016300652
ENSBTAG00000014390	MTMR9	80.747	112.601	-0.480	0.016374596
ENSBTAG00000034613	MROH6	9.391	20.433	-1.122	0.016400608
ENSBTAG00000015426	PDLIM4	1350.710	1688.038	-0.322	0.016440978
ENSBTAG00000007461	C20H5orf34	143.084	106.412	0.427	0.01649187
ENSBTAG00000017812	ALS2CL	917.971	1057.033	-0.203	0.016571729
ENSBTAG00000007809	PPP1R36	412.750	511.485	-0.309	0.016571729
ENSBTAG00000011591	KRR1	471.502	391.181	0.269	0.016578401
ENSBTAG00000004877	TRAIP	33.448	19.846	0.753	0.016699603
ENSBTAG00000020032	CEP126	38.913	63.036	-0.696	0.01674559
ENSBTAG00000034580	TMSB4X	249.713	200.751	0.315	0.016758798
ENSBTAG00000015293	NXPH3	23.685	40.902	-0.788	0.016840605
ENSBTAG00000038696	RAB8A	1590.498	1369.457	0.216	0.016863946
ENSBTAG00000017063	EPB41L4B	1624.993	1800.121	-0.148	0.016975205
ENSBTAG00000030648	MPST	582.123	476.641	0.288	0.01708364
ENSBTAG00000047827	RENBP	52.307	81.734	-0.644	0.017188281
ENSBTAG00000018731		42.436	27.356	0.633	0.017222037
ENSBTAG00000031107	HS3ST3A1	36.983	57.800	-0.644	0.017222037
ENSBTAG00000004931	POLE2	98.981	69.348	0.513	0.01741161
ENSBTAG00000020334	ENTPD5	365.847	301.434	0.279	0.01741161
ENSBTAG00000004187	WDR66	71.118	101.425	-0.512	0.017443283
ENSBTAG00000019581	PLEKHF2	224.561	176.818	0.345	0.01747662
ENSBTAG00000016572	USP37	234.350	182.310	0.362	0.017640457
ENSBTAG00000012858	NT5C2	2011.786	1706.496	0.237	0.017640457
ENSBTAG00000018423	DDX5	7993.590	6826.575	0.228	0.017640457
ENSBTAG00000006755	C15H11orf58	2143.499	1836.660	0.223	0.017640457
ENSBTAG00000007767	TBX15	27.628	44.201	-0.678	0.017640457
ENSBTAG00000014151	RCSD1	616.116	760.038	-0.303	0.017692258
ENSBTAG00000023629		46.880	71.302	-0.605	0.017811542
ENSBTAG00000003109	ITM2B	8861.246	7377.328	0.264	0.017880284
ENSBTAG00000012239	SLC37A3	837.541	962.288	-0.200	0.017880284
ENSBTAG00000046176	SPEG	1520.448	1778.082	-0.226	0.017880284
ENSBTAG00000031933	ALOX12E	37.520	62.153	-0.728	0.018017313
ENSBTAG00000018589	RFC2	268.804	202.801	0.406	0.018070757
ENSBTAG00000001332	MYO1C	4342.129	4898.464	-0.174	0.018070757
ENSBTAG00000015766	ZFPM1	2548.055	3091.456	-0.279	0.018070757
ENSBTAG00000005313	EPHB3	332.930	417.071	-0.325	0.018070757
ENSBTAG00000014916	GJC2	42.762	64.413	-0.591	0.018070757
ENSBTAG00000004387	MTPAP	457.771	385.921	0.246	0.01814512
ENSBTAG00000014727	RFC4	184.807	136.962	0.432	0.018191223

GeneID	Gene	Mean Counts Juxt	Mean Counts NoEmbryos	Log2 Fold-Change	P-Value (FDR adj)
ENSBTAG00000020308	EIF4G2	18517.327	21139.444	-0.191	0.018199418
ENSBTAG00000035319	MAD2L1	83.195	55.812	0.576	0.018239335
ENSBTAG00000020485	ARRB1	133.610	202.232	-0.598	0.018302832
ENSBTAG00000010731	CDKN2D	45.541	28.449	0.679	0.018321304
ENSBTAG00000039015	TMEM145	119.473	152.250	-0.350	0.018321304
ENSBTAG00000021744	PSMC3	1363.766	1113.002	0.293	0.018398896
ENSBTAG00000020164	BAZ1A	541.688	453.726	0.256	0.01841852
ENSBTAG00000009434	PAQR6	76.385	112.147	-0.554	0.018551596
ENSBTAG00000020547	BCAP31	666.656	569.699	0.227	0.018569697
ENSBTAG00000006951	LMO2	7.316	2.227	1.716	0.018616594
ENSBTAG00000007395	ALS2	1038.207	826.628	0.329	0.018616594
ENSBTAG00000016961	RAP2B	829.017	980.834	-0.243	0.018657601
ENSBTAG00000004786	TMEM134	166.945	128.324	0.380	0.01867659
ENSBTAG00000007330	STXBP3	735.730	600.003	0.294	0.018765953
ENSBTAG00000003619	SEC24D	2701.188	3350.706	-0.311	0.018788512
ENSBTAG00000011997	ZMIZ2	1280.831	1612.501	-0.332	0.018788512
ENSBTAG00000021919	NAV1	940.099	1170.023	-0.316	0.018835492
ENSBTAG00000021639	ARC	4.684	13.367	-1.513	0.018932779
ENSBTAG00000020444	MAST2	1708.015	1479.364	0.207	0.01905993
ENSBTAG00000014226	RPL34	3982.779	5044.507	-0.341	0.019178999
ENSBTAG00000000559	PLTP	108.440	158.992	-0.552	0.01948117
ENSBTAG00000007960	TOP1	1335.721	1129.691	0.242	0.019501723
ENSBTAG00000015885	PPFIA4	426.314	526.401	-0.304	0.019530219
ENSBTAG00000015535	NEK8	125.682	97.385	0.368	0.019555038
ENSBTAG00000020748	FAM76B	298.251	232.649	0.358	0.019555038
ENSBTAG00000010682	DDR1	6733.195	7683.391	-0.190	0.019555038
ENSBTAG00000009103	UBLCP1	1287.319	1084.082	0.248	0.019662456
ENSBTAG00000038335		255.175	329.020	-0.367	0.019674158
ENSBTAG00000009618	NEK2	45.519	28.215	0.690	0.019755075
ENSBTAG00000019838	SHC1	6029.687	5514.567	0.129	0.019835063
ENSBTAG00000038477	GGCX	1134.068	1306.973	-0.205	0.019835063
ENSBTAG00000002936	PRRX2	38.424	58.432	-0.605	0.019835063
ENSBTAG00000002340	STEAP4	121.901	296.446	-1.282	0.019835063
ENSBTAG00000014804	HNRNPDL	3419.624	2842.127	0.267	0.019996621
ENSBTAG00000019267	MMP2	9899.986	12073.346	-0.286	0.02009882
ENSBTAG00000000875	CEP131	380.832	456.694	-0.262	0.020134398
ENSBTAG00000007217	TMEM94	1682.495	1968.281	-0.226	0.02017247
ENSBTAG00000021025	P3H2	1631.893	1233.971	0.403	0.020278104
ENSBTAG00000019298	STRADB	478.559	400.855	0.256	0.020278104
ENSBTAG00000006108	MMP11	108.944	145.123	-0.414	0.020305952
ENSBTAG00000020964	STRIP1	469.774	367.910	0.353	0.020336677
ENSBTAG00000012059	MVD	312.252	252.369	0.307	0.020356348
ENSBTAG00000012582	IARS2	1218.621	1408.743	-0.209	0.020449377
ENSBTAG00000003757	DNAJA2	1405.422	1201.484	0.226	0.020584383
ENSBTAG00000003894	NDRG4	10.435	22.878	-1.132	0.020612089
ENSBTAG00000004855	PRDX6	4429.812	3719.622	0.252	0.020622117
ENSBTAG00000000137	FRYL	2224.671	1943.625	0.195	0.020622117
ENSBTAG00000019133	ZNF326	1032.291	831.103	0.313	0.020683441
ENSBTAG00000019053	MAP9	52.641	73.794	-0.487	0.020756368
ENSBTAG00000014891	SRSF7	1445.341	1139.287	0.343	0.020830266
ENSBTAG00000033248	CDH3	799.706	1008.427	-0.335	0.0211163
ENSBTAG00000018363	RBM48	246.342	200.558	0.297	0.021124929
ENSBTAG00000006326	ALDH1L2	658.105	860.578	-0.387	0.021124929
ENSBTAG00000038020		117.134	91.220	0.361	0.021152783
ENSBTAG00000002576	GLDN	96.781	150.966	-0.641	0.021286102
ENSBTAG00000013669	KIF22	193.473	138.470	0.483	0.021326218
ENSBTAG00000039196		155.116	209.782	-0.436	0.021480785
ENSBTAG00000000494	PDE4D	108.117	150.846	-0.480	0.021490118
ENSBTAG00000010627	SF3B3	3321.411	3007.713	0.143	0.021499292
ENSBTAG00000015183	TPCN2	737.650	869.173	-0.237	0.021499675
ENSBTAG00000013392	PLD2	1428.927	1634.881	-0.194	0.021527325
ENSBTAG00000000977	CADM1	524.791	654.308	-0.318	0.021537382
ENSBTAG00000010635	RAB3A	56.646	79.864	-0.496	0.021540871
ENSBTAG00000001948	VTI1B	445.742	524.234	-0.234	0.021635785
ENSBTAG00000003458	CDCA7	166.061	112.400	0.563	0.021774329
ENSBTAG00000002620	DNA2	53.223	34.097	0.642	0.021793186
ENSBTAG00000012880	DNLZ	99.128	145.051	-0.549	0.021874937
ENSBTAG00000004155	SPATA20	375.787	443.867	-0.240	0.02194398
ENSBTAG00000016746	UBE2C	260.017	174.926	0.572	0.022001908
ENSBTAG00000030384		4926.353	5659.264	-0.200	0.022140352

GeneID	Gene	Mean Counts Juxt	Mean Counts NoEmbryos	Log2 Fold-Change	P-Value (FDR adj)
ENSBTAG00000011424	TPM2	1161.673	1513.070	-0.381	0.022140352
ENSBTAG00000020567	HNRNPLL	1183.937	962.281	0.299	0.022235945
ENSBTAG00000009736	CDC42BPG	259.534	333.194	-0.360	0.022377406
ENSBTAG00000010531	CYP1B1	478.104	770.647	-0.689	0.022421312
ENSBTAG00000017672	HAS1	12.766	23.912	-0.905	0.022539152
ENSBTAG00000046364		1686.016	2013.901	-0.256	0.0227037
ENSBTAG00000006016	GTPBP2	636.117	551.716	0.205	0.022721198
ENSBTAG00000002282	EIF1	1709.335	2044.690	-0.258	0.022721198
ENSBTAG00000006862	MEIS3	494.839	633.337	-0.356	0.022721198
ENSBTAG00000014358	EVA1B	165.742	223.855	-0.434	0.022739182
ENSBTAG00000013290	DYSF	139.508	175.039	-0.327	0.022991633
ENSBTAG00000012044	RPL13	8535.356	10479.337	-0.296	0.02306579
ENSBTAG00000006296	VMA21	914.672	778.202	0.233	0.02309971
ENSBTAG00000018088	SETBP1	44.425	64.087	-0.529	0.023102217
ENSBTAG00000003947	SSBP4	644.815	776.225	-0.268	0.023162001
ENSBTAG00000011179	PDCD2	265.321	214.321	0.308	0.023273241
ENSBTAG00000008134	BDNF	1409.297	1615.567	-0.197	0.023273241
ENSBTAG00000016465	DHCR7	1050.984	870.647	0.272	0.023340408
ENSBTAG00000009493	BCL3	803.490	1078.056	-0.424	0.023560909
ENSBTAG00000002917	PRKAG2	652.167	764.233	-0.229	0.023582207
ENSBTAG00000040042	GRIN2C	33.504	53.265	-0.669	0.023582207
ENSBTAG00000007833		982.764	1200.090	-0.288	0.023598556
ENSBTAG00000040338	OBSL1	417.176	512.646	-0.297	0.023598556
ENSBTAG00000012687	INSR	777.854	987.943	-0.345	0.023598556
ENSBTAG00000007503	STRC	1.133	7.613	-2.748	0.023611357
ENSBTAG00000018635	ATP1A3	35.371	51.466	-0.541	0.023752562
ENSBTAG00000000436	TNFAIP3	79.010	157.748	-0.998	0.023835406
ENSBTAG00000020441	HMG20A	1333.605	1186.826	0.168	0.023977032
ENSBTAG00000010982	UBE2B	1436.693	1112.435	0.369	0.024068745
ENSBTAG00000014883	GABARAP	3680.809	4376.912	-0.250	0.024158435
ENSBTAG00000020938	TWF1	611.986	514.688	0.250	0.024322306
ENSBTAG00000009384	AGTRAP	1851.233	1643.136	0.172	0.024322306
ENSBTAG00000019672		375.648	467.001	-0.314	0.02436101
ENSBTAG00000017873	USF1	829.204	717.474	0.209	0.024376107
ENSBTAG00000004291		278.464	335.507	-0.269	0.024376107
ENSBTAG00000000220	NEK10	39.442	57.832	-0.552	0.024384274
ENSBTAG00000015109	TOB2	1214.497	1510.141	-0.314	0.024410299
ENSBTAG00000047658	PHF7	143.171	178.977	-0.322	0.02442432
ENSBTAG00000010849	ANKRD23	63.306	90.338	-0.513	0.024690581
ENSBTAG00000017527	CRYBG1	1126.640	916.167	0.298	0.02476546
ENSBTAG00000024787	HAUS3	329.979	250.861	0.395	0.024822252
ENSBTAG00000043571	ND2	47336.714	63118.267	-0.415	0.024822252
ENSBTAG00000007036	SLC17A7	21.804	36.180	-0.731	0.024822252
ENSBTAG00000006716	PTGS1	158.456	115.096	0.461	0.02483668
ENSBTAG00000006843	UTP15	702.275	606.342	0.212	0.024963042
ENSBTAG00000020243	SVEP1	169.036	225.968	-0.419	0.024963042
ENSBTAG00000011635	CENPN	73.992	49.069	0.593	0.024980271
ENSBTAG00000025964	MAST4	602.163	765.454	-0.346	0.024981932
ENSBTAG00000003505	DCN	40273.046	34349.820	0.230	0.025061352
ENSBTAG00000018613	NOL8	977.458	835.095	0.227	0.025073444
ENSBTAG00000007130	ESF1	481.938	386.016	0.320	0.025083528
ENSBTAG00000013406	CSRP2	258.853	326.460	-0.335	0.025083528
ENSBTAG00000004742	RUNX1	295.449	380.446	-0.365	0.025083528
ENSBTAG00000008409	MYC	4185.186	3568.020	0.230	0.025113059
ENSBTAG00000011083	POLD1	304.901	240.664	0.341	0.025134972
ENSBTAG00000016794		8.356	19.129	-1.195	0.025172747
ENSBTAG00000006404	CENPT	118.871	83.384	0.512	0.025491829
ENSBTAG00000019743	CHTF18	147.758	106.126	0.477	0.025579852
ENSBTAG00000011578	CD44	3904.687	4715.175	-0.272	0.025756827
ENSBTAG00000017604	RAB13	1023.089	1241.715	-0.279	0.025756827
ENSBTAG00000014782	STAB1	49.231	71.323	-0.535	0.025756827
ENSBTAG00000002527	ZSWIM4	267.926	362.424	-0.436	0.02578019
ENSBTAG00000004662	SLC16A12	20.285	9.913	1.033	0.025888368
ENSBTAG00000001328	SLBP	603.650	493.546	0.291	0.025888368
ENSBTAG00000005969	EIF2S2	1847.983	1626.015	0.185	0.025910208
ENSBTAG00000016224	RPS7	13085.812	15632.585	-0.257	0.02598242
ENSBTAG00000000638	CDT1	105.952	69.773	0.603	0.026161706
ENSBTAG00000002918	RAD51	185.143	149.702	0.307	0.026429447
ENSBTAG00000007963	KIDINS220	2982.220	3605.531	-0.274	0.026491847
ENSBTAG00000002341	ETS1	392.266	513.089	-0.387	0.026524001

GeneID	Gene	Mean Counts Juxt	Mean Counts NoEmbryos	Log2 Fold-Change	P-Value (FDR adj)
ENSBTAG00000001617	G2E3	433.517	327.783	0.403	0.026552974
ENSBTAG00000027626	GOLGA7	941.134	802.054	0.231	0.026588117
ENSBTAG00000018744	MGAT5	126.364	180.300	-0.513	0.026589501
ENSBTAG00000017164	LARP4	405.704	325.793	0.316	0.026665059
ENSBTAG00000018908	GFOD2	76.542	105.372	-0.461	0.026894303
ENSBTAG00000007753	KIFC2	340.109	407.932	-0.262	0.026926905
ENSBTAG00000009287	EBP	247.428	204.182	0.277	0.026986489
ENSBTAG00000009214	ETS2	196.055	151.502	0.372	0.027139096
ENSBTAG00000015363	CDC42SE1	953.268	1066.934	-0.163	0.027334088
ENSBTAG00000009345	AMZ2	656.353	757.607	-0.207	0.027344359
ENSBTAG00000009470	CLIC4	4977.137	5997.112	-0.269	0.027344359
ENSBTAG00000032427	FHOD1	393.378	490.428	-0.318	0.027399087
ENSBTAG00000000245	NHSL1	448.381	337.424	0.410	0.027434952
ENSBTAG00000039731	RND3	2857.923	2305.918	0.310	0.027434952
ENSBTAG00000020824	KRT10	29.082	50.043	-0.783	0.027471361
ENSBTAG00000011487	PLEKHS1	11.274	28.672	-1.347	0.027678906
ENSBTAG00000021576	LMOD1	46.417	72.616	-0.646	0.027730212
ENSBTAG00000001564	PDE4DIP	2333.213	2724.474	-0.224	0.027862056
ENSBTAG00000005523	XYLT1	263.048	458.515	-0.802	0.027888118
ENSBTAG00000017866	CD36	26.494	14.599	0.860	0.027890575
ENSBTAG00000004147	FBH1	1250.566	1410.982	-0.174	0.027890575
ENSBTAG00000012851	SLC5A1	11.171	22.852	-1.033	0.028143683
ENSBTAG00000017150	EHF	1.538	7.402	-2.267	0.028143683
ENSBTAG00000001872	ORC6	129.354	97.935	0.401	0.028606661
ENSBTAG00000019984	GINS1	396.069	312.728	0.341	0.02863994
ENSBTAG00000030470		926.233	1074.441	-0.214	0.028649698
ENSBTAG00000030646	KCTD17	371.184	443.000	-0.255	0.028649698
ENSBTAG00000010620	ATP6V1B1	293.333	356.005	-0.279	0.028662547
ENSBTAG00000014211	FOXP4	1549.923	1888.942	-0.285	0.028662547
ENSBTAG00000026909		462.648	399.726	0.211	0.028752271
ENSBTAG00000017086	GRB10	565.924	664.900	-0.233	0.028752271
ENSBTAG00000004028	POLK	975.506	804.277	0.278	0.028834515
ENSBTAG00000014731	GAPDH	14932.668	17785.702	-0.252	0.028906403
ENSBTAG00000010502	SERTAD3	456.500	379.743	0.266	0.02892281
ENSBTAG00000016026	PCOLCE2	1186.055	996.274	0.252	0.02892281
ENSBTAG00000018828	ATN1	5048.638	5919.207	-0.230	0.02892281
ENSBTAG00000011885	NNT	1406.817	1683.125	-0.259	0.029130204
ENSBTAG00000010047	TIAM2	108.176	138.559	-0.357	0.029130204
ENSBTAG00000002758	THBD	1073.797	696.015	0.626	0.029160403
ENSBTAG00000016984	PTPN9	863.244	956.823	-0.148	0.029160403
ENSBTAG00000010526	PLPP1	1368.783	1610.475	-0.235	0.029160403
ENSBTAG00000002846	TRAF3IP3	218.833	277.709	-0.344	0.029160403
ENSBTAG00000004005	WDR7	385.411	514.177	-0.416	0.029160403
ENSBTAG00000019777	CDCA3	117.452	80.869	0.538	0.029167845
ENSBTAG00000044092	IQCK	365.451	439.161	-0.265	0.029315619
ENSBTAG00000032137	PNPLA6	590.633	723.948	-0.294	0.029662627
ENSBTAG00000004259	HPCAL1	200.858	264.075	-0.395	0.029662627
ENSBTAG00000018046	B3GNT2	258.361	199.601	0.372	0.029693871
ENSBTAG00000017318	TMEM178A	104.091	75.648	0.460	0.029697567
ENSBTAG00000007605	FKBP4	1321.806	1123.159	0.235	0.029697567
ENSBTAG00000020115	UBE2O	1019.179	1181.698	-0.213	0.029697567
ENSBTAG00000038375	STOM	809.581	1044.933	-0.368	0.029697567
ENSBTAG00000014724	EIF4A2	5561.945	4903.423	0.182	0.02970034
ENSBTAG00000020548	AZIN2	24.983	42.543	-0.768	0.02970034
ENSBTAG00000006616	PTPN1	680.979	567.709	0.262	0.029721196
ENSBTAG00000001257	AGTPBP1	242.899	288.523	-0.248	0.02973661
ENSBTAG00000000667	APOL3	8.494	30.140	-1.827	0.029788486
ENSBTAG00000037921	OVCH2	13.989	29.035	-1.053	0.029851508
ENSBTAG00000012030	TTLL1	210.894	259.040	-0.297	0.029889534
ENSBTAG00000047083		260.509	215.028	0.277	0.029933355
ENSBTAG00000013185	TIMD4	108.354	83.878	0.369	0.030019475
ENSBTAG00000013727	UMPS	616.458	523.525	0.236	0.030019475
ENSBTAG00000046556	SOX4	201.912	267.705	-0.407	0.030019475
ENSBTAG00000012184	PTTG1	114.694	76.158	0.591	0.03015889
ENSBTAG00000025280	SERPINB6	3075.675	2720.822	0.177	0.030247608
ENSBTAG00000020619	PKD1	1409.806	1700.823	-0.271	0.030247608
ENSBTAG00000003033	GADD45G	1511.226	1152.554	0.391	0.030423699
ENSBTAG00000019658	ASB16	43.229	59.982	-0.473	0.030595479
ENSBTAG00000012873	SNX6	1203.444	1048.232	0.199	0.030609576
ENSBTAG00000005314	MFN2	923.446	770.211	0.262	0.030612233

GeneID	Gene	Mean Counts Juxt	Mean Counts NoEmbryos	Log2 Fold-Change	P-Value (FDR adj)
ENSBTAG00000020714	DDX19B	613.547	532.501	0.204	0.030628689
ENSBTAG00000002981	PIMREG	64.632	41.001	0.657	0.030670671
ENSBTAG00000001323	CENPC	656.275	528.216	0.313	0.030670671
ENSBTAG00000006160	SUOX	316.253	378.810	-0.260	0.030743501
ENSBTAG00000006989	SEMA4F	1068.536	1207.146	-0.176	0.030935279
ENSBTAG00000021447	SIM2	515.866	611.827	-0.246	0.031031675
ENSBTAG00000008633	SLX1A	661.978	779.009	-0.235	0.031064064
ENSBTAG00000021469	CTTNBP2	2935.500	3473.341	-0.243	0.031095487
ENSBTAG00000025931	NEU3	269.783	209.502	0.365	0.031110592
ENSBTAG00000006239		97.079	74.018	0.391	0.031170786
ENSBTAG00000006353	TXNL4B	339.576	268.860	0.337	0.031180261
ENSBTAG00000000501	KLHL13	18.905	32.080	-0.763	0.031180261
ENSBTAG00000001776	SIRT2	1335.738	1586.247	-0.248	0.031274644
ENSBTAG00000018579	DOK1	237.830	193.101	0.301	0.031363034
ENSBTAG00000015019	STN1	262.824	214.796	0.291	0.031363034
ENSBTAG00000014764	CD9	6555.670	5866.662	0.160	0.031363034
ENSBTAG00000016057	CSRP1	4316.472	5082.737	-0.236	0.031417999
ENSBTAG00000039190	SLC9A5	53.942	130.945	-1.279	0.031600574
ENSBTAG00000005726	HNRNPA2B1	6849.541	5883.304	0.219	0.031704333
ENSBTAG00000048017	PRR16	25.918	39.434	-0.605	0.031710086
ENSBTAG00000017618	MAP3K10	361.047	439.242	-0.283	0.031781661
ENSBTAG00000005654	TMSB10	2865.040	3727.776	-0.380	0.032045071
ENSBTAG00000017284	RHBDL1	651.096	808.663	-0.313	0.032101536
ENSBTAG00000013099	ALDOC	337.943	399.174	-0.240	0.032190535
ENSBTAG00000045550	TSPAN6	713.154	589.781	0.274	0.032212845
ENSBTAG00000015510	EPHB6	827.278	683.684	0.275	0.032273471
ENSBTAG00000020169	CEPT1	420.523	347.521	0.275	0.032552463
ENSBTAG00000021965	SUB1	2198.467	1823.796	0.270	0.032616101
ENSBTAG00000021410	C1GALT1C1	374.722	315.154	0.250	0.03268083
ENSBTAG00000038171		18.254	35.248	-0.949	0.03268083
ENSBTAG00000017846	F11R	3898.373	3345.321	0.221	0.032691047
ENSBTAG00000020983	RRAS	848.693	1194.328	-0.493	0.032691047
ENSBTAG00000023106		325.566	385.509	-0.244	0.032728583
ENSBTAG00000004976	CDCA7L	319.116	234.629	0.444	0.032736871
ENSBTAG00000009738	MGAT4B	1610.279	1399.659	0.202	0.032736871
ENSBTAG00000019463	SLC25A39	2113.719	2498.395	-0.241	0.032736871
ENSBTAG00000047214	TRAPPC1	314.559	388.181	-0.303	0.032736871
ENSBTAG00000006383		515.603	695.559	-0.432	0.032736871
ENSBTAG00000005244	RASL11A	143.299	194.485	-0.441	0.032736871
ENSBTAG00000021252	TMEM35A	8.280	18.346	-1.148	0.032810091
ENSBTAG00000017375	FAM241A	108.798	80.510	0.434	0.03287405
ENSBTAG00000006703	PTGDR	1215.406	1046.441	0.216	0.03287405
ENSBTAG00000008696	FAM120A	3266.606	3859.683	-0.241	0.03287405
ENSBTAG00000030335	ALDH4A1	632.706	740.215	-0.226	0.032877248
ENSBTAG00000011562	STK32C	120.534	153.602	-0.350	0.032973831
ENSBTAG00000044070	SNX30	142.217	195.154	-0.457	0.032983425
ENSBTAG00000007390	VAT1	5938.046	7112.235	-0.260	0.03329754
ENSBTAG00000007385	EMC7	625.124	527.408	0.245	0.033505024
ENSBTAG00000015556	UBA3	1003.259	828.500	0.276	0.033554577
ENSBTAG00000019453	PTGES	277.068	519.252	-0.906	0.033594867
ENSBTAG00000011859	IPPK	371.011	295.095	0.330	0.033614548
ENSBTAG00000019611	MAGI3	729.628	604.086	0.272	0.033614548
ENSBTAG00000021535	CROT	204.579	161.374	0.342	0.033697278
ENSBTAG00000015182	STARD10	56.072	84.667	-0.595	0.033762869
ENSBTAG00000019806	YPEL2	873.650	1111.275	-0.347	0.03391124
ENSBTAG00000001473	ARVCF	578.174	735.264	-0.347	0.033939212
ENSBTAG00000008674	FAM136A	748.711	644.209	0.217	0.033989203
ENSBTAG00000047077	ENTPD7	185.554	235.797	-0.346	0.03411803
ENSBTAG00000019251	EPB41L3	255.738	310.809	-0.281	0.034241968
ENSBTAG00000012312	ROR1	184.128	236.516	-0.361	0.034312218
ENSBTAG00000005596	IGFBP2	18642.212	15208.643	0.294	0.034438424
ENSBTAG00000012113	HCCS	497.662	423.628	0.232	0.034557034
ENSBTAG00000030578	PTOV1	2037.279	2522.508	-0.308	0.034561058
ENSBTAG00000018563	SFRP2	73902.307	62639.414	0.239	0.034578718
ENSBTAG00000004126	MLF1	64.985	91.868	-0.499	0.034632765
ENSBTAG00000013671	UTP14A	3390.135	3104.809	0.127	0.034807799
ENSBTAG00000018965	PRDM16	22.968	12.182	0.915	0.034841255
ENSBTAG00000003015	SESN1	458.668	562.659	-0.295	0.034956528
ENSBTAG00000036087	ARMC2	119.554	143.891	-0.267	0.034981529
ENSBTAG00000004114	MAP3K11	491.513	591.116	-0.266	0.035126375

GeneID	Gene	Mean Counts Juxt	Mean Counts NoEmbryos	Log2 Fold-Change	P-Value (FDR adj)
ENSBTAG00000005702	CNGB1	6.277	1.904	1.721	0.035206855
ENSBTAG00000003499	ENPP4	288.150	240.625	0.260	0.035206855
ENSBTAG00000014558	DDX21	1793.888	1533.442	0.226	0.035253618
ENSBTAG00000007860	ASPM	307.334	238.049	0.369	0.035286969
ENSBTAG00000018979	PUM1	4664.618	3964.925	0.234	0.035305179
ENSBTAG00000019639	SNX16	479.267	395.133	0.278	0.035328283
ENSBTAG00000010208	ZER1	1031.734	876.444	0.235	0.035328283
ENSBTAG00000048071	EXOSC2	384.636	327.016	0.234	0.035328283
ENSBTAG00000031800	PPDPF	4128.210	4792.754	-0.215	0.03536607
ENSBTAG00000008013	LRRC2	42.993	65.651	-0.611	0.035410203
ENSBTAG00000021575	BRD7	1552.662	1365.104	0.186	0.035545886
ENSBTAG00000000371	DIS3L	1381.088	1520.401	-0.139	0.035550777
ENSBTAG00000000894	PGK1	2407.885	2104.661	0.194	0.035562584
ENSBTAG00000021073	KIAA1549	244.745	317.162	-0.374	0.035626044
ENSBTAG00000014458	MROH1	1263.982	1461.387	-0.209	0.035661466
ENSBTAG00000005989	LAP3	601.811	509.273	0.241	0.035768292
ENSBTAG00000046054	RHOB	4576.355	5315.346	-0.216	0.035768292
ENSBTAG00000006185	SPC24	103.223	73.930	0.482	0.035904296
ENSBTAG00000017363	SAT1	9509.223	7942.591	0.260	0.036013815
ENSBTAG00000020266	SLC19A2	134.234	103.047	0.381	0.036164381
ENSBTAG00000001848	KATNB1	300.886	247.100	0.284	0.036164381
ENSBTAG00000031165	TRPM7	1281.665	1472.467	-0.200	0.03620783
ENSBTAG00000020286	GAREM1	33.194	21.320	0.639	0.036277841
ENSBTAG00000003552	MED17	706.930	622.204	0.184	0.036322508
ENSBTAG00000006797		79.033	111.660	-0.499	0.036322508
ENSBTAG00000006305	AK1	142.681	180.867	-0.342	0.036335608
ENSBTAG00000014960	SCHIP1	923.376	787.143	0.230	0.036394748
ENSBTAG00000018954	ELP2	686.602	586.739	0.227	0.036394748
ENSBTAG00000021143	DNMT3A	348.138	419.183	-0.268	0.036474578
ENSBTAG00000015392	TTF2	433.597	375.451	0.208	0.036511761
ENSBTAG00000017402	OSBPL2	711.287	798.427	-0.167	0.036613591
ENSBTAG00000019277	KCNH3	49.538	69.162	-0.481	0.036632218
ENSBTAG00000020934	SHF	1004.577	851.149	0.239	0.036641961
ENSBTAG00000006001	STAP2	140.749	208.330	-0.566	0.036656056
ENSBTAG00000009543	ESYT1	2817.060	3231.558	-0.198	0.036703219
ENSBTAG00000011507	NUP88	1266.498	1114.797	0.184	0.03679111
ENSBTAG00000017001	RBM28	281.732	231.394	0.284	0.036886565
ENSBTAG00000017894	CAD	992.672	1193.196	-0.265	0.036911534
ENSBTAG00000009770	GPD2	896.393	708.581	0.339	0.036929263
ENSBTAG00000001867	SACS	1272.643	1506.185	-0.243	0.036929263
ENSBTAG00000001252	HIVEP1	1237.366	1465.422	-0.244	0.036929263
ENSBTAG00000006785	ARF2	136.640	199.477	-0.546	0.036929263
ENSBTAG00000014585	PTGIR	24.048	39.046	-0.699	0.036929263
ENSBTAG00000002028	FAM69A	234.937	285.350	-0.280	0.036937876
ENSBTAG00000020060	TXNIP	980.396	819.848	0.258	0.037163028
ENSBTAG00000033731	PRCP	332.848	284.849	0.225	0.037163028
ENSBTAG00000020665	GFRA2	430.816	534.492	-0.311	0.037185486
ENSBTAG00000018425	PSMD7	877.035	743.326	0.239	0.037422478
ENSBTAG00000038107	MAPKAPK2	1347.304	1540.475	-0.193	0.037468454
ENSBTAG00000009879	PCGF6	192.965	150.414	0.359	0.037674382
ENSBTAG00000018415	TTLL4	271.038	328.742	-0.278	0.037712121
ENSBTAG00000008181	CHAF1A	291.155	217.034	0.424	0.037817148
ENSBTAG00000031383	SMIM24	5.736	14.634	-1.351	0.03807936
ENSBTAG00000009709	TAF5	146.935	115.971	0.341	0.038242504
ENSBTAG00000015711	BTG2	187.947	367.379	-0.967	0.038378863
ENSBTAG00000033449	SLC25A40	32.449	18.823	0.786	0.038379239
ENSBTAG00000033299	IGFALS	1.871	8.358	-2.159	0.038379239
ENSBTAG00000011112	KCNK5	60.093	94.354	-0.651	0.038445758
ENSBTAG00000017685	JUP	6277.656	5540.576	0.180	0.038563125
ENSBTAG00000000721	GPATCH1	519.906	446.688	0.219	0.038639684
ENSBTAG00000035584		397.577	334.482	0.249	0.038683944
ENSBTAG00000012545	CASC4	1889.076	1696.669	0.155	0.038920915
ENSBTAG00000001481	IGSF9	384.815	474.092	-0.301	0.038920915
ENSBTAG00000000205	MMD	360.201	459.246	-0.350	0.038920915
ENSBTAG00000021519	CAMLG	432.837	360.495	0.264	0.038968599
ENSBTAG00000003866	PPP1R8	585.306	500.918	0.225	0.039342688
ENSBTAG00000020367	SLC30A9	700.788	601.301	0.221	0.039348551
ENSBTAG00000011228	FASTK	1049.013	1254.018	-0.258	0.039541438
ENSBTAG00000006103	XRCC6	745.799	654.527	0.188	0.039569811
ENSBTAG00000000456	CPB1	97.468	70.799	0.461	0.039619201

GeneID	Gene	Mean Counts Juxt	Mean Counts NoEmbryos	Log2 Fold-Change	P-Value (FDR adj)
ENSBTAG00000017095	DENND4A	531.966	673.504	-0.340	0.039676572
ENSBTAG00000038639	CXCL9	203.642	158.895	0.358	0.039793878
ENSBTAG00000001597	PITPNM2	208.874	269.831	-0.369	0.039965297
ENSBTAG00000010456	TADA1	416.446	348.763	0.256	0.04007822
ENSBTAG00000040521	SAMD14	41.289	59.683	-0.532	0.040220438
ENSBTAG00000015677	KARS	3136.860	3418.959	-0.124	0.040329112
ENSBTAG00000003825	PTPN12	1090.091	940.317	0.213	0.040442142
ENSBTAG00000007659	CORO2A	427.619	492.543	-0.204	0.040493628
ENSBTAG00000008113	OSR1	504.298	604.967	-0.263	0.04049497
ENSBTAG00000000720	CTSL	257.801	195.958	0.396	0.040548939
ENSBTAG00000003585	CD47	4149.531	3493.628	0.248	0.040548939
ENSBTAG00000034396	PIGW	281.348	232.662	0.274	0.040574304
ENSBTAG00000002768	SLC35A2	256.429	312.577	-0.286	0.040574304
ENSBTAG00000004386	SOCS1	69.615	44.939	0.631	0.04062995
ENSBTAG00000013505	IQCA1	75.146	98.469	-0.390	0.040653018
ENSBTAG00000006639	CSTF1	600.549	515.743	0.220	0.040695849
ENSBTAG00000012068	BRIP1	81.604	58.165	0.489	0.040715696
ENSBTAG00000020803		27.624	14.831	0.897	0.040901032
ENSBTAG00000030599	SMOC1	1260.465	1086.376	0.214	0.040901032
ENSBTAG00000005947	PLAU	471.320	760.062	-0.689	0.040901032
ENSBTAG00000015888	PDE7B	11.717	5.552	1.077	0.041140428
ENSBTAG00000008072	SRSF10	7250.496	5856.028	0.308	0.041296962
ENSBTAG00000013670	SLC46A2	15.597	28.424	-0.866	0.041449623
ENSBTAG00000017832	PDK3	467.198	544.980	-0.222	0.04167102
ENSBTAG00000002882	LMNB1	257.970	191.550	0.429	0.041700402
ENSBTAG00000000195		159.804	128.451	0.315	0.041815776
ENSBTAG00000013008	PMCH	50.209	33.311	0.592	0.041976555
ENSBTAG00000016206	MAOA	23.605	39.782	-0.753	0.042093739
ENSBTAG00000047591	C23H6orf141	59.239	39.079	0.600	0.042519682
ENSBTAG00000014337	EIF2S3	3534.838	3920.904	-0.150	0.042519682
ENSBTAG00000047998	COL5A1	12413.021	15275.300	-0.299	0.042725476
ENSBTAG00000013105	SYT3	34.376	48.959	-0.510	0.042744766
ENSBTAG00000032640	FOPNL	345.405	279.193	0.307	0.042760185
ENSBTAG00000016349	TEAD2	739.202	850.538	-0.202	0.042878347
ENSBTAG00000016362	POU6F1	90.325	66.849	0.434	0.042907286
ENSBTAG00000021245	SPRY1	1519.881	1703.061	-0.164	0.042990445
ENSBTAG00000009654	LPAR1	48.101	68.188	-0.503	0.042990445
ENSBTAG00000001805	TWSG1	1444.665	1267.453	0.189	0.043157248
ENSBTAG00000017211	SERINC4	436.280	555.696	-0.349	0.043157248
ENSBTAG00000014599	LRRC66	20.985	31.909	-0.605	0.043157248
ENSBTAG00000001112	SMOX	202.079	245.836	-0.283	0.043393036
ENSBTAG00000003516	TM2D2	636.591	552.477	0.204	0.043402848
ENSBTAG00000003345	FAT4	5.106	12.023	-1.235	0.043569518
ENSBTAG00000024604		1041.626	1320.625	-0.342	0.043729332
ENSBTAG00000010196	NUP43	307.651	243.946	0.335	0.043746688
ENSBTAG00000017834	PRELP	852.496	684.695	0.316	0.043795943
ENSBTAG00000004423	ARHGAP42	2027.692	2634.217	-0.378	0.043821608
ENSBTAG00000032705	CALM	329.653	251.588	0.390	0.043867307
ENSBTAG00000018256	SMC6	871.104	766.423	0.185	0.043950146
ENSBTAG00000004749	NEK4	445.268	512.306	-0.202	0.044040653
ENSBTAG00000010493	SERTAD1	426.508	332.818	0.358	0.044082558
ENSBTAG00000007712	SEC22B	3369.008	3712.891	-0.140	0.044082558
ENSBTAG00000017350	PCLO	2226.638	2678.233	-0.266	0.044082558
ENSBTAG00000025130	HIC1	31.036	49.401	-0.671	0.044082558
ENSBTAG00000001513	PDIK1L	66.557	45.367	0.553	0.044259516
ENSBTAG00000014217	HHEX	52.431	37.608	0.479	0.044346138
ENSBTAG00000018116	MTFP1	145.643	115.904	0.330	0.044346138
ENSBTAG00000007156	AGAP2	29.258	43.397	-0.569	0.045001776
ENSBTAG00000013822	GAS2L3	63.371	41.493	0.611	0.045111486
ENSBTAG00000009780	GTF2I	4203.055	3849.667	0.127	0.045111486
ENSBTAG00000010885	TSPYL1	1834.101	1616.726	0.182	0.045156095
ENSBTAG00000038134	ZDHHC1	506.876	617.668	-0.285	0.045156095
ENSBTAG00000019313	ZMIZ1	2988.380	3877.505	-0.376	0.045166263
ENSBTAG00000004651	NME1	109.867	138.924	-0.339	0.045435312
ENSBTAG00000010304	CHKA	1285.115	1100.216	0.224	0.045587193
ENSBTAG00000020611	GLB1L	479.707	406.076	0.240	0.045613634
ENSBTAG00000027924	SNX18	2638.798	2227.228	0.245	0.045686134
ENSBTAG00000021870	FAM98B	283.657	235.829	0.266	0.04570929
ENSBTAG00000002083	AUTS2	81.854	105.573	-0.367	0.045851885
ENSBTAG00000014371	CHPF2	723.109	845.572	-0.226	0.046026907

GeneID	Gene	Mean Counts Juxt	Mean Counts NoEmbryos	Log2 Fold-Change	P-Value (FDR adj)
ENSBTAG00000004496	TVP23B	836.422	957.046	-0.194	0.046048015
ENSBTAG00000018025	IQCG	114.967	145.486	-0.340	0.046048015
ENSBTAG00000013956	BCL2L13	2571.518	2902.749	-0.175	0.046066762
ENSBTAG00000004745	NAA15	1099.170	948.484	0.213	0.046173518
ENSBTAG00000048107	CANX	10873.425	9831.418	0.145	0.046304572
ENSBTAG00000026657	IFT27	190.087	230.154	-0.276	0.046304572
ENSBTAG00000010691	USP39	655.428	560.129	0.227	0.046454731
ENSBTAG00000038716	SKI	1180.745	1376.931	-0.222	0.046454731
ENSBTAG00000003809	PLCD4	71.467	51.275	0.479	0.046623367
ENSBTAG00000004782	PTPRCAP	71.926	96.487	-0.424	0.046623367
ENSBTAG00000007850	ITIH4	16.876	30.224	-0.841	0.046646961
ENSBTAG00000011946	ODR4	506.914	419.474	0.273	0.046975443
ENSBTAG00000013489	CYP27A1	166.963	201.037	-0.268	0.046988742
ENSBTAG00000017482	ISYNA1	214.234	259.011	-0.274	0.047081825
ENSBTAG00000000744	DCTN6	1263.959	1071.534	0.238	0.047150583
ENSBTAG00000014426	PRKAG1	571.281	508.634	0.168	0.047161224
ENSBTAG00000019309		97.480	131.895	-0.436	0.047161224
ENSBTAG00000002391	TGFB1I1	702.282	852.388	-0.279	0.04734895
ENSBTAG00000009906	DDX1	1822.981	1658.579	0.136	0.047996295
ENSBTAG00000005300	TMEM51	258.739	373.416	-0.529	0.047996295
ENSBTAG00000001221	NKX3-1	10.823	5.181	1.063	0.048080096
ENSBTAG00000021945	NID2	16727.906	13937.430	0.263	0.048080096
ENSBTAG00000017801	ATP6AP2	1856.140	1604.263	0.210	0.048080096
ENSBTAG00000003319	FLRT3	1359.030	1112.251	0.289	0.048153444
ENSBTAG00000031788		63.851	46.411	0.460	0.048255754
ENSBTAG00000002350	PIK3R2	1743.155	2019.568	-0.212	0.048299
ENSBTAG00000012938	JARID2	217.695	260.965	-0.262	0.048299
ENSBTAG00000011738	TFR2	83.232	62.130	0.422	0.048300666
ENSBTAG00000003837	RSPO1	222.914	181.068	0.300	0.048307593
ENSBTAG00000009596	C8H9orf43	24.861	40.026	-0.687	0.048385374
ENSBTAG00000006941	ATAT1	585.405	696.307	-0.250	0.048426209
ENSBTAG00000004171	GPHN	314.667	264.133	0.253	0.048715021
ENSBTAG00000012629	ZNF362	394.453	474.318	-0.266	0.048746134
ENSBTAG00000004344	ACSL1	341.692	403.835	-0.241	0.04897524
ENSBTAG00000004307	VPS36	1437.822	1267.363	0.182	0.049229439
ENSBTAG00000038617	SH3D21	242.165	291.861	-0.269	0.049233391
ENSBTAG00000020839	MEGF6	171.011	226.217	-0.404	0.049233391
ENSBTAG00000005517	NOP58	1683.259	1422.887	0.242	0.049240512
ENSBTAG00000020852	SLC16A11	634.234	716.360	-0.176	0.049311298
ENSBTAG00000000130	TNFSF13	72.468	98.591	-0.444	0.049327692
ENSBTAG00000020756	GSK3A	1004.825	1169.164	-0.219	0.049390039
ENSBTAG00000004075	IDI1	525.774	411.973	0.352	0.049491029
ENSBTAG00000003708	SEC23A	2097.645	2341.542	-0.159	0.049495791
ENSBTAG00000000191	SLC25A20	162.115	200.908	-0.310	0.049568478
ENSBTAG00000021897	B4GALT3	239.865	284.875	-0.248	0.049589893
ENSBTAG00000026825	TMEM37	5.473	12.518	-1.194	0.049737827
ENSBTAG00000048157	ABI3BP	220.453	280.881	-0.349	0.049804028
ENSBTAG00000000211		1594.691	1406.272	0.181	0.04990235
ENSBTAG00000019121	IFT122	983.052	1091.066	-0.150	0.04990235
ENSBTAG00000015258		139.020	179.190	-0.366	0.04990235
ENSBTAG00000014614	ACTA2	2758.885	4083.196	-0.566	0.04990235

Supplementary Dataset S14. Gene ID, mean normalized counts per group, Log2 Fold-Change, and FDR adjusted P-Values for differentially expressed genes (DEGs) in BEECs between NoEmbryos versus Non-juxt conditions. (Continued)

GeneID	Gene	Mean Counts Non-juxt	Mean Counts NoEmbryos	Log2 Fold-Change	P-Value (FDR adj)
ENSBTAG00000030913	MX1	11972.060	100.966	6.890	0
ENSBTAG00000037527	OAS1X	4724.012	50.446	6.549	0
ENSBTAG00000007881	IFIT1	7449.302	96.570	6.269	0
ENSBTAG00000045588		2270.826	32.124	6.143	0
ENSBTAG00000003152	IFI27	11618.040	169.423	6.100	0
ENSBTAG00000039861	OAS1Y	6077.797	102.107	5.895	0
ENSBTAG00000016661	USP18	2254.213	73.030	4.948	0
ENSBTAG00000021791	PARP9	1694.570	133.619	3.665	0
ENSBTAG00000012335	UBA7	3540.778	169.368	4.386	1.7E-277
ENSBTAG00000012406	ZBP1	985.540	9.578	6.685	1.76E-269
ENSBTAG00000030932	IFI44L	1804.894	60.527	4.898	7.82E-268
ENSBTAG00000014628	OAS2	535.213	10.187	5.715	1.94E-249
ENSBTAG00000011343	XAF1	762.175	13.673	5.801	1.32E-248
ENSBTAG00000003366	DDX58	4305.116	357.543	3.590	3.8E-234
ENSBTAG00000017367	IFIT5	5034.332	1013.969	2.312	1.65E-228
ENSBTAG00000009933	DTX3L	1770.313	170.731	3.374	7.89E-210
ENSBTAG00000016546	PARP12	2167.096	389.494	2.476	6.24E-207
ENSBTAG00000005816	IRF9	2614.848	389.725	2.746	1.23E-198
ENSBTAG00000046580	DHX58	1322.491	81.267	4.024	3.25E-198
ENSBTAG00000032265	RTP4	490.903	14.708	5.061	8.96E-197
ENSBTAG00000016656	PARP14	2630.783	395.511	2.734	2.34E-178
ENSBTAG00000008703	EIF2AK2	6417.122	1128.725	2.507	3.73E-174
ENSBTAG00000012894	SAMD9	1024.896	60.392	4.085	2.07E-166
ENSBTAG00000018994	TNFSF10	574.358	26.832	4.420	1.36E-145
ENSBTAG00000034349	IFI44	353.026	1.187	8.216	2.11E-143
ENSBTAG00000019015	IFITM3	11222.616	2130.631	2.397	8.64E-136
ENSBTAG00000014529	GBP4	228.958	1.707	7.067	1.78E-132
ENSBTAG00000019054	EPSTI1	963.270	162.935	2.564	5.44E-128
ENSBTAG00000008142	IFIH1	1143.312	109.727	3.381	1.52E-127
ENSBTAG00000009677	PARP10	2624.099	623.675	2.073	3.24E-127
ENSBTAG00000019017	IFITM2	1764.054	201.706	3.129	2.36E-120
ENSBTAG00000022489		6628.486	884.552	2.906	8.98E-120
ENSBTAG00000019018		2010.509	255.097	2.978	1.37E-112
ENSBTAG00000007554	IFI6	6003.365	56.043	6.743	2.26E-112
ENSBTAG00000020166	ZNFX1	4640.350	865.448	2.423	2.79E-104
ENSBTAG00000013900	TRIM21	738.679	192.324	1.941	3.41E-99
ENSBTAG00000007867	STAT1	5497.898	1854.287	1.568	3.23E-97
ENSBTAG00000031750	PLAC8	661.195	3.372	7.615	1.01E-81
ENSBTAG00000038710		1376.119	439.489	1.647	3.56E-79
ENSBTAG00000015779	PML	2629.955	730.555	1.848	4.22E-78
ENSBTAG00000014707	ISG15	2426.217	12.447	7.607	4.07E-73
ENSBTAG00000019979	CMPK2	538.169	55.189	3.286	1.05E-72
ENSBTAG00000007519	ADAR	2823.729	856.937	1.720	2.02E-72
ENSBTAG00000037465	TRIM34	577.464	148.748	1.957	2.84E-72
ENSBTAG00000017670		458.899	94.936	2.273	1.49E-71
ENSBTAG00000011511		175.111	12.355	3.825	1.39E-69
ENSBTAG00000003719	TDRD7	1124.203	418.307	1.426	5.16E-69
ENSBTAG00000015752		741.600	248.890	1.575	1.39E-58
ENSBTAG00000001368	LGALS3BP	8265.069	3499.035	1.240	4.11E-47
ENSBTAG00000008909	PNPT1	1887.343	621.358	1.603	7.85E-44
ENSBTAG00000001143		333.236	90.135	1.886	9.34E-44
ENSBTAG00000014297	MOV10	2166.168	1290.466	0.747	8.76E-40
ENSBTAG00000020538	HERC5	772.542	238.285	1.697	8.23E-38
ENSBTAG00000012330	B2M	8230.160	3321.168	1.309	1.26E-37
ENSBTAG00000009664		456.940	161.302	1.502	3.77E-37
ENSBTAG00000027317	RNF114	2272.003	1203.789	0.916	1.11E-35
ENSBTAG00000000312	GRINA	2390.492	1056.786	1.178	4.28E-35
ENSBTAG00000009206	FOXS1	192.650	28.538	2.755	4.48E-33
ENSBTAG00000017091	CMTR1	1915.598	1105.439	0.793	5.04E-32
ENSBTAG00000017040	LY6E	5017.023	1874.443	1.420	8.64E-29
ENSBTAG00000021452	TRANK1	8291.792	3814.284	1.120	1.01E-28
ENSBTAG00000015636	C7H19orf66	462.443	179.648	1.364	1.26E-28

GeneID	Gene	Mean Counts Non-juxt	Mean Counts NoEmbryos	Log2 Fold-Change	P-Value (FDR adj)
ENSBTAG00000002416		102.763	9.182	3.484	3.6E-28
ENSBTAG00000008707	SULT6B1	130.392	28.268	2.206	3.61E-28
ENSBTAG00000009177	PLEKHA4	1456.702	615.534	1.243	8.92E-27
ENSBTAG00000038536		896.727	427.150	1.070	2.72E-26
ENSBTAG00000016061	RSAD2	1684.903	11.241	7.228	6.64E-26
ENSBTAG00000022227	PLSCR2	2091.844	1088.691	0.942	1.2E-25
ENSBTAG00000020536	HERC6	7967.499	4476.249	0.832	1.14E-24
ENSBTAG00000037702	SP140L	202.610	74.964	1.434	1.61E-24
ENSBTAG00000011936	ATP8B4	312.458	94.728	1.722	2.37E-24
ENSBTAG00000031214		108.586	18.870	2.525	3.09E-23
ENSBTAG00000011304	XRN2	2261.310	1457.992	0.633	2.42E-22
ENSBTAG00000006801	TMEM106A	1031.358	498.763	1.048	5.09E-22
ENSBTAG00000004272	ISG12(B)	116.279	45.903	1.341	3.39E-19
ENSBTAG00000016217	RBM43	228.859	92.222	1.311	6.04E-18
ENSBTAG00000021395	PSME1	1489.432	841.761	0.823	1.72E-17
ENSBTAG00000001702	TMEM107	30.186	87.690	-1.539	3.98E-17
ENSBTAG00000012989	UBE2L6	137.924	55.686	1.308	4.66E-17
ENSBTAG00000003495	KDM7A	267.782	140.877	0.927	1.4E-16
ENSBTAG00000020884	CASP4	1773.744	984.480	0.849	3.09E-16
ENSBTAG00000018523	TRIM38	496.838	284.272	0.806	3.6E-16
ENSBTAG00000032369	NMI	785.552	436.399	0.848	5E-16
ENSBTAG00000000892	CGAS	116.903	39.221	1.576	9.22E-16
ENSBTAG00000047367	CMTR2	421.100	187.306	1.169	2.99E-15
ENSBTAG00000010166	MIC1	1367.937	868.490	0.655	1.07E-14
ENSBTAG00000007389	IFI35	302.421	135.695	1.156	7.7E-14
ENSBTAG00000037989		29.786	2.779	3.422	1.55E-13
ENSBTAG00000002435	PTPRE	1577.222	998.797	0.659	2.39E-13
ENSBTAG00000009183	SHISA5	1006.058	602.048	0.741	2.94E-13
ENSBTAG00000017002	RBCK1	1322.369	798.446	0.728	1.05E-12
ENSBTAG00000034918	IFIT2	261.212	15.689	4.057	1.25E-12
ENSBTAG00000011876	MORC3	712.435	463.800	0.619	1.37E-12
ENSBTAG00000019386	BOLA-NC1	226.938	134.287	0.757	3.14E-12
ENSBTAG00000008021		51.844	0.357	7.184	4.19E-12
ENSBTAG00000003039	PSMB8	514.458	290.722	0.823	4.38E-12
ENSBTAG00000005815	RNF31	993.080	695.120	0.515	6.17E-12
ENSBTAG00000005814	PSME2	817.402	447.587	0.869	8.15E-12
ENSBTAG00000034519		290.967	149.504	0.961	2.81E-11
ENSBTAG00000005251		45.294	8.719	2.377	2.87E-11
ENSBTAG00000018417	PSMF1	989.749	592.847	0.739	8.58E-11
ENSBTAG00000005146		369.706	234.723	0.655	2.08E-10
ENSBTAG00000000504	GTF2B	650.538	391.571	0.732	2.18E-10
ENSBTAG00000040244	APOL3	50.020	14.940	1.743	2.28E-10
ENSBTAG00000007077	ABHD1	158.218	76.869	1.041	2.33E-10
ENSBTAG00000009091	RNASEL	127.018	59.651	1.090	8.7E-10
ENSBTAG00000002069	BOLA	1563.657	903.588	0.791	2.76E-09
ENSBTAG00000006633	IRF3	1510.771	1048.694	0.527	7.76E-09
ENSBTAG00000025762	CNP	1528.603	1100.743	0.474	8.17E-09
ENSBTAG00000012107	SLC25A28	862.864	621.553	0.473	0.000000012
ENSBTAG00000009948	TRIM25	1126.237	573.782	0.973	0.000000015
ENSBTAG00000021687	JADE2	208.598	115.694	0.850	1.63E-08
ENSBTAG00000011647	SLC25A15	219.773	326.537	-0.571	0.000000023
ENSBTAG00000039275	ERAP2	749.414	489.910	0.613	2.53E-08
ENSBTAG00000002691	ELMOD1	84.192	42.235	0.995	2.86E-08
ENSBTAG00000000990	PSMA2	1237.139	861.939	0.521	3.32E-08
ENSBTAG00000016830	DAXX	1596.805	1102.913	0.534	0.000000301
ENSBTAG00000004679	WARS	4812.058	3326.253	0.533	0.000000689
ENSBTAG00000044019	KAT2A	780.695	585.304	0.416	0.000000744
ENSBTAG00000003743		74.127	36.102	1.038	0.000000862
ENSBTAG00000009132	TMPRSS2	44.808	0.157	8.161	0.000000897
ENSBTAG00000020225	TBXAS1	21.971	3.428	2.680	0.00000157
ENSBTAG00000000639	APRT	962.697	659.172	0.546	0.00000174
ENSBTAG00000024492		27.093	9.030	1.585	0.00000181
ENSBTAG00000003639	ELMO2	1727.137	1328.510	0.379	0.00000261
ENSBTAG00000022590		1355.723	931.627	0.541	0.00000317
ENSBTAG00000007450	C2	4430.357	3438.165	0.366	0.00000326
ENSBTAG00000019989	PXK	515.031	367.242	0.488	0.00000416

GeneID	Gene	Mean Counts Non-juxt	Mean Counts NoEmbryos	Log2 Fold-Change	P-Value (FDR adj)
ENSBTAG00000004380	STAT2	1024.248	757.656	0.435	0.00000782
ENSBTAG00000021617	ZC3HAV1	2004.180	1481.788	0.436	0.00000818
ENSBTAG00000015718	CASP8	677.335	472.571	0.519	0.0000109
ENSBTAG00000011934	PCK2	452.273	342.463	0.401	0.0000119
ENSBTAG00000019614	FAM76A	293.333	217.992	0.428	0.0000136
ENSBTAG00000003636	LIPA	791.235	583.070	0.440	0.000018
ENSBTAG00000003381	PAPD7	907.352	697.396	0.380	0.0000256
ENSBTAG00000016092	SPATS2L	1282.574	900.135	0.511	0.0000382
ENSBTAG00000000706	ADAMTS1	2461.837	3634.067	-0.562	0.000055
ENSBTAG00000008682	TLR3	322.386	235.119	0.455	0.00006
ENSBTAG00000000995	FAM46A	102.910	67.021	0.619	0.000150812
ENSBTAG00000046699		22.285	6.285	1.826	0.000216228
ENSBTAG00000015778	SASS6	293.659	199.622	0.557	0.000246482
ENSBTAG00000005454	FUT10	281.763	209.223	0.429	0.000256773
ENSBTAG00000013557	ERAP1	575.351	427.429	0.429	0.00050701
ENSBTAG00000007935	CALCOCO2	1151.508	907.108	0.344	0.000692564
ENSBTAG00000009768	IFIT3	218.691	42.949	2.348	0.000755703
ENSBTAG00000005182	BoLA	567.259	381.015	0.574	0.00080054
ENSBTAG00000007755	APOBEC3Z3	190.363	134.125	0.505	0.000841903
ENSBTAG00000018065	YARS	1108.750	919.327	0.270	0.000844327
ENSBTAG00000015509	NAMPT	386.027	263.868	0.549	0.000880649
ENSBTAG00000020116	JSP.1	109.097	59.309	0.879	0.001027258
ENSBTAG00000001296	TMEM50A	1894.869	1497.692	0.339	0.001027258
ENSBTAG00000008406	TREX1	164.483	86.732	0.923	0.001030672
ENSBTAG00000007431	CEMIP	14154.172	20631.006	-0.544	0.001501963
ENSBTAG00000040584	DSC2	962.911	1228.783	-0.352	0.001573851
ENSBTAG00000000204	TMEM268	331.372	262.802	0.334	0.001574554
ENSBTAG00000024272		18.948	2.457	2.947	0.001620534
ENSBTAG00000003751	MACC1	126.029	211.491	-0.747	0.001938681
ENSBTAG00000006974	PLEKHA7	317.006	217.110	0.546	0.002395082
ENSBTAG00000008353	CDKN1A	5408.030	6758.760	-0.322	0.002670724
ENSBTAG00000012774	RAB7B	228.680	294.287	-0.364	0.002883559
ENSBTAG00000010665	CBLN3	380.107	277.678	0.453	0.002942194
ENSBTAG00000006638	BCL2L12	837.276	647.752	0.370	0.002998646
ENSBTAG00000012383	CHMP5	978.843	743.565	0.397	0.003409177
ENSBTAG00000008744	PDK2	443.744	542.062	-0.289	0.003524284
ENSBTAG00000018016	NUPR1	4507.625	3171.971	0.507	0.003632895
ENSBTAG00000006016	GTPBP2	668.300	551.716	0.277	0.003683648
ENSBTAG00000007399	LAMP2	5172.185	4220.090	0.293	0.003880974
ENSBTAG00000008953	TAP1	387.540	252.853	0.616	0.003930837
ENSBTAG00000014060	LSM6	552.168	435.455	0.343	0.003932396
ENSBTAG00000038625		13.554	2.722	2.316	0.004112151
ENSBTAG00000011467	BATF2	34.587	16.398	1.077	0.004222401
ENSBTAG00000031306	PLSCR1	24.192	11.332	1.094	0.004344244
ENSBTAG00000003038		1221.049	1009.831	0.274	0.004376085
ENSBTAG00000030648	MPST	613.050	476.641	0.363	0.004734651
ENSBTAG00000037533	C4A	2462.485	1679.501	0.552	0.004952707
ENSBTAG00000005063	THEM6	29.870	13.153	1.183	0.005147487
ENSBTAG00000014650	NFATC2IP	181.849	136.835	0.410	0.005172037
ENSBTAG00000001867	SACS	1191.117	1506.185	-0.339	0.00544123
ENSBTAG00000020030	FITM2	515.018	685.215	-0.412	0.005488063
ENSBTAG00000016529	SLC25A30	674.085	530.864	0.345	0.005976266
ENSBTAG00000005066	HSPBAP1	262.534	178.886	0.553	0.00610273
ENSBTAG00000020989	SUSD4	890.999	1080.769	-0.279	0.006488581
ENSBTAG00000006506	GIT2	1950.109	2363.401	-0.277	0.006563979
ENSBTAG00000038938		11.453	1.609	2.831	0.006885919
ENSBTAG00000004117	AZI2	955.382	791.820	0.271	0.006885919
ENSBTAG00000007129	MRVI1	266.094	371.763	-0.482	0.007102876
ENSBTAG00000000957	CDKN2AIP	358.941	266.062	0.432	0.007176875
ENSBTAG00000046512	XIRP1	293.400	462.075	-0.655	0.009130475
ENSBTAG00000006615	CASP7	97.529	69.117	0.497	0.010176446
ENSBTAG00000004378	IL23A	258.614	187.775	0.462	0.010176446
ENSBTAG00000011458	CPXM1	431.025	343.886	0.326	0.01135297
ENSBTAG00000019437		121.926	80.370	0.601	0.012214445
ENSBTAG00000000555	ACO1	943.659	1092.564	-0.211	0.012214445
ENSBTAG00000030435	PNRC2	3902.842	3073.324	0.345	0.01414231

GeneID	Gene	Mean Counts Non-juxt	Mean Counts NoEmbryos	Log2 Fold-Change	P-Value (FDR adj)
ENSBTAG00000012038	TRIM56	207.578	129.805	0.677	0.014200282
ENSBTAG00000011798	STK38L	1105.569	1453.449	-0.395	0.014304956
ENSBTAG00000007075		76.667	52.580	0.544	0.01483859
ENSBTAG00000002271	CDADC1	351.112	255.334	0.460	0.01483859
ENSBTAG00000000806	ATAD1	1124.990	883.208	0.349	0.01483859
ENSBTAG00000021474	GSDMD	270.279	196.595	0.459	0.014934216
ENSBTAG00000037377	ABHD14B	2404.244	2148.100	0.163	0.016397159
ENSBTAG00000031231	IRF1	220.149	133.792	0.718	0.017162749
ENSBTAG00000014465	SERPINE1	1224.814	2053.723	-0.746	0.017162749
ENSBTAG00000014728	TAPBPL	659.740	517.992	0.349	0.018099084
ENSBTAG00000038619		137.173	88.756	0.628	0.018976871
ENSBTAG00000003616	DCLRE1B	249.670	313.680	-0.329	0.019078968
ENSBTAG00000013191	AGRN	7944.526	5785.091	0.458	0.020452169
ENSBTAG00000020575	IFITM5	220.858	169.902	0.378	0.021778135
ENSBTAG00000016828	TAPBP	4056.155	3285.470	0.304	0.024279141
ENSBTAG00000012673	CDK18	241.337	185.758	0.378	0.024345084
ENSBTAG00000031718	OGFR	635.233	486.550	0.385	0.025158714
ENSBTAG00000009428	GAN	116.671	176.296	-0.596	0.025484351
ENSBTAG00000020313	FNBP1	1320.848	1581.008	-0.259	0.027686702
ENSBTAG00000011412	LAMB1	20149.983	23593.507	-0.228	0.028305982
ENSBTAG00000003807	CNOT9	857.659	734.357	0.224	0.028457722
ENSBTAG00000002357	TICAM2	433.447	367.590	0.238	0.02893655
ENSBTAG00000018040	PSMB10	214.046	148.344	0.529	0.029996332
ENSBTAG00000008607	ARID3A	239.894	305.072	-0.347	0.030601955
ENSBTAG00000002717	INA	118.613	78.394	0.597	0.033266692
ENSBTAG00000015046	MST1R	219.115	164.248	0.416	0.034745872
ENSBTAG00000020277	PPP2R1B	3016.776	3347.355	-0.150	0.038785404
ENSBTAG00000004459	TMEM45A	156.327	199.198	-0.350	0.038785404
ENSBTAG00000015772	STOML1	130.738	98.787	0.404	0.042264201
ENSBTAG00000002605		190.493	145.333	0.390	0.043975862
ENSBTAG00000002915	GPR63	64.517	38.430	0.747	0.045083144
ENSBTAG00000000820	GNG11	2321.875	1861.833	0.319	0.046032355
ENSBTAG00000038233		6.781	0.171	5.309	0.048102415
ENSBTAG00000008954	PSMB9	83.269	45.959	0.857	0.048102415
ENSBTAG00000021151	MYH10	10948.586	14364.128	-0.392	0.048768688
ENSBTAG00000021903	KIAA0319	21.373	35.613	-0.737	0.049317708

Supplementary Dataset S15. Gene ID, mean normalized counts per group, Log2 Fold-Change, and FDR adjusted P-Values for differentially expressed genes (DEGs) in BEECs between Juxt versus Non-juxt conditions. (Continued)

GeneID	Gene	Mean Counts Juxt	Mean Counts Non-juxt	Log2 Fold-Change	P-Value (FDR adj)
ENSBTAG00000014529	GBP4	869.347	228.958	1.925	1.23E-51
ENSBTAG00000034349	IFI44	1561.642	353.026	2.145	6.9E-50
ENSBTAG00000011936	ATP8B4	1348.566	312.458	2.110	1.28E-47
ENSBTAG00000012406	ZBP1	3082.706	985.540	1.645	3E-38
ENSBTAG00000032265	RTP4	1286.875	490.903	1.390	4.08E-33
ENSBTAG00000034918	IFIT2	2094.095	261.212	3.003	4.56E-32
ENSBTAG00000007867	STAT1	10249.789	5497.898	0.899	9.14E-32
ENSBTAG00000038710		2700.708	1376.119	0.973	2.87E-29
ENSBTAG00000031214		444.078	108.586	2.032	3.77E-29
ENSBTAG00000009206	FOXS1	759.033	192.650	1.978	4.74E-29
ENSBTAG00000030932	IFI44L	4580.486	1804.894	1.344	6.77E-28
ENSBTAG00000019979	CMPK2	1736.875	538.169	1.690	2.4E-27
ENSBTAG00000017670		1074.593	458.899	1.228	1.72E-26
ENSBTAG00000018994	TNFSF10	1569.377	574.358	1.450	2.18E-26
ENSBTAG00000008142	IFIH1	2965.725	1143.312	1.375	6.13E-26
ENSBTAG00000002416		415.702	102.763	2.016	8.17E-25
ENSBTAG00000011511		499.736	175.111	1.513	3.21E-24
ENSBTAG00000008021		317.376	51.844	2.614	4.61E-24
ENSBTAG00000021791	PARP9	2845.556	1694.570	0.748	6.9E-24
ENSBTAG00000009933	DTX3L	3600.750	1770.313	1.024	1.21E-22
ENSBTAG00000007881	IFIT1	16307.409	7449.302	1.130	2.06E-22
ENSBTAG00000030913	MX1	26814.051	11972.060	1.163	5.57E-22
ENSBTAG00000016546	PARP12	3666.142	2167.096	0.758	2.86E-21
ENSBTAG00000019054	EPSTI1	1879.235	963.270	0.964	3.16E-21
ENSBTAG00000018417	PSMF1	1987.983	989.749	1.006	5.49E-21
ENSBTAG00000020538	HERC5	1774.309	772.542	1.200	7.97E-21
ENSBTAG00000045588		4894.733	2270.826	1.108	8.53E-21
ENSBTAG00000037527	OAS1X	8857.437	4724.012	0.907	2.6E-20
ENSBTAG00000018125	KIF5C	90.260	11.091	3.025	5.39E-20
ENSBTAG00000013900	TRIM21	1278.781	738.679	0.792	3.31E-19
ENSBTAG00000001143		715.939	333.236	1.103	1.5E-18
ENSBTAG00000007431	CEMIP	6129.304	14154.172	-1.207	1.93E-18
ENSBTAG00000024272		108.653	18.948	2.520	2.34E-18
ENSBTAG00000016661	USP18	3803.554	2254.213	0.755	3.09E-18
ENSBTAG00000011343	XAF1	1605.704	762.175	1.075	3.57E-18
ENSBTAG00000037989		107.239	29.786	1.848	1.48E-17
ENSBTAG00000039275	ERAP2	1362.611	749.414	0.863	1.65E-17
ENSBTAG00000017367	IFIT5	7797.873	5034.332	0.631	2.22E-17
ENSBTAG00000012894	SAMD9	2242.560	1024.896	1.130	2.32E-17
ENSBTAG00000012330	B2M	15246.081	8230.160	0.889	2.73E-17
ENSBTAG00000012335	UBA7	7138.319	3540.778	1.012	3.07E-17
ENSBTAG00000003719	TDRD7	1805.483	1124.203	0.683	5.17E-17
ENSBTAG00000009664		875.319	456.940	0.938	6.02E-17
ENSBTAG00000037702	SP140L	414.925	202.610	1.034	3.38E-16
ENSBTAG00000016092	SPATS2L	2348.048	1282.574	0.872	3.93E-16
ENSBTAG00000011304	XRN2	3279.526	2261.310	0.536	5.79E-16
ENSBTAG00000008471	MX2	1678.997	53.997	4.959	1.21E-15
ENSBTAG00000038625		62.843	13.554	2.213	1.45E-15
ENSBTAG00000009768	IFIT3	1159.098	218.691	2.406	6.15E-15
ENSBTAG00000031750	PLAC8	2014.683	661.195	1.607	1.11E-14
ENSBTAG00000015752		1235.108	741.600	0.736	4.35E-14
ENSBTAG00000038619		332.049	137.173	1.275	4.68E-14
ENSBTAG00000017040	LY6E	9861.644	5017.023	0.975	8.37E-14
ENSBTAG00000016061	RSAD2	6549.763	1684.903	1.959	8.49E-14
ENSBTAG00000003495	KDM7A	459.353	267.782	0.779	1.51E-13
ENSBTAG00000005146		605.134	369.706	0.711	1.51E-13
ENSBTAG00000014297	MOV10	2919.171	2166.168	0.430	3.3E-13
ENSBTAG00000015779	PML	4426.102	2629.955	0.751	4.15E-13
ENSBTAG00000022489		12723.211	6628.486	0.941	4.52E-13
ENSBTAG00000038536		1495.143	896.727	0.738	7.33E-13
ENSBTAG00000003366	DDX58	7544.599	4305.116	0.809	8.83E-13
ENSBTAG00000007554	IFI6	16397.473	6003.365	1.450	1.7E-12
ENSBTAG00000039861	OAS1Y	8768.631	6077.797	0.529	2.02E-12
ENSBTAG00000008909	PNPT1	3381.717	1887.343	0.841	2.41E-12
ENSBTAG00000004380	STAT2	1561.471	1024.248	0.608	2.53E-12
ENSBTAG00000046580	DHX58	2444.223	1322.491	0.886	2.55E-12

GeneID	Gene	Mean Counts Juxt	Mean Counts Non-juxt	Log2 Fold-Change	P-Value (FDR adj)
ENSBTAG00000004679	WARS	7787.986	4812.058	0.695	3.6E-12
ENSBTAG00000016656	PARP14	4250.004	2630.783	0.692	3.6E-12
ENSBTAG00000027317	RNF114	3268.460	2272.003	0.525	8.74E-12
ENSBTAG00000020166	ZNFX1	8076.849	4640.350	0.800	1.38E-11
ENSBTAG00000019437		254.338	121.926	1.061	2.46E-11
ENSBTAG00000038233		33.628	6.781	2.310	3.17E-11
ENSBTAG00000006882	IQGAP3	377.637	210.675	0.842	3.17E-11
ENSBTAG00000019314	USP25	1299.781	833.453	0.641	3.28E-11
ENSBTAG00000002298	CKAP2L	238.629	113.961	1.066	5.32E-11
ENSBTAG00000007519	ADAR	4447.305	2823.729	0.655	1.52E-10
ENSBTAG00000009177	PLEKHA4	2484.335	1456.702	0.770	1.7E-10
ENSBTAG00000018523	TRIM38	769.223	496.838	0.631	1.7E-10
ENSBTAG00000014628	OAS2	883.092	535.213	0.722	1.71E-10
ENSBTAG00000017091	CMTR1	2608.186	1915.598	0.445	4.6E-10
ENSBTAG00000043550	CYTB	43070.691	77878.948	-0.855	5.59E-10
ENSBTAG00000008772	SMC2	543.067	320.983	0.759	9.02E-10
ENSBTAG00000002444		1462.307	774.738	0.916	0.000000001
ENSBTAG00000002331	DLGAP5	174.747	87.582	0.997	1.23E-09
ENSBTAG00000016217	RBM43	427.631	228.859	0.902	1.55E-09
ENSBTAG00000002717	INA	246.398	118.613	1.055	1.78E-09
ENSBTAG00000009218	ANLN	1115.069	639.956	0.801	1.89E-09
ENSBTAG00000037465	TRIM34	916.245	577.464	0.666	2.07E-09
ENSBTAG00000005251		120.273	45.294	1.409	2.77E-09
ENSBTAG00000020536	HERC6	11396.044	7967.499	0.516	3.02E-09
ENSBTAG00000012443	DIAPH3	380.572	220.941	0.785	3.4E-09
ENSBTAG00000003639	ELMO2	2352.366	1727.137	0.446	3.97E-09
ENSBTAG00000019262	TOP2A	691.592	391.633	0.820	4.9E-09
ENSBTAG00000006697	RICTOR	1447.697	1012.777	0.515	6.58E-09
ENSBTAG00000010166	MIC1	1938.144	1367.937	0.503	9.99E-09
ENSBTAG00000008140	FAP	1083.360	1506.043	-0.475	9.99E-09
ENSBTAG00000008703	EIF2AK2	9469.259	6417.122	0.561	1.08E-08
ENSBTAG00000016131	NCAPG2	272.416	173.279	0.653	1.46E-08
ENSBTAG00000032369	NMI	1198.171	785.552	0.609	1.72E-08
ENSBTAG00000000988	BRCA2	599.601	414.912	0.531	2.48E-08
ENSBTAG00000001244	PLAT	2065.532	1597.878	0.370	2.63E-08
ENSBTAG00000043546	ND6	22717.010	37403.490	-0.719	2.73E-08
ENSBTAG00000024449	CENPF	631.739	361.474	0.805	2.92E-08
ENSBTAG00000002435	PTPRE	2254.725	1577.222	0.516	2.92E-08
ENSBTAG00000011876	MORC3	1004.592	712.435	0.496	2.98E-08
ENSBTAG00000012451	BOLA-DMB	112.643	51.443	1.131	3.57E-08
ENSBTAG00000033441	SHCBP1	109.141	51.340	1.088	5.11E-08
ENSBTAG00000030921	FAM3B	14.805	1.751	3.080	6.52E-08
ENSBTAG00000000892	CGAS	228.260	116.903	0.965	6.72E-08
ENSBTAG00000008744	PDK2	317.048	443.744	-0.485	7.02E-08
ENSBTAG00000040244	APOL3	106.259	50.020	1.087	9.16E-08
ENSBTAG00000006801	TMEM106A	1580.922	1031.358	0.616	9.97E-08
ENSBTAG00000007860	ASPM	307.334	177.080	0.795	0.000000177
ENSBTAG00000009677	PARP10	3705.873	2624.099	0.498	0.000000178
ENSBTAG00000000706	ADAMTS1	1532.691	2461.837	-0.684	0.0000002
ENSBTAG00000010721	MCM3	708.627	476.458	0.573	0.000000231
ENSBTAG00000018643	PRC1	367.755	244.373	0.590	0.000000265
ENSBTAG00000020884	CASP4	2635.428	1773.744	0.571	0.000000277
ENSBTAG00000043563	ND5	67997.442	108761.384	-0.678	0.000000278
ENSBTAG00000043559	ND4L	5703.555	8845.347	-0.633	0.000000335
ENSBTAG00000001368	LGALS3BP	11621.324	8265.069	0.492	0.000000357
ENSBTAG00000003039	PSMB8	789.804	514.458	0.618	0.000000381
ENSBTAG00000037533	C4A	4241.017	2462.485	0.784	0.000000641
ENSBTAG00000000995	FAM46A	165.225	102.910	0.683	0.000000648
ENSBTAG00000019716	CXCL8	56.113	124.607	-1.151	0.000000648
ENSBTAG00000024851	TRIM14	129.977	72.183	0.849	0.000000678
ENSBTAG00000007237	BUB1B	276.217	155.895	0.825	0.000000717
ENSBTAG00000003152	IFI27	17435.707	11618.040	0.586	0.00000072
ENSBTAG00000043577	ND4	60652.455	99932.365	-0.720	0.000000728
ENSBTAG00000018775	TPX2	503.391	293.882	0.776	0.000000817
ENSBTAG00000021687	JADE2	338.870	208.598	0.700	0.000000848
ENSBTAG00000012925	NCAPH	162.370	92.564	0.811	0.000000913
ENSBTAG00000008758	KIF20A	416.727	257.152	0.696	0.000000942
ENSBTAG00000022227	PLSCR2	2929.016	2091.844	0.486	0.000000978
ENSBTAG00000013557	ERAP1	832.224	575.351	0.533	0.000000981
ENSBTAG00000000806	ATAD1	1626.014	1124.990	0.531	0.00000119

GeneID	Gene	Mean Counts Juxt	Mean Counts Non-juxt	Log2 Fold-Change	P-Value (FDR adj)
ENSBTAG00000003066	NSA2	691.629	931.142	-0.429	0.00000134
ENSBTAG00000008934	ESPL1	210.391	122.810	0.777	0.0000014
ENSBTAG00000016387	GDAP2	405.856	286.858	0.501	0.00000146
ENSBTAG00000047367	CMTR2	700.412	421.100	0.734	0.00000156
ENSBTAG00000015778	SASS6	460.259	293.659	0.648	0.00000162
ENSBTAG00000002826	CLSPN	129.653	62.502	1.053	0.00000188
ENSBTAG00000021069	PBK	134.525	67.691	0.991	0.00000208
ENSBTAG00000008953	TAP1	679.302	387.540	0.810	0.00000208
ENSBTAG00000009383	KIF11	321.099	183.528	0.807	0.00000226
ENSBTAG00000006792	EHD4	450.694	249.213	0.855	0.00000246
ENSBTAG00000006846	LGALS9	16.982	3.347	2.343	0.00000247
ENSBTAG00000013100	SPAG5	194.788	111.257	0.808	0.00000253
ENSBTAG00000002069	BOLA	2438.096	1563.657	0.641	0.00000266
ENSBTAG00000003636	LIPA	1093.994	791.235	0.467	0.0000029
ENSBTAG00000005456	TTK	104.787	55.653	0.913	0.00000294
ENSBTAG00000007935	CALCOCO2	1537.218	1151.508	0.417	0.00000341
ENSBTAG00000009983	KIF23	387.787	216.091	0.844	0.00000455
ENSBTAG00000021452	TRANK1	11883.620	8291.792	0.519	0.00000493
ENSBTAG00000020100		168.227	91.325	0.881	0.00000507
ENSBTAG00000015509	NAMPT	608.341	386.027	0.656	0.00000526
ENSBTAG00000011839	HMGCS1	931.626	648.774	0.522	0.00000594
ENSBTAG00000000990	PSMA2	1677.918	1237.139	0.440	0.00000676
ENSBTAG00000043584	ATP6	67089.976	98699.594	-0.557	0.0000074
ENSBTAG00000012074	MYB	573.133	414.749	0.467	0.00000769
ENSBTAG00000002691	ELMOD1	139.663	84.192	0.730	0.00000781
ENSBTAG00000012216	MLKL	193.767	118.845	0.705	0.0000086
ENSBTAG00000019278	KNTC1	171.699	100.775	0.769	0.00000886
ENSBTAG00000024726	HJURP	169.418	93.991	0.850	0.00000913
ENSBTAG00000012861	KIF4A	201.274	124.776	0.690	0.00000913
ENSBTAG00000011465	MYBPH	64.230	150.481	-1.228	0.00000954
ENSBTAG00000008436	CDC25B	173.839	101.523	0.776	0.0000098
ENSBTAG00000019017	IFITM2	2765.574	1764.054	0.649	0.0000103
ENSBTAG00000019822	TPPP3	18.462	58.290	-1.659	0.0000105
ENSBTAG00000015172	MCM6	584.568	440.205	0.409	0.0000108
ENSBTAG00000010313	DDX52	589.948	449.318	0.393	0.0000115
ENSBTAG00000014707	ISG15	5149.006	2426.217	1.086	0.0000123
ENSBTAG00000002271	CDADC1	541.191	351.112	0.624	0.0000135
ENSBTAG00000013573	BIRC5	197.931	123.421	0.681	0.0000161
ENSBTAG00000001631	KIFC1	315.153	214.309	0.556	0.0000161
ENSBTAG00000015718	CASP8	955.840	677.335	0.497	0.0000168
ENSBTAG00000004971	GRAMD1C	174.208	115.007	0.599	0.0000174
ENSBTAG00000012314	LDLR	1609.169	1170.630	0.459	0.0000174
ENSBTAG00000000204	TMEM268	438.629	331.372	0.405	0.0000174
ENSBTAG00000006551	ESCO2	120.894	64.429	0.908	0.0000182
ENSBTAG00000006587	ZNF367	178.631	119.105	0.585	0.0000184
ENSBTAG00000016936	MISP3	94.766	158.027	-0.738	0.0000194
ENSBTAG00000038938		32.573	11.453	1.508	0.0000222
ENSBTAG00000009183	SHISA5	1386.183	1006.058	0.462	0.0000277
ENSBTAG00000017446	E2F8	125.643	57.219	1.135	0.000028
ENSBTAG00000017271	MASTL	123.917	61.555	1.009	0.0000287
ENSBTAG00000021673	NDC80	146.975	77.576	0.922	0.0000287
ENSBTAG00000007593	AIDA	870.048	636.790	0.450	0.0000313
ENSBTAG00000046512	XIRP1	153.319	293.400	-0.936	0.0000337
ENSBTAG00000004943	CCNA2	269.535	154.086	0.807	0.0000339
ENSBTAG00000000240	AKAP7	191.315	117.294	0.706	0.0000353
ENSBTAG00000022520	BRCA1	394.004	273.260	0.528	0.000036
ENSBTAG00000002586	TCF12	2067.782	1535.018	0.430	0.000036
ENSBTAG00000019386	BOLA-NC1	312.768	226.938	0.463	0.0000378
ENSBTAG00000024648		198.269	102.337	0.954	0.00004
ENSBTAG00000033690	BARD1	72.328	38.806	0.898	0.0000402
ENSBTAG00000016529	SLC25A30	905.424	674.085	0.426	0.0000419
ENSBTAG00000013405	FAM92A	378.702	516.159	-0.447	0.0000426
ENSBTAG00000014239	CCNB1	185.744	101.386	0.873	0.0000457
ENSBTAG00000015978	ANXA1	11737.549	8775.048	0.420	0.0000461
ENSBTAG00000021686	MELK	126.328	71.772	0.816	0.0000484
ENSBTAG00000043560	COX3	94657.863	140998.007	-0.575	0.0000496
ENSBTAG00000012397	DCK	277.562	183.471	0.597	0.0000501
ENSBTAG00000001343	DEPDC1	116.417	59.546	0.967	0.0000506
ENSBTAG00000021162	CKAP2	1010.308	659.762	0.615	0.000052
ENSBTAG00000012989	UBE2L6	210.199	137.924	0.608	0.0000523

GeneID	Gene	Mean Counts Juxt	Mean Counts Non-juxt	Log2 Fold-Change	P-Value (FDR adj)
ENSBTAG00000000590	POLE	374.969	247.410	0.600	0.0000523
ENSBTAG00000014099	YTHDC2	674.605	518.530	0.380	0.0000588
ENSBTAG00000016726	KIF15	114.866	58.622	0.970	0.0000598
ENSBTAG00000015230	PLA2G12A	483.087	373.062	0.373	0.0000598
ENSBTAG00000018003	ARHGEF25	243.189	342.098	-0.492	0.0000598
ENSBTAG00000000042	PYCR1	1435.771	2040.583	-0.507	0.0000598
ENSBTAG00000003120	ZNF385B	73.894	141.400	-0.936	0.0000598
ENSBTAG00000010077	FANCD2	161.779	100.465	0.687	0.0000605
ENSBTAG00000002918	RAD51	185.143	129.519	0.515	0.0000712
ENSBTAG00000003743		124.266	74.127	0.745	0.0000728
ENSBTAG00000021181	BUB1	384.950	266.966	0.528	0.0000743
ENSBTAG00000003314	SKA3	208.751	146.554	0.510	0.0000747
ENSBTAG00000003733	TM4SF5	94.048	155.774	-0.728	0.000077
ENSBTAG00000005413	NLRC5	88.595	42.505	1.060	0.0000847
ENSBTAG00000012252	MOCOS	333.278	228.334	0.546	0.0000863
ENSBTAG00000008963	CIT	288.337	197.203	0.548	0.0000887
ENSBTAG00000019989	PXK	689.215	515.031	0.420	0.0000898
ENSBTAG00000003807	CNOT9	1063.386	857.659	0.310	0.0000898
ENSBTAG00000006707	ACSL5	3775.635	3296.070	0.196	0.0000898
ENSBTAG00000015016	CALCOCO1	4882.189	5969.729	-0.290	0.0000898
ENSBTAG00000021799	RCN3	1236.299	1734.171	-0.488	0.0000898
ENSBTAG00000010007	MAPK13	206.786	291.771	-0.497	0.0000928
ENSBTAG00000005454	FUT10	377.083	281.763	0.420	0.0000983
ENSBTAG00000020837	ARHGEF16	117.259	74.843	0.648	0.0000993
ENSBTAG00000007397	FOLH1B	62.370	33.440	0.899	0.000105718
ENSBTAG00000009047	YPEL3	1520.450	1984.802	-0.384	0.000111277
ENSBTAG00000014694	JTB	320.104	424.500	-0.407	0.00011372
ENSBTAG00000000660	FAM83D	117.981	66.111	0.836	0.000129653
ENSBTAG00000009091	RNASEL	199.494	127.018	0.651	0.000137878
ENSBTAG00000021780	SCO1	868.594	693.448	0.325	0.000137878
ENSBTAG00000010774	NUSAP1	251.778	143.834	0.808	0.0001405
ENSBTAG00000013245	ITPR3	7702.084	6332.118	0.283	0.000144945
ENSBTAG00000012225	KPNA2	720.285	505.873	0.510	0.00015078
ENSBTAG00000006974	PLEKHA7	475.934	317.006	0.586	0.000160182
ENSBTAG00000013254	XPO1	2332.785	1669.502	0.483	0.00016251
ENSBTAG00000021395	PSME1	1988.616	1489.432	0.417	0.000169747
ENSBTAG00000005498	SQLE	957.491	685.586	0.482	0.000192321
ENSBTAG00000016557	MTMR2	763.474	608.588	0.327	0.000192321
ENSBTAG00000010517	EVPL	3184.623	4301.754	-0.434	0.000200838
ENSBTAG00000007799	MTFR2	104.166	56.052	0.894	0.000203695
ENSBTAG00000020905	RPL11	7872.941	9537.056	-0.277	0.000203943
ENSBTAG00000021177	ADAMTS14	185.693	298.841	-0.686	0.000205599
ENSBTAG00000008186	UBXN6	696.850	856.035	-0.297	0.000222528
ENSBTAG00000043564	ATP8	9128.072	12842.860	-0.493	0.000222528
ENSBTAG00000008633	SLX1A	661.978	849.996	-0.361	0.000222541
ENSBTAG00000015636	C7H19orf66	657.276	462.443	0.507	0.000230983
ENSBTAG00000007840	HMGCR	708.283	515.036	0.460	0.000237175
ENSBTAG00000002615	LONRF3	568.671	329.041	0.789	0.000241634
ENSBTAG00000046837	ZNF358	1241.778	1595.185	-0.361	0.000241634
ENSBTAG00000007247	NUF2	178.894	105.655	0.760	0.000256387
ENSBTAG00000011467	BATF2	67.892	34.587	0.973	0.000259709
ENSBTAG00000012046	JUNB	3153.365	4467.087	-0.502	0.000268176
ENSBTAG00000010225	POLR2D	746.307	575.912	0.374	0.000271443
ENSBTAG00000004064	BPNT1	510.028	364.225	0.486	0.000303966
ENSBTAG00000013160	GFRA4	587.407	813.503	-0.470	0.000322231
ENSBTAG00000016265	DNAJA1	1740.757	1335.792	0.382	0.000324266
ENSBTAG00000005305	NTS	112.293	59.943	0.906	0.000325317
ENSBTAG00000047827	RENBP	52.307	95.138	-0.863	0.000337809
ENSBTAG00000039462	PCLAF	123.318	64.890	0.926	0.000340692
ENSBTAG00000047694	SERF2	3125.332	4514.957	-0.531	0.000340692
ENSBTAG00000013855	ORMDL3	927.602	1423.644	-0.618	0.000340692
ENSBTAG00000017557	QRSL1	421.542	320.495	0.395	0.000358213
ENSBTAG00000000752	SGO1	73.688	38.820	0.925	0.000364196
ENSBTAG00000018569	CUL4B	1446.186	1071.927	0.432	0.000364196
ENSBTAG00000023814	ECT2	290.639	174.245	0.738	0.000366832
ENSBTAG00000019461	NUMBL	449.525	586.021	-0.383	0.000380275
ENSBTAG00000004240	TMPO	1130.896	842.222	0.425	0.000421615
ENSBTAG00000027655	TIFA	84.290	48.637	0.793	0.000427403
ENSBTAG00000003068	MSMO1	2284.990	1659.277	0.462	0.000429222
ENSBTAG00000019857	OTUD4	1639.126	1319.192	0.313	0.000429222

GeneID	Gene	Mean Counts Juxt	Mean Counts Non-juxt	Log2 Fold-Change	P-Value (FDR adj)
ENSBTAG00000011484	ZDHHC3	898.146	740.448	0.279	0.000438621
ENSBTAG00000021681	PRR11	64.241	31.868	1.011	0.000452916
ENSBTAG00000005862	SMC4	942.926	681.909	0.468	0.000475299
ENSBTAG00000018548	INTS7	724.686	572.838	0.339	0.000479435
ENSBTAG00000001992	CYP51A1	817.507	595.547	0.457	0.000483517
ENSBTAG00000043558	ND1	47222.788	71489.863	-0.598	0.000486086
ENSBTAG00000003381	PAPD7	1129.642	907.352	0.316	0.00051237
ENSBTAG00000009607	LARGE2	251.996	333.758	-0.405	0.000513749
ENSBTAG00000011146	RAB8B	856.977	631.328	0.441	0.000518406
ENSBTAG00000009617	SLC2A1	546.636	402.018	0.443	0.000560604
ENSBTAG00000016406	MCM10	274.943	198.459	0.470	0.000580196
ENSBTAG00000011405	CEP72	165.219	103.844	0.670	0.000583236
ENSBTAG00000002224	UHRF1	379.085	235.542	0.687	0.000588118
ENSBTAG00000000504	GTF2B	883.719	650.538	0.442	0.00059332
ENSBTAG00000031231	IRF1	381.583	220.149	0.794	0.000596901
ENSBTAG00000011549	TRPC2	138.478	91.455	0.599	0.000600042
ENSBTAG00000014633	ABCD4	441.914	349.769	0.337	0.000643983
ENSBTAG00000031461	SNX7	175.335	116.452	0.590	0.000671044
ENSBTAG00000016830	DAXX	2084.512	1596.805	0.385	0.000671044
ENSBTAG00000005063	THEM6	57.252	29.870	0.939	0.000672604
ENSBTAG00000010109	CDK1	153.025	95.053	0.687	0.00067503
ENSBTAG00000015604	ZNF385A	3862.529	4772.671	-0.305	0.000677795
ENSBTAG00000009812	CXCL5	1096.475	1794.411	-0.711	0.000678476
ENSBTAG00000018142	DTL	182.000	110.154	0.724	0.000744372
ENSBTAG00000008353	CDKN1A	4290.803	5408.030	-0.334	0.000744372
ENSBTAG00000012519	XDH	2099.885	2970.229	-0.500	0.000752496
ENSBTAG00000009681	PPP2R3C	366.950	263.709	0.477	0.000787761
ENSBTAG00000006615	CASP7	139.553	97.529	0.517	0.00079285
ENSBTAG00000006225	RPA2	407.645	300.876	0.438	0.000814748
ENSBTAG00000007077	ABHD1	236.838	158.218	0.582	0.000879485
ENSBTAG00000006851		148.422	90.018	0.721	0.000896467
ENSBTAG00000005708	KIF20B	237.848	155.919	0.609	0.000896467
ENSBTAG00000008113	OSR1	504.298	663.450	-0.396	0.000902329
ENSBTAG00000007389	IFI35	445.308	302.421	0.558	0.000908255
ENSBTAG00000005588	DXO	325.141	417.203	-0.360	0.000908255
ENSBTAG00000009618	NEK2	45.519	23.197	0.973	0.000925076
ENSBTAG00000002249	NAALADL1	88.833	131.193	-0.563	0.000925076
ENSBTAG00000001592	INSIG1	557.504	384.205	0.537	0.000961784
ENSBTAG00000006015	POLH	506.786	396.548	0.354	0.000965919
ENSBTAG00000000767	DCP2	302.961	208.200	0.541	0.001018271
ENSBTAG00000005979	HELLS	282.481	185.080	0.610	0.001027974
ENSBTAG00000000087	HSD17B12	851.626	649.559	0.391	0.001027974
ENSBTAG00000015713	TLK2	777.544	636.943	0.288	0.001065353
ENSBTAG00000001637	FUNDC1	418.142	313.309	0.416	0.001067105
ENSBTAG00000020116	JSP.1	186.444	109.097	0.773	0.00109029
ENSBTAG00000021442	CRTAP	1407.045	1758.792	-0.322	0.00111208
ENSBTAG00000040131	CD58	5745.834	4677.011	0.297	0.001127946
ENSBTAG00000014326	CDCA8	118.419	70.309	0.752	0.001143831
ENSBTAG00000021582	NCAPG	272.708	171.920	0.666	0.001143831
ENSBTAG00000021372		2472.505	2003.096	0.304	0.001143831
ENSBTAG00000020852	SLC16A11	634.234	765.139	-0.271	0.001143831
ENSBTAG00000045794	STMP1	2149.610	2482.849	-0.208	0.001165247
ENSBTAG00000012044	RPL13	8535.356	11318.781	-0.407	0.001172632
ENSBTAG00000044006	GINS2	110.896	70.580	0.652	0.001200985
ENSBTAG00000015683	HSPA4	2332.000	1972.119	0.242	0.001321965
ENSBTAG00000015875	FOXM1	98.523	59.487	0.728	0.00132573
ENSBTAG00000012068	BRIP1	81.604	50.005	0.707	0.00132573
ENSBTAG00000039556	WIPI1	540.979	678.060	-0.326	0.001359118
ENSBTAG00000023938	CENPA	139.552	89.913	0.634	0.001385146
ENSBTAG00000019614	FAM76A	364.278	293.333	0.313	0.001398685
ENSBTAG00000021301	ACSF2	575.857	746.170	-0.374	0.001485722
ENSBTAG00000043568	ND3	12891.720	20192.265	-0.647	0.001485722
ENSBTAG00000005825	NEIL3	43.829	22.744	0.946	0.001496419
ENSBTAG00000012432	FDFT1	831.421	670.118	0.311	0.001569887
ENSBTAG00000024081	ECM2	2578.027	1875.038	0.459	0.001585675
ENSBTAG00000014291	WNT2B	1646.634	1366.679	0.269	0.001654745
ENSBTAG00000011437		292.107	207.452	0.494	0.001660254
ENSBTAG00000001250	TFAP2A	1554.195	1993.610	-0.359	0.001660254
ENSBTAG00000014435	TCF19	113.946	65.052	0.809	0.001704157
ENSBTAG00000016766	TMEM176B	67.303	109.849	-0.707	0.001727303

GeneID	Gene	Mean Counts Juxt	Mean Counts Non-juxt	Log2 Fold-Change	P-Value (FDR adj)
ENSBTAG00000014380	MCM2	901.795	653.248	0.465	0.001738718
ENSBTAG00000006928	OAT	8732.094	7133.600	0.292	0.001756276
ENSBTAG00000024493	DHRS3	1293.329	2268.441	-0.811	0.00180391
ENSBTAG00000014820	OXA1L	1745.189	2132.348	-0.289	0.001914951
ENSBTAG00000005269	CCNB2	115.084	70.051	0.716	0.00192084
ENSBTAG00000011859	IPPK	371.011	271.000	0.453	0.00192084
ENSBTAG00000007755	APOBEC3Z3	257.079	190.363	0.433	0.001921895
ENSBTAG00000016043	GNB3	185.803	273.683	-0.559	0.001946954
ENSBTAG00000006751	PAPD4	784.695	585.583	0.422	0.001972126
ENSBTAG00000003330	ATL3	2441.326	1872.146	0.383	0.002070085
ENSBTAG00000023607	HACD2	783.100	603.701	0.375	0.002115362
ENSBTAG00000017329	GMNN	205.066	121.306	0.757	0.002142948
ENSBTAG00000008216	RRM2	853.998	473.476	0.851	0.002211234
ENSBTAG00000046450		226.685	300.923	-0.409	0.002267481
ENSBTAG00000004378	IL23A	360.071	258.614	0.477	0.002269057
ENSBTAG00000009830	PLEKHB1	392.606	501.677	-0.354	0.002370264
ENSBTAG00000003418	MSN	16395.903	19335.078	-0.238	0.002457883
ENSBTAG00000002027	FAM167B	93.639	133.557	-0.512	0.002458491
ENSBTAG00000024803	ENDOD1	821.637	653.201	0.331	0.002514725
ENSBTAG00000000137	FRYL	2224.671	1870.469	0.250	0.002514725
ENSBTAG00000002792	FUT11	431.907	529.681	-0.294	0.002525533
ENSBTAG00000011836	OMD	509.555	246.726	1.046	0.002608178
ENSBTAG00000001741	DLGAP4	1625.180	2030.352	-0.321	0.002608178
ENSBTAG00000014226	RPL34	3982.779	5383.906	-0.435	0.002608178
ENSBTAG00000024756	DENND6B	312.837	392.862	-0.329	0.002635047
ENSBTAG00000016224	RPS7	13085.812	16560.829	-0.340	0.002667556
ENSBTAG00000006836	FBXO33	647.932	480.554	0.431	0.00269843
ENSBTAG00000004805	ITFG1	2138.667	1842.323	0.215	0.002835537
ENSBTAG00000000202	SLC25A19	309.260	215.184	0.523	0.002895915
ENSBTAG00000044066	CATSPERE	40.101	18.436	1.121	0.003018169
ENSBTAG00000026246	MOSPD3	393.251	486.692	-0.308	0.00303189
ENSBTAG00000014091	ARHGEF3	626.325	472.023	0.408	0.003046533
ENSBTAG00000002357	TICAM2	515.905	433.447	0.251	0.003046533
ENSBTAG00000009522	EIF4E	862.772	693.031	0.316	0.003118151
ENSBTAG00000016709	NT5C3A	505.499	371.479	0.444	0.003133081
ENSBTAG00000033727	RBPMS	2198.232	2599.755	-0.242	0.003136794
ENSBTAG00000020059	GEN1	194.286	129.157	0.589	0.003177267
ENSBTAG00000017002	RBCK1	1694.143	1322.369	0.357	0.003177267
ENSBTAG00000011133	AP1S3	937.678	741.647	0.338	0.003191234
ENSBTAG00000008827	SPOCK2	1715.856	2054.443	-0.260	0.003402515
ENSBTAG00000004999	KIAA1551	8917.116	6019.947	0.567	0.00343687
ENSBTAG00000043561	COX1	485698.972	621071.314	-0.355	0.003485571
ENSBTAG00000018383	ATAD5	146.309	92.430	0.663	0.003570984
ENSBTAG00000018189	CSTB	416.996	621.946	-0.577	0.003570984
ENSBTAG00000016650	TIGAR	66.978	41.270	0.699	0.003732259
ENSBTAG00000011636	DDIAS	258.304	181.902	0.506	0.003768765
ENSBTAG00000011986	PLSCR4	976.318	745.916	0.388	0.003777145
ENSBTAG00000002515		98.681	138.992	-0.494	0.00383587
ENSBTAG00000001938	CKS2	180.099	114.459	0.654	0.003859747
ENSBTAG00000030557	LIN52	749.669	604.854	0.310	0.003874557
ENSBTAG00000000021	WASHC3	875.172	1080.839	-0.305	0.003912958
ENSBTAG00000013631	GLUL	5685.490	6807.147	-0.260	0.003921515
ENSBTAG00000012749	CUL7	3190.927	3791.456	-0.249	0.004199201
ENSBTAG00000002690	BLZF1	559.330	457.265	0.291	0.004199923
ENSBTAG00000015527	MYO1D	15525.541	18659.968	-0.265	0.00428725
ENSBTAG00000000146	FARP1	831.676	997.639	-0.262	0.004486314
ENSBTAG00000002573	UBA2	1626.140	1380.687	0.236	0.004487674
ENSBTAG00000006383		515.603	761.074	-0.562	0.004570302
ENSBTAG00000003405	TP53I3	372.199	446.053	-0.261	0.004577193
ENSBTAG00000013669	KIF22	193.473	127.153	0.606	0.004589513
ENSBTAG00000012070	INTS2	217.866	166.119	0.391	0.004685607
ENSBTAG00000010627	SF3B3	3321.411	2937.559	0.177	0.004751601
ENSBTAG00000005129	CEP55	112.796	72.295	0.642	0.004929299
ENSBTAG00000021680	SKA2	433.451	324.340	0.418	0.004930971
ENSBTAG00000014793	C16H1orf112	143.114	104.894	0.448	0.004957827
ENSBTAG00000001100	IL22RA1	67.382	44.921	0.585	0.004976936
ENSBTAG00000016501	ARHGAP1	4946.673	5839.013	-0.239	0.005198125
ENSBTAG00000024042	MORN2	108.263	157.082	-0.537	0.005273331
ENSBTAG00000024539	SPSB1	1214.564	1592.522	-0.391	0.005325905
ENSBTAG00000016017	CCDC40	30.593	48.739	-0.672	0.005325905

GeneID	Gene	Mean Counts Juxt	Mean Counts Non-juxt	Log2 Fold-Change	P-Value (FDR adj)
ENSBTAG00000020301	BLM	162.368	116.221	0.482	0.005380505
ENSBTAG00000014784	NT5DC2	579.274	735.950	-0.345	0.005380505
ENSBTAG00000012880	DNLZ	99.128	155.810	-0.652	0.005380505
ENSBTAG00000039529	BTBD19	232.355	293.450	-0.337	0.005392404
ENSBTAG00000010048	SPC25	51.925	26.683	0.961	0.00561025
ENSBTAG00000019246	SC5D	1276.550	1047.318	0.286	0.00561025
ENSBTAG00000026375	RMI2	147.391	107.647	0.453	0.005647335
ENSBTAG00000005607	ERCC6L	69.978	44.383	0.657	0.005792088
ENSBTAG00000000690	THEM5	388.294	493.488	-0.346	0.00580368
ENSBTAG00000020528	PCOLCE	197.812	260.467	-0.397	0.005840078
ENSBTAG00000001465	P2RY1	435.706	307.065	0.505	0.005882133
ENSBTAG00000044175	CENPK	104.055	59.086	0.816	0.005977931
ENSBTAG00000018216	SKA1	71.408	37.571	0.926	0.006005289
ENSBTAG00000003514	HSF4	557.582	715.038	-0.359	0.006018177
ENSBTAG00000043553	GPX3	159.405	235.904	-0.566	0.006033547
ENSBTAG00000019312	TFCP2	1188.793	983.704	0.273	0.006126418
ENSBTAG00000008320		233.389	297.261	-0.349	0.006133576
ENSBTAG00000012784	RACGAP1	398.513	310.582	0.360	0.006280667
ENSBTAG00000008733	MAGED1	3761.515	4498.116	-0.258	0.006280667
ENSBTAG00000014762	ISG20	79.145	49.997	0.663	0.006286267
ENSBTAG00000011421	CD37	122.400	166.737	-0.446	0.006484937
ENSBTAG00000020780	SBNO2	1689.242	2051.832	-0.281	0.006511938
ENSBTAG00000007644	GNG7	449.610	555.091	-0.304	0.006638343
ENSBTAG00000016174	NCL	6512.279	5815.486	0.163	0.006729412
ENSBTAG00000016254	HDAC5	1885.407	2377.414	-0.335	0.006729412
ENSBTAG00000014773	HMMR	250.977	186.144	0.431	0.006732989
ENSBTAG00000047214	TRAPPC1	314.559	410.229	-0.383	0.006732989
ENSBTAG00000000312	GRINA	3012.301	2390.492	0.334	0.006740963
ENSBTAG00000008097	WNT2	1075.809	871.701	0.304	0.006762308
ENSBTAG00000000668	SLC22A5	273.606	352.603	-0.366	0.006762308
ENSBTAG00000004463	KDELR1	1940.522	2280.913	-0.233	0.006848724
ENSBTAG00000007429	SPNS2	192.457	255.292	-0.408	0.006848724
ENSBTAG00000008499	TROAP	193.916	122.440	0.663	0.006888084
ENSBTAG00000044079	SMIM4	102.493	156.464	-0.610	0.006902768
ENSBTAG00000017037	PKN1	1064.386	1344.554	-0.337	0.006992069
ENSBTAG00000004688	DHCR24	639.958	439.886	0.541	0.007018378
ENSBTAG00000010170	MBTPS1	1570.326	1932.143	-0.299	0.007118661
ENSBTAG00000047416	HEPH	299.912	222.194	0.433	0.007187123
ENSBTAG00000035544	CYP46A1	39.635	64.377	-0.700	0.007201811
ENSBTAG00000003800	LRRC27	275.374	338.969	-0.300	0.007229493
ENSBTAG00000010304	CHKA	1285.115	1047.485	0.295	0.007230113
ENSBTAG00000015225	NUP58	1350.773	1128.981	0.259	0.007230113
ENSBTAG00000002014	SNX1	1654.575	1461.417	0.179	0.007230113
ENSBTAG00000020139	RPL7	8982.419	11308.463	-0.332	0.007384138
ENSBTAG00000002363	SESN2	412.712	339.981	0.280	0.007421876
ENSBTAG00000015280	KIF2C	103.245	64.433	0.680	0.007459134
ENSBTAG00000007494	SMARCA2	2097.148	2479.514	-0.242	0.007623487
ENSBTAG00000000897	IQGAP2	112.310	148.104	-0.399	0.007660471
ENSBTAG00000037634		14.500	5.779	1.327	0.007660723
ENSBTAG00000020734	ARL6IP1	1002.566	771.098	0.379	0.007660723
ENSBTAG00000000095	CD274	38.198	21.805	0.809	0.00768798
ENSBTAG00000000604	GPNMB	143.637	203.417	-0.502	0.007701049
ENSBTAG00000013009	AURKA	171.715	125.687	0.450	0.007825011
ENSBTAG00000007303	RAD21	2480.193	2060.336	0.268	0.007825011
ENSBTAG00000047268	WT1	5577.288	6479.557	-0.216	0.007825011
ENSBTAG00000002562	PRAF2	773.122	954.829	-0.305	0.007825011
ENSBTAG00000011187	FAM13A	527.371	428.501	0.300	0.008106172
ENSBTAG00000014705	HES4	19.245	7.214	1.416	0.008135752
ENSBTAG00000011505	RABEP1	3175.901	2671.240	0.250	0.008135752
ENSBTAG00000024097	MRPS15	290.739	395.921	-0.445	0.008135752
ENSBTAG00000013929	RRAD	11.085	26.881	-1.278	0.008135752
ENSBTAG00000001694	TYRO3	3102.572	3722.996	-0.263	0.008184039
ENSBTAG00000008180	SPDL1	102.559	61.362	0.741	0.008532542
ENSBTAG00000037558	GRO1	86.821	140.071	-0.690	0.008575915
ENSBTAG00000017549	KITLG	721.792	474.651	0.605	0.00863902
ENSBTAG00000014728	TAPBPL	833.194	659.740	0.337	0.008770916
ENSBTAG00000012873	SNX6	1203.444	1016.690	0.243	0.008770916
ENSBTAG00000046325		237.945	173.579	0.455	0.008998242
ENSBTAG00000021176	CRISPLD2	1703.424	2077.314	-0.286	0.008998242
ENSBTAG00000005015	SFXN3	296.787	387.827	-0.386	0.009240354

GeneID	Gene	Mean Counts Juxt	Mean Counts Non-juxt	Log2 Fold-Change	P-Value (FDR adj)
ENSBTAG00000031800	PPDPF	4128.210	4975.260	-0.269	0.009274092
ENSBTAG00000003072	ACADVL	2143.012	2507.204	-0.226	0.009360764
ENSBTAG00000009441	RBBP6	3128.478	2628.151	0.251	0.009564447
ENSBTAG00000014382	KANK4	714.303	577.206	0.307	0.009625567
ENSBTAG00000016156	MAPK3	2162.188	2565.555	-0.247	0.009712301
ENSBTAG00000003947	SSBP4	644.815	799.155	-0.310	0.01000816
ENSBTAG00000006305	AK1	142.681	190.137	-0.414	0.01000816
ENSBTAG00000032996	P4HA1	2836.203	2354.826	0.268	0.010131308
ENSBTAG00000002526	BDH2	753.092	920.421	-0.289	0.010359697
ENSBTAG00000017674	SCNN1D	63.354	89.531	-0.499	0.010678304
ENSBTAG00000015541	DLC1	2959.300	2305.646	0.360	0.010687654
ENSBTAG00000008635	SULT1A1	6556.951	7857.146	-0.261	0.010687654
ENSBTAG00000007208	HDAC11	236.324	304.159	-0.364	0.010687654
ENSBTAG00000004490	TRIM31	45.716	66.572	-0.542	0.010687654
ENSBTAG00000013624	LMNB2	293.633	215.673	0.445	0.010822556
ENSBTAG00000032951	ABHD17C	1194.789	1397.962	-0.227	0.010846278
ENSBTAG00000007639	SDAD1	715.922	603.917	0.245	0.011028399
ENSBTAG00000020179	AAAS	185.724	250.500	-0.432	0.011028399
ENSBTAG00000043556	COX2	45293.065	61798.134	-0.448	0.011028399
ENSBTAG00000009819	CDC20	152.154	101.205	0.588	0.011035248
ENSBTAG00000008453	LBR	169.862	131.129	0.373	0.011128656
ENSBTAG00000013822	GAS2L3	63.371	37.412	0.760	0.01125543
ENSBTAG00000002613	MIS18BP1	327.889	234.908	0.481	0.01144815
ENSBTAG00000014626	RARS	1079.142	922.134	0.227	0.01144815
ENSBTAG00000003826	SCN1B	128.631	188.725	-0.553	0.011488229
ENSBTAG00000013949	AHCTF1	1298.390	1110.051	0.226	0.011489229
ENSBTAG00000027081	ATP10A	1021.037	857.593	0.252	0.011544415
ENSBTAG00000009886	KDELR3	1432.533	1829.254	-0.353	0.011544415
ENSBTAG00000003959	ARHGAP24	1334.301	1664.714	-0.319	0.011661
ENSBTAG00000018240	CYP2S1	152.881	98.883	0.629	0.011828687
ENSBTAG00000002747	ABCA5	208.856	272.432	-0.383	0.011828687
ENSBTAG00000006695	VCPIP1	587.961	441.324	0.414	0.011863451
ENSBTAG00000019864	MAPK15	46.746	69.863	-0.580	0.011863451
ENSBTAG00000021071	TRIM8	859.527	1128.398	-0.393	0.011872696
ENSBTAG00000000957	CDKN2AIP	469.864	358.941	0.388	0.011928161
ENSBTAG00000012927	ALDOA	5515.422	6625.921	-0.265	0.011928161
ENSBTAG00000022590		1710.328	1355.723	0.335	0.011997695
ENSBTAG00000014100	BAIAP3	8.698	20.681	-1.250	0.011997695
ENSBTAG00000017021		245.589	172.379	0.511	0.011999056
ENSBTAG00000017266	ITGA6	1693.114	1384.074	0.291	0.012069395
ENSBTAG00000007753	KIFC2	340.109	419.928	-0.304	0.012310833
ENSBTAG00000013191	AGRN	10743.235	7944.526	0.435	0.012438948
ENSBTAG00000018040	PSMB10	304.366	214.046	0.508	0.012470665
ENSBTAG00000005745	HPSE	1430.359	1076.849	0.410	0.012586759
ENSBTAG00000015582	HMOX1	1496.800	1967.692	-0.395	0.012586759
ENSBTAG00000035319	MAD2L1	83.195	53.128	0.647	0.012939578
ENSBTAG00000017844	STIL	75.458	50.446	0.581	0.013057739
ENSBTAG00000008355	CPSF1	1307.820	1579.476	-0.272	0.013057739
ENSBTAG00000013162	HSPA8	20422.727	17731.447	0.204	0.013069489
ENSBTAG00000005793	PEA15	15919.877	18376.587	-0.207	0.013071081
ENSBTAG00000009035	CENPE	245.776	161.430	0.606	0.013257347
ENSBTAG00000006482	PTCD3	714.464	601.198	0.249	0.013291456
ENSBTAG00000011228	FASTK	1049.013	1303.279	-0.313	0.013429471
ENSBTAG00000001920	POLQ	59.202	36.203	0.710	0.013435009
ENSBTAG00000019794	SYPL1	1972.732	1646.521	0.261	0.013440909
ENSBTAG00000008181	CHAF1A	291.155	202.679	0.523	0.013493195
ENSBTAG00000037456	AHDC1	1107.452	1363.173	-0.300	0.013524126
ENSBTAG00000032521	PLEKHH2	1288.419	986.444	0.385	0.013549202
ENSBTAG00000037581	MZF1	791.640	918.581	-0.215	0.013565539
ENSBTAG00000010935	EML4	1824.273	1402.722	0.379	0.013605241
ENSBTAG00000005110	CADPS2	104.040	66.177	0.653	0.013695964
ENSBTAG00000012107	SLC25A28	1024.028	862.864	0.247	0.013695964
ENSBTAG00000016619	MIS18A	39.670	20.389	0.960	0.013718562
ENSBTAG00000013275	MAD2L2	366.575	272.209	0.429	0.013741397
ENSBTAG00000046358	PABPC1	19398.330	22579.341	-0.219	0.013741397
ENSBTAG00000010532	KCTD11	452.112	608.144	-0.428	0.013771409
ENSBTAG00000044192	MAF	584.315	820.874	-0.490	0.013816877
ENSBTAG00000008636	PDE4B	817.057	566.406	0.529	0.014457955
ENSBTAG00000017405	RORC	489.281	610.506	-0.319	0.014457955
ENSBTAG00000048017	PRR16	25.918	42.097	-0.700	0.014457955

GeneID	Gene	Mean Counts Juxt	Mean Counts Non-juxt	Log2 Fold-Change	P-Value (FDR adj)
ENSBTAG00000017133	GINS4	67.224	43.559	0.626	0.014510033
ENSBTAG00000031752	TMEM256	351.494	468.052	-0.413	0.014889451
ENSBTAG00000001578	ADPGK	979.964	825.730	0.247	0.015210026
ENSBTAG00000021957	LTBP2	36044.878	66735.988	-0.889	0.015234797
ENSBTAG00000039015	TMEM145	119.473	155.599	-0.381	0.015297355
ENSBTAG00000005957	CSE1L	1825.256	1522.651	0.262	0.015425718
ENSBTAG00000031579	SGO2	358.698	288.000	0.317	0.015444165
ENSBTAG00000015046	MST1R	284.373	219.115	0.376	0.015788589
ENSBTAG00000000571	ARHGAP27	50.086	27.548	0.862	0.015936323
ENSBTAG00000019120	WDHD1	285.823	199.102	0.522	0.015967228
ENSBTAG00000012016	LMTK3	139.379	176.394	-0.340	0.015973794
ENSBTAG00000002736	DNMT1	1066.466	880.580	0.276	0.016131621
ENSBTAG00000012184	PTTG1	114.694	70.825	0.695	0.016142699
ENSBTAG00000002620	DNA2	53.223	32.453	0.714	0.016319576
ENSBTAG00000020371	ACOT8	251.184	310.198	-0.304	0.016319576
ENSBTAG00000007117	CTC1	623.650	508.957	0.293	0.016322863
ENSBTAG00000008954	PSMB9	143.893	83.269	0.789	0.016450376
ENSBTAG00000026971	CDCA5	97.532	61.669	0.661	0.016450376
ENSBTAG00000017616	ADSSL1	161.136	201.782	-0.325	0.016455013
ENSBTAG00000017164	LARP4	405.704	316.950	0.356	0.016548919
ENSBTAG00000032077	KCND2	96.155	64.400	0.578	0.016639611
ENSBTAG00000016264	FKBP8	3053.723	3522.034	-0.206	0.016731159
ENSBTAG00000018566	SFRP5	253.951	482.727	-0.927	0.016731159
ENSBTAG00000016355	UVRAG	344.567	262.904	0.390	0.016758955
ENSBTAG00000015106	DSP	3018.424	2529.805	0.255	0.0168156
ENSBTAG00000025931	NEU3	269.783	202.753	0.412	0.016920202
ENSBTAG00000011911		174.190	128.480	0.439	0.017219729
ENSBTAG00000000639	APRT	1198.919	962.697	0.317	0.017219729
ENSBTAG00000021506	ARL6IP5	2542.026	2115.143	0.265	0.017219729
ENSBTAG00000015163	TM4SF1	2944.783	2294.161	0.360	0.017222768
ENSBTAG00000014730	NCAPD2	1069.760	875.450	0.289	0.017278535
ENSBTAG00000010584	AP2S1	604.587	751.440	-0.314	0.017278535
ENSBTAG00000017284	RHBDL1	651.096	835.614	-0.360	0.017401466
ENSBTAG00000012586	HSPD1	1598.558	1416.806	0.174	0.017659772
ENSBTAG00000011661	CEP152	91.311	62.561	0.546	0.017802282
ENSBTAG00000019156	CCT2	2375.640	2099.488	0.178	0.017818468
ENSBTAG00000037778	CXCL3	605.357	904.431	-0.579	0.017927786
ENSBTAG00000007415	SLC7A8	1810.504	2094.644	-0.210	0.017953247
ENSBTAG00000014208	RPL35A	4811.499	5837.186	-0.279	0.017986413
ENSBTAG00000001497	MRAS	1089.571	1391.275	-0.353	0.018336852
ENSBTAG00000003038		1422.653	1221.049	0.220	0.018371155
ENSBTAG00000020636	SYN3	7595.496	8652.416	-0.188	0.018384041
ENSBTAG00000008504	SYNGR3	175.452	233.288	-0.411	0.018411063
ENSBTAG00000014863	GYPC	445.256	655.088	-0.557	0.018411063
ENSBTAG00000012434	ENOX1	211.459	266.932	-0.336	0.018445035
ENSBTAG00000011824	OGN	1857.258	993.899	0.902	0.018522175
ENSBTAG00000023780	SYCE1L	66.198	104.177	-0.654	0.018562814
ENSBTAG00000007447	NUDT4	1653.653	1420.816	0.219	0.018599423
ENSBTAG00000015457	FGFR1	3283.241	3887.199	-0.244	0.018599423
ENSBTAG00000008406	TREX1	256.216	164.483	0.639	0.018807063
ENSBTAG00000021517	TMEM216	72.752	100.308	-0.463	0.018807063
ENSBTAG00000014744	TXNDC15	765.431	646.187	0.244	0.018937233
ENSBTAG00000003155	IFI27L2	139.441	205.371	-0.559	0.019088515
ENSBTAG00000009888	DRAM2	494.884	402.515	0.298	0.019163926
ENSBTAG00000003222	ASNS	1148.574	1340.392	-0.223	0.019163926
ENSBTAG00000044038	TEN1	322.622	391.445	-0.279	0.019163926
ENSBTAG00000013111	RRM1	1107.220	929.544	0.252	0.019176714
ENSBTAG00000000828	CAPN6	131.521	182.076	-0.469	0.019176714
ENSBTAG00000012205	CPT1C	107.997	142.939	-0.404	0.019198717
ENSBTAG00000009132	TMPRSS2	93.999	44.808	1.069	0.0193242
ENSBTAG00000011184	FTH1	7104.314	8486.625	-0.256	0.019513795
ENSBTAG00000019463	SLC25A39	2113.719	2559.225	-0.276	0.019702351
ENSBTAG00000013479	SLC9A3R2	58.535	84.064	-0.522	0.019712332
ENSBTAG00000015593	KIAA0753	429.922	357.523	0.266	0.019769298
ENSBTAG00000031299	TTC17	938.101	825.316	0.185	0.019965288
ENSBTAG00000018800	RPS4X	7841.905	9394.933	-0.261	0.019965288
ENSBTAG00000006052	PLCD3	428.367	515.507	-0.267	0.019965288
ENSBTAG00000044083	LIMK1	540.274	428.911	0.333	0.020034548
ENSBTAG00000004307	VPS36	1437.822	1236.428	0.218	0.020121717
ENSBTAG00000019554	FBP2	143.232	186.378	-0.380	0.020268265

GeneID	Gene	Mean Counts Juxt	Mean Counts Non-juxt	Log2 Fold-Change	P-Value (FDR adj)
ENSBTAG00000015346	NASP	871.459	703.445	0.309	0.020332972
ENSBTAG00000015831	RPL18A	10115.760	11926.806	-0.238	0.020393635
ENSBTAG00000030503	H2AFJ	398.417	513.457	-0.366	0.020705771
ENSBTAG00000001151	APLP1	490.188	600.913	-0.294	0.021165711
ENSBTAG00000017258	ACSL3	592.382	473.772	0.322	0.021250144
ENSBTAG00000018936	LSS	573.374	463.953	0.305	0.021250144
ENSBTAG00000002117	KIF18A	135.927	95.931	0.503	0.021502895
ENSBTAG00000033315	DNAJC1	370.818	283.587	0.387	0.021522474
ENSBTAG00000021691	PSMD14	890.473	751.551	0.245	0.021522474
ENSBTAG00000003711	EPAS1	3782.739	4947.859	-0.387	0.02162945
ENSBTAG00000021102	GALM	1456.631	1210.452	0.267	0.021854119
ENSBTAG00000006633	IRF3	1811.001	1510.771	0.262	0.022036756
ENSBTAG00000015519	GFM2	482.914	411.507	0.231	0.022129092
ENSBTAG00000016315	COTL1	3231.219	3928.570	-0.282	0.022129092
ENSBTAG00000012219	CSPG4	455.364	638.091	-0.487	0.022290783
ENSBTAG00000014401	SORBS3	3007.241	3739.599	-0.314	0.022337735
ENSBTAG00000011044	TACC3	340.724	238.402	0.515	0.022343005
ENSBTAG00000006779	LDHD	28.871	46.878	-0.699	0.022355765
ENSBTAG00000025219		28.337	13.171	1.105	0.022472994
ENSBTAG00000012212	CYP26B1	42.113	23.985	0.812	0.022472994
ENSBTAG00000020535	PYCARD	132.559	175.309	-0.403	0.022521055
ENSBTAG00000006255	MDM4	544.393	417.256	0.384	0.022833581
ENSBTAG00000025450	SYNE2	1714.440	1390.318	0.302	0.022833581
ENSBTAG00000005372	DLGAP1	182.177	238.994	-0.392	0.022833581
ENSBTAG00000001662	EHD3	1291.971	1532.593	-0.246	0.022880655
ENSBTAG00000007356	ELF1	1135.104	970.866	0.225	0.022883645
ENSBTAG00000003457	ATF5	829.006	1002.695	-0.274	0.023178754
ENSBTAG00000011134	USE1	345.844	418.377	-0.275	0.023178754
ENSBTAG00000011971	NRP2	927.134	693.471	0.419	0.023260337
ENSBTAG00000016413	DUSP26	14.735	29.149	-0.984	0.023326995
ENSBTAG00000003791	LPAR3	443.775	578.198	-0.382	0.023416578
ENSBTAG00000020238	RIMS1	95.506	66.242	0.528	0.023495513
ENSBTAG00000004448	CKAP5	1457.567	1253.688	0.217	0.023678844
ENSBTAG00000008774	UROC1	64.067	92.020	-0.522	0.023698503
ENSBTAG00000008135	SLIRP	605.597	762.492	-0.332	0.024071945
ENSBTAG00000003168	HNRNPUL1	4814.626	5628.879	-0.225	0.024490354
ENSBTAG00000018650	HEPACAM	19.411	37.050	-0.933	0.024707257
ENSBTAG00000009960	FLOT1	1748.214	1981.921	-0.181	0.024717115
ENSBTAG00000011563		19.847	9.540	1.057	0.024796648
ENSBTAG00000006065	PCNA	653.698	479.783	0.446	0.024981326
ENSBTAG00000026613	MSTO1	185.198	228.527	-0.303	0.025028449
ENSBTAG00000017721	METTL13	264.215	210.971	0.325	0.025055801
ENSBTAG00000010196	NUP43	307.651	236.269	0.381	0.02529915
ENSBTAG00000020975	SYNGAP1	394.426	489.870	-0.313	0.02529915
ENSBTAG00000007102	GTSE1	205.749	155.515	0.404	0.025306486
ENSBTAG00000013259	POLR3A	995.604	877.081	0.183	0.025364219
ENSBTAG00000007093	DDX11	189.191	140.599	0.428	0.025632823
ENSBTAG00000026025		86.457	59.802	0.532	0.025715613
ENSBTAG00000009535	RPS2	36524.377	43996.244	-0.269	0.02573491
ENSBTAG00000008170	POLA1	405.693	310.805	0.384	0.025744492
ENSBTAG00000009948	TRIM25	1560.343	1126.237	0.470	0.025836742
ENSBTAG00000020407	MTSS1	381.174	523.051	-0.457	0.026010253
ENSBTAG00000016838	SRPK1	1021.177	877.230	0.219	0.026022788
ENSBTAG00000013346	SIX5	399.708	489.182	-0.291	0.026062126
ENSBTAG00000006984	CD55	10979.372	8951.623	0.295	0.026097395
ENSBTAG00000005814	PSME2	1050.465	817.402	0.362	0.026298652
ENSBTAG00000020277	PPP2R1B	2729.518	3016.776	-0.144	0.026298652
ENSBTAG00000031933	ALOX12E	37.520	62.344	-0.733	0.026298652
ENSBTAG00000048151	PRPF40A	1760.622	1509.976	0.222	0.026332093
ENSBTAG00000012658	TMA16	616.765	501.095	0.300	0.026341202
ENSBTAG00000021469	CTTNBP2	2935.500	3530.832	-0.266	0.026376698
ENSBTAG00000003089	RHPN2	816.855	669.216	0.288	0.026535557
ENSBTAG00000032481	DAPL1	53.534	80.224	-0.584	0.026535557
ENSBTAG00000015318	NECTIN2	331.607	259.914	0.351	0.026706134
ENSBTAG00000007937	PRIM2	323.625	257.931	0.327	0.026713645
ENSBTAG00000047376	PIN4	94.397	120.749	-0.355	0.026810462
ENSBTAG00000026008	METTL5	158.979	193.678	-0.285	0.026818568
ENSBTAG00000008632		258.865	327.063	-0.337	0.026818568
ENSBTAG00000017460	PRORSD1	135.359	185.678	-0.456	0.026818568
ENSBTAG00000020367	SLC30A9	700.788	589.625	0.249	0.026866457

GeneID	Gene	Mean Counts Juxt	Mean Counts Non-juxt	Log2 Fold-Change	P-Value (FDR adj)
ENSBTAG00000018223	CHI3L1	2539.725	3179.997	-0.324	0.026938058
ENSBTAG00000027654	EIF4EBP1	411.813	520.307	-0.337	0.026938058
ENSBTAG00000016828	TAPBP	4892.096	4056.155	0.270	0.027043622
ENSBTAG00000011943	TPR	2474.548	2180.978	0.182	0.027155527
ENSBTAG00000018622	PCBP4	1756.928	2017.956	-0.200	0.02737651
ENSBTAG00000012516	SLC1A7	29.591	52.028	-0.814	0.02737651
ENSBTAG00000014450	NOSIP	477.882	586.771	-0.296	0.027596074
ENSBTAG00000011395	DNM1L	412.388	330.196	0.321	0.02770099
ENSBTAG00000021066	CAPN11	5.588	16.585	-1.570	0.02770099
ENSBTAG00000031435	SELENOT	1073.153	890.478	0.269	0.027712725
ENSBTAG00000000599	CCNI	3392.944	3954.246	-0.221	0.027712725
ENSBTAG00000048077	MAGED4B	777.263	952.267	-0.293	0.027712725
ENSBTAG00000004085	ASF1B	93.449	58.988	0.664	0.028181869
ENSBTAG00000020169	CEPT1	420.523	342.861	0.295	0.028188573
ENSBTAG00000018025	IQCG	114.967	150.526	-0.389	0.028281105
ENSBTAG00000016746	UBE2C	260.017	171.700	0.599	0.02837937
ENSBTAG00000006862	MEIS3	494.839	639.250	-0.369	0.028693512
ENSBTAG00000007960	TOP1	1335.721	1126.472	0.246	0.028844818
ENSBTAG00000014648	RPN2	3238.529	2786.034	0.217	0.028844818
ENSBTAG00000009199	GLIS2	2753.426	3270.605	-0.248	0.028844818
ENSBTAG00000009396	EXO1	51.879	29.870	0.796	0.029008407
ENSBTAG00000005573	SCAND1	993.851	1245.033	-0.325	0.029088825
ENSBTAG00000019018		2633.348	2010.509	0.389	0.02910624
ENSBTAG00000001209	PHLDB2	3579.271	3984.349	-0.155	0.02910624
ENSBTAG00000031849	TMEM119	55.410	81.195	-0.551	0.02910624
ENSBTAG00000001553	HNRNPA1	7567.400	6410.689	0.239	0.02910903
ENSBTAG00000020480	SPTLC2	1137.514	931.989	0.287	0.029170229
ENSBTAG00000001745	LUM	6254.832	4874.392	0.360	0.029245664
ENSBTAG00000021020	RIF1	897.233	687.028	0.385	0.029414534
ENSBTAG00000010505	INTS4	579.054	497.627	0.219	0.029633825
ENSBTAG00000006877	MMP16	182.634	239.459	-0.391	0.029713009
ENSBTAG00000020647	RASL11B	154.679	233.492	-0.594	0.029911392
ENSBTAG00000000629	MMS22L	167.036	126.275	0.404	0.030011909
ENSBTAG00000019636	SCARA5	16.556	32.076	-0.954	0.030027914
ENSBTAG00000007121	TK1	284.599	217.515	0.388	0.03007663
ENSBTAG00000020710	CENPQ	103.914	71.775	0.534	0.030211055
ENSBTAG00000013392	PLD2	1428.927	1640.480	-0.199	0.030323612
ENSBTAG00000006160	SUOX	316.253	383.521	-0.278	0.030564188
ENSBTAG00000005092	ROR2	111.529	153.277	-0.459	0.030566909
ENSBTAG00000010956	SCARB2	3622.600	3065.244	0.241	0.030810371
ENSBTAG00000015426	PDLIM4	1350.710	1683.515	-0.318	0.031236405
ENSBTAG00000038844	ANKRD35	83.872	58.290	0.525	0.031351233
ENSBTAG00000013218	GORASP2	3062.748	3461.422	-0.177	0.031351233
ENSBTAG00000001840	INO80B	478.394	574.398	-0.264	0.031351233
ENSBTAG00000000281	MND1	65.782	41.826	0.653	0.031358593
ENSBTAG00000019105	NPLOC4	934.208	798.847	0.226	0.031358593
ENSBTAG00000018884	RING1	935.660	1156.668	-0.306	0.031641222
ENSBTAG00000017448	EFEMP1	13655.592	11172.833	0.289	0.031665408
ENSBTAG00000005475	TCAF2	457.954	372.633	0.297	0.031786881
ENSBTAG00000002094	ATP5MF	610.129	759.403	-0.316	0.031875445
ENSBTAG00000018967	YIPF3	2024.303	2371.214	-0.228	0.032069362
ENSBTAG00000021193	FBXO5	97.020	67.853	0.516	0.032076593
ENSBTAG00000014278	TBX2	96.005	135.040	-0.492	0.032096383
ENSBTAG00000019015	IFITM3	13750.853	11222.616	0.293	0.032135756
ENSBTAG00000001057	ARFGAP3	757.372	866.457	-0.194	0.032135756
ENSBTAG00000000288	UPF2	856.488	728.337	0.234	0.032990746
ENSBTAG00000017026	DEPDC1B	46.292	28.377	0.706	0.033059294
ENSBTAG00000021045	E2F3	234.190	189.642	0.304	0.033150973
ENSBTAG00000004092	AK8	265.743	327.597	-0.302	0.033288485
ENSBTAG00000027213		182.580	271.511	-0.572	0.033288485
ENSBTAG00000021971	SNCAIP	143.754	193.020	-0.425	0.033351377
ENSBTAG00000011111	COPS7A	920.724	1117.905	-0.280	0.033869486
ENSBTAG00000007808	ANTXR1	2820.382	3512.595	-0.317	0.033971936
ENSBTAG00000013249	SALL2	193.740	244.741	-0.337	0.033971936
ENSBTAG00000001776	SIRT2	1335.738	1601.886	-0.262	0.034133119
ENSBTAG00000000064	FEN1	179.907	133.851	0.427	0.034142051
ENSBTAG00000037377	ABHD14B	2184.555	2404.244	-0.138	0.034142051
ENSBTAG00000016368	LRPPRC	1447.571	1249.526	0.212	0.034198087
ENSBTAG00000044029	AVEN	686.072	594.464	0.207	0.034198087
ENSBTAG00000016002	FAM169A	162.769	129.313	0.332	0.03479364

GeneID	Gene	Mean Counts Juxt	Mean Counts Non-juxt	Log2 Fold-Change	P-Value (FDR adj)
ENSBTAG00000008743	ALDH2	1242.582	1480.797	-0.253	0.03495171
ENSBTAG00000009231	NSDHL	562.262	454.744	0.306	0.035198856
ENSBTAG00000005066	HSPBAP1	353.621	262.534	0.430	0.035233356
ENSBTAG00000003553	ZFP36L2	1553.331	1973.803	-0.346	0.035233356
ENSBTAG00000030966	TAF6	1292.610	1524.115	-0.238	0.03524582
ENSBTAG00000018065	YARS	1255.249	1108.750	0.179	0.035730306
ENSBTAG00000014246	CENPH	95.872	64.548	0.571	0.035822527
ENSBTAG00000040076	ILF3	2122.284	1898.497	0.161	0.035945686
ENSBTAG00000001440	PMM2	859.792	1025.872	-0.255	0.035945686
ENSBTAG00000047658	PHF7	143.171	180.636	-0.335	0.036024269
ENSBTAG00000012317	PNP	2165.482	2475.675	-0.193	0.036236141
ENSBTAG00000009291	CFAP61	59.696	84.820	-0.507	0.036243943
ENSBTAG00000006754	DBP	270.372	336.555	-0.316	0.036453176
ENSBTAG00000001395	C1H21orf91	195.071	149.156	0.387	0.036482865
ENSBTAG00000006579	P4HA3	66.478	92.248	-0.473	0.036482865
ENSBTAG00000004257	TAF4B	190.052	144.948	0.391	0.036501028
ENSBTAG00000017812	ALS2CL	917.971	1052.467	-0.197	0.036634719
ENSBTAG00000020548	AZIN2	24.983	43.434	-0.798	0.036650773
ENSBTAG00000027320	KCNB1	149.555	183.738	-0.297	0.036676582
ENSBTAG00000017604	RAB13	1023.089	1246.082	-0.284	0.036766935
ENSBTAG00000005786	ATXN3	251.016	195.925	0.357	0.036941953
ENSBTAG00000021741	RPS6KA2	106.928	142.165	-0.411	0.037088147
ENSBTAG00000002176	NSMCE1	508.191	608.375	-0.260	0.037132204
ENSBTAG00000026966	RASSF9	173.949	127.191	0.452	0.037205035
ENSBTAG00000037470		86.322	131.896	-0.612	0.037328538
ENSBTAG00000012139	SIX1	97.487	71.586	0.446	0.037394427
ENSBTAG00000007393	RND2	257.389	325.410	-0.338	0.037472182
ENSBTAG00000015595	MCM5	579.175	428.282	0.435	0.037500093
ENSBTAG00000004745	NAA15	1099.170	934.652	0.234	0.037500093
ENSBTAG00000015101	HMGB2	447.220	337.170	0.408	0.037622712
ENSBTAG00000004997	CTNNAL1	1614.909	1336.733	0.273	0.037632893
ENSBTAG00000043571	ND2	47336.714	63388.261	-0.421	0.03766985
ENSBTAG00000015312	LTBR	1240.131	1496.656	-0.271	0.037737103
ENSBTAG00000002467	FAM173A	199.056	273.916	-0.461	0.037743143
ENSBTAG00000019023	NANS	246.963	314.603	-0.349	0.037845604
ENSBTAG00000025496	SORD	72.529	99.044	-0.450	0.037898477
ENSBTAG00000000266	NAB1	1656.106	1376.732	0.267	0.038195513
ENSBTAG00000004374	CNPY2	529.900	675.911	-0.351	0.038415965
ENSBTAG00000000153	LRFN3	166.605	212.184	-0.349	0.038530088
ENSBTAG00000003458	CDCA7	166.061	112.083	0.567	0.038661444
ENSBTAG00000013562	SKP2	262.201	212.563	0.303	0.038661444
ENSBTAG00000020989	SUSD4	760.802	890.999	-0.228	0.038661444
ENSBTAG00000000160	CBS	442.478	525.072	-0.247	0.038661444
ENSBTAG00000012918	CRISP3	23.392	80.577	-1.784	0.038661444
ENSBTAG00000005182	BoLA	742.735	567.259	0.389	0.038723219
ENSBTAG00000018894	PEX11G	358.851	420.674	-0.229	0.038723219
ENSBTAG00000016349	TEAD2	739.202	860.878	-0.220	0.038965119
ENSBTAG00000002260	NCAPD3	401.775	332.068	0.275	0.039086444
ENSBTAG00000002981	PIMREG	64.632	40.227	0.684	0.039100939
ENSBTAG00000012634	NDUFB7	337.388	426.266	-0.337	0.039101153
ENSBTAG00000012919	MMP15	88.475	67.289	0.395	0.039286003
ENSBTAG00000011932	PRG4	569.677	450.879	0.337	0.039286003
ENSBTAG00000043958	TMEM33	435.183	344.840	0.336	0.039286003
ENSBTAG00000030933	ZNF576	292.832	355.048	-0.278	0.039286003
ENSBTAG00000006515	ESPN	88.241	121.223	-0.458	0.039286003
ENSBTAG00000046166		25.959	41.129	-0.664	0.039286003
ENSBTAG00000047166	SH2D7	43.183	62.032	-0.523	0.039381485
ENSBTAG00000000854	SEC16B	1.793	7.275	-2.020	0.039758439
ENSBTAG00000007783	MYBL2	518.728	363.904	0.511	0.039797352
ENSBTAG00000010002	IRF2	524.014	440.331	0.251	0.039899854
ENSBTAG00000005197	BAZ1B	1902.055	1716.645	0.148	0.039899854
ENSBTAG00000003191	FSCN1	5206.808	6321.403	-0.280	0.039899854
ENSBTAG00000006864		211.503	134.000	0.658	0.039927752
ENSBTAG00000002915	GPR63	96.951	64.517	0.588	0.039939401
ENSBTAG00000034875	ALPK1	403.842	317.702	0.346	0.039979226
ENSBTAG00000005211	RPL4	21037.288	24450.015	-0.217	0.041088844
ENSBTAG00000003604	ADAMTSL4	399.362	523.062	-0.389	0.04135026
ENSBTAG00000003165	ADAMTS9	1799.940	2317.938	-0.365	0.041475275
ENSBTAG00000014883	GABARAP	3680.809	4372.528	-0.248	0.041833324
ENSBTAG00000005833	ETNK1	537.383	423.372	0.344	0.041964554

GeneID	Gene	Mean Counts Juxt	Mean Counts Non-juxt	Log2 Fold-Change	P-Value (FDR adj)
ENSBTAG00000012509	DYRK1B	687.992	835.121	-0.280	0.041964554
ENSBTAG00000000030	RDM1	62.054	40.098	0.630	0.042025768
ENSBTAG00000019234	BMP6	256.626	337.530	-0.395	0.042034503
ENSBTAG00000000773	TTC9C	378.927	318.048	0.253	0.042071642
ENSBTAG00000046362		120.113	154.491	-0.363	0.042231112
ENSBTAG00000011963	RPS19	7152.580	8856.212	-0.308	0.042271244
ENSBTAG00000021617	ZC3HAV1	2368.502	2004.180	0.241	0.042278327
ENSBTAG00000048210		30.289	52.078	-0.782	0.042967013
ENSBTAG00000004203	VPS33A	395.202	460.862	-0.222	0.043266234
ENSBTAG00000018810	THBS2	215.105	289.084	-0.426	0.043266234
ENSBTAG00000009345	AMZ2	656.353	757.251	-0.206	0.043388627
ENSBTAG00000009175	RPS6KB2	275.170	335.811	-0.287	0.043388627
ENSBTAG00000001296	TMEM50A	2226.558	1894.869	0.233	0.043404795
ENSBTAG00000000405	VKORC1	640.192	801.477	-0.324	0.043443416
ENSBTAG00000017816	FXYD1	11.292	26.903	-1.252	0.043443416
ENSBTAG00000016869	POLD3	364.564	298.201	0.290	0.043672704
ENSBTAG00000005124	JADE3	1235.649	973.943	0.343	0.043725038
ENSBTAG00000010357	ST6GAL1	176.274	232.849	-0.402	0.04417979
ENSBTAG00000014390	MTMR9	80.747	110.446	-0.452	0.04417979
ENSBTAG00000004387	MTPAP	457.771	389.082	0.235	0.044341026
ENSBTAG00000005670	ARHGEF19	47.186	68.356	-0.535	0.044407365
ENSBTAG00000024815	ANKRD28	345.083	288.401	0.259	0.044574649
ENSBTAG00000018070	SCNM1	235.285	290.083	-0.302	0.044682049
ENSBTAG00000011528	SMIM11A	87.931	116.434	-0.405	0.044728082
ENSBTAG00000007503	STRC	1.133	7.265	-2.681	0.044728082
ENSBTAG00000011635	CENPN	73.992	49.224	0.588	0.044751767
ENSBTAG00000011224	CITED2	4286.229	5053.961	-0.238	0.044775191
ENSBTAG00000018732	HSPA12B	234.716	284.448	-0.277	0.044775191
ENSBTAG00000039090	MAGEH1	168.105	217.669	-0.373	0.044826558
ENSBTAG00000034449		738.811	377.155	0.970	0.04485157
ENSBTAG00000016547	CEP57	362.986	303.307	0.259	0.04485157
ENSBTAG00000008552	PLXNA3	886.580	1042.288	-0.233	0.04485157
ENSBTAG00000019538	FBXO28	461.773	380.832	0.278	0.044896668
ENSBTAG00000009783		322.154	475.072	-0.560	0.044925081
ENSBTAG00000005310	GPR180	89.131	67.294	0.405	0.044933757
ENSBTAG00000000647	SELENOO	609.900	746.722	-0.292	0.044934281
ENSBTAG00000034360	SERF1A	109.101	151.478	-0.473	0.044934281
ENSBTAG00000001081	PALLD	1375.230	1636.164	-0.251	0.045170028
ENSBTAG00000017739	TNK1	292.142	355.790	-0.284	0.045544077
ENSBTAG00000002164	AXDND1	10.078	3.821	1.399	0.045674905
ENSBTAG00000040442		106.124	79.067	0.425	0.045674905
ENSBTAG00000019214	USP14	812.658	683.786	0.249	0.045781254
ENSBTAG00000018164	FNDC4	156.346	210.964	-0.432	0.045781254
ENSBTAG00000033449	SLC25A40	32.449	18.309	0.826	0.046080069
ENSBTAG00000002605		237.163	190.493	0.316	0.046216168
ENSBTAG00000008579	RCC2	1494.491	1317.702	0.182	0.046216168
ENSBTAG00000039477	TPBG	273.820	227.015	0.270	0.046233808
ENSBTAG00000020421	SUPT16H	1744.221	1530.238	0.189	0.046451199
ENSBTAG00000010718	RALGPS2	443.379	352.386	0.331	0.046543833
ENSBTAG00000004956	CHEK2	154.789	116.767	0.407	0.046996153
ENSBTAG00000006755	C15H11orf58	2143.499	1854.699	0.209	0.047266675
ENSBTAG00000031723	RPL6	11482.384	13125.903	-0.193	0.047630702
ENSBTAG00000011340	NSL1	162.783	126.751	0.361	0.047884206
ENSBTAG00000039922	ARAP2	2732.828	2228.511	0.294	0.047884206
ENSBTAG00000023369	GRIN2D	118.909	151.131	-0.346	0.047884206
ENSBTAG00000006526	BCL2L1	696.812	800.977	-0.201	0.048106564
ENSBTAG00000014318	SLC33A1	962.124	841.101	0.194	0.048159086
ENSBTAG00000014375	TMCC3	629.282	535.113	0.234	0.048560117
ENSBTAG00000014371	CHPF2	723.109	854.036	-0.240	0.04862865
ENSBTAG00000015032	CD14	81.371	109.025	-0.422	0.04862865
ENSBTAG00000015198	DZIP1L	192.797	241.913	-0.327	0.049118925
ENSBTAG00000047161	ARSH	65.105	42.484	0.616	0.049377869
ENSBTAG00000013544	LGALS8	251.215	198.582	0.339	0.049662416

SUPPLEMENTARY FIGURES

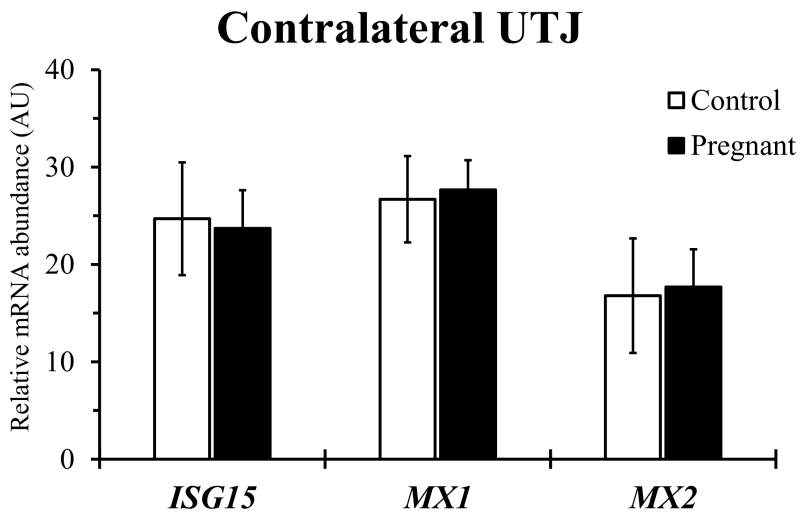

Figure S1. Relative mRNA abundance of interferon-stimulated genes (arbitrary units; AU; mean ± SEM) for control (white bars) and pregnant (black bars) cows in the uterotubal junction of the uterine horn contralateral to the CL. No significant mean differences were detected ($P > 0.1$).

APPENDICES

APPENDIX A

PLOS ONE

RESEARCH ARTICLE

Pre-hatching embryo-dependent and -independent programming of endometrial function in cattle

Mariana Sponchiado[1], Nathália Souza Gomes[1], Patrícia Kubo Fontes[2], Thiago Martins[1], Maite del Collado[3], Athos de Assumpção Pastore[4], Guilherme Pugliesi[5], Marcelo Fábio Gouveia Nogueira[6], Mario Binelli[1]*

1 School of Veterinary Medicine and Animal Science, University of São Paulo, Pirassununga, São Paulo, Brazil, **2** Department of Pharmacology, São Paulo State University, Botucatu, São Paulo, Brazil, **3** Department of Veterinary Medicine, Faculty of Animal Science and Food Engineering, University of São Paulo, Pirassununga, São Paulo, Brazil, **4** Androvet, Sertãozinho, São Paulo, Brazil, **5** Department of Clinic and Surgery of Veterinary, School of Veterinary, Minas Gerais Federal University, Belo Horizonte, Minas Gerais, Brazil, **6** Department of Biological Science, São Paulo State University, Assis, São Paulo, Brazil

* binelli@usp.br

OPEN ACCESS

Citation: Sponchiado M, Gomes NS, Fontes PK, Martins T, del Collado M, Pastore AdA, et al. (2017) Pre-hatching embryo-dependent and -independent programming of endometrial function in cattle. PLoS ONE 12(4): e0175954. https://doi.org/10.1371/journal.pone.0175954

Editor: Eric Asselin, Universite du Quebec a Trois-Rivieres, CANADA

Received: December 26, 2016

Accepted: April 3, 2017

Published: April 19, 2017

Data Availability Statement: All relevant data are within the paper and its Supporting Information files.

Funding: This work was supported by Conselho Nacional de Desenvolvimento Científico e Tecnológico (CNPq): MS; Fundação de Amparo à Pesquisa do Estado de São Paulo (FAPESP): MB (grant number 2011/03226-4) and NSG (grant number 2015/21831-3).

Competing interests: The authors have declared that no competing interests exist.

Abstract

The bovine pre-implantation embryo secretes bioactive molecules from early development stages, but effects on endometrial function are reported to start only after elongation. Here, we interrogated spatially defined regions of the endometrium transcriptome for responses to a day 7 embryo *in vivo*. We hypothesize that exposure to an embryo changes the abundance of specific transcripts in the cranial region of the pregnant uterine horn. Endometrium was collected from the uterotubal junction (UTJ), anterior (IA), medial (IM) and posterior (IP) regions of the uterine horn ipsilateral to the CL 7 days after estrus from sham-inseminated (Con) or artificially inseminated, confirmed pregnant (Preg) cows. Abundance of 86 transcripts was evaluated by qPCR using a microfluidic platform. Abundance of 12 transcripts was modulated in the Preg endometrium, including classical interferon-stimulated genes (*ISG15*, *MX1*, *MX2* and *OAS1Y*), prostaglandin biosynthesis genes (*PTGES*, *HPGD* and *AKR1C4*), water channel (*AQP4*) and a solute transporter (*SLC1A4*) and this was in the UTJ and IA mainly. Additionally, for 71 transcripts, abundance varied according to region of the reproductive tract. Regulation included downregulation of genes associated with proliferation (*IGF1*, *IGF2*, *IGF1R* and *IGF2R*) and extracellular matrix remodeling (*MMP14*, *MMP19* and *MMP2*) and upregulation of anti-adhesive genes (*MUC1*) in the cranial regions of uterine horn. Physical proximity to the embryo provides paracrine regulation of endometrial function. Embryo-independent regulation of the endometrial transcriptome may support subsequent stages of embryo development, such as elongation and implantation. We speculate that successful early embryo-dependent and -independent programming fine-tune endometrial functions that are important for maintenance of pregnancy in cattle.